

***Dual Purpose
Canister Reactivity
and Groundwater
Absorption Analyses***

Spent Fuel and Waste Disposition

***Prepared for
US Department of Energy
Office of Spent Fuel and Waste
Science and Technology
A. M. Shaw
Oak Ridge National Laboratory***

***J. B. Clarity, L.P. Miller, K. Banerjee
Pacific Northwest National Laboratory***

September 30, 2022

M3SF-22OR0103050810

FCRD-UFD-2014-000520, Revision 8

ORNL/SPR-2022/2609

DISCLAIMER

This information was prepared as an account of work sponsored by an agency of the U.S. Government. Neither the U.S. Government nor any agency thereof, nor any of their employees, makes any warranty, expressed or implied, or assumes any legal liability or responsibility for the accuracy, completeness, or usefulness, of any information, apparatus, product, or process disclosed, or represents that its use would not infringe privately owned rights. References herein to any specific commercial product, process, or service by trade name, trademark, manufacturer, or otherwise, does not necessarily constitute or imply its endorsement, recommendation, or favoring by the U.S. Government or any agency thereof. The views and opinions of authors expressed herein do not necessarily state or reflect those of the U.S. Government or any agency thereof.

This is a technical paper that does not take into account contractual limitations or obligations under the Standard Contract for Disposal of Spent Nuclear Fuel and/or High-Level Radioactive Waste (Standard Contract) (10 CFR Part 961). For example, under the provisions of the Standard Contract, spent nuclear fuel in multi-assembly canisters is not an acceptable waste form, absent a mutually agreed to contract amendment. To the extent discussions or recommendations in this paper conflict with the provisions of the Standard Contract, the Standard Contract governs the obligations of the parties, and this paper in no manner supersedes, overrides, or amends the Standard Contract. This paper reflects technical work, which could support future decision making by DOE. No inferences should be drawn from this paper regarding future actions by DOE, which are limited both by the terms of the Standard Contract and Congressional appropriations for the Department to fulfill its obligations under the Nuclear Waste Policy Act including licensing and construction of a spent nuclear fuel repository

REVISION HISTORY

Version	Description
FCRD-UFD-2014-000520	Initial Release
FCRD-UFD-2014-000520, Revision 1	Appendix A is added. Appendix A contains (1) post-closure criticality results with principal set of 29 isotopes (recommended for post-closure criticality analysis) for eight sites (total 215 DPCs), (2) reactivity reduction study results by groundwater species applied to as-loaded DPCs, and (3) reactivity impact of filler material applied to as-loaded DPCs. In the main body, Figures 2, 5–9, and 11 are updated to be consistent with FCRD-UFD-2014-000069, <i>Investigation of Dual-Purpose Canister Direct Disposal Feasibility</i> (FY14). Changes in the main body are identified by a black vertical line in the margin.
FCRD-UFD-2014-000520, Revision 2	Appendix B is added. Appendix B contains (1) post-closure criticality results for 16 new sites (total 339 DPCs), and (2) reactivity reduction study by groundwater species (NaCl) applied to as-loaded DPCs at 16 sites. Changes in the main body are identified by a black vertical line in the margin.
FCRD-UFD-2014-000520, Revision 3	Appendix C is added. Appendix C contains a misload methodology for as-loaded disposal calculations and an evaluation for misload of 3 sites and 99 canisters. Changes in the main body are identified by a black vertical line in the margin.
FCRD-UFD-2014-000520, Revision 4	Appendix D is added. Appendix D contains (1) a description of the criticality models for the NUHOMS® 24PT1-DSC and NUHOMS® 32 PT-DSC DPCs, (2) post-closure criticality calculation results for five sites (total 60 DPCs), (3) reactivity reduction study results by groundwater species applied to as-loaded DPCs, (4) misload analyses assuming the worst fuel assembly configuration in an as-loaded canister, and (5) a filler height scoping calculation.
FCRD-UFD-2014-000520, Revision 5	Appendix E is added. Appendix E contains: (1) a description of the criticality models for the NUHOMS® 32 PT-DSC and NUHOMS® 61 BT-DSC loss of absorber models, (2) post-closure criticality calculation results for five sites (total 92 DPCs), (3) reactivity reduction study results by groundwater species applied to as-loaded DPCs, and (4) misload analyses assuming the worst fuel assembly configuration in an as-loaded canister.
FCRD-UFD-2014-000520, Revision 6	Appendix F is added. Appendix F contains calculations that (1) extend the analytical timeline for the 708 canisters analyzed through FY19 from 22,000 years to 1,100,000 years, (2) characterize the effects of cementitious filler materials have on post closure criticality scenarios, (3) provide post-closure criticality calculation results for four sites (66 new DPCs), (4) provide reactivity reduction study results by groundwater species applied to as-loaded DPCs, and (5) present misload analyses assuming the worst fuel assembly configuration in an as-loaded canister.

FCRD-UFD-2014-000520, Revision 7	Appendix G is added. Appendix G contains (1) a summary of previous FY21 research activities, including the reactivity assessment of basket modification techniques and an investigation of canister loading optimization techniques which consider disposal reactivity, (2) post-closure criticality calculation results for ten sites (155 new DPCs), (3) reactivity reduction study results by groundwater species applied to as-loaded DPCs, and (4) misload analyses assuming the worst fuel assembly configuration in an as-loaded canister.
FCRD-UFD-2014-000520, Revision 8	Appendix H is added. Appendix H contains (1) post-closure criticality calculation results for fourteen sites (225 new DPCs), (2) reactivity reduction study results by groundwater species applied to as-loaded DPCs, and (3) misload analyses assuming the worst fuel assembly configuration in an as-loaded canister.

This page is intentionally left blank.

CONTENTS

REVISION HISTORY.....	iii
CONTENTS.....	vi
FIGURES.....	ix
TABLES	xix
ACRONYMS.....	xxii
1. INTRODUCTION.....	1
2. REVIEW OF LITERATURE.....	3
3. CODES AND METHODS	5
3.1 Axial Burnup Profile.....	6
3.2 Isotopes Included in the Criticality Mode.....	7
3.3 Subcritical Limit	7
3.4 Degradation Scenarios	8
4. IMPACTS OF GROUNDWATER DISSOLVED AQUEOUS SPECIES.....	11
4.1 Groundwater Study Results.....	13
4.2 Hypothetical High Reactivity Configuration	19
5. ANALYSIS BY APPLYING THE ACTUAL CANISTER-SPECIFIC LOADING	21
5.1 Maine Yankee	22
5.2 Connecticut Yankee	25
5.3 Rancho Seco.....	28
5.4 Trojan.....	32
5.5 Sequoyah.....	34
5.6 Component Credit.....	35
6. CONCLUSION	39
7. REFERENCES	41
APPENDIX A. FY15 Criticality Study	A-1
A.1. Introduction.....	A-3
A.2. Disposal-Isotopes	A-3
A.3. New Sites	A-6
A.4. As-Loaded Criticality Analysis with Chlorides in Groundwater.....	A-10
A.5. As-Loaded Criticality Analysis with Engineering Filler Materials.....	A-11
A.6. Reactivity Impact of ¹⁰ B Areal Density for As-Loaded DPCs.....	A-12
A.7. Conclusion	A-13

A.8. References.....	A-14
APPENDIX B. FY16 Criticality Study	B-1
B.1. Introduction.....	B-3
B.2. BWR As-Loaded Criticality Analysis Approach.....	B-3
B.3. Sites Analyzed.....	B-3
B.4. As-Loaded Criticality Analysis with Chlorides in Groundwater	B-5
B.5. Conclusion	B-6
B.6. References.....	B-7
APPENDIX C. FY17 Criticality Study	C-1
C.1. Introduction.....	C-3
C.2. Misload Definition and Regulatory Guidance	C-3
C.3. Assembly Misload Methodology	C-4
C.4. Results.....	C-9
C.5. Conclusion	C-16
C.6. References.....	C-17
APPENDIX D. FY 2018 Criticality Study	D-1
D.1. Introduction.....	D-3
D.2. NUHOMS® 24PT1-DSC.....	D-4
D.3. NUHOMS® 32PT-DSC.....	D-10
D.4. Filler Height Scoping Calculation.....	D-15
D.5. Conclusions.....	D-17
D.6. References.....	D-18
APPENDIX E. FY 2019 Criticality Study	E-1
E.1. Introduction.....	E-3
E.2. NUHOMS® 61BT-DSC loss of Neutron Absorber Model	E-4
E.3. Nine Mile Point, Cooper, and Monticello Criticality Calculations.....	E-4
E.4. NUHOMS® 32PTH-DSC loss of Neutron Absorber Model.....	E-7
E.5. Crystal River Criticality Calculations	E-8
E.6. Kewaunee Criticality Calculations.....	E-10
E.7. Conclusions.....	E-14
E.8. Reference	E-15
APPENDIX F. FY 2020 Criticality Study	F-1
F.1. Introduction.....	F-2
F.2. Extension of DPC calculations to Beyond 1,000,000 Years.....	F-3
F.3. Evaluation of Cementitious Filler Materials for Criticality Control	F-9
F.4. Seabrook Criticality Calculations	F-19
F.5. Vogtle Criticality Calculations.....	F-21
F.6. Hope Creek Criticality Calculations	F-23

F.7.	Salem Criticality Calculations.....	F-25
F.8.	Conclusions.....	F-27
F.9.	Reference	F-29
APPENDIX G.	FY 2021 Criticality Study	G-30
G.1.	Introduction.....	G-31
G.2.	Other Direct Disposal of DPCs activities in FY2021	G-32
G.3.	Braidwood Criticality Calculations.....	G-37
G.4.	Diablo Canyon Criticality Calculations	G-39
G.5.	Byron Criticality Calculations.....	G-41
G.6.	La Salle Criticality Calculations	G-43
G.7.	North Anna Criticality Calculations.....	G-46
G.8.	Sequoyah Criticality Calculations.....	G-48
G.9.	Surry Criticality Calculations.....	G-51
G.10.	Callaway Criticality Calculations	G-52
G.11.	Watts Bar Criticality Calculations	G-54
G.12.	Browns Ferry Criticality Calculations	G-56
G.13.	Conclusions.....	G-58
G.14.	Reference	G-60
APPENDIX H.	FY 2022 Criticality Study	H-1
H.1.	Introduction.....	H-2
H.2.	Clinton Criticality Calculations.....	H-3
H.3.	Fermi Criticality Calculations	H-5
H.4.	Saint Lucie Criticality Calculations	H-7
H.5.	McGuire Criticality Calculations	H-8
H.6.	Palo Verde Criticality Calculations.....	H-12
H.7.	Summer Criticality Calculations	H-13
H.8.	Susquehanna Criticality Calculations	H-15
H.9.	Brown’s Ferry Criticality Calculations	H-17
H.10.	Fitzpatrick Criticality Calculations	H-18
H.11.	Waterford Criticality Calculations	H-20
H.12.	Perry Criticality Calculations	H-22
H.13.	Farley Criticality Calculations	H-24
H.14.	Indian Point Criticality Calculations.....	H-26
H.15.	Comanche Peak Criticality Calculations.....	H-28
H.16.	Conclusions.....	H-30

FIGURES

Figure 1. Pressurized-water reactor (PWR) 18 nodes, with 1 being the bottom of the assembly, axial burnup profiles with normalized distribution.....	7
Figure 2. Reactivity impact of B ¹⁰ areal density variation.....	9
Figure 3. Graphical depiction of the center plane of the MPC-32 KENO model used for groundwater composition studies with varying B ¹⁰ areal density in the neutron absorber panels.....	12
Figure 4. KENO depiction of the MPC-32 degraded basket scenario.....	13
Figure 5. (a) Reactivity impact of Cl concentration in groundwater for different levels of neutron absorber; (b) reactivity impact of Cl concentration in groundwater for degraded basket configuration.....	14
Figure 6. (a) Reactivity impact of Li concentration in groundwater for different levels of neutron absorber; (b) reactivity impact of Li concentration in groundwater for degraded basket configuration.....	15
Figure 7. (a) Reactivity impact of B concentration in groundwater for different levels of neutron absorber; (b) reactivity impact of B concentration in groundwater for degraded basket configuration.....	16
Figure 8. (a) Reactivity impact of Br and Mn concentration in groundwater for complete loss of neutron absorber; (b) reactivity impact of Br and Mn concentration in groundwater for degraded basket configuration.....	17
Figure 9. (a) Reactivity impact of the rest of the ions' concentration in groundwater for complete loss of neutron absorber; (b) reactivity impact of the rest of the ions' concentration in groundwater for degraded basket configuration.....	18
Figure 10. Disintegrated fuel rods configuration as modeled in KENO.....	19
Figure 11. Reactivity impact of Cl concentration in groundwater for high reactivity configuration.....	20
Figure 12. NAC UMS 24-assembly basket without neutron absorber panels as modeled in SCALE.....	23
Figure 13. Calculated k_{eff} results for as-loaded MY 24-assembly DPCs with loss of neutron absorber panels.....	24
Figure 14. Radial layout of the CY MPC-26 without neutron absorber panels as modeled in SCALE.....	25
Figure 15. Radial layout of the CY MPC-24 without neutron absorber panels as modeled in SCALE.....	26
Figure 16. Calculated k_{eff} results for as-loaded CY DPCs with loss of neutron absorber panels.....	27
Figure 17. 3D representation of the RS DPC as modeled in SCALE.....	29
Figure 18. (a) Loss of neutron absorber configuration (RS) as modeled in KENO; (b) k_{eff} as a function of time based on actual loading.....	30
Figure 19. (a) Degraded spacer disks configuration (RS) as modeled in KENO; (b) k_{eff} as a function of time based on actual loading.....	31
Figure 20. Radial layout of the MPC-24E/EF without neutron absorber panels as modeled in SCALE.....	32

Figure 21. Calculated k_{eff} results for as-loaded TJ DPCs with loss of neutron absorber panels.	33
Figure 22. Radial layout of the MPC-32 without neutron absorber panels as modeled in SCALE.	34
Figure 23. Calculated k_{eff} results for as-loaded SQ casks with loss of neutron absorber panels.	35
Figure 24. Radial view of the WABAs in the guide tube as modeled in SCALE for SQ DPCs.	37
Figure 25. DPC criticality analyses roadmap as described in Ref. [4] with the completion status; Yellow: work in progress and Green: completed.	40
Figure A-1. Comparison (in terms of reactivity) between disposal-isotopes and storage- transportation-isotopes for CY DPCs in the calendar year 9999.	A-4
Figure A-2. k_{eff} vs. calendar year for the loss-of-neutron-absorber case based on actual loading and disposal-isotopes.	A-5
Figure A-3. k_{eff} vs. calendar year for the RS basket degradation case based on actual loading and disposal-isotopes.	A-6
Figure A-4. Holtec's MPC-HB 80-assembly basket without neutron absorber panels as modeled in KENO VI.	A-7
Figure A-5. k_{eff} vs. calendar year for the loss-of-neutron-absorber case, based on actual loading and disposal isotopes.	A-9
Figure A-6. k_{eff} vs. NaCl concentration for the loss-of-neutron-absorber (MY, SQ CY, SL, and HB) and degraded basket (RS) cases based on actual loading.	A-11
Figure A-7. Reactivity as a function of aluminum and gibbsite volume fraction for DPCs at SQ site.	A-12
Figure A-8. Reactivity impact of ^{10}B areal density variation for as-loaded SQ DPCs.	A-13
Figure B-1. k_{eff} vs. calendar year for the loss-of-neutron-absorber case, based on actual loading and disposal-isotopes. The number within the bracket indicates number of DPCs.	B-4
Figure B-2. k_{eff} vs. NaCl concentration for the DPCs with $k_{eff} > 0.98$ for the loss-of-neutron- absorber scenario. (Numbers in brackets = number of DPCs).	B-6
Figure B-3. DPC criticality analyses roadmap as described in Ref. [4] with the completion status; Yellow: work in progress and Green: completed.	B-7
Figure C-1. Example distribution of k_{inf} for all assemblies in a pool at the time of loading a specific canister at a specific site. Y-axis shows number of assemblies in each bin.	C-5
Figure C-2. The single severely underburned assembly (circled in red in the left plot) is the assembly with the highest k_{inf} . The multiple moderately underburned assemblies (circled in red in the right plot) are selected as the number of assemblies corresponding to 50% of the cask payload with the lowest available reactivity that bounds 90% (red line in right plot) of the assemblies available in the pool. Y-axis shows number of assemblies in each bin.	C-5
Figure C-3. A loading independent criticality importance map (left) generated by ranking the highest (indicated by 1) to lowest number of fissions generated in each position (canister cell) of a uniformly loaded MPC-32 canister. Both E (edge) and C (corner) are excluded from misloads due to high leakage. The right figure shows the fission reaction rate at each cell location.	C-6
Figure C-4. Number of fissions (left) and individual assembly reactivity (right) for each position of an as-loaded MPC-32 cask.	C-7

Figure C-5. Identified position for single assembly misload using highest reactivity approach (left) and neighbor nearest center with lowest reactivity approach (right).....	C-7
Figure C-6. Increase in reactivity from misloading the position with the single severely underburned assembly.	C-8
Figure C-7. Loading priority for an example as-loaded canister with multiple moderately underburned assembly misload based on the importance map and position cell number. The red positions indicate misloaded positions, while the others are still the as-loaded positions.....	C-8
Figure C-8. Individual assembly reactivity distribution for the pool inventory at Sequoyah 1 and 2. Y-axis shows number of assemblies in each bin.	C-9
Figure C-9. The red markers indicate the reactivity of the loaded canisters at Sequoyah, and the black lines are the ranges between optimum and worst possible loading for reactivity using the same canister inventory.....	C-10
Figure C-10. Reactivity increase in pcm for each misload type and canister loaded at Sequoyah. Single Fission is the single assembly misload method misloading the position with the highest fission density, Single React is the single assembly misload method misloading the neighbor with lowest reactivity closest to the center, multiple is the multiple moderately underburned assembly misload and worst is the worst configuration misload.....	C-11
Figure C-11. The as-loaded reactivity and the most bounding of the misload types.	C-11
Figure C-12. Individual assembly reactivity distribution for the pool inventory at Zion 1 and 2. Y-axis shows number of assemblies in each bin.....	C-12
Figure C-13. Red markers indicate the reactivity of the loaded canisters at Zion, and the black lines are the ranges between optimized and worst possible loading for reactivity using the same canister inventory.	C-12
Figure C-14. Reactivity increase in pcm for each misload type and canister loaded at Zion. Single Fission is the single assembly misload method misloading the position with the highest fission density, Single React is the single assembly misload method misloading the neighbor with lowest reactivity closest to the center, multiple is the multiple moderately underburned assembly misload and worst is the worst configuration misload.....	C-13
Figure C-15. The as-loaded reactivity and the most bounding of the misload types.	C-14
Figure C-16. Individual assembly reactivity distribution for the pool inventory at Browns Ferry 2 and 3. Y-axis shows number of assemblies in each bin.....	C-14
Figure C-17. Red markers indicate the reactivity of the loaded canisters at Browns Ferry, and black lines are the range between optimized and worst possible loading for reactivity using the same canister inventory. Notice that the range in k_{eff} is much smaller than for Sequoyah and Zion.	C-15
Figure C-18. Reactivity increase in pcm for each misload type and canister loaded at Browns Ferry. Single Fission is the single assembly misload method misloading the position with the highest fission density, Single React is the single assembly misload method misloading the neighbor with lowest reactivity closest to the center, multiple is the multiple moderately underburned assembly misload and worst is the worst configuration misload.	C-15

Figure C-19. The as-loaded reactivity and the most bounding of the misload types.	C-16
Figure C-20. DPC criticality analyses roadmap as described in Ref. [4], with the color yellow indicating a work in progress and green indicating completion.	C-17
Figure D-1. Horizontal cross-sectional view of the XSO14W fuel assembly model.	D-5
Figure D-2. Horizontal cross-sectional view of the MOX fuel assembly model.	D-5
Figure D-3. Horizontal cross-sectional view of the NUHOMS® 24PT1-DSC model through a disc plate for the loss-of-neutron-absorber scenario.	D-7
Figure D-4. Horizontal cross-sectional view of the NUHOMS® 24PT1-DSC model for the degraded basket scenario.	D-7
Figure D-5. Illustration of fuel assembly ranking for the worst-misload configuration of the NUHOMS® 24PT1-DSC.	D-8
Figure D-6. k_{eff} vs. calendar year for the SONGS1 SNF canisters with degraded basket materials, no neutron absorber, and regular configurations.	D-9
Figure D-7. k_{eff} vs. NaCl concentration for SONGS1 SNF canisters with $k_{eff} > 0.98$ for the degraded basket scenario (numbers in brackets = number of DPCs).	D-10
Figure D-8. k_{eff} increase between the worst-misload scenario and the as-loaded configuration for six SONGS1 SNF canisters.	D-10
Figure D-9. Horizontal cross-sectional view of the XPA15C fuel assembly model.	D-12
Figure D-10. Horizontal cross-sectional view of the NUHOMS® 32PT-DSC model for the loss-of-neutron-absorber scenario.	D-12
Figure D-11. Illustration of fuel assembly ranking in the worst-misload configuration for the NUHOMS® 32PT-DSC.	D-13
Figure D-12. k_{eff} vs. calendar year for the loss-of-neutron-absorber scenario, based on actual loading and disposal isotopes (numbers in brackets = number of DPCs).	D-14
Figure D-13. k_{eff} vs. NaCl concentration for the DPCs with $k_{eff} > 0.98$ for the loss-of-neutron-absorber scenario (numbers in brackets = number of DPCs).	D-14
Figure D-14. k_{eff} increase between the worst-misload scenario and the as-loaded configuration (numbers in brackets = number of DPCs).	D-15
Figure D-15. (a) Vertical cross-sectional view and (b) horizontal cross-section view of the MPC-32 disposal criticality model for filler height studies.	D-16
Figure E-1. Horizontal cross-sectional view of the NUHOMS® 61BT-DSC model for the loss-of-neutron-absorber scenario.	E-4
Figure E-2. k_{eff} vs. calendar year for the loss-of-neutron-absorber scenario based on actual loading and disposal isotopes for SNF canisters at Nine Mile Point, Cooper, and Monticello.	E-5
Figure E-3. k_{eff} increase between the worst-misload scenario and the as-loaded configuration for 6 Nine Mile Point SNF canisters.	E-6
Figure E-4. k_{eff} increase between the worst-misload scenario and the as-loaded configuration for 8 Cooper SNF canisters.	E-6
Figure E-5. k_{eff} increase between the worst misload scenario and the as-loaded configuration for 10 Monticello SNF canisters.	E-7

Figure E-6. Horizontal cross-sectional view of the NUHOMS® 32PTH-DSC model for the loss-of-neutron-absorber scenario.	E-8
Figure E-7. k_{eff} vs. calendar year for the loss-of-neutron-absorber scenario based on actual loading and disposal isotopes for SNF canisters at Crystal River.	E-9
Figure E-8. k_{eff} increase between the worst misload scenario and the as-loaded configuration for Crystal River SNF canisters.....	E-9
Figure E-9. k_{eff} vs. calendar year for the loss-of-neutron-absorber scenario based on actual loading and disposal isotopes for all SNF canisters at Kewaunee.....	E-11
Figure E-10. k_{eff} vs. calendar year for the degraded basket scenario, based on actual loading and disposal isotopes for the TSC-37 canisters at Kewaunee.	E-11
Figure E-11. k_{eff} vs. NaCl concentration for the DPCs with $k_{eff} > 0.98$ for the TSC-37 canisters at Kewaunee under the degraded basket scenario.	E-12
Figure E-12. k_{eff} increase between the worst-misload scenario and the as-loaded configuration for the NUHOMS® 32PTH-DSCs at Kewaunee.	E-12
Figure E-13. k_{eff} increase between the worst-misload scenario and the as-loaded configuration for the TSC-37 SNF canisters at Kewaunee.....	E-13
Figure F-1. Degraded absorber calculations for PWR DPCs.....	F-4
Figure F-2. Degraded absorber calculations for BWR DPCs.	F-5
Figure F-3. Degraded basket calculations for PWR DPCs.	F-6
Figure F-4. Degraded absorber reactivity trajectory for TSC-37 canister MAG-TSC-30026086-004 at Kewaunee.	F-7
Figure F-5. Degraded basket reactivity trajectory for TSC-37 canister MAG-TSC-30026086-004 at Kewaunee.	F-8
Figure F-6. Radial view of the complete filling models for the NA case (left) and the DB case (right).	F-10
Figure F-7. Radial view of the damaged fuel filler exclusion models for the NA case (left) and the DB case (right).	F-11
Figure F-8. Radial view of the guide tube filler exclusion models for the NA case (left) and the DB case (right).	F-11
Figure F-9. Axial view of the incomplete axial filling model showing the top seven of 18 nodes unfilled.	F-12
Figure F-10. Canister reactivity vs. porosity for the complete filling and damaged fuel exclusion NA cases.	F-14
Figure F-11. Canister reactivity vs. porosity for the complete filling and damaged fuel exclusion DB cases.	F-15
Figure F-12. Canister reactivity vs. porosity for the guide tube filler exclusion NA case.	F-16
Figure F-13. Canister reactivity vs. porosity for the guide tube filler exclusion DB case.	F-17
Figure F-14. Canister reactivity vs. length of top portion of assembly uncovered for NA and DB cases (guide tubes water filled, 50% porosity elsewhere).	F-18

Figure F-15. k_{eff} vs. calendar year for the loss-of-neutron-absorber scenario based on actual loading and disposal isotopes for the SNF canisters at Seabrook.....	F-19
Figure F-16. k_{eff} vs. NaCl concentration for the DPCs with $k_{eff} > 0.98$ for the canisters at Seabrook under the loss-of-neutron-absorber scenario (calendar year 22,000).	F-20
Figure F-17. k_{eff} increase between the worst-misload scenario and the as-loaded configuration for the NUHOMS® 32PTH-DSCs at Seabrook (calendar year 22,000).	F-20
Figure F-18. k_{eff} vs. calendar year for the loss-of-neutron-absorber scenario based on actual loading and disposal isotopes for the SNF canisters at Vogtle.....	F-21
Figure F-19. k_{eff} vs. NaCl concentration for the DPCs with $k_{eff} > 0.98$ for the canisters at Vogtle under the loss-of-neutron-absorber scenario (calendar year 22,000).....	F-22
Figure F-20. k_{eff} increase between the worst-misload scenario and the as-loaded configuration for the MPC-32s at Vogtle (calendar year 22,000).	F-22
Figure F-21. k_{eff} vs. calendar year for the loss-of-neutron-absorber scenario based on actual loading and disposal isotopes for the SNF canisters at Hope Creek.....	F-23
Figure F-22. k_{eff} increase between the worst-misload scenario and the as-loaded configuration for the MPC-68s at Hope Creek (calendar year 22,000).	F-24
Figure F-23. k_{eff} vs. calendar year for the loss-of-neutron-absorber scenario based on actual loading and disposal isotopes for the SNF canisters at Salem.....	F-25
Figure F-24. k_{eff} vs. NaCl concentration for the DPCs with $k_{eff} > 0.98$ for the canisters at Salem under the loss-of-neutron-absorber scenario (calendar year 22,000).....	F-26
Figure F-25. k_{eff} increase between the worst-misload scenario and the as-loaded configuration for the MPC-32s at Salem (calendar year 22,000).	F-26
Figure F-26. Summary plot of the post closure criticality calculations performed this year (66 DPCs + other canisters at Salem) including as-loaded (gray line) and best- and worst-case misload (pink band) scenarios.	F-28
Figure G-1. SCALE-generated renderings of the DCRA (upper left), ANA chevron insert (upper right), and ANA fuel channel replacement (lower) concepts.	G-33
Figure G-2. Box plots for the single-site reloading analysis.....	G-35
Figure G-3. Diagram of the canister k_{eff} predicting neural network used with the input, output and hidden layers labeled.	G-36
Figure G-4. Training and validation errors for the neural network.....	G-37
Figure G-5. k_{eff} vs. calendar year for the loss-of-neutron-absorber scenario based on actual loading and disposal isotopes for the SNF canisters at Braidwood.....	G-38
Figure G-6. k_{eff} vs. NaCl concentration for the DPCs with $k_{eff} > 0.98$ for the canisters at Braidwood under the loss-of-neutron-absorber scenario (calendar year 22,000).	G-38
Figure G-7. k_{eff} increase between the worst-misload scenario and the as-loaded configuration for the MPC-32s at Braidwood (calendar year 22,000).	G-39
Figure G-8. k_{eff} vs. calendar year for the loss-of-neutron-absorber scenario based on actual loading and disposal isotopes for the SNF canisters at Diablo Canyon.	G-40
Figure G-9. k_{eff} vs. NaCl concentration for the DPCs with $k_{eff} > 0.98$ for the canisters at Diablo Canyon under the loss-of-neutron-absorber scenario (calendar year 22,000).	G-40

Figure G-10. k_{eff} increase between the worst-misload scenario and the as-loaded configuration for the MPC-32s at Diablo Canyon (calendar year 22,000).....	G-41
Figure G-11. k_{eff} vs. calendar year for the loss-of-neutron-absorber scenario based on actual loading and disposal isotopes for the SNF canisters at Byron.....	G-42
Figure G-12. k_{eff} vs. NaCl concentration for the DPCs with $k_{eff} > 0.98$ for the canisters at Byron under the loss-of-neutron-absorber scenario (calendar year 22,000).....	G-42
Figure G-13. k_{eff} increase between the worst-misload scenario and the as-loaded configuration for the MPC-32s at Byron (calendar year 22,000).	G-43
Figure G-14. k_{eff} vs. calendar year for the loss-of-neutron-absorber scenario based on actual loading and disposal isotopes for the MPC-68 SNF canisters at La Salle.....	G-44
Figure G-15. k_{eff} vs. calendar year for the DB scenario based on actual loading and disposal isotopes for the MPC-68M SNF canisters at La Salle.....	G-44
Figure G-16. k_{eff} vs. NaCl concentration for the DPCs with $k_{eff} > 0.98$ for the canisters analyzed in 2021 at La Salle under the DB scenario (calendar year 22,000).	G-45
Figure G-17. k_{eff} increase between the worst-misload scenario and the as-loaded configuration for the MPC-68s at La Salle (calendar year 22,000).	G-45
Figure G-18. k_{eff} increase between the worst-misload scenario and the as-loaded configuration for the MPC-68Ms at La Salle (calendar year 22,000).	G-46
Figure G-19. k_{eff} vs. calendar year for the loss-of-neutron-absorber scenario based on actual loading and disposal isotopes for the SNF canisters at North Anna.....	G-47
Figure G-20. k_{eff} increase between the worst-misload scenario and the as-loaded configuration for the NUHOMS® 32PTH-DSCs at North Anna (calendar year 22,000).	G-47
Figure G-21. k_{eff} vs. calendar year for the loss-of-neutron-absorber scenario based on actual loading and disposal isotopes for the MPC-32 SNF canisters at Sequoyah.	G-48
Figure G-22. k_{eff} vs. calendar year for the loss-of-neutron-absorber scenario based on actual loading and disposal isotopes for the MPC-37 SNF canisters at Sequoyah.	G-49
Figure G-23. k_{eff} vs. NaCl concentration for the DPCs with $k_{eff} > 0.98$ for the canisters analyzed in 2021 at Sequoyah under the loss-of-neutron-absorber and DB scenarios (calendar year 22,000).....	G-49
Figure G-24. k_{eff} increase between the worst-misload scenario and the as-loaded configuration for the MPC-32s at Sequoyah (calendar year 22,000).	G-50
Figure G-25. k_{eff} increase between the worst-misload scenario and the as-loaded configuration for the MPC-37s at Sequoyah (calendar year 22,000).	G-50
Figure G-26. k_{eff} vs. calendar year for the loss-of-neutron-absorber scenario based on actual loading and disposal isotopes for the SNF canisters at Surry.....	G-51
Figure G-27. k_{eff} increase between the worst-misload scenario and the as-loaded configuration for the NUHOMS® 32PTH-DSCs at Surry (calendar year 22,000).	G-52
Figure G-28. k_{eff} vs. calendar year for the DB scenario based on actual loading and disposal isotopes for the SNF canisters at Callaway.	G-53
Figure G-29. k_{eff} vs. NaCl concentration for the DPCs with $k_{eff} > 0.98$ for the canisters analyzed at Callaway under the DB scenario (calendar year 22,000).	G-53

Figure G-30. k_{eff} increase between the worst-misload scenario and the as-loaded configuration for the MPC-37s at Callaway (calendar year 22,000).	G-54
Figure G-31. k_{eff} vs. calendar year for the DB scenario based on actual loading and disposal isotopes for the SNF canisters at Watts Bar.	G-55
Figure G-32. k_{eff} vs. NaCl concentration for the DPCs with $k_{eff} > 0.98$ for the canisters analyzed at Watts Bar under the DB scenario (calendar year 22,000).	G-55
Figure G-33. k_{eff} increase between the worst-misload scenario and the as-loaded configuration for the MPC-37s at Watts Bar (calendar year 22,000).	G-56
Figure G-34. k_{eff} vs. calendar year for the DB scenario based on actual loading and disposal isotopes for the SNF canisters at Browns Ferry.	G-57
Figure G-35. k_{eff} vs. NaCl concentration for the DPCs with $k_{eff} > 0.98$ for the canisters analyzed at Browns Ferry under the DB scenario (calendar year 22,000).	G-57
Figure G-36. k_{eff} increase between the worst-misload scenario and the as-loaded configuration for the MPC-89s at Browns Ferry (calendar year 22,000).	G-58
Figure H-1. k_{eff} vs. calendar year for the loss-of-neutron-absorber scenario based on actual loading and disposal isotopes for the SNF canisters at Clinton.	H-4
Figure H-2. k_{eff} vs. NaCl concentration for the DPCs with $k_{eff} > 0.98$ for the canisters at Clinton under the loss-of-neutron-absorber scenario (calendar year 22,000).	H-4
Figure H-3. k_{eff} increase between the worst-misload scenario and the as-loaded configuration for the MPC-89s at Clinton (calendar year 22,000).	H-5
Figure H-4. k_{eff} vs. calendar year for the loss-of-neutron-absorber scenario based on actual loading and disposal isotopes for the SNF canisters at Fermi.	H-6
Figure H-5. k_{eff} increase between the worst-misload scenario and the as-loaded configuration for the MPC-68s at Fermi (calendar year 22,000).	H-6
Figure H-6. k_{eff} vs. calendar year for the loss-of-neutron-absorber scenario based on actual loading and disposal isotopes for the SNF canisters at Saint Lucie.	H-7
Figure H-7. k_{eff} increase between the worst-misload scenario and the as-loaded configuration for the NUHOMS [®] 32PTHs at Saint Lucie (calendar year 22,000).	H-8
Figure H-8. k_{eff} vs. calendar year for the loss-of-neutron-absorber scenario based on actual loading and disposal isotopes for the TSC-37 SNF canisters at McGuire.	H-9
Figure H-9. k_{eff} vs. calendar year for the DB scenario based on actual loading and disposal isotopes for the TSC-37 SNF canisters at McGuire.	H-9
Figure H-10. k_{eff} vs. NaCl concentration for the DPCs with $k_{eff} > 0.98$ for the canisters analyzed in 2022 at McGuire under the NA scenario (calendar year 22,000).	H-10
Figure H-11. k_{eff} vs. NaCl concentration for the DPCs with $k_{eff} > 0.98$ for the canisters analyzed in 2022 at McGuire under the DB scenario (calendar year 22,000).	H-10
Figure H-12. k_{eff} increase between the NA worst-misload scenario and the as-loaded configuration for the TSC-37s at McGuire (calendar year 22,000).	H-11
Figure H-13. k_{eff} increase between the DB worst-misload scenario and the as-loaded configuration for the TSC-37s at McGuire (calendar year 22,000).	H-11

Figure H-14. k_{eff} vs. calendar year for the loss-of-neutron-absorber scenario based on actual loading and disposal isotopes for the TSC-24 SNF canisters at Palo Verde.	H-12
Figure H-15. k_{eff} increase between the worst-misload scenario and the as-loaded configuration for the TSC-24s at Palo Verde (calendar year 22,000).	H-13
Figure H-16. k_{eff} vs. calendar year for the DB scenario based on actual loading and disposal isotopes for the SNF canisters at Summer.	H-14
Figure H-17. k_{eff} vs. NaCl concentration for the DPCs with $k_{eff} > 0.98$ for the canisters analyzed at Summer under the DB scenario (calendar year 22,000).	H-14
Figure H-18. k_{eff} increase between the worst-misload scenario and the as-loaded configuration for the MPC-37s at Summer (calendar year 22,000).	H-15
Figure H-19. k_{eff} vs. calendar year for the loss-of-neutron-absorber scenario based on actual loading and disposal isotopes for the NUHOMS® canisters at Susquehanna.	H-16
Figure H-20. k_{eff} increase between the worst-misload scenario and the as-loaded configuration for the NUHOMS® canisters at Susquehanna (calendar year 22,000).	H-16
Figure H-21. k_{eff} vs. calendar year for the NA scenario based on actual loading and disposal isotopes for the SNF canisters at Brown’s Ferry.	H-17
Figure H-22. k_{eff} increase between the worst-misload scenario and the as-loaded configuration for the MPC-68s at Browns Ferry (calendar year 22,000).	H-18
Figure H-23. k_{eff} vs. calendar year for the DB scenario based on actual loading and disposal isotopes for the SNF canisters at Fitzpatrick.	H-19
Figure H-24. k_{eff} vs. NaCl concentration for the DPCs with $k_{eff} > 0.98$ for the canisters analyzed at Fitzpatrick under the DB scenario (calendar year 22,000).	H-19
Figure H-25. k_{eff} increase between the worst-misload scenario and the as-loaded configuration for the MPC-68Ms at Fitzpatrick (calendar year 22,000).	H-20
Figure H-26. k_{eff} vs. calendar year for the loss-of-neutron-absorber scenario based on actual loading and disposal isotopes for the SNF canisters at Waterford.	H-21
Figure H-27. k_{eff} vs. NaCl concentration for the DPCs with $k_{eff} > 0.98$ for the canisters analyzed at Waterford under the NA scenario (calendar year 22,000).	H-21
Figure H-28. k_{eff} increase between the worst-misload scenario and the as-loaded configuration for the MPC-32s at Waterford (calendar year 22,000).	H-22
Figure H-29. k_{eff} vs. calendar year for the NA scenario based on actual loading and disposal isotopes for the SNF canisters at Perry.	H-23
Figure H-30. k_{eff} increase between the worst-misload scenario and the as-loaded configuration for the MPC-68s at Perry (calendar year 22,000).	H-23
Figure H-31. k_{eff} vs. calendar year for the loss-of-neutron-absorber scenario based on actual loading and disposal isotopes for the SNF canisters at Farley.	H-24
Figure H-32. k_{eff} vs. NaCl concentration for the DPCs with $k_{eff} > 0.98$ for the canisters analyzed at Farley under the NA scenario (calendar year 22,000).	H-25
Figure H-33. k_{eff} increase between the worst-misload scenario and the as-loaded configuration for the MPC-32s at Farley (calendar year 22,000).	H-25

Figure H-34. k_{eff} vs. calendar year for the loss-of-neutron-absorber scenario based on actual loading and disposal isotopes for the SNF canisters at Indian Point.	H-26
Figure H-35. k_{eff} vs. NaCl concentration for the DPCs with $k_{eff} > 0.98$ for the canisters analyzed at Indian Point under the NA scenario (calendar year 22,000).....	H-27
Figure H-36. k_{eff} increase between the worst-misload scenario and the as-loaded configuration for the MPC-32s at Indian Point (calendar year 22,000).....	H-27
Figure H-37. k_{eff} vs. calendar year for the loss-of-neutron-absorber scenario based on actual loading and disposal isotopes for the SNF canisters at Comanche Peak.	H-28
Figure H-38. k_{eff} vs. NaCl concentration for the DPCs with $k_{eff} > 0.98$ for the canisters analyzed at Comanche Peak under the NA scenario (calendar year 22,000).	H-29
Figure H-39. k_{eff} increase between the worst-misload scenario and the as-loaded configuration for the MPC-32s at Comanche Peak (calendar year 22,000).	H-29

TABLES

Table 1. 18 node axial burnup profiles as a function of discharge burnup	6
Table 2. Isotope set—actinides + 16 fission products.....	7
Table 3. Representative Rancho Seco DPC (NUHOMS-FC24P-P03) loading map (Service date: 07-19-2001)	22
Table 4. Calculated degraded absorber k_{eff} for the MY DPC with design basis fuel	22
Table 5. Final MY DPC statistics in the year 9999.....	24
Table 6. Type and number of DPCs in the CY ISFSI.....	25
Table 7. Calculated degraded absorber k_{eff} for the CY DPC with design basis fuel	26
Table 8. Final CY DPC statistics in the year 9999	27
Table 9. Calculated k_{eff} s for the RS degradation scenarios with design basis fuel.....	28
Table 10. Final RS statistics in the year 9999.....	32
Table 11. Calculated degraded absorber k_{eff} for the TJ DPC with design basis fuel.....	33
Table 12. Final TJ statistics in the year 9999.....	33
Table 13. Calculated degraded absorber k_{eff} for the SQ DPC with design basis fuel.....	34
Table 14. Final SQ statistics in the year 9999.....	35
Table 15. Reactivity reduction from the components for SQ DPCs with loss of neutron absorber.....	38
Table 16. Analyses summary	40
Table A-1. Principal set of isotopes for burnup credit post-closure criticality analysis	A-4
Table A-2. Number of DPCs above subcritical limit with disposal-isotopes and storage- transportation-isotopes in the calendar year 9999	A-6
Table A-3. Calculated degraded absorber k_{eff} for the MPC-HB with design basis fuel	A-7
Table A-4. Summary of DPC As-loaded Criticality Analyses in the Calendar Year 9999	A-9
Table B-1. List of sites and number of loaded DPCs assessed for criticality	B-4
Table B-2. Summary of DPC as-loaded criticality analyses in calendar year 9999	B-5
Table D-1. Final NUHOMS® 32PT-DSC statistics in the year 22,000.....	D-15
Table D-2. k_{eff} as a function of filler height.....	D-16
Table E-1. Summary of the number of canisters meeting the subcritical limit.....	E-15
Table F-1. Chemical composition of filler materials.	F-9
Table F-2. Summary of the number of canisters meeting the subcritical limit.....	F-28
Table G-1. Summary of Sites Analyzed in FY21.	G-31
Table G-2. Summary of FY21 DPC reactivity assessment results.	G-59
Table G-3. Summary of the number of canisters meeting the subcritical limit.....	G-60
Table H-1. Summary of Sites Analyzed in FY22.	H-2
Table H-2. Summary of FY22 DPC reactivity assessment results.	H-31

Table H-3. Summary of the number of canisters meeting the subcritical limit.H-32

This page is intentionally left blank.

ACRONYMS

2D	two-dimensional
ANA	advanced neutron absorber
ANN	artificial neural network
B&W	Babcock & Wilcox
BPRA	burnable poison rod assemblies
BWR	boiling water reactor
CRA	control rod assembly
CTB	Catawba
CY	Connecticut Yankee Site
DB	degraded basket
DCRA	disposal control rodlet assembly
DFC	damaged fuel can
DOE	US Department of Energy
DPC	dual-purpose canister
DSC	dry shielded canisters
EPRI	Electric Power Research Institute
FEP	features, events, processes
FSAR	final safety analysis report
GWd/MTU	gigawatt-days per metric ton of uranium
HB	Humboldt Bay
ISFSI	independent spent fuel storage installation
ISG	interim staff guidance
MPC	multipurpose canister
MY	Maine Yankee Site
NA	loss of neutron absorber
NE	DOE Office of Nuclear Energy
OFA	optimized fuel assembly
PA	performance assessment
PWR	pressurized water reactor
RS	Rancho Seco
SFP	spent fuel pool
SL	Salem
SNF	spent nuclear fuel*

* Note that the terms *used* and *spent* are used interchangeably by various organizations to describe nuclear fuel that has been irradiated in a nuclear reactor.

SQ	Sequoyah Nuclear Plan
STD	standard assembly
UMS	universal MPC system
UNF	used nuclear fuel*
UNF-ST&DARDS	UNF-Storage, Transportation & Disposal Analysis Resource and Data System
WABA	wet annular burnable absorbers

SPENT FUEL AND WASTE SCIENCE AND TECHNOLOGY

DUAL PURPOSE CANISTER REACTIVITY AND GROUNDWATER ABSORPTION ANALYSES

1. INTRODUCTION

The current spent nuclear fuel (SNF) management strategy includes reliance on dry storage. Utilities are meeting their interim storage needs on an individual basis with use of large-capacity dry storage casks, with a current focus on meeting existing storage and transportation requirements, as disposal requirements are not currently available. These casks are commonly known as dual-purpose (i.e., storage and transportation) canisters (DPCs). However, a small percentage of single-purpose (storage only) systems is also being used to meet storage needs. These are included under the “DPC” heading. This report investigates the postclosure criticality safety aspects of DPCs.

Placing large, heavy waste packages containing DPCs into a repository for direct disposal has not yet been implemented domestically or internationally. Therefore, direct disposal of DPCs represents new engineering and scientific challenges. Some of the engineering challenges that have already been addressed include handling and placement, use of ramps vs. shafts, use of hoists, use of transport equipment, and thermal management. Additionally, some studies have been conducted in the past regarding the feasibility of direct disposal from a criticality analysis perspective and have concluded that while possible, demonstrating subcriticality over the disposal time period is a challenge [1,2]. The alternative to direct disposal of DPCs into a repository is to repackage the SNF into different canisters. The direct disposal of DPCs without cutting them open and repackaging is appealing because it could be more cost-effective, reduce the complexity of fuel management operations both in and outside reactor facilities, and result in less cumulative worker dose during interim storage and handling before eventual disposal in a deep geologic repository.

The performance of the neutron absorber material as a function of time inside the canister is a key factor to demonstrating subcriticality. The neutron absorber panel material used in the majority of currently loaded DPCs is Boral[®]. Boral[®] is composed of B₄C particles and alloy 1100 aluminum that are hot rolled together to form a neutron-absorbing core. The neutron-absorbing core is then bonded to two outer layers of alloy 1100 aluminum. Various corrosion tests have been performed on this material because it is used in existing casks and in spent fuel pools (SFPs). Some of the corrosion tests were conducted under pool chemistry conditions and showed a 0.28 mil-per-year rate of cladding material loss, which equates to about a 40-year service (in the presence of water) life before degradation of the neutron-absorbing core. [1] Additionally, some tests of Boral[®] under simulated vacuum drying processes have shown the formation of blisters within the Boral[®] induced by the drying process. [3] Considering that the repository periods of interest are expected to be at least 10,000 years, it is not likely that the Boral[®] neutron absorber will maintain its criticality control function this long if the package cavity is exposed to an aqueous environment.

Within a repository performance assessment (PA), features, events, processes (FEPs), and sequences of FEPs that might affect the repository are examined. Criticality is considered an event within the FEPs nomenclature that has the potential to affect repository performance. Prior to conducting a PA, the FEPs that can affect repository performance are screened for inclusion or exclusion. Based on previous screening criteria, options available for excluding a FEP consisted of a low-probability criterion, a low-consequence criterion, and by regulation. The objective of this report is to provide a baseline assessment

of potential DPC reactivity changes over repository time frames and reactivity suppressing attributes that may be available to assist future FEP screening justifications. Reference [4] describes a comprehensive analysis framework for the evaluation of DPC postclosure criticality risks.

This report assesses potential DPC reactivity changes over repository time frames primarily because of various degradation mechanisms. Note that if water can be excluded from the repository or from entering a package, there would be essentially no potential for criticality. Licensed DPCs are loaded using well-defined assembly loading criteria such as specifications for approved contents in a storage cask system's certificate of compliance. These specifications define limiting (bounding) loading conditions and characteristics for which the DPC's safety analysis report has demonstrated compliance with the applicable regulatory requirements. In practice, because of the diversity in the discharged SNF available for loading (e.g., variations in SNF assembly burnup values, initial enrichments, and discharge date), it is not possible to load a DPC with SNF assemblies that correspond exactly to the limiting licensing conditions. Hence, DPCs are typically loaded with assemblies that satisfy the limiting loading conditions with some amount of unquantified, uncredited safety margin. By leveraging detailed information on the reactor in-service history of the assemblies and cask loadings, more realistic safety margins inherent within each loaded DPC can be determined. These safety margins may compensate for the reactivity increases during disposal time periods. This report examines (1) the uncredited margins associated with actual fuel loading compared with the regulatory licensing limits and (2) the increased reactivity resulting from canister flooding and the associated material and structural changes that can occur as a result of that flooding. As-loaded criticality analyses are performed for DPCs loaded at the decommissioned Maine Yankee (MY), Connecticut Yankee (CY), Rancho Seco (RS), and Trojan (TJ) nuclear power plant sites, as well as the Sequoyah Nuclear Plant (SQ). Additional as-loaded DPCs are evaluated in the appendices of this report. This report also investigates the reactivity impact of various dissolved aqueous species that could be present in the groundwater of a repository. In the main body of this report, generic loading configurations are used to evaluate the reactivity impact of various aqueous species and to determine the most viable aqueous species that could be credited in a licensing application. As-loaded configurations with the most viable aqueous species are then assessed in the appendices of this report. The results of the study presented in this report indicate that DPC disposal criticality safety demonstration could benefit from, and may require detailed canister-specific evaluation and credit for, neutron absorbers present in groundwater. This report is a continuation of the extension of the work presented in Ref. [5], where preliminary as-loaded canister-specific evaluations are documented for the MY and SQ sites. Throughout this report, a vendor-specific storage/transport canister (e.g., multipurpose canister [MPC], dry shielded canister [DSC], or transportable storage canister), is referred to as a DPC.

This report is organized as follows. The literature survey is presented in Sect. 2. Relevant information regarding the analysis codes and methods are provided in Sect. 3. Section 4 presents the groundwater composition studies relative to canister criticality, while Sect. 5 describes the as-loaded criticality assessment for five sites. Finally, Sect. 6 provides the conclusion. Appendix A presents (1) criticality analyses with 29 principal isotopes set recommended for post-closure criticality analysis [4], (2) additional as-loaded DPCs (total 36), (3) reactivity reduction study by groundwater species applied to as-loaded DPCs, and the (4) reactivity impact of filler material applied to as-loaded DPCs. Appendix B contains (1) post-closure criticality results for 16 new sites (total 339 DPCs), and (2) reactivity reduction study by groundwater species (NaCl) applied to as-loaded DPCs at 16 sites. Note that the results in Appendixes A and B supersede all previous results presented to date. A total of 554 canisters have been analyzed and are presented in this report and its appendices. Appendix C presents an assembly misload analysis methodology for as-loaded calculations including a misload evaluation for 99 canisters at three different sites and three different canister models. Appendix D provides post-closure criticality analyses for as-loaded canisters at 5 new sites (60 DPCs), including (1) k_{eff} values for intact and material degradation configurations, (2) reactivity reduction by groundwater species (NaCl) applied to as-loaded canisters, (3) misload analyses assuming worst fuel assembly configuration in an as-loaded canister, and (4) a scoping calculation evaluating filler height requirements to prevent canister criticality due to

complete loss-of-neutron absorber. Appendix E provides post-closure criticality analyses for as-loaded canisters at 5 new sites (92 DPCs), including (1) k_{eff} values for intact and material degradation configurations, (2) reactivity reduction by groundwater species (NaCl) applied to as-loaded canisters, (3) misload analyses assuming worst fuel assembly configuration in an as-loaded canister, and (4) criticality analysis models for the NUHOMS® 61BT-DSC and NUHOMS® 32PTH-DSC canister types. Appendix F provides post-closure criticality analyses for as-loaded canisters at 4 new sites (66 DPCs), including (1) k_{eff} values for intact and material degradation configurations, (2) reactivity reduction by groundwater species (NaCl) applied to as-loaded canisters, (3) misload analyses assuming worst fuel assembly configuration in an as-loaded canister, and (4) calculations to determine the impact on post closure criticality of adding filler material to canisters. Appendix G provides post-closure criticality analyses for as-loaded canisters at 10 new sites (155 DPCs), including (1) k_{eff} values for material degradation configurations, (2) reactivity reduction by groundwater species (NaCl) applied to as-loaded canisters, (3) misload analyses assuming worst fuel assembly configuration in an as-loaded canister, and (4) the analysis of fuel assembly/basket modification concepts and the initial investigation of DPC loading optimization while considering criticality as a criterion. Appendix H provides post-closure criticality analyses for as-loaded canisters at 14 new sites (225 DPCs), including (1) k_{eff} values for material degradation configurations, (2) reactivity reduction by groundwater species (NaCl) applied to as-loaded canisters, and (3) misload analyses assuming worst fuel assembly configuration in an as-loaded canister.

2. REVIEW OF LITERATURE

Reference [1] documents work performed by the Electric Power Research Institute (EPRI) to examine the feasibility of directly disposing DPCs. For this work, two loaded MPC -32s were selected with assembly average burnup between approximately 30 gigawatt-days per metric ton of uranium (GWd/MTU) and 43 GWd/MTU. The MPC-32s were chosen at random from the SQ site, and their reactivity was examined given the fuel inventory under the assumption of fully degraded neutron absorbers but with the canister otherwise intact. The study used three different sets of burnup credit isotopes containing 5, 6, and 16 most important fission products with respect to fuel reactivity, respectively. Each of the sets of isotopes was evaluated at 5 years of cooling time. In addition to examining the as-loaded reactivity of the canisters, the study also analyzed the potential reactivity-suppressing effects of adding used burnable poison rod assemblies (BPRAs), surrogate control rods, and the use of alternative loading patterns in future canister loadings.

The EPRI study concluded that crediting the five most important fission products with respect to fuel reactivity was insufficient to show that the two canisters in question were subcritical; however, it showed that the canisters were marginally acceptable for disposal conditions by including the six most important fission products ($k_{eff} \sim 0.995$). The study also showed that there is significant uncredited margin even when accounting for the 16 fission products when compared with the full inventory of fission products in the lattice code used in the study. Additionally, the study also showed a 2% Δk_{eff} decrease for modeling the used BPRAs in the canister.

This page is intentionally left blank.

3. CODES AND METHODS

Taking credit for the reduction in reactivity that results from fuel burnup is commonly referred to as *burnup credit*. Burnup credit criticality safety analysis for SNF in storage systems requires the determination of isotopic number densities for fuel assemblies by applying assembly-specific irradiation histories, commonly known as a *depletion calculation*. A depletion calculation is followed by a canister criticality evaluation which uses the isotopic number densities of the fuel from the depletion step to determine the neutron multiplication factor, k_{eff} (also referred to as reactivity in this report). Both of these calculations—depletion and criticality—require different tools and methods to complete.

Various modules of the SCALE [6] code system are employed for the criticality analyses presented in this paper. The TRITON two-dimensional (2D) depletion sequence is used to perform depletion calculations that generate cross section libraries for generic assembly/reactor-specific classes and a range of fuel operating conditions. This information can subsequently be used by ORIGEN-ARP for rapid processing of problem-dependent cross sections. The TRITON 2D depletion calculation sequence employs CENTRM for multigroup cross section processing, NEWT for 2D discrete-ordinates transport calculations, and ORIGEN-S for depletion and decay calculations. The resultant nuclide concentrations are passed to the criticality analysis codes. The SCALE CSAS6 criticality analysis sequence is used to perform criticality calculations for a loaded fuel cask using the KENO-VI Monte Carlo code with the continuous-energy ENDF/B-VII cross section library to determine the effective neutron multiplication factor, k_{eff} . Note that a pre-released version of SCALE 6.2, which is under development, is used for decay and continuous-energy criticality calculations.

The computational analysis of site-specific DPCs is evaluated by employing a comprehensive and integrated data and analysis tool—UNF-Storage, Transportation & Disposal Analysis Resource and Data System (UNF-ST&DARDS)—which is being developed at Oak Ridge National Laboratory [7] through a collaborative effort between multiple national laboratories and industry participants. UNF-ST&DARDS employs the depletion, decay, and criticality analysis modules discussed previously. Although the groundwater study uses the criticality models developed within UNF-ST&DARDS, the models are executed separately.

Reference [8] documents the UNF-ST&DARDS detailed depletion calculation methodology, including the template generation scheme. Bounding irradiation parameters [8], which are intended to estimate the upper limit of the neutron multiplication after discharge, are used in this report.

Reference [9] reports the UNF-ST&DARDS criticality model development activity with detailed model description. Criticality calculations are performed applying 18 node bounding axial burnup profiles for assemblies. Additionally, 12 actinides and 16 fission products are credited in the criticality analyses as described in Sect. 3.2.

The major conservative assumptions applied to the criticality evaluation are as follows.

- Depletion: Bounding depletion conditions are employed for the SNF isotopic composition determination including the burnable poison rod to be inserted in the fuel assembly guide tubes throughout the irradiation time.
- Criticality: Control elements (control rod assemblies, BPRAs, etc.) are not conservatively considered in the criticality calculations except for SQ. A conservative approach, as described in Sect. 5.6, is employed for the SQ as-loaded DPCs to account for the water displacement aspect of the control elements. Burnup is not credited for damaged fuels in the damaged fuel cans (DFCs). Instead, the canister's design basis assembly or bounding assembly for the DFC, as determined in the final safety analysis report (FSAR), is modeled for damaged fuel. However, high burnup (> 45 GWD/MTU) assemblies in a DFC (e.g., MY) are modeled as intact with

accumulated burnup. As described below, bounding axial burnup profiles are used for the criticality calculations.

Therefore, the criticality analyses documented in this report are expected to be reasonably conservative.

3.1 Axial Burnup Profile

The axial burnup distribution is an important factor in determining the reactivity of fuel at a given average burnup. For example, two fuel assemblies with the same initial enrichment and average burnup could yield different reactivity levels depending on the axial burnup profiles of the assemblies at discharge. Reference [10] provides a set of bounding profiles based on the statistical analysis of 3,169 axial profiles taken from plant operating data covering 106 cycles of operation. Bounding axial burnup profiles, as shown in Table , are implemented through UNF-ST&DARDS and are used in the criticality analysis of PWR fuel. Additionally, Figure 1 illustrates the burnup profiles.

Table 1. 18 node axial burnup profiles as a function of discharge burnup

Axial zone no.	Fraction of active fuel height	Burnup < 18 GWd/MTU	18 ≤ Burnup < 30 GWd/MTU	Burnup ≥ 30 GWd/MTU
1	0.0278	0.649	0.668	0.652
2	0.0833	1.044	1.034	0.967
3	0.1389	1.208	1.15	1.074
4	0.1944	1.215	1.094	1.103
5	0.25	1.214	1.053	1.108
6	0.3056	1.208	1.048	1.106
7	0.3611	1.197	1.064	1.102
8	0.4167	1.189	1.095	1.097
9	0.4722	1.188	1.121	1.094
10	0.5278	1.192	1.135	1.094
11	0.5833	1.195	1.14	1.095
12	0.6389	1.19	1.138	1.096
13	0.6944	1.156	1.13	1.095
14	0.75	1.022	1.106	1.086
15	0.8056	0.756	1.049	1.059
16	0.8611	0.614	0.933	0.971
17	0.9167	0.481	0.669	0.738
18	0.9722	0.284	0.373	0.462

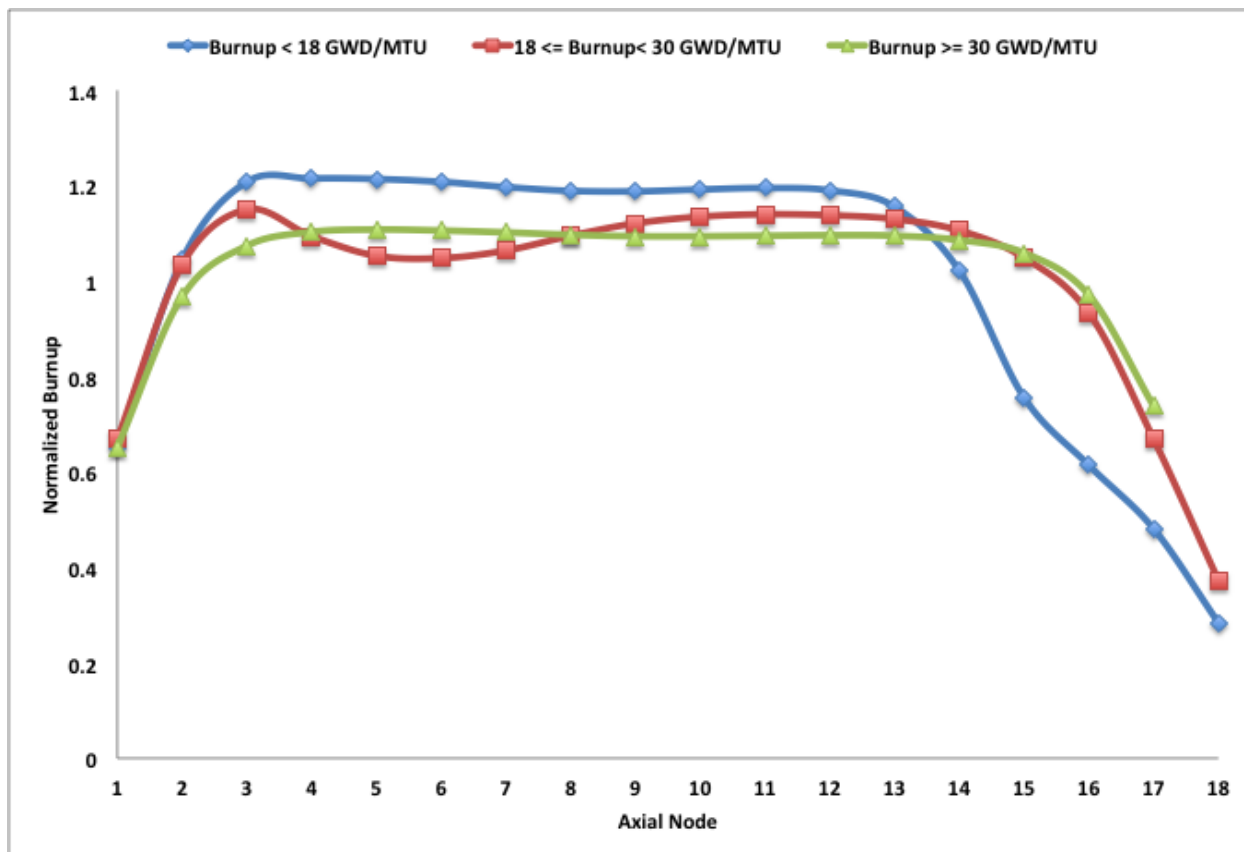


Figure 1. Pressurized-water reactor (PWR) 18 nodes, with 1 being the bottom of the assembly, axial burnup profiles with normalized distribution.

3.2 Isotopes Included in the Criticality Mode

The isotope set credited in the criticality calculations is selected based on the burnup credit isotopes recommended by NUREG/CR-7108 and -7109 [11,12] for SNF storage and transportation. The credited isotopes are listed in Table . This list will be revised in future to match with the principal isotopes provided in Ref. [13] for SNF disposal.

Table 2. Isotope set—actinides + 16 fission products

Actinides					
²³⁴ U	²³⁵ U	²³⁶ U	²³⁸ U	²³⁸ Pu	²³⁹ Pu
²⁴⁰ Pu	²⁴¹ Pu	²⁴² Pu	²⁴¹ Am	²⁴³ Am	²³⁷ Np
Fission products					
⁹⁵ Mo	⁹⁹ Tc	¹⁰¹ Ru	¹⁰³ Rh	¹⁰⁹ Ag	¹³³ Cs
¹⁴³ Nd	¹⁴⁵ Nd	¹⁴⁷ Sm	¹⁴⁹ Sm	¹⁵⁰ Sm	¹⁵¹ Sm
¹⁵² Sm	¹⁵¹ Eu	¹⁵³ Eu	¹⁵⁵ Gd		

3.3 Subcritical Limit

For simplicity, computational biases and uncertainties are not considered in this report. These uncertainties are simply estimated to be 2% (Δk_{eff}), resulting in a subcritical limit of $k_{eff} < 0.98$. Time-

dependent reactivity calculation results are provided for the time range between the calendar years 2001 and 9999 (i.e., approximately 8,000 years). Note that after the initial decrease, reactivity increases gradually from approximately 100 years to 10,000 years and beyond, and it reaches a second reactivity peak. [14] However, the expected reactivity increase between 8,000 years (used in this paper) and the second reactivity peak is not significant (less than $0.005 \Delta k_{eff}$). [14] As mentioned above, UNF-ST&DARDS is employed to carry out the as-loaded criticality analyses. Currently, a database restriction allows UNF-ST&DARDS to perform analyses only up to calendar year 9999. This restriction will be resolved in future to perform automated as-loaded calculations using UNF-ST&DARDS beyond the calendar year 9999.

3.4 Degradation Scenarios

For criticality analysis, it is important to make the assumption that water enters a waste package at some point over the repository time frame. While different geologic settings and material degradation mechanisms might yield a large number of potential configurations, two simplified and potentially conservative configurations are used in this report to assess DPC reactivity changes that may occur over repository time frames:

1. total loss of neutron absorber from unspecified degradation and material transport processes, and
2. loss of the internal basket structure (including the neutron absorber) resulting in elimination of assembly-to-assembly spacing.

In this report, the aforementioned two configurations (degradation scenarios) are analyzed for DPCs flooded with fresh water as well as groundwater with different dissolved aqueous species. Criticality models from Ref. [9] are modified to represent the above two scenarios. The degradation mechanisms for both neutron absorber and basket structure components over repository timeframes are not well understood. However, sufficient information is not currently available to support a basis for assuming the neutron absorber's continued presence in the basket to provide criticality control. Therefore, the reactivity effect of gradual loss of the neutron absorber is also studied in this report. Figure 2 presents the reactivity reduction in terms of negative Δk_{eff} of a 32-assembly PWR canister as a function of ^{10}B areal density in the neutron absorber panels, assuming the DPC is flooded with fresh water. For all the cases, Δk_{eff} for each step is calculated with respect to the k_{eff} corresponding to 0% of the minimum ^{10}B areal density. This 32-assembly canister is the type of canister used in the SQ nuclear power plant. It contains Westinghouse (W) $17 \times 17\text{WL}$ (Lopar design) fuel assemblies. Reference [9] presents the detailed canister model description. The B^{10} areal density study is performed for three uniform canister loadings: 10 GWd/MTU, 20 GWd/MTU, and 30 GWd/MTU assemblies. The study uses 100 years of cooling time in all 32 locations. Consistent with NUREG-1536, [15] DPC licensing evaluations typically credit 75% of the minimum B^{10} areal density. Figure 2 indicates that loss of neutron absorber from the basket up to a certain threshold ^{10}B areal density would not significantly increase reactivity. However, when the loss of neutron absorber from the basket passes the threshold ^{10}B areal density, significant reactivity increase is expected. The actual extent of basket material degradation that must be accounted for should be revisited in the future, when more thorough corrosion data will be available under repository conditions and time frames.

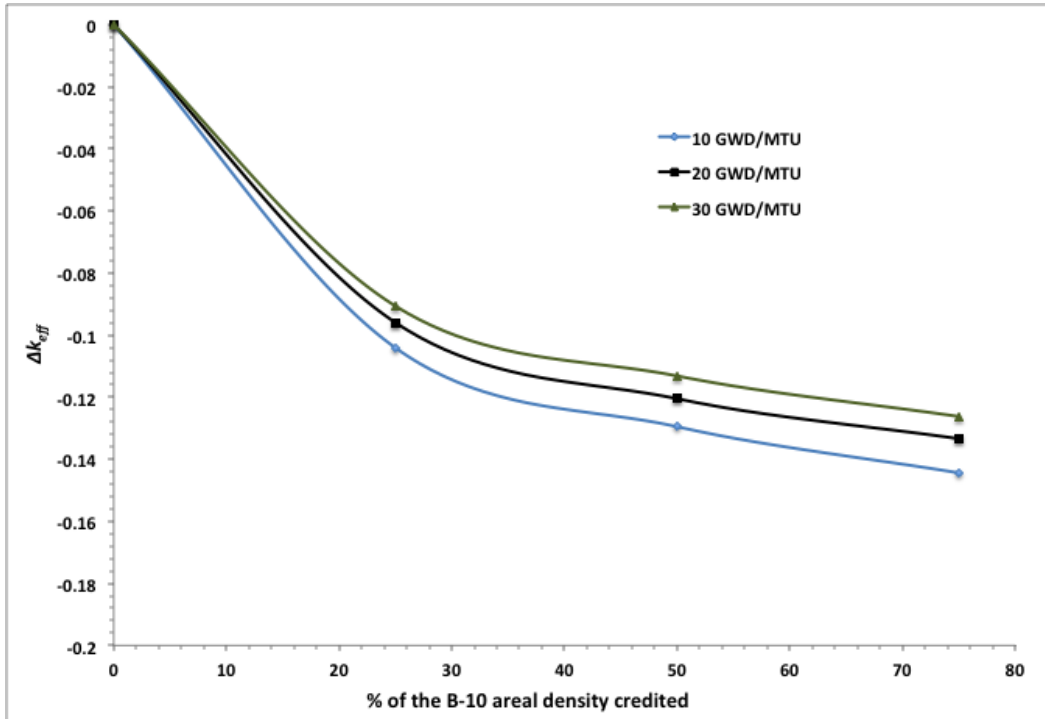


Figure 2. Reactivity impact of B¹⁰ areal density variation.

This page is intentionally left blank.

4. IMPACTS OF GROUNDWATER DISSOLVED AQUEOUS SPECIES

As mentioned previously, water (moderator) is needed to form a critical waste package configuration. However, the groundwater (pore water) that may breach the waste package confinement contains various dissolved aqueous species. The dissolved aqueous species in the groundwater can (1) act as a neutron absorber (e.g., ^{35}Cl and ^6Li), and (2) displace moderating elements (e.g., H). Currently, a location for permanent geologic disposal has not been identified, and hence various geologic options for a repository are under consideration, including crystalline rock, clay/shale, bedded salt, and sedimentary rock, among others [16]. A brief review of available literature [17,18,19] shows that dissolved aqueous species available in the pore water vary widely, depending on the geochemistry of the repository concept. For example, pore water in Opalinus clay contains about 10,000 mg/L (ppm) of Cl, [17] while the Cl content of a salt formation (brine) could be more than 150,000 mg/L. [18] However, it is observed that the following are the most common dissolved aqueous species in various pore water compositions:

- Ca, Li, Na, Mg, K, Fe, Al, Si, Ba, B, Mn, Sr, Cl, S, Br, N, and F.

In the absence of a defined chemical composition of the repository groundwater, the reactivity impact of each dissolved aqueous species is determined by varying the concentration levels over a wide range. Note that in this study, emphasis is given on the neutron absorption characteristics of the dissolved aqueous species. As mentioned in Sect. 3.4, the following two configurations are studied:

1. canister with different amounts of neutron absorber, and
2. canister with complete loss of basket structural components.

These studies are performed using Holtec International's MPC-32. [9] Uniform loading with specified burnup at all locations is assumed. Figure 3 and Figure 4 illustrate the criticality models with varying amounts of neutron absorber and complete loss of basket structures, respectively. The conceptual representation of the loss of basket structure in this section consists of the assembly-to-assembly spacing being reduced uniformly and forming into a close-packed cylindrical geometric configuration. This close-packed configuration increases neutron interaction in the system, which in turn increases system reactivity. The corrosion products from the basket materials are represented as displaced from between the fuel assemblies and flushed from the system.

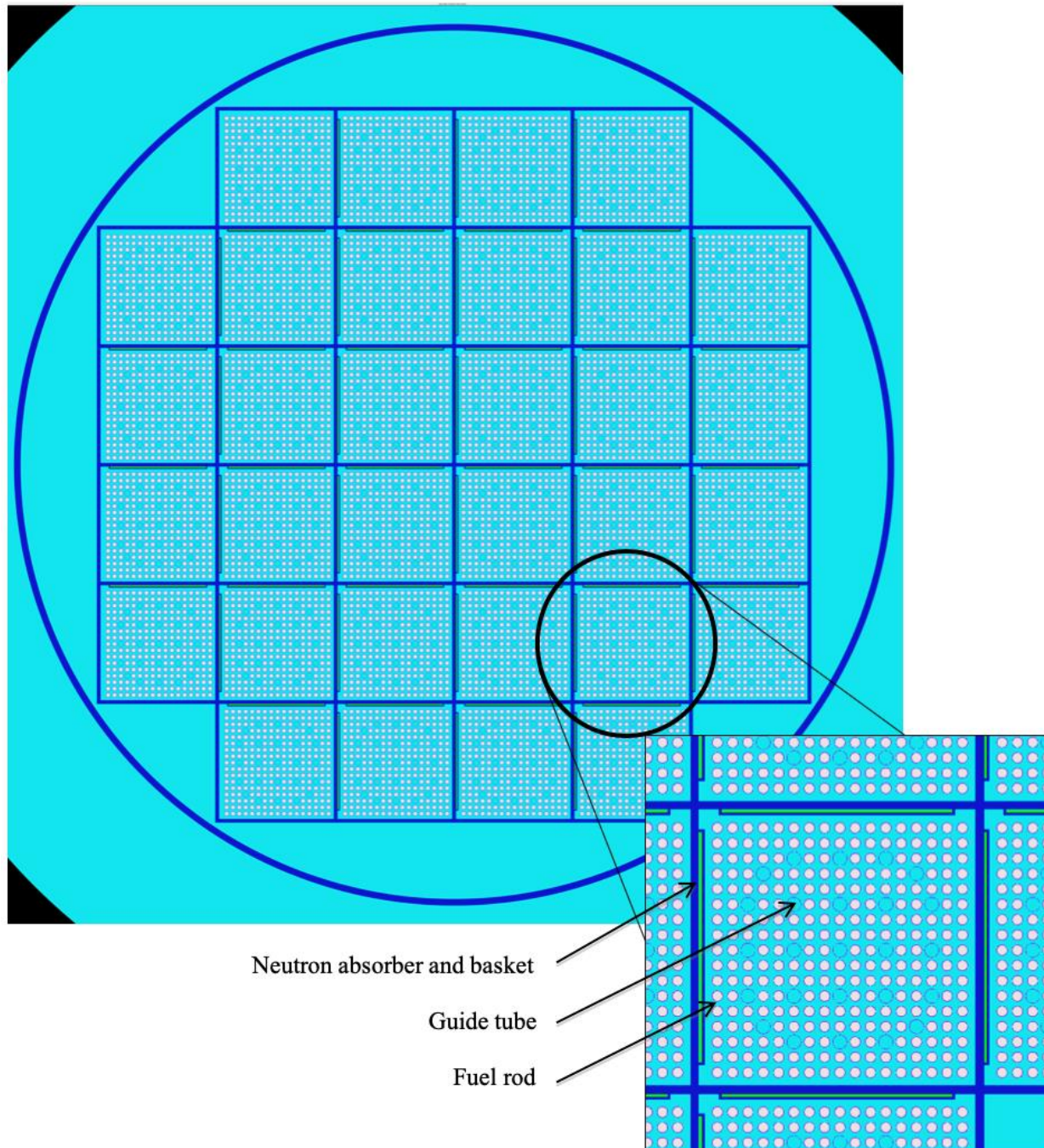


Figure 3. Graphical depiction of the center plane of the MPC-32 KENO model used for groundwater composition studies with varying B^{10} areal density in the neutron absorber panels.

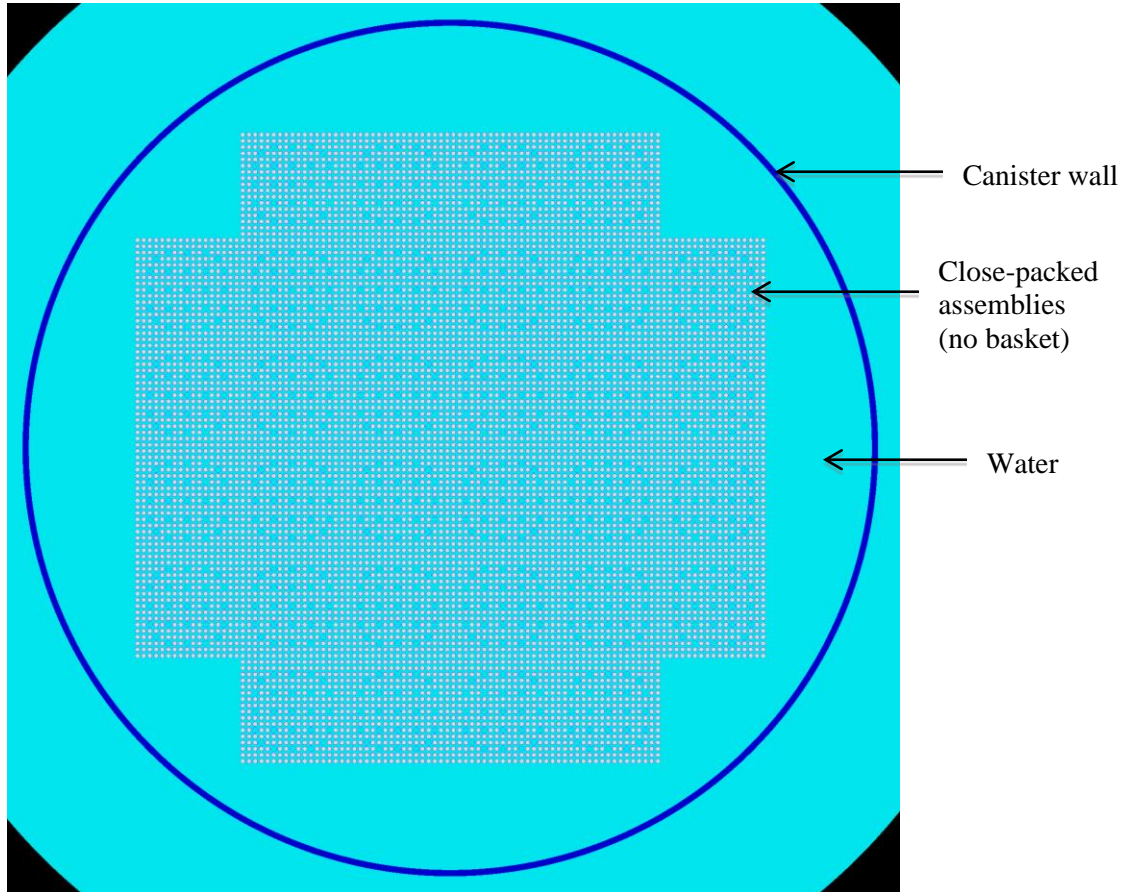


Figure 4. KENO depiction of the MPC-32 degraded basket scenario.

4.1 Groundwater Study Results

Among the dissolved aqueous species listed previously, Cl, Li, and B have the maximum reduction in canister reactivity because of their large neutron absorption cross sections. Figure 5(a) presents the impact of Cl concentration in groundwater on the reactivity of DPCs with different levels of neutron absorber in the basket, while Figure 5(b) illustrates the same for a degraded basket configuration. The negative Δk_{eff} indicates reactivity reduction with respect to the k_{eff} that corresponds to a configuration with fresh water. Similarly, Figure 6 and Figure 7 present the reactivity reduction as a function of Li and B content, respectively, in the groundwater for the two analyzed configurations. For the complete loss of basket (degraded basket), the dissolved aqueous species concentration is varied up to 150,000 ppm because the degraded basket configuration (see Figure 4) is more reactive than the degraded absorber plate configuration (see Figure 3) due to its compact geometry. For the gradual loss of neutron absorber scenario, Li and B concentrations are varied up to 12,000 ppm, while Cl concentration is varied up to 100,000 ppm. Li and B concentrations are varied up to 12,000 ppm for the gradual loss of neutron absorber case because of their potentially limited availability in the groundwater. These plots could be used to determine the reactivity impact (Δk_{eff}) for a specified amount of a dissolved element. For example, 100,000 ppm (mg/L) of Cl in brine provides around -0.20 Δk_{eff} for a configuration with complete loss of neutron absorber and minimum burnup of 10 GWd/MTU, which could be enough to show subcriticality of any perceivable configuration. It is observed that Cl is available in most of the repository concepts under consideration, including salt, clay/shale, granite, and crystalline rock. However, the quantity of available Cl in the groundwater varies widely between geological media. Additionally, currently available groundwater compositions show limited availability of the other important dissolved aqueous species (e.g., Li and B) that can provide any noticeable reactivity impact.

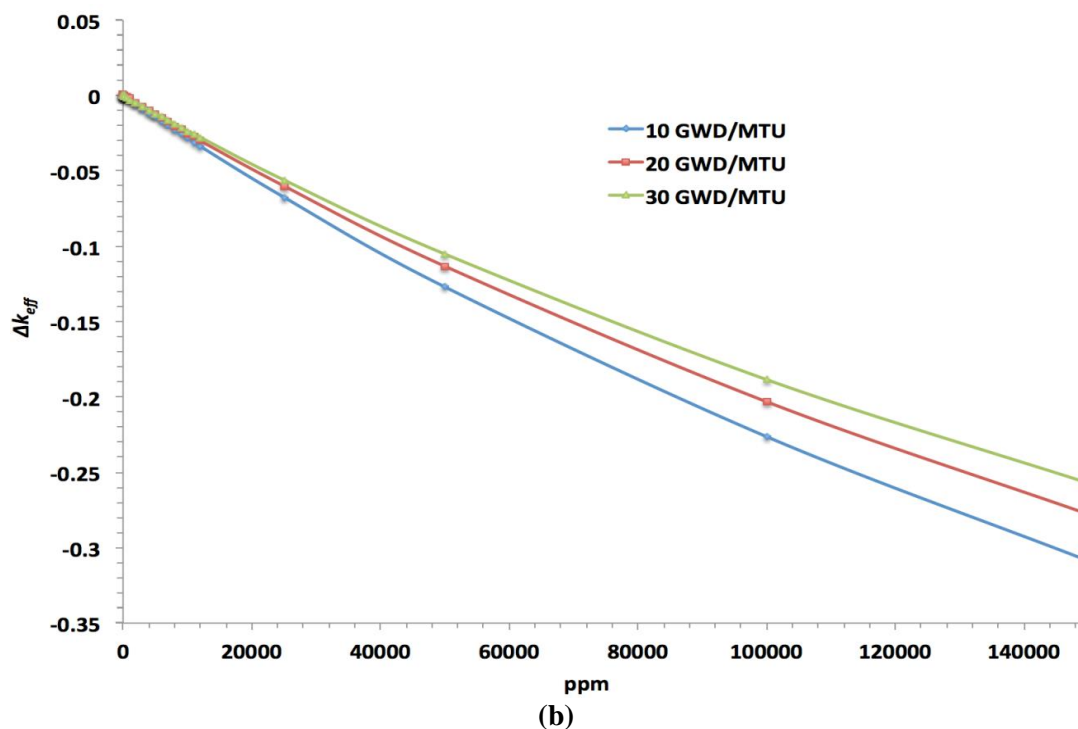
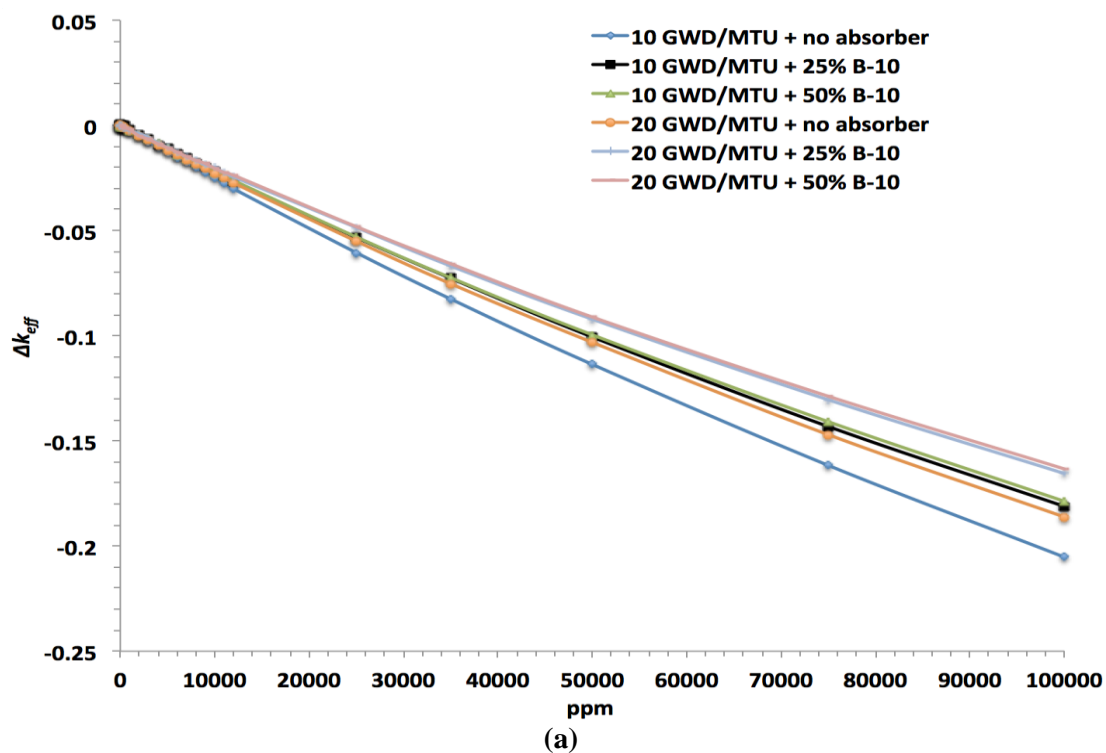


Figure 5. (a) Reactivity impact of Cl concentration in groundwater for different levels of neutron absorber; (b) reactivity impact of Cl concentration in groundwater for degraded basket configuration.

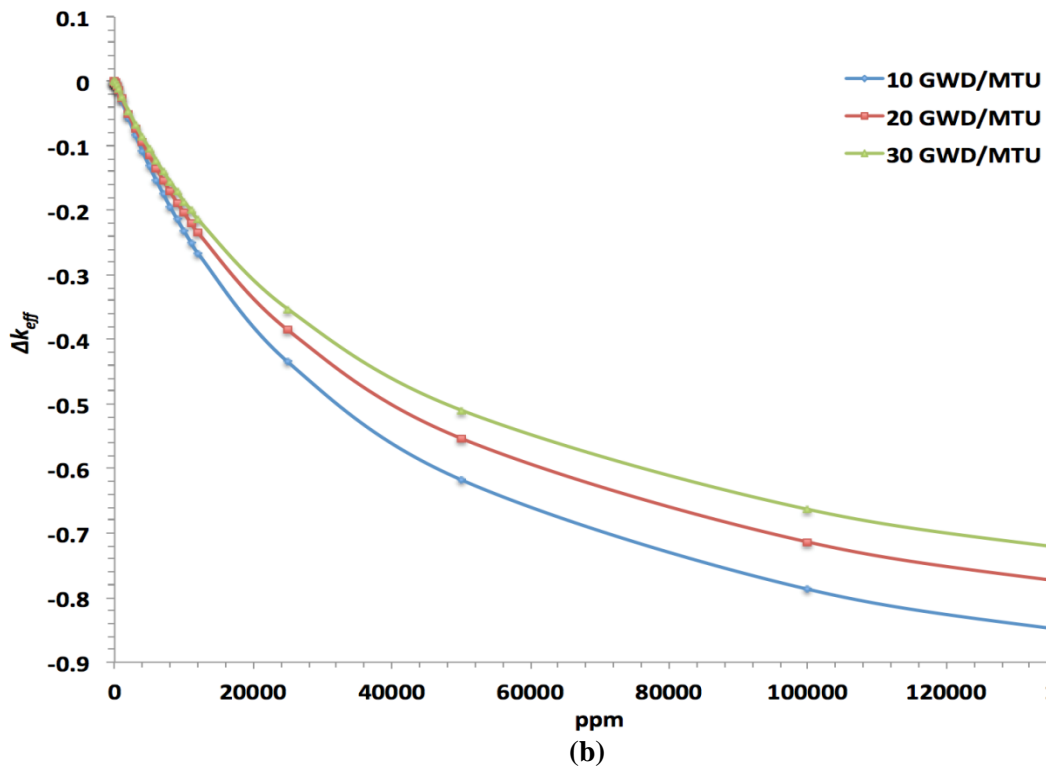
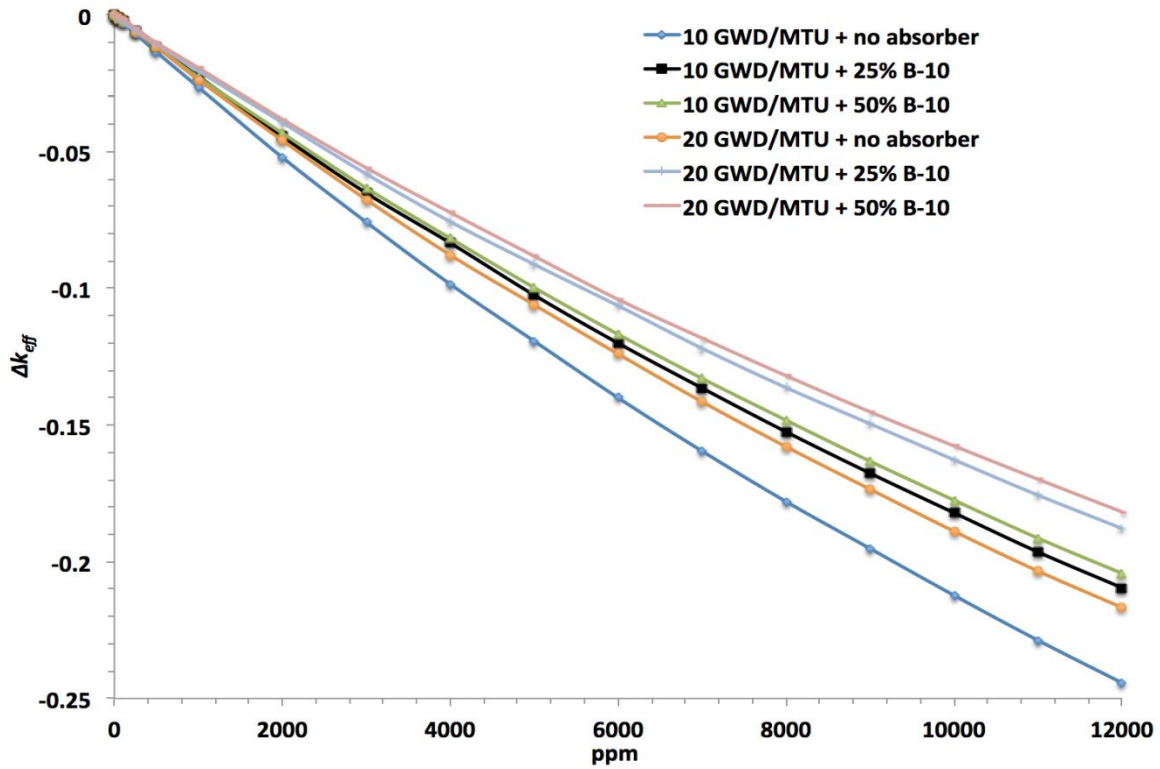


Figure 6. (a) Reactivity impact of Li concentration in groundwater for different levels of neutron absorber; (b) reactivity impact of Li concentration in groundwater for degraded basket configuration.

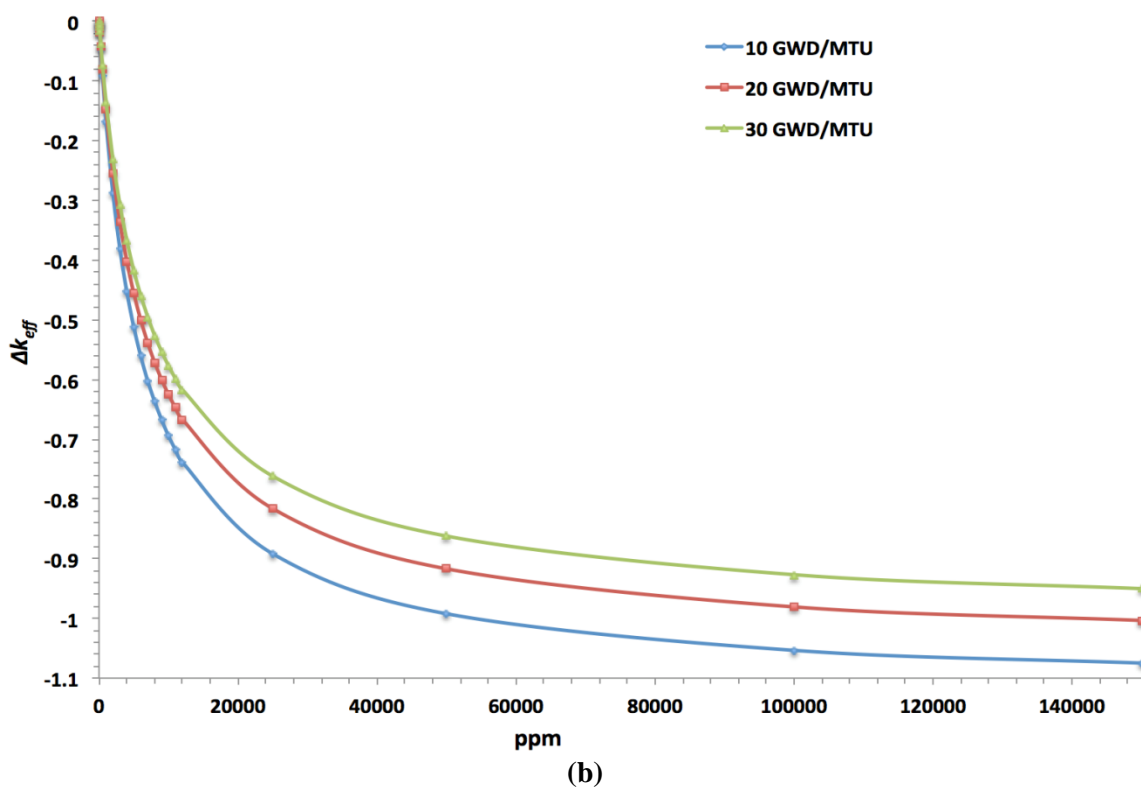
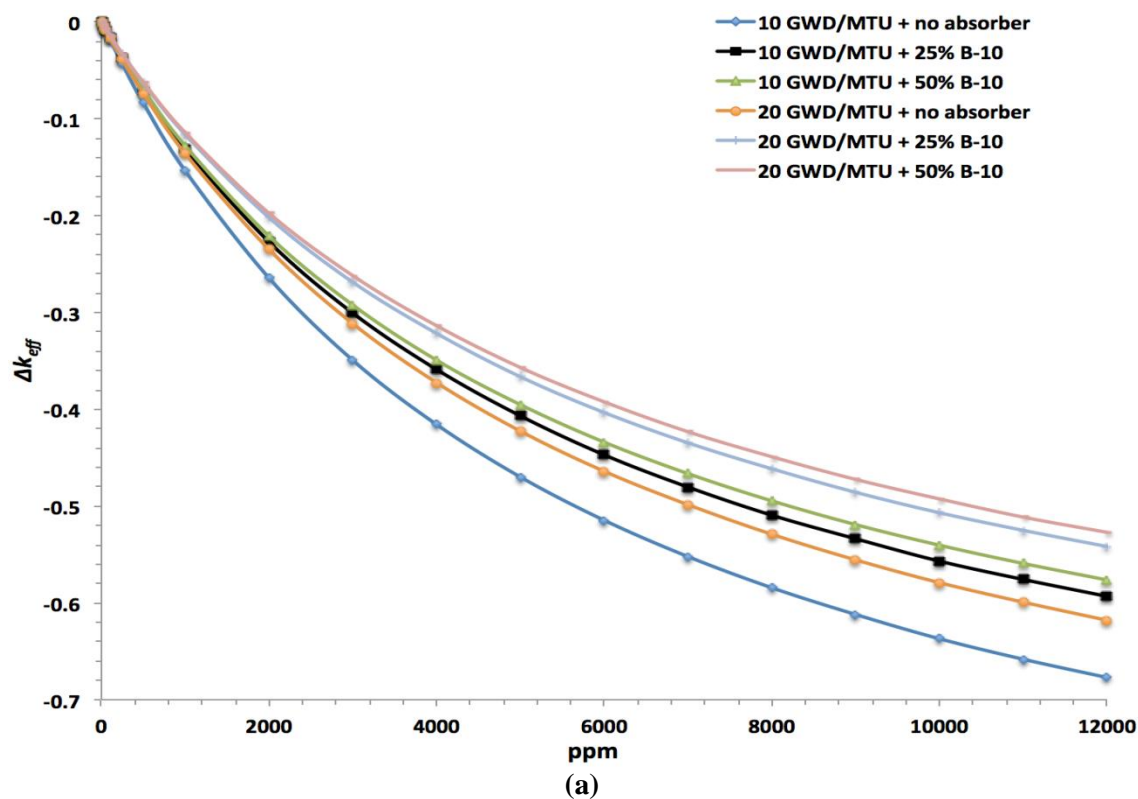


Figure 7. (a) Reactivity impact of B concentration in groundwater for different levels of neutron absorber; (b) reactivity impact of B concentration in groundwater for degraded basket configuration.

It is also observed that Br and Mn offer minor reactivity reduction, while the remaining the dissolved aqueous species (N, Ba, Mg, F, S, Na, K, Sr, Ca, Fe, Al, and Si) do not have any significant impact. The Br and Mn study is presented in Figure 8, while Figure 9 depicts the reactivity changes as functions of the remaining ion concentrations for the two degraded configurations analyzed in this report.

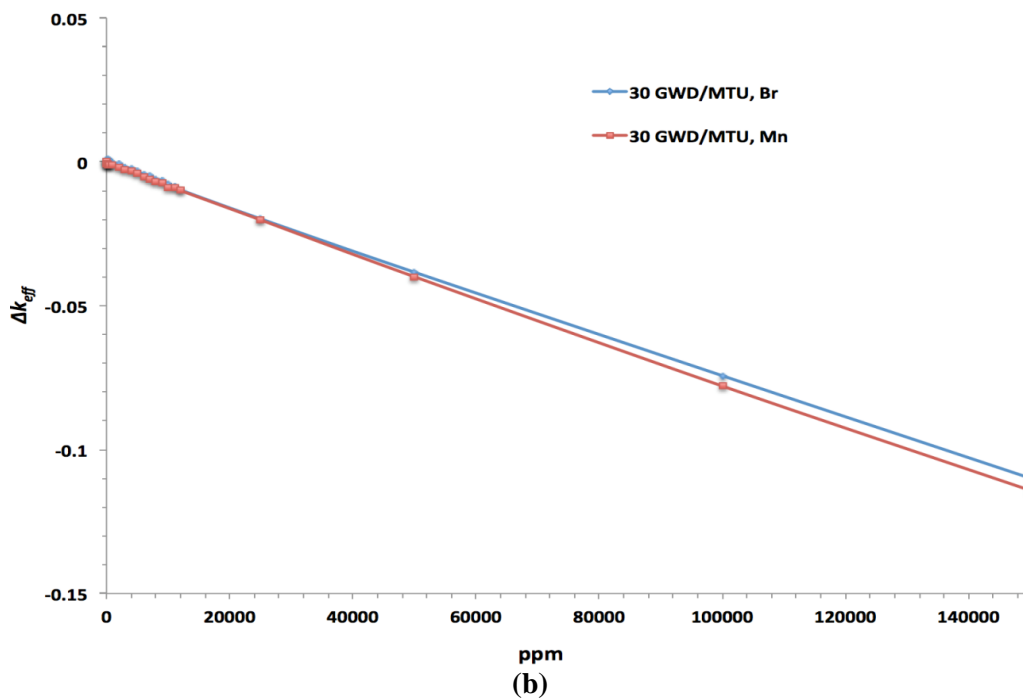
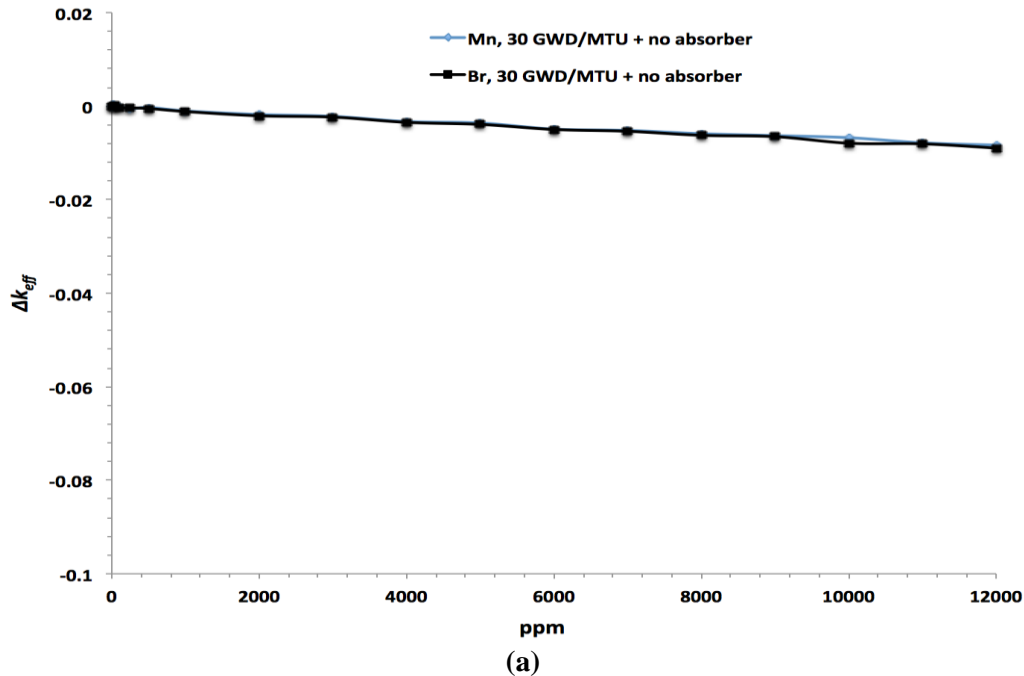


Figure 8. (a) Reactivity impact of Br and Mn concentration in groundwater for complete loss of neutron absorber; (b) reactivity impact of Br and Mn concentration in groundwater for degraded basket configuration.

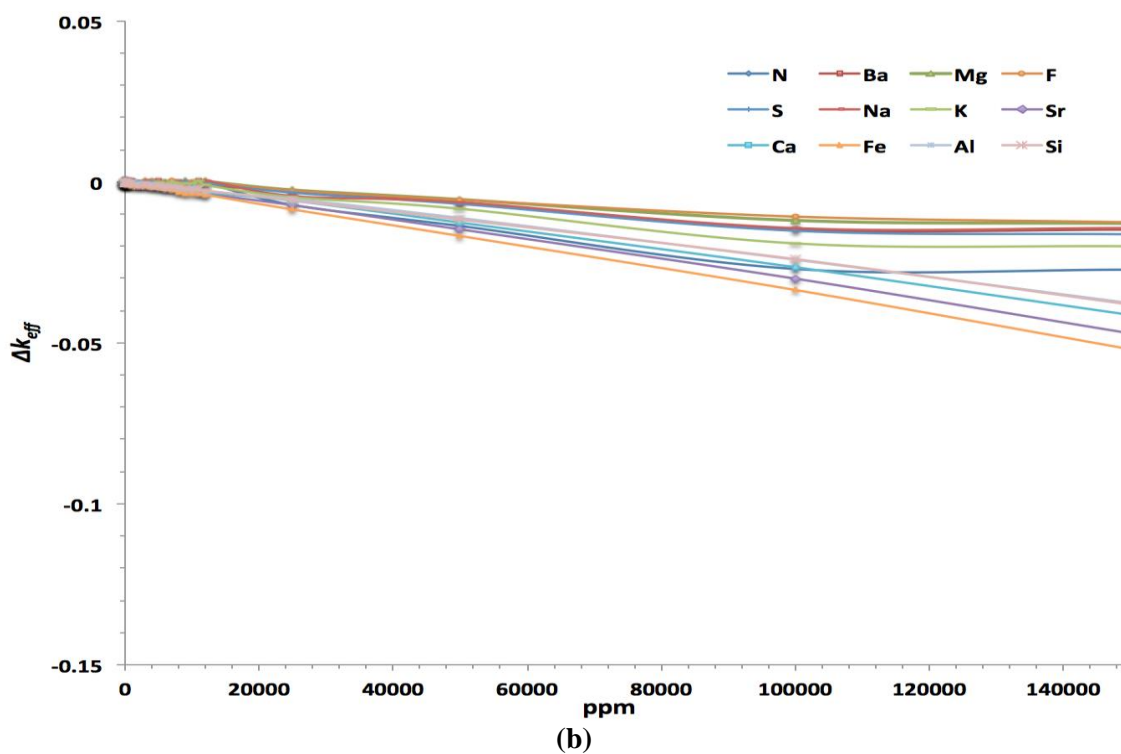
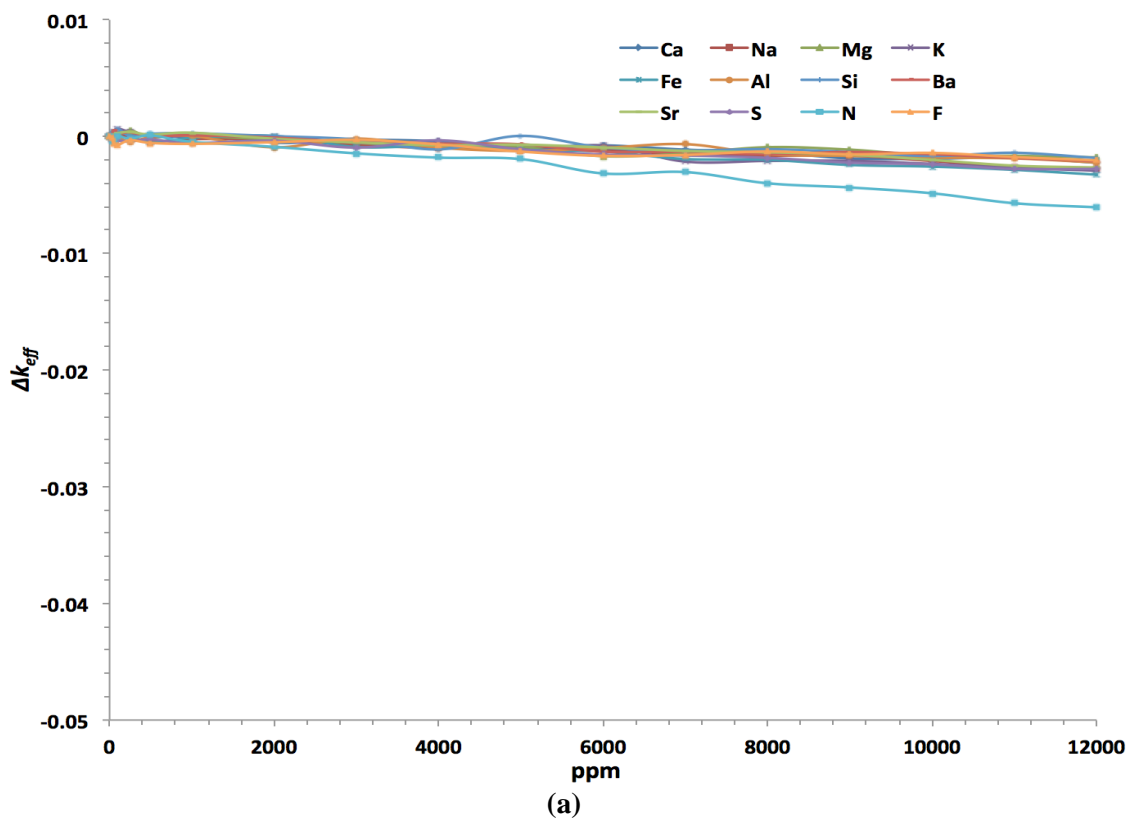


Figure 9. (a) Reactivity impact of the rest of the ions' concentration in groundwater for complete loss of neutron absorber; (b) reactivity impact of the rest of the ions' concentration in groundwater for degraded basket configuration.

4.2 Hypothetical High Reactivity Configuration

A hypothetical high reactivity configuration that includes complete loss of basket structure and loss of lattice arrangement is studied. This configuration is developed for the purpose of using a conservative configuration with high reactivity to estimate the upper limit on the amount of CI that may be needed to maintain subcriticality. Hence, this configuration is not intended to be credible. This scenario consists of intact fuel rods from the fuel assemblies distributed on a triangular pitch within the canister boundary. The following assumptions are used:

1. An MPC-32 loaded with W 17 × 17WL assemblies is employed for this study, and 32 W17 × 17WL assemblies will contain 8,448 intact fuel rods for dispersal in the system. Because the model was simplified to use an infinite hexagonal array of intact fuel rods bounded by the canister boundary, the pitch of the hexagonal array is adjusted to model approximately 8,448 rods (e.g., calculated number of rods for the model used is 8,619) in the canister.
2. Guide tubes are not considered.
3. The fuel rods are modeled as fresh UO₂ fuel with 4 wt% and 5 wt% ²³⁵U enrichment, and also with three uniform burnup distributions of 10, 20 and 30 GWd/MTU.

Although the objective of this study is to estimate the CI requirement for a bounding scenario, a simple modeling approach, as described above, is used in this report. A sensitivity study is not performed to determine the absolute bounding fissile material configuration for the system. Therefore, future sensitivity studies are required to verify the bounding nature of the analysis presented here. Figure 10 illustrates the cross section of the canister with dispersed fuel rods as modeled in KENO, while Figure 11 presents the reactivity as a function of CI concentration for this scenario. A saturated NaCl brine has a concentration of approximately 6 molal (~158,000 ppm 5), which could ensure subcriticality of fresh fuel with 4% enrichment, or irradiated fuel with 5% enrichment and at least 10 GWd/MTU burnup (Figure 11). Because concentrated CI brine would be needed to ensure subcriticality of these cases, the bounding-type approach is suited mainly for DPC disposal in salt.

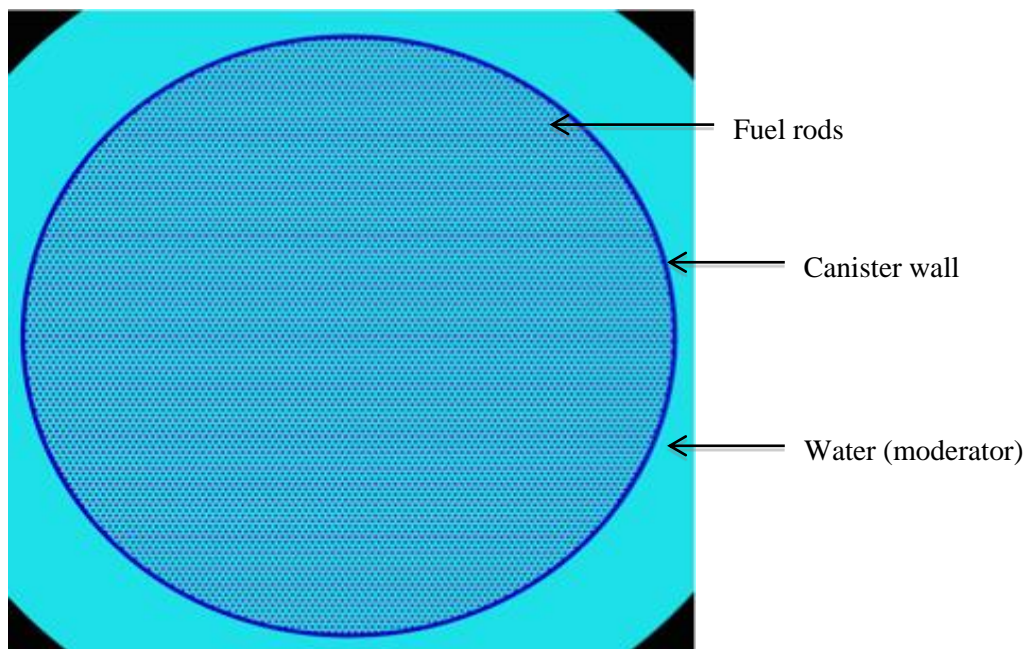


Figure 10. Disintegrated fuel rods configuration as modeled in KENO.

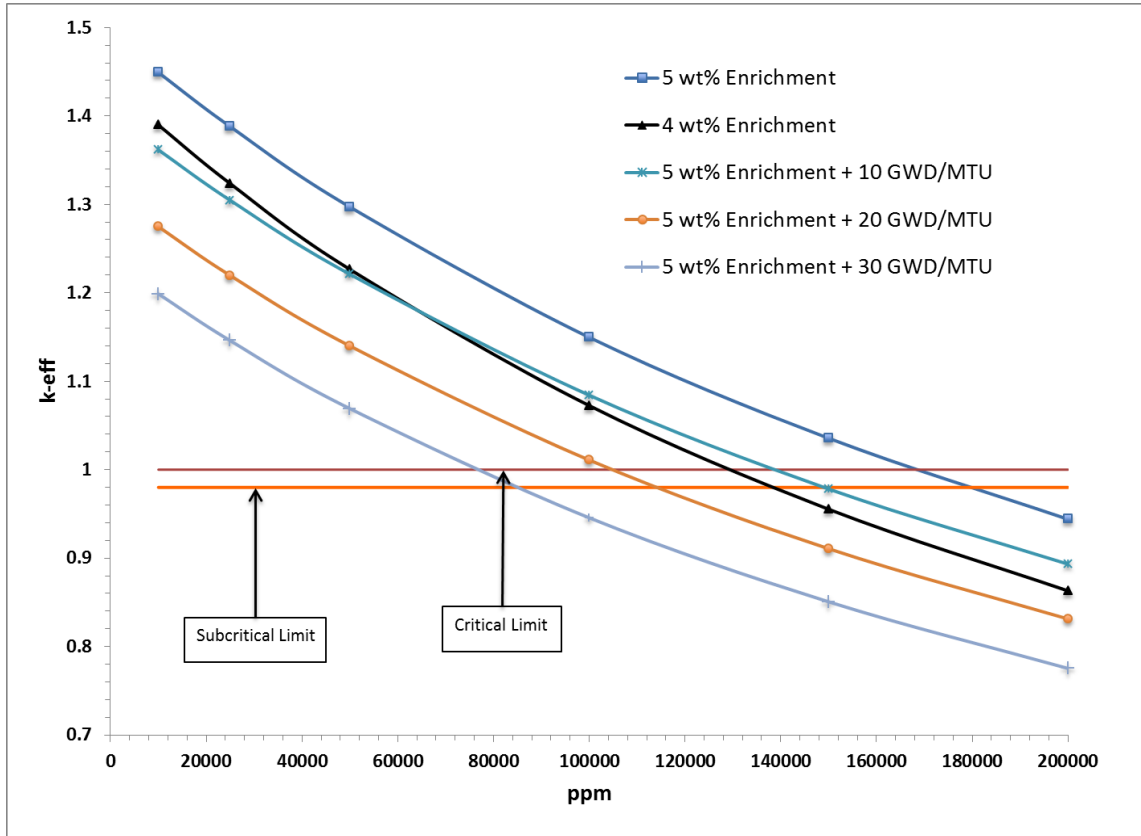


Figure 11. Reactivity impact of Cl concentration in groundwater for high reactivity configuration.

5. ANALYSIS BY APPLYING THE ACTUAL CANISTER-SPECIFIC LOADING

The FSAR for a particular cask system documents the bounding models and calculations used to demonstrate that the system meets the regulatory requirements under all credible and hypothetical conditions (10 CFR 71.55 and 71.73). Note that FSAR calculations and approved content specifications are intended to be bounding in nature to certify cask systems for a variety of fuel characteristics without placing stringent used fuel-loading requirements. Therefore, in general, licensed cask systems possess excess and uncredited safety margins. The calculations performed in this report replicate representative conditions documented in the FSARs to the extent applicable, but with specific as-loaded fuel to determine the inherent uncredited safety margins. This section examines and quantifies these uncredited margins that could offset the reactivity increases because of canister flooding and associated structural changes over the repository time frame. It is assumed that the canister will be flooded with fresh water to produce significant moderation and that neutron absorber materials (panels) and coated carbon steel structural components will be completely degraded and transported away from the system. However, it is considered that the stainless steel structural components will maintain functional integrity over the repository time frame (e.g., 10,000 years). These assumptions should be scrutinized in the future when corrosion data are available to represent the specific disposal environment and time frame. Canisters loaded at five sites are investigated in this section including MY, CY, RS, TJ and SQ.

UNF-ST&DARDS is employed for the as-loaded criticality analyses. UNF-ST&DARDS performs neutronics calculations for each unique assembly design (e.g., Westinghouse 17×17 optimized fuel assembly [OFA] or standard assembly [STD]), initial enrichment and burnup, and decay time of each assembly stored at the different sites, and it generates explicit criticality models of each fuel assembly in its respective loading pattern as identified from canister-specific loading maps. Table 3 presents a typical RS DPC (NUHOMS-FC24P-P03) loading map. In this report, the criticality models are based on nominal dimensions. Additionally, the same criticality model is used for the design basis and as-loaded calculations. In the following subsections, the MY evaluations are described first, followed by the CY, RS, TJ, and SQ criticality analyses.

**Table 3. Representative Rancho Seco DPC (NUHOMS-FC24P-P03) loading map
(Service date: 07-19-2001)**

Assembly ID	Assembly average burnup (MWd/MTU)	Initial enrichment	Assembly location
NJ03GM	10,000	3.062	1
NJ02GF	28,000	3.143	2
1B06	25,397	2.673	3
1B50	25,736	2.676	4
NJ01GZ	32,000	3.21	5
NJ02F8	21,000	3.144	6
NJ030H	20,000	3.19	7
1C07	31,914	2.99	8
1B27	35,360	2.67	9
NJ00DN	38,016	3.2	10
1B14	25,706	2.671	11
1A17	16,998	2.007	12
1C24	29,320	2.998	13
1B54	28,420	2.664	14
NJ00E0	36,545	3.19	15
1C04	35,311	2.993	16
1B20	27,611	2.671	17
NJ03GA	10,000	3.06	18
NJ03FA	10,000	3.056	19
NJ017Y	32,000	3.041	20
NJ016G	34,000	3.041	21
NJ00DH	28,054	3.188	22
NJ0179	24,804	3.042	23
NJ02FN	21,000	3.141	24

5.1 Maine Yankee

The MY Nuclear Power Plant, located at Wiscasset, Maine, began electricity production in 1972 and was closed for operation in 1996. The 1,434 SNF assemblies produced during MY's 25 years of service [20] are stored in 60 NAC, International's universal MPC system (UMS). [21] The UMS canisters (DPCs) used in MY can house up to 24 PWR fuel assemblies. Fuel assemblies inside the DPC are maintained in place by the stainless steel fuel tubes. Neutron absorber sheets are attached on the four sides of the fuel tube. The MY DPC basket components are stainless steel construction; hence, complete loss of neutron absorber is only considered as the potential degradation scenario. Figure 12 illustrates the MY 24-assembly DPC basket without neutron absorber.

The UMS system applies 4.2 wt % enriched Westinghouse 17 × 17 OFA as the design basis. [21] shows the reactivity of the complete loss of neutron absorber scenario with the design basis assembly.

Table 4. Calculated degraded absorber k_{eff} for the MY DPC with design basis fuel

Enrichment (w/o ^{235}U)	Burnup (GWd/MTU)	k_{eff}
4.2	0	1.16584 ± 0.00040

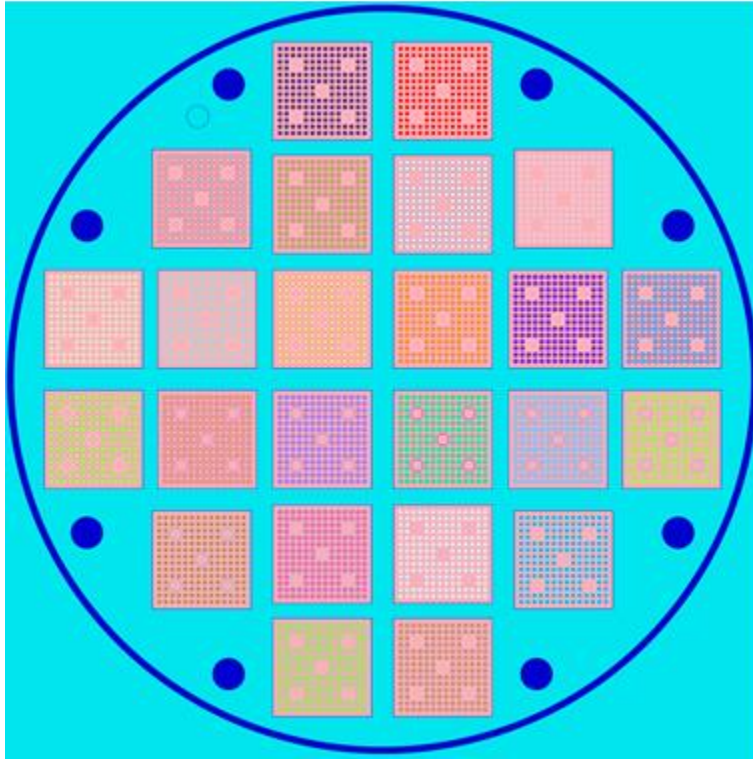


Figure 12. NAC UMS 24-assembly basket without neutron absorber panels as modeled in SCALE.

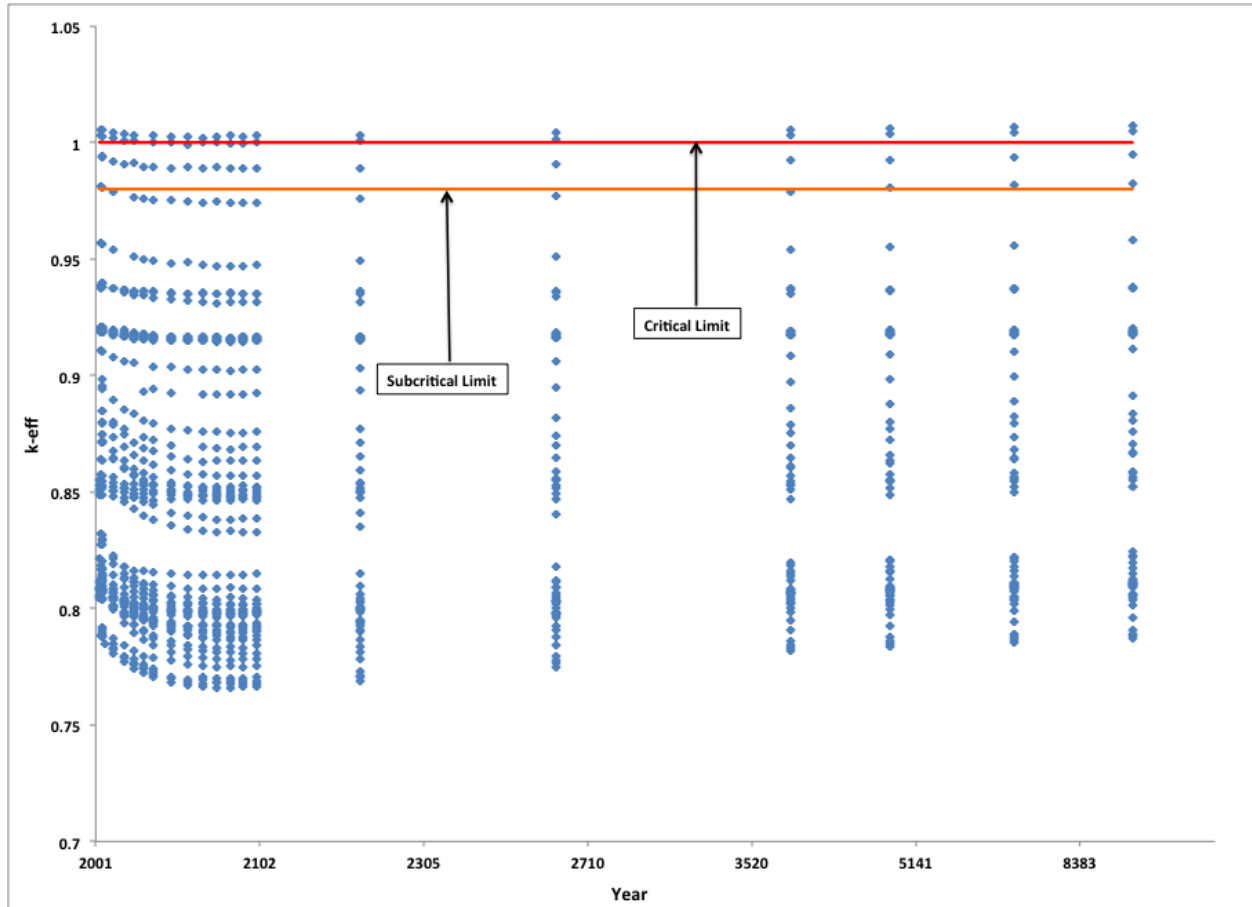


Figure 13. Calculated k_{eff} results for as-loaded MY 24-assembly DPCs with loss of neutron absorber panels.

Figure 13 presents the k_{eff} of the loss of neutron absorber scenario as a function of time. Figure 13 shows that a substantial number of DPCs over the analyzed time period are below the subcritical limit (0.98) defined in this report. This is attributed to the detailed modeling using actinides and fission product burnup credit in conjunction with canister-specific loading. As shown in Table 4, an analysis of this configuration using the design basis fuel assembly for which the DPC has been licensed results in $k_{eff} > 1$ for all the DPCs. Table 5 shows the number of MY DPCs above the subcritical limit and the maximum k_{eff} . Table 5 also reports the approximate amount of Cl required to maintain subcritical condition in the four identified canisters, which are above the subcritical limit with fresh water. The approximate Cl requirement is calculated by linearly interpolating the data presented in Figure 5(a).

Table 5. Final MY DPC statistics in the year 9999

Description	Values
Number of canisters	60
Number of canisters with $k_{eff} > 0.98$ (design basis analysis)	60
Number of canisters with $k_{eff} > 0.98$ (as-loaded analysis)	4
Maximum k_{eff}	1.00696
Approximate Cl requirement (linear interpolation) ^a	13,500 ppm (mg/L)

^a Cl reactivity worth based on a 32-assembly configuration is assumed to be applicable for this DPC.

5.2 Connecticut Yankee

The CY Nuclear Power Plant began electricity production in 1967 and ceased operation in 1996. During CY's ~30 years of electricity generation, 1,019 SNF assemblies [20] were discharged and are now stored in 40 NAC International's CY-MPC. However, the analyses are performed for 39 of the 40 MPCs. The fuel loading information for the canister with serial number 01, which is a 26-assembly basket, is not available at this time. The CY-MPC (DPC) fuel basket is available for both 26 and 24 assembly configurations. These two baskets are identical except that the top weldment of the 24 assembly configuration consists of 24 fuel tube penetrations. [22] The 24 assembly basket is designed to accommodate higher enriched fuel assemblies than the 26 assembly basket. CY baskets are made of stainless steel. Therefore, the potential degradation scenario considered for CY is the loss of neutron absorber panels. Table 6 presents the number of each type of DPC loaded at the CY independent spent fuel storage installation (ISFSI). Figure 14 illustrates the 26 assembly basket without neutron absorber panels, while Figure 15 represents the 24 assembly basket without neutron absorber panels as modeled in SCALE.

Table 6. Type and number of DPCs in the CY ISFSI

CY-MPC configuration	Count
26 assembly	37
24 assembly	3

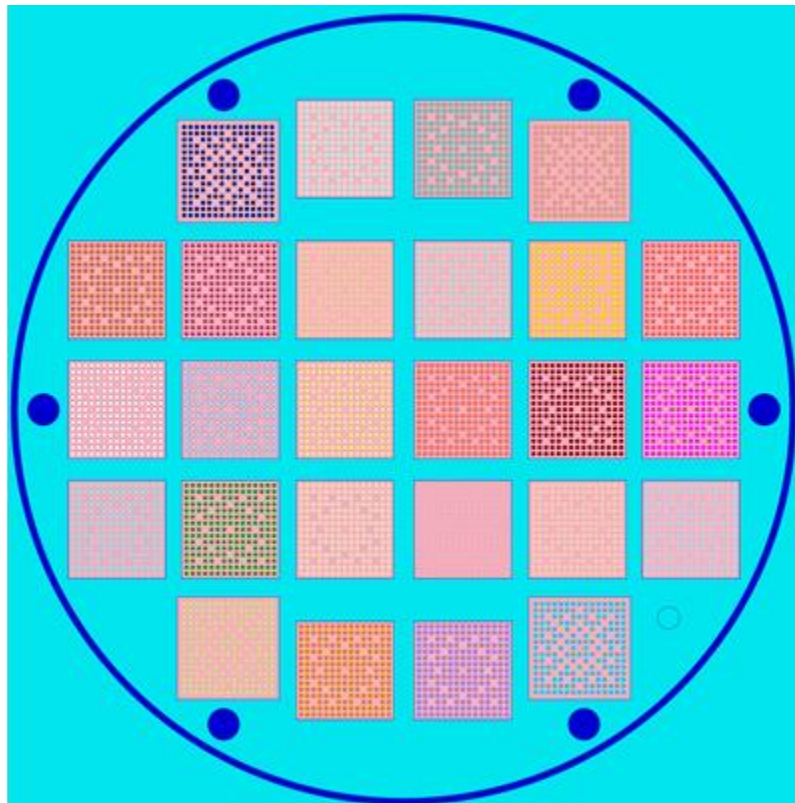


Figure 14. Radial layout of the CY MPC-26 without neutron absorber panels as modeled in SCALE.

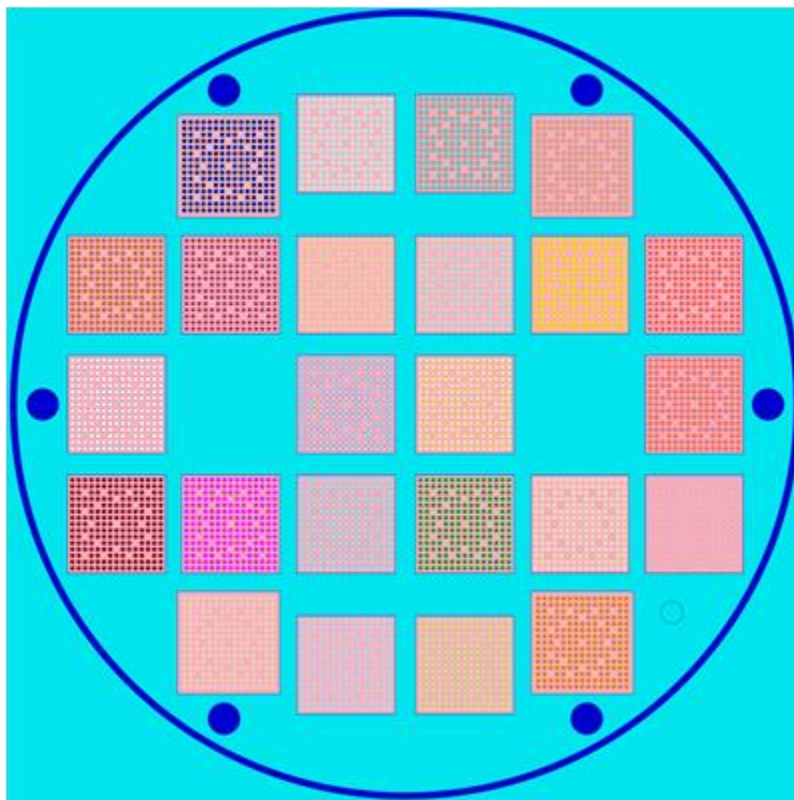


Figure 15. Radial layout of the CY MPC-24 without neutron absorber panels as modeled in SCALE.

CY licensing basis evaluations are performed using unirradiated (fresh) fuel assemblies. The licensing basis fuel assembly characteristics are defined as follows: [22]

- 26 assembly basket:
 - 15 × 15 Zircaloy-clad fuel (Babcock and Wilcox [B&W]) up to 3.93 wt % initial enrichment.
 - 15 × 15 stainless steel-clad fuel up to 4.03 wt % initial enrichment. However, the stainless steel-clad assembly is bounded by the 3.93 wt % Zircaloy-clad fuel.
- 24 assembly basket:
 - 15 × 15 Zircaloy-clad fuel (Westinghouse Vantage 5H) up to 4.61 wt % initial enrichment.
 - Assemblies allowed in the 26 assembly basket.

Table 7 shows the reactivity of the complete loss of neutron absorber scenario with the design basis assembly.

Table 7. Calculated degraded absorber k_{eff} for the CY DPC with design basis fuel

MPC type	Enrichment (w/o ^{235}U)	Burnup (GWd/MTU)	k_{eff}
24 assembly	4.61	0	1.14546 ± 0.00023
26 assembly	3.93	0	1.14809 ± 0.00024

Figure 16 presents the k_{eff} for the loss of neutron absorber scenario as a function of time. Figure 16 shows that majority of the DPCs over the analyzed time period are below the subcritical limit (0.98) defined in this report as a result of the detailed modeling using actinides and fission product burnup credit in

conjunction with canister-specific loading. As shown in Table 7, an analysis of the loss of neutron absorber configuration using the design basis fuel assemblies for which the canisters have been licensed yields $k_{eff} > 1$ for all canisters. Table 8 reports the number of CY DPCs above the subcritical limit and the maximum k_{eff} . Table 8 also shows the approximate amount of CI required to maintain subcritical condition in the three identified DPCs, which are above the subcritical limit with fresh water. The CI requirement is calculated by linearly interpolating the data presented in Figure 5(a).

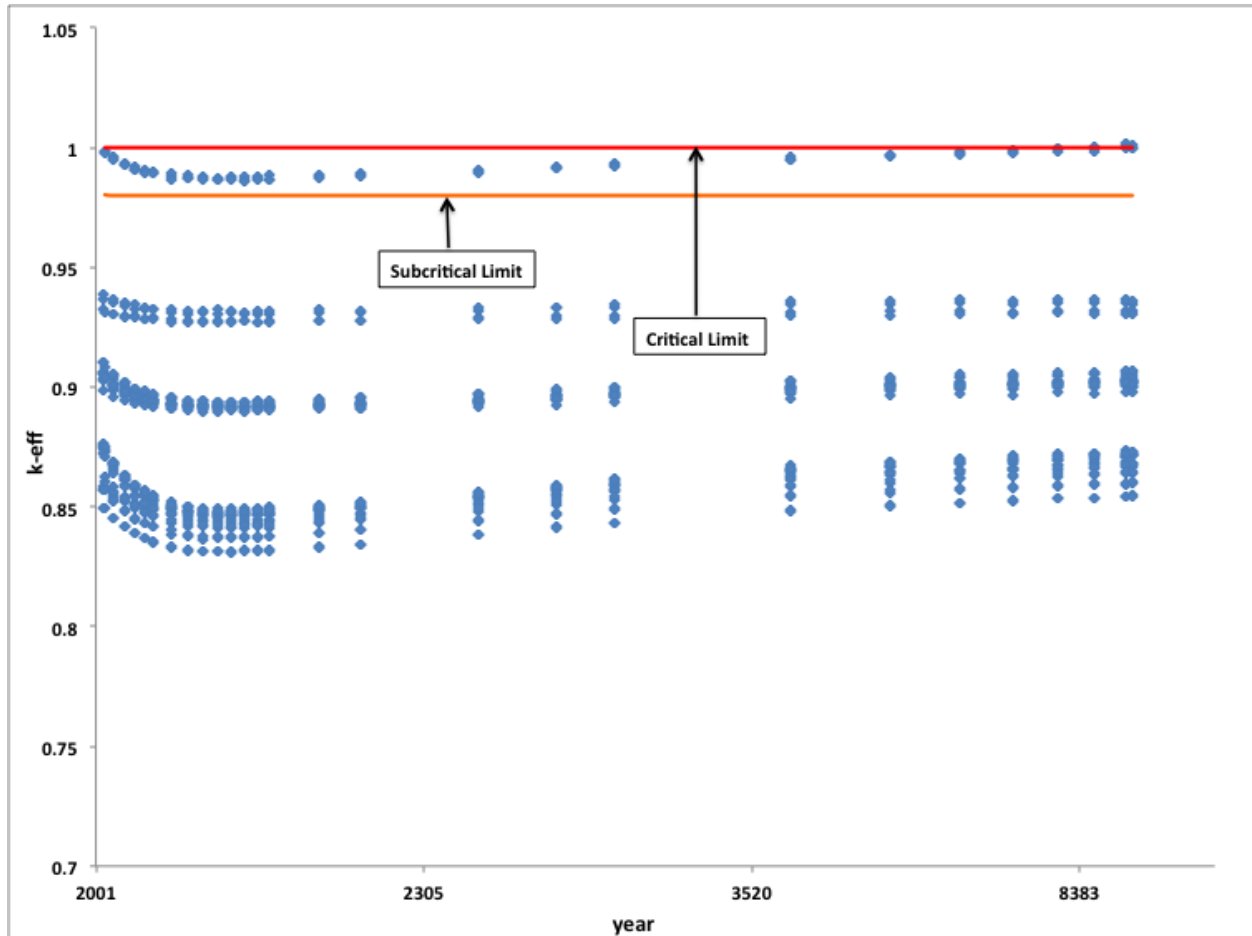


Figure 16. Calculated k_{eff} results for as-loaded CY DPCs with loss of neutron absorber panels.

Table 8. Final CY DPC statistics in the year 9999

Description	Values
Number of canisters	39
Number of canisters with $k_{eff} > 0.98$ (design basis analysis)	39
Number of canisters with $k_{eff} > 0.98$ (as-loaded analysis)	3
Maximum k_{eff}	1.00118
Approximate CI requirement (linear interpolation) ^a	11,000 ppm (mg/L)

^a CI reactivity worth based on a 32 assembly configuration is assumed to be applicable for this DPC.

5.3 Rancho Seco

The Rancho Seco (RS) Nuclear Generation Station, operated by the Sacramento Municipal Utility District, began electricity production in 1975 and ceased operation in 1989. During its nuclear electricity generation lifetime, the plant produced 493 SNF assemblies. [20] These 493 assemblies are stored in 21 NUHOMS dry shielded canisters (DSCs). [23] RS DSCs (DPCs) can accommodate 24 intact PWR assemblies. Design basis criticality analyses are performed applying 3.43 wt % enriched B&W 15 × 15 Mark B4 PWR intact fuel assemblies. [23]

As-loaded criticality calculations are performed for 20 DPCs. One of the DPCs (13 assembly configuration) only stores damaged fuel assemblies. The nature of damage to this fuel is not known sufficiently for criticality analysis, hence crediting burnup for such damaged fuel may lead to non-conservative k_{eff} estimation and is not being implemented at this time. This failed fuel DPC is being treated as the design basis as defined in Ref. [23].

Fuel assemblies inside the DPCs are maintained in place by guide sleeves. Each guide sleeve assembly is made of stainless steel and neutron absorber panels. Neutron absorber panels are attached to the sides of every guide sleeve that faces another guide sleeve. The gaps between the neutron absorber panels facing each other form the flux-trap design. The guide sleeves are arranged inside the canister using axial spacer disks made of coated carbon steel to maintain the flux-trap configuration. Figure 17 illustrates the guide sleeves and the coated carbon steel spacer disk located axially. Because of the carbon steel component present in the DPC, the following two degradation scenarios are considered for RS.

1. Loss of neutron absorber. In this configuration, the neutron absorber is replaced by a moderator (freshwater). It is assumed that the degraded absorber materials are transported away from the canister while the guide sleeves are still in their original positions supported by the spacer disks. This hypothetical configuration could result from the likely situation in which the corrosion-resistant properties of the fuel assemblies, stainless steel guide sleeves, and coated carbon steel spacer disks are superior to that of the neutron absorber. Figure 18(a) depicts the cross section of the canister as modeled in SCALE, while Figure 18(b) presents the k_{eff} as a function of time. Figure 18(b) shows that the k_{eff} values over the analyzed time interval are all substantially below the subcritical limit defined in this report (0.98) using actinides and fission product burnup credit in conjunction with canister-specific loading. However, the design basis k_{eff} for this scenario, presented in Table 9, is greater than 1.
2. Degraded basket. In this case, the loss of neutron absorber configuration is extended to include complete degradation of the coated carbon steel spacer disks, resulting in a close-packed configuration of collapsed guide sleeves. The degraded material is replaced by freshwater. Figure 19(a) illustrates the cross section of the collapsed guide sleeves as modeled in KENO. The results of this analysis are presented in Figure 19(b), which shows that the k_{eff} values associated with some of the DPCs are above the subcritical limit defined in this report. An analysis of this configuration using the design basis fuel, as shown in Table 9, for which the DPC has been licensed results in $k_{eff} > 1$ for all the DPCs.

Table 9. Calculated k_{eff} s for the RS degradation scenarios with design basis fuel

Degradation scenario	Enrichment (w/o ^{235}U)	Burnup (GWd/MTU)	k_{eff}
Loss of neutron absorber	3.43	0	1.09358 ± 0.00024
Loss of neutron absorber and spacer disks	3.43	0	1.27754 ± 0.00019

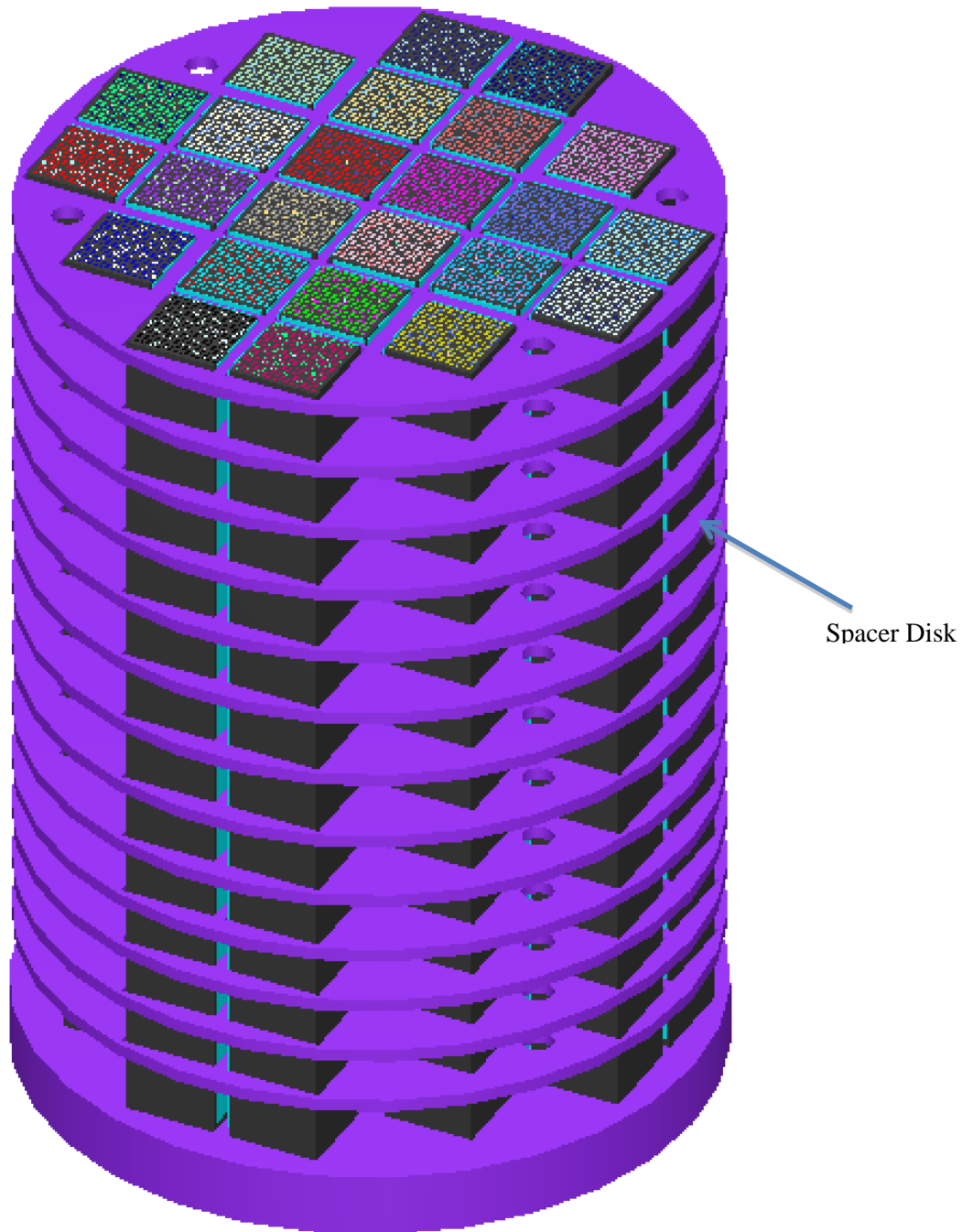
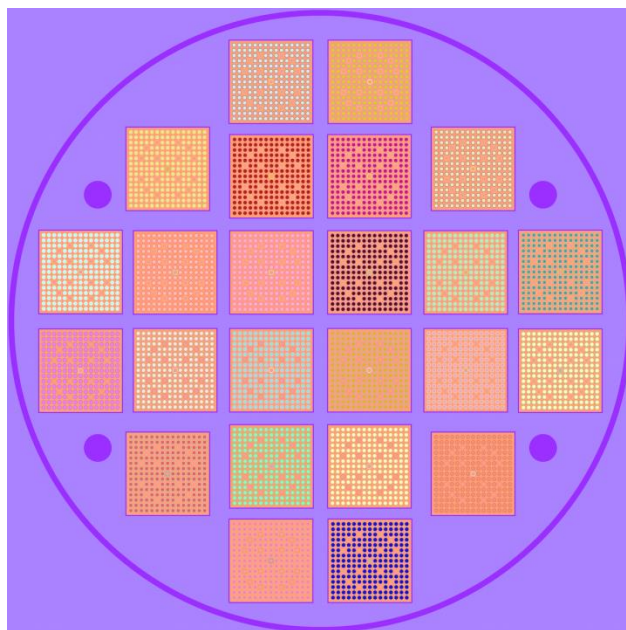
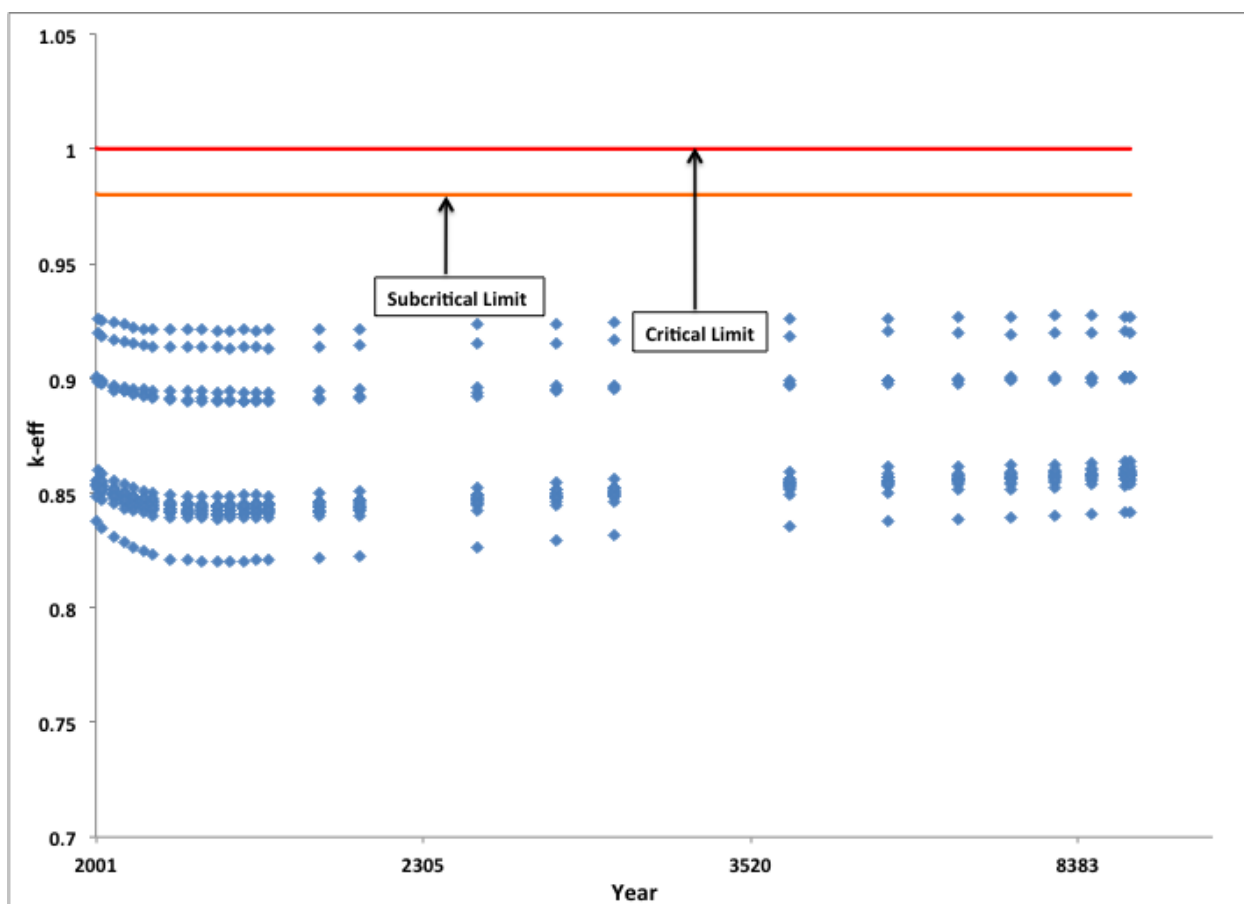


Figure 17. 3D representation of the RS DPC as modeled in SCALE.

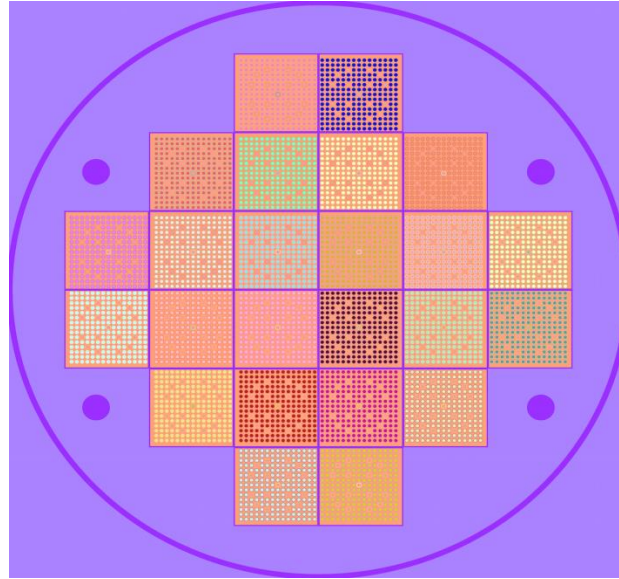


(a)

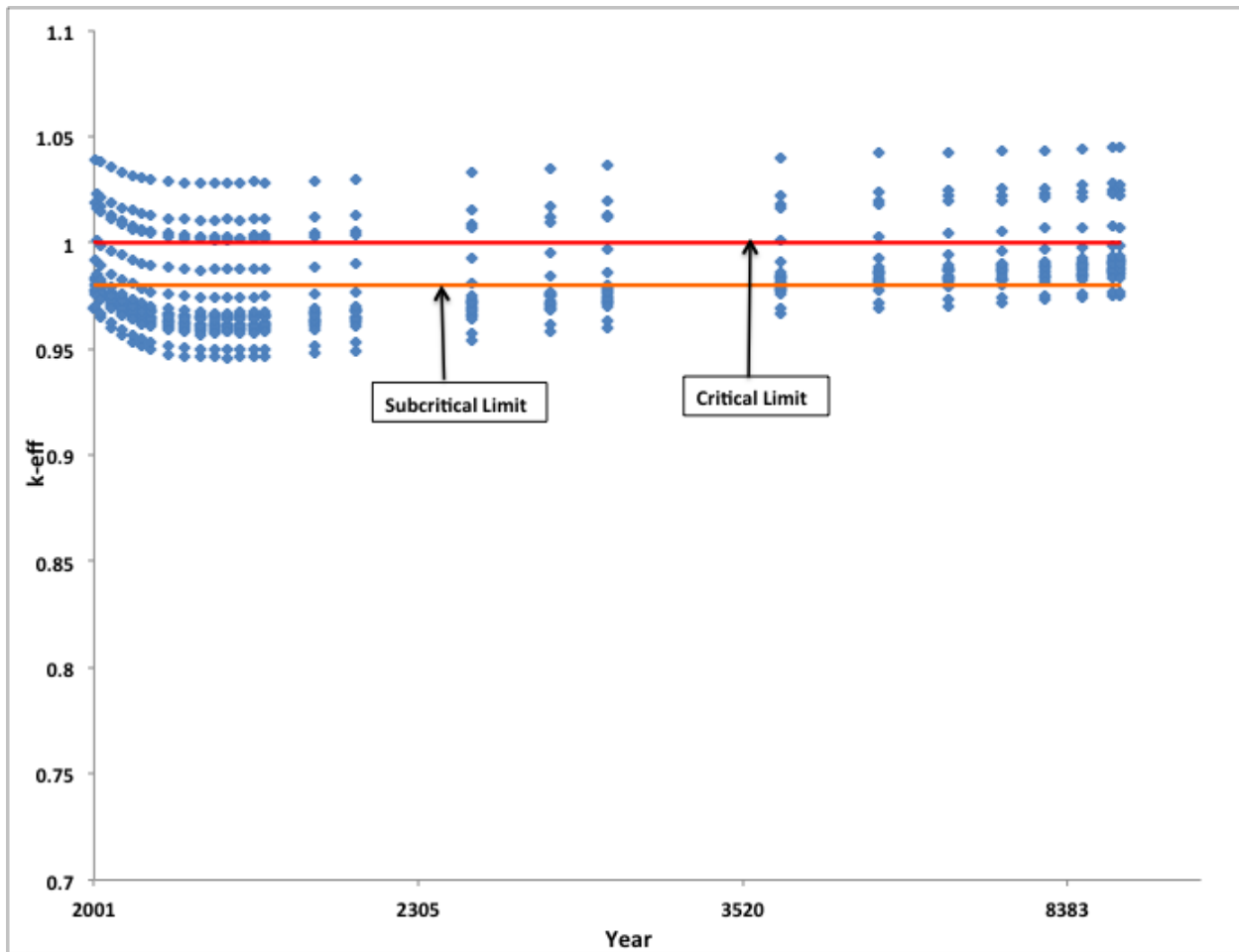


(b)

Figure 18. (a) Loss of neutron absorber configuration (RS) as modeled in KENO;
(b) k_{eff} as a function of time based on actual loading.



(a)



(b)

Figure 19. (a) Degraded spacer disks configuration (RS) as modeled in KENO;
(b) k_{eff} as a function of time based on actual loading.

Table 10 summarizes RS DPC results for the two analyzed degradation scenarios. Estimated CI requirement for the degraded basket scenario to maintain subcritical configuration over the repository time frame is also presented in Table 10.

Table 10. Final RS statistics in the year 9999

Description	Values for loss of neutron absorber	Values for degraded basket
Number of DSCs	20	20
Number of DSCs with $k_{eff} > 0.98$ (design basis analysis)	20	20
Number of DSCs with $k_{eff} > 0.98$ (as-loaded analysis)	0	18
Maximum k_{eff}	0.92691	1.04468
Approximate CI requirement (linear interpolation) ^a	not applicable	32,500 ppm (mg/L)

^aCI reactivity worth based on a 32-assembly configuration is assumed to be applicable for this DPC.

5.4 Trojan

The Trojan (TJ) Nuclear Power Plant, located at Rainier, Oregon, began electricity production in 1976 and ceased operation in 1993. TJ SNF assemblies are stored in 34 Holtec International’s MPC-24E/EF canisters (DPC). [24] The MPC-24E/EF can accommodate up to 24 SNF assemblies. The TJ basket is stainless steel construction; therefore, complete loss of neutron absorber is the only degradation scenario considered. Figure 20 illustrates the MPC-24E/EF basket without neutron absorber.

The MPC-24E/EF system applies 4.4 wt % enriched W 17×17 STD as the design basis. [24] Table 4 shows the reactivity of the complete loss of neutron absorber scenario with the design basis assembly.

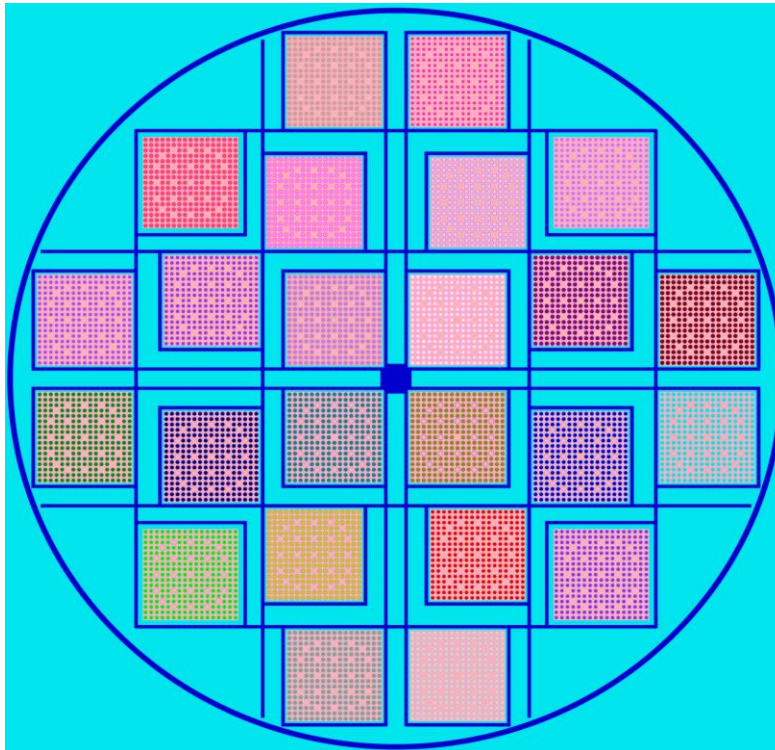


Figure 20. Radial layout of the MPC-24E/EF without neutron absorber panels as modeled in SCALE.

Figure 21 presents the k_{eff} of the loss of neutron absorber scenario as a function of time. Figure 21 shows that all of the canisters over the analyzed time period are below the subcritical limit (0.98) defined in this report. As shown in Table 11, an analysis of this configuration using the design basis fuel assembly for which the canister has been licensed yields $k_{eff} > 1$ for all the canisters. Table 12 summarizes the TJ nuclear site results.

Table 11. Calculated degraded absorber k_{eff} for the TJ DPC with design basis fuel

Enrichment (w/o ^{235}U)	Burnup (GWd/MTU)	k_{eff}
3.7	0	1.00569 ± 0.00020

Table 12. Final TJ statistics in the year 9999

Description	Values
Number of canisters	34
Number of canisters with $k_{eff} > 0.98$ (design basis analysis)	34
Number of canisters with $k_{eff} > 0.98$ (as-loaded analysis)	0
Maximum k_{eff}	0.90476
Approximate CI requirement (linear interpolation)	NA

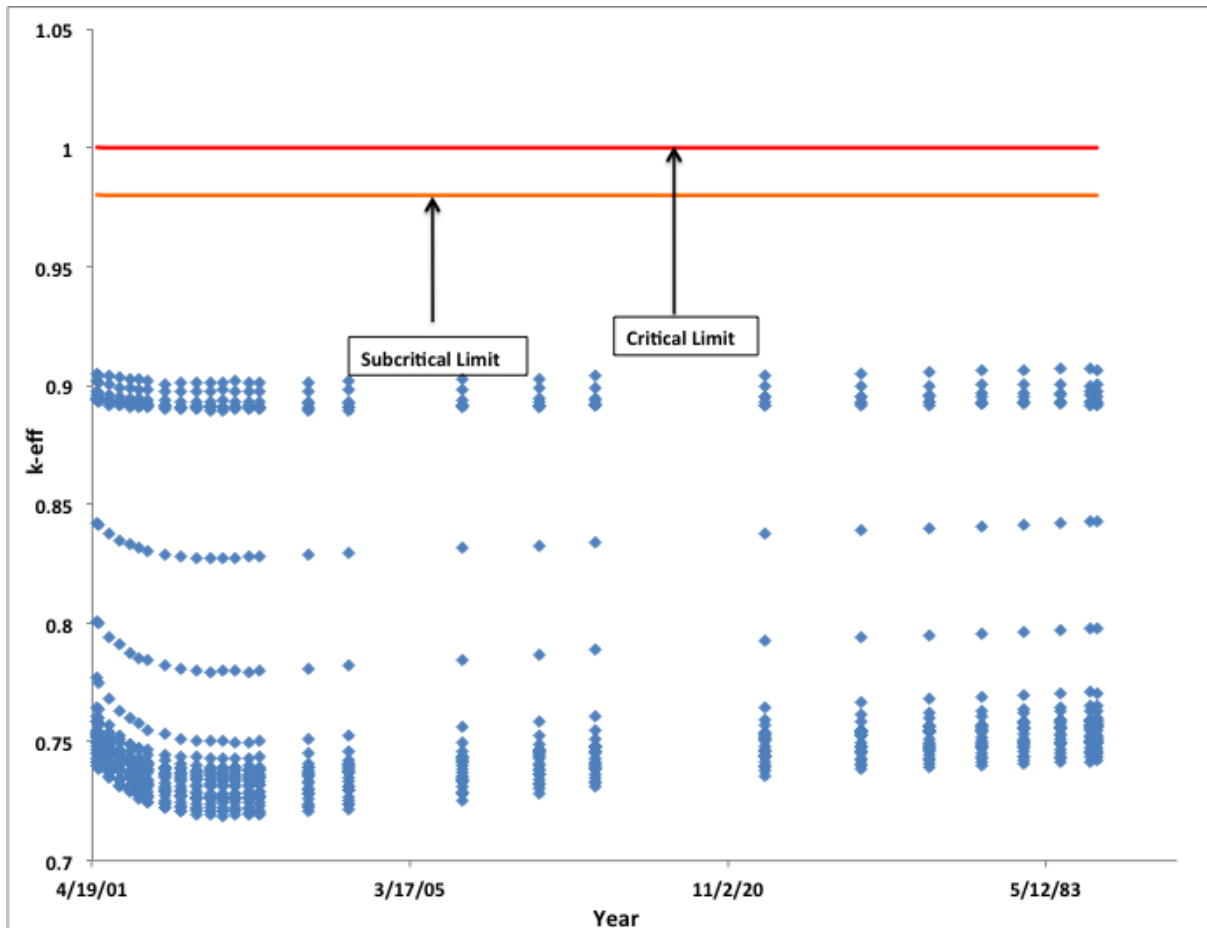


Figure 21. Calculated k_{eff} results for as-loaded TJ DPCs with loss of neutron absorber panels.

5.5 Sequoyah

The Sequoyah Nuclear Plant (SQ) is the only operating plant investigated in this report. SQ unit 1 started its operation in 1981, while unit 2 started producing electricity in 1982. SQ employs Holtec international's HI-STORM 100 systems with MPC-32 canisters (DPCs) for storing SNF. [25] The MPC-32 is an all stainless steel canister that can accommodate 32 PWR assemblies and uses an egg-crate basket design with a single neutron absorber panel between adjacent assemblies. Accordingly, loss of neutron absorber is the only degradation scenario considered for the MPC-32. Figure 22 presents a cross section view of the SCALE MPC-32 model used for criticality analyses. Twenty-six loaded MPC-32 canisters for SQ are examined in this report.

Because of its high density, the MPC-32 is licensed (for transportation) by applying burnup credit. Table 13 presents the design basis reactivity for the complete loss of neutron absorber case. Design basis parameters are selected from Ref. 26.

Table 13. Calculated degraded absorber k_{eff} for the SQ DPC with design basis fuel

Fuel type [26]	Configuration [26]	Enrichment (w/o ^{235}U)	Burnup (GWd/MTU)	k_{eff}
17 × 17A,B,C	B	4.0	49	1.06812 ± 0.00040

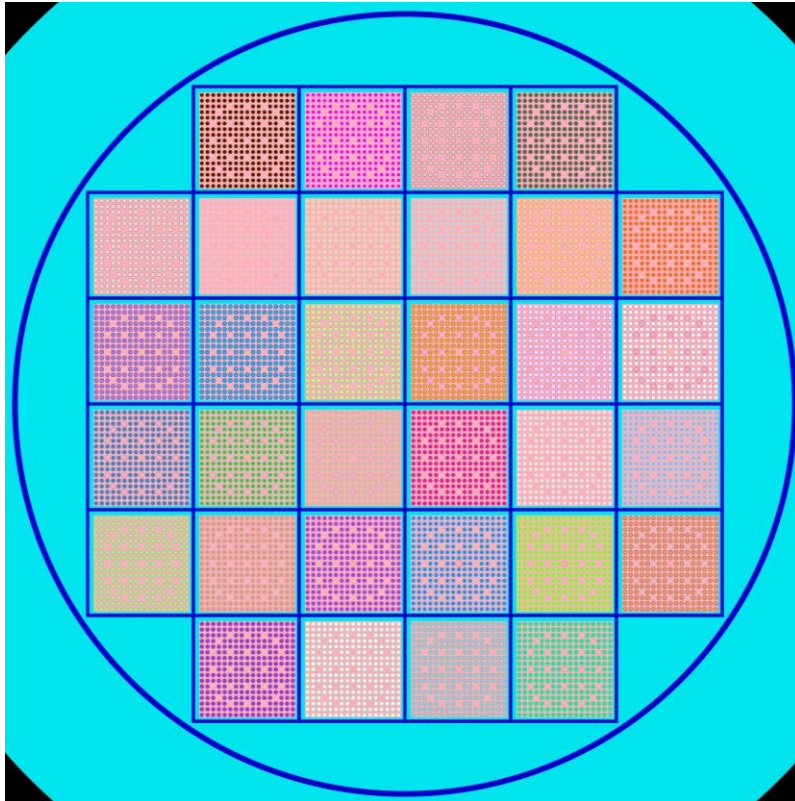


Figure 22. Radial layout of the MPC-32 without neutron absorber panels as modeled in SCALE.

Figure 23 presents the k_{eff} of the loss of neutron absorber scenario as a function of time. As described in the following subsection, if components in the guide tubes are present, they are credited in this calculation. Figure 23 shows that some of the canisters over the analyzed time period are below the subcritical limit (0.98) defined in this report. As shown in Table 13, an analysis of this configuration

using the design basis fuel assembly yields $k_{eff} > 1$ for all the canisters. Table 14 shows the number of SQ DPCs above the subcritical limit and the maximum k_{eff} . Table 14 also indicates the approximate amount of CI required to maintain subcritical condition in the 16 identified DPCs, which are above subcritical limit with fresh water.

Table 14. Final SQ statistics in the year 9999

Description	Values
Number of canisters	26
Number of canisters with $k_{eff} > 0.98$ (design basis analysis)	26
Number of canisters with $k_{eff} > 0.98$ (as-loaded analysis)	16
Maximum k_{eff}	1.00623
Approximate CI requirement (linear interpolation) ^a	13,500 ppm (mg/L)

^aCI reactivity worth based on a 32-assembly configuration is assumed to be applicable for this DPC.

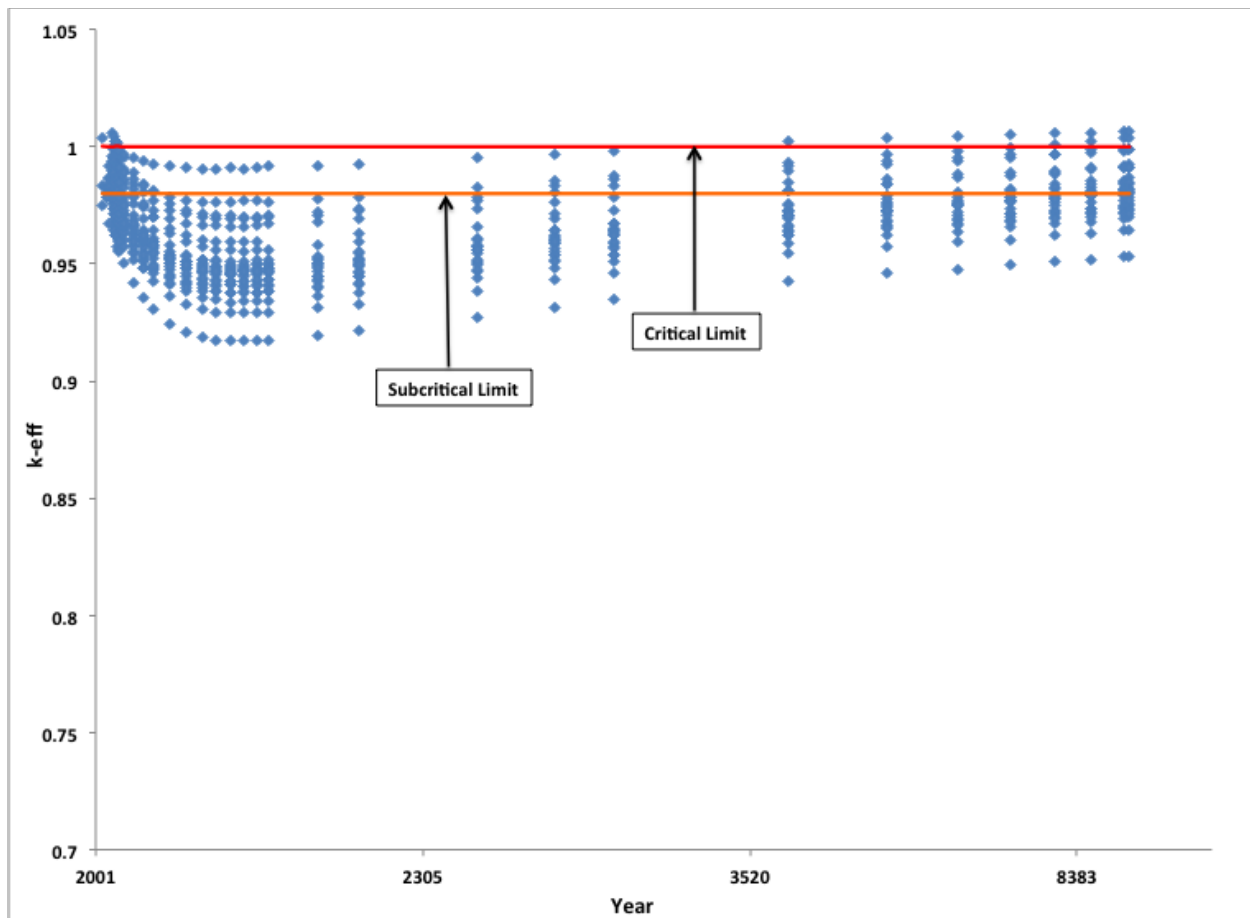


Figure 23. Calculated k_{eff} results for as-loaded SQ casks with loss of neutron absorber panels.

5.6 Component Credit

Many utilities are currently placing discharged non-fuel components into the used fuel assemblies that are placed in DPCs. Interim Staff Guidance (ISG) – 9 [27] indicates that materials positioned or operated within the envelope of the fuel assembly during reactor operation may be approved for storage in the

DPC. This includes items such as discharged burnable poison rods and control rods. ISG-9 states: “Credit for water displacement may be taken provided adequate structural integrity and placement under accident conditions is demonstrated.”

Different types of components are currently stored in the guide tubes of the SNF assemblies, including BPRAs, wet annular burnable absorbers (WABAs), and control rod assemblies (CRAs). BPRAs are either solid or annular (with dry annular gap) in design, while WABAs contain wet annular gaps. CRAs also contain solid rods. The number of rods (rodlets) in each type of component can also vary (e.g., W17 × 17, number of component rods varies from 4 to 24).

Some of the DPCs at SQ contain discharged components that include BPRAs and WABAs, with the number of rods varying from 4 to 24, including asymmetric configurations (e.g., with 9 rods). The results presented in Sect. 5.5 include a conservative model of components if they are stored with an assembly. Note that components are used in this analysis to credit the water displacement aspect only. A simplistic approach is used, because enough information is not presently available to model specific geometries of different components. The following assumptions are utilized:

- WABA design is considered for all the components, as it provides the least amount of water displacement because of its wet annular gap. Reference [28] provides the radial dimensions of the WABA. Although a WABA is longer than the active fuel length, when placed in the guide tube, the bottom end of a WABA is about 11 cm higher than that of the active fuel. In this analysis, WABAs are modeled to cover the entire axial length of the active fuel. However, the upper part of the WABA above the active length is not credited for water displacement. Figure 24 illustrates a cross section view of the WABA model used for the SQ DPCs.
- 16 WABA rods are considered for all components irrespective of the actual number of rods.
- The absorber material (e.g., $\text{Al}_2\text{O}_3\text{-B}_4\text{C}$) is modeled as void.

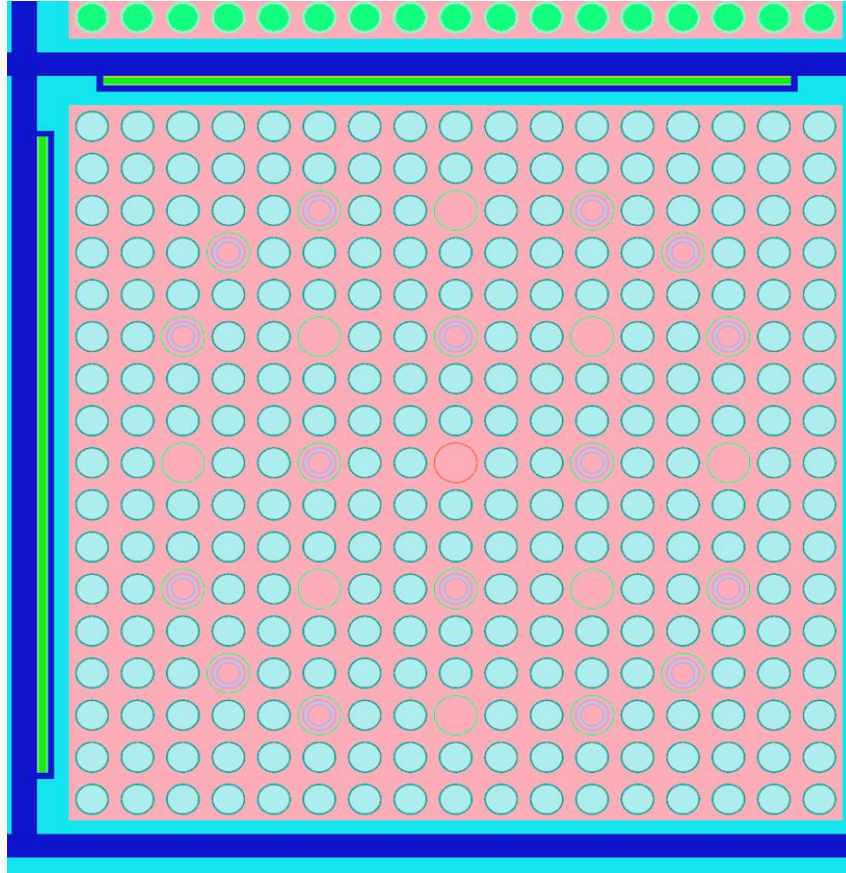


Figure 24. Radial view of the WABAs in the guide tube as modeled in SCALE for SQ DPCs.

This approach will be refined in the future to include the actual number and geometry of the components when more data will be available. Table 15 presents the typical reactivity reduction obtained from the water displacement by the components in the guide tubes. It is observed that a reactivity worth of approximately $0.06 \Delta k_{eff}$ is obtained with the simplified approach used in this report.

Table 15. Reactivity reduction from the components for SQ DPCs with loss of neutron absorber

SQ DPC	k_{eff} without component @ 9999	k_{eff} with component @ 9999	Δk
MPC-005	1.0048	0.99868	0.00612
MPC-006	0.9808	0.97466	0.00614
MPC-0109	0.9705	0.96418	0.00632
MPC-0110	0.95872	0.95314	0.00558
MPC-0177	0.99812	0.99254	0.00558
MPC-068	0.98747	0.9818	0.00567
MPC-070	0.97858	0.97276	0.00582

6. CONCLUSION

The analyses presented in this paper assume that waste package breach occurs at a relatively early time in the repository, allowing flooding of the canister to produce significant moderation and to degrade the internal components. Note that if water can be excluded or significantly delayed from entering the repository or from entering a package, there is little potential for criticality. Criticality analyses are performed (using fresh water) for two cases of canister degradation—loss-of-absorber and basket degradation—and for five types of DPCs located at five sites. Degraded material was assumed to be replaced by water moderator and to be completely removed from the DPC. Additionally, component credit to displace moderator from the guide tubes is applied for the DPCs at SQ ISFSI. The main sources of reactivity margin (relative to licensing design basis analyses) investigated in this paper include:

- burnup credit for 28 actinide and fission product nuclides previously demonstrated to exhibit a significant effect on fuel reactivity,
- use of actual as-loaded DPCs, and
- radionuclide inventory decay.

Analyses are also performed to generate the reactivity curves as functions of the concentration of various dissolved species in groundwater. These curves can be used to determine the reactivity impact for a specified amount of an element in different DPC configurations. However, currently available groundwater data indicates that Cl is the only naturally abundant, neutron-absorbing element in groundwater that can offer noticeable reactivity reduction. Table 16 summarizes the analyses performed in this report. Based on as-loaded canister-specific analyses, it can be concluded that credit for neutron absorbers present in groundwater is needed for 13% of the evaluated DPCs with loss of neutron absorber over the repository time frame, while credit for neutron absorbers present in groundwater is required for 23% of the analyzed DPC if degradation scenario includes loss of carbon steel structures and neutron absorber panels. Table 16 also presents the approximate Cl requirements to maintain subcritical configurations in all the 179 DPCs evaluated for both the degradation scenarios. About 2,000 DPCs have already been loaded with SNF and stationed in storage casks on ISFSI pads throughout the nation. Therefore, more DPCs are required to be evaluated to improve the overall statistics (probability of forming critical configurations over the repository time frame) following the criticality approach outlined in Ref. [4] for DPC direct disposal. The criticality roadmap from Ref. [4] is presented in Figure 25 with the completion status marked by yellow (work in progress) and green (completed) colors.

The analyses performed in this report indicate that subcriticality can be demonstrated for typical DPCs by detailed canister-specific analysis and by crediting the available groundwater composition if required. However, better understanding of the corrosion process of basket structural materials and their physical degradation mechanisms, as well as the probability of flooding or partial flooding, could further and significantly influence the projected likelihood of criticality events. Further, the possibility of one or more criticality events is not by itself a definitive indication that direct disposal of DPCs is infeasible for a given geologic setting and disposal concepts. In the past, stylized analyses have shown that the consequences of criticality, if properly weighted by probability, might not have a significant impact on waste isolation performance such that radionuclide releases from a repository would exceed safety standards. [29]

Table 16. Analyses summary

Description	Values	
Total DPC analyzed	179	
Fail subcriticality test with design basis analysis	179 (100%)	
Fail subcriticality test with as-loaded analysis	Loss of neutron absorber	Loss of neutron absorber and carbon steel structures
	23 (13%)	41 (23%)
Approximate Cl requirement	13,500 ppm (mg/L)	32,500 ppm (mg/L)

Criticality Analysis Roadmap					
Feasibility Assessment	Identify sources of water and potential for pooling in DPC by host media				
	Perform DPC model development to establish baseline	Develop and apply misload analysis methodology	Assess radiolysis rates required for significant impact to in-package chemistry	Groundwater analyses for different geologies	Identify performance assessment parameters directly influenced by criticality consequence
	Review neutron absorber and basket material performance data for existing DPCs	Development of BWR burnup credit methodology	Evaluation of chemistry ranges inside DPCs and corrosion rates on primary components	Develop probability based sampling framework for generic distributions	
	Perform envelope analysis on key parameters that lead to criticality	Evaluate probability of criticality	Develop geochemistry models accounting for in-package chemistry effects	Establish model for evaluating reaction kinetics and impacts on PA parameters	
	Evaluate envelope parameters against geochemistry model results to refine credible range	Evaluate criticality consequence effects on repository distributions		Generate risk curves per influence parameter	
Licensing Determination	Criticality validation (e.g., experiments with Cl ⁻ in solution, relevant configurations)	Justify and incorporate site-specific parameter distributions	Justify use of non-bounding assumptions	Validate site-specific geochemistry models	

Figure 25. DPC criticality analyses roadmap as described in Ref. [4] with the completion status; Yellow: work in progress and Green: completed.

7. REFERENCES

1. *Feasibility of Direct Disposal of Dual-Purpose Canisters: Options for Assuring Criticality Control*, Electric Power Research Institute, Palo Alto, Calif., 2008.
2. *The Potential of Using Commercial Dual Purpose Canisters for Direct Disposal*, TDR-CRW-SE-000030 Rev 00, US Department of Energy, Office of Civilian Radioactive Waste Management, November 2003.
3. *Handbook of Neutron Absorber Materials for Spent Nuclear Fuel Transportation and Storage Applications*, Electric Power Research Institute, Palo Alto, Calif., 2009.
4. J. M. Scaglione et al., *Criticality Analysis Process for Direct Disposal of Dual Purpose Canisters*, ORNL/LTR-2014/80, Oak Ridge National Laboratory, Oak Ridge, TN, March 2014.
5. J. B. Clarity et al., *Feasibility of Direct Disposal of Dual Purpose Canisters – Criticality Evaluations*, ORNL/LTR-2013/213, Oak Ridge National Laboratory, Oak Ridge, TN, June 2013.
6. Oak Ridge National Laboratory, *SCALE: A Comprehensive Modeling and Simulation Suite for Nuclear Safety Analysis and Design*, ORNL/TM-2005/39, Version 6.1, Radiation Safety Information Computational Center at Oak Ridge National Laboratory, Oak Ridge, Tenn., 2011.
7. J. M. Scaglione et al., *Integrated Data and Analysis System for Commercial Used Nuclear Fuel Safety Assessments*, Proceedings of the 17th International Symposium on the Packaging and Transportation of Radioactive Materials (PATRAM), August 18–23, 2013, San Francisco, Calif.
8. H. Smith et al., *Fuel Assembly Modeling for the Modeling and Simulation Toolset*, ORNL/LTR-2012-555, Oak Ridge National Laboratory, Oak Ridge, Tenn., November 2012.
9. J. Clarity et al., *Report Documenting Models for Criticality Safety Analyses*, Oak Ridge, TN, September 2013. (Draft report)
10. J. C. Wagner et al. *Recommendations for Addressing Axial Burnup in PWR Burnup Credit Analyses*, NUREG/CR-6801 (ORNL/TM-2001/273), prepared for the US Nuclear Regulatory Commission by Oak Ridge National Laboratory, Oak Ridge, Tenn., March 2003.
11. G. Radulescu et al., *An Approach for Validating Actinide and Fission Product Burnup Credit Criticality Safety Analyses–Isotopic Composition Predictions*, NUREG/CR-7108 (ORNL/TM-2011/509), prepared for the US Nuclear Regulatory Commission by Oak Ridge National Laboratory, Oak Ridge, Tenn., April 2012.
12. J. M. Scaglione et al. *An Approach for Validating Actinide and Fission Product Burnup Credit Criticality Safety Analyses–Criticality (k_{eff}) Predictions*, NUREG/CR-7109 (ORNL/TM-2011/514), prepared for the US Nuclear Regulatory Commission by Oak Ridge National Laboratory, Oak Ridge, Tenn., April 2012.
13. US Department of Energy, *Disposal Criticality Analysis Methodology Topical Report*, YMP/TR-004Q, Revision 0, Office of Civilian Radioactive Waste Management, November 1998.
14. J. C. Wagner et al., *Recommendations on the Credit for Cooling Time in PWR Burnup Credit Analyses*, NUREG/CR-6781 (ORNL/TM-2001/272), prepared for the US Nuclear Regulatory Commission by Oak Ridge National Laboratory, Oak Ridge, Tenn., January 2003.
15. *Standard Review Plan for Spent Fuel Dry Storage Systems at a General License Facility*, NUREG-1536, Rev. 1, Office of Nuclear Material Safety and Safeguards, July 2010.
16. E. Hardin et al., *Repository Reference Disposal Concepts and Thermal Management Analysis*. FCRD-USED-2012-000219 Rev. 2, US Department of Energy, Used Fuel Disposition R&D Campaign, November 2012.
17. Y. Wang et al., *Integrated Tool Development for Used Fuel Disposition Natural System Evaluation–Phase I Report*, prepared for the US Department of Energy Used Fuel Disposition, FCRD-UFD-2012-000229 SAND2012-7073P, 2012.
18. J. Winterle et al., *Geological Disposal of High-Level Radioactive Waste in Salt Formation*, Center for Nuclear Waste Regulatory Analyses, San Antonio, Texas, March 2012.

19. C. F. Jove Colon et al., *Disposal Systems Evaluations and Tool Development—Engineered Barrier System (EBS) Evaluation*, prepared for the US Department of Energy Used Fuel Disposition Campaign, SAND2010-8200, 2011.
20. E. I. A., *RW-859 Nuclear Fuel Data*, Washington, D.C.(Oct. 2004), Washington, DC, EIA, 2004.
21. NAC-UMS Final Safety Analyses Report, Rev. 3, US NRC Docket No. 72-1015, NAC International, January 2004.
22. NAC-STC Safety Analysis Report, Revision 15, US NRC Docket No. 71-9235, March 2004.
23. Transnuclear, Inc., *Multi-Purpose Cask*, Rev. 17, Safety Analysis Report-NUHOMS-MP187, Transnuclear, Inc., Fremont, Calif., July 2003 (Vendor Provided).
24. Holtec International, "*HI-STAR SAR Report HI-951251*", USNRC Docket No. 72-1014, Revision 15, October 11, 2010.
25. Holtec Final Safety Analysis Report for the HI-STORM 100 Cask System, Revision 9, February 13, 2010. ADAMS Accession Number ML101400161.
26. NRC Certificate Number 9261, Revision 8, Certificate of Compliance HI-STAR 100 for Radioactive Material Packages – HI-STAR 100.
27. U.S. Nuclear Regulatory Commission, *Interim Staff Guidance – 9, Revision 1, Storage of Components Associated with Fuel Assemblies*, Spent Fuel Project Office (2002).
28. Summary Report of Commercial Reactor Criticality Data for Sequoyah Unit 2, Revision 01, Civilian Radioactive Waste Management System, April 14, 1998.
29. S. Mohanty et al., *System-Level Performance Assessment of the Proposed Repository at Yucca Mountain Using the TPA Version 4.1 Code*, Center for Nuclear Waste Regulatory Analyses, San Antonio, Texas, Revision 2, March 2004.

This page is intentionally left blank.

APPENDIX A. FY15 Criticality Study

This page is intentionally left blank.

A.1. INTRODUCTION

This appendix documents work performed supporting the US Department of Energy (DOE) Nuclear Energy (NE) Fuel Cycle Technologies Used Fuel Disposition under work breakdown structure element 1.02.08.16 - DR, "Disposal of Dual Purpose Canisters." In particular, this appendix fulfills the M4 milestone, M4FT-15OR0816011, "Direct Disposal of DPC Reactivity and Criticality Evaluations" within work package FT-15OR0816001, "Disposal of Dual Purpose Canisters-ORNL."

This appendix presents the dual purpose canister (DPC) criticality evaluations performed in FY15 to support the feasibility determination of direct disposal of DPCs. This appendix extends the work reported in the main body of this report (performed in FY14). This appendix features:

1. updated criticality results with a set of 29 principal isotopes (henceforth referred to as disposal-isotopes) from Ref. A-1;
2. three new sites including a boiling water reactor (BWR) site (additional 36 DPCs);
3. reactivity reduction by groundwater species (Cl) applied to as-loaded DPCs (generic reactivity impact of groundwater is discussed in the main body);
4. reactivity impact of filler material applied to as-loaded DPCs; and
5. reactivity impact of ^{10}B areal density variation applied to as-loaded DPCs.

A.2. DISPOSAL-ISOTOPES

The criticality results reported in the main body of this report were generated applying the isotopic set reported in Table 2 (main body). The set of isotopes reported in Table 2 is recommended for spent nuclear fuel (SNF) storage and transportation (henceforth referred to as *storage-transportation-isotopes*) burnup credit criticality analyses. This set of storage-transportation-isotopes is the default burnup credit criticality analysis option within UNF-ST&DARDS. However, the storage-transportation-isotopes set is slightly different than that recommended in Ref. A-1 for disposal (post-closure) burnup credit criticality analyses. Table A-1 presents the principal set of isotopes for post-closure burnup credit criticality analysis. As stated in Ref. A-1, the principal isotopes for burnup credit includes a subset of the isotopes present in irradiated commercial fuel. They were selected considering the nuclear, physical, and chemical properties of the irradiated commercial fuel isotopes, such as cross sections and half-lives of the isotopes, concentrations (amount present in the irradiated fuel), and state (solid, liquid, or gas) of the isotopes, as well as volatility and solubility of the isotopes. Isotopic decay and build-up, as well as relative importance of isotopes for criticality (combination of cross sections and concentrations), were also considered in this selection process. No isotopes with significant positive reactivity effects (fissile isotopes with significant concentrations) were removed from consideration. Thus, the selection process was conservative.

UNF-ST&DARDS has been recently updated to include disposal-isotopes for the post-closure criticality analysis. Figure A-1 presents a reactivity comparison between the disposal-isotopes and storage-transportation-isotopes. This reactivity comparison study was performed for all the CY DPCs in the calendar year 9999. Figure A-1 shows that the disposal-isotopes set yields marginally higher k_{eff} s (up to 0.0038 Δk_{eff}) than that of the storage-transportation-isotopes. The secondary axis plotting differences is defined by the following equation:

$$\Delta k_{eff} = k_{eff}(\text{disposal} - \text{isotopes}) - k_{eff}(\text{storage} - \text{transportation} - \text{isotopes})$$

Perhaps this is because of the fission product isotope ^{133}Cs (a neutron poison), which is not present in the disposal-isotopes set.

Table A-1. Principal set of isotopes for burnup credit post-closure criticality analysis

⁹⁵ Mo	¹⁴⁵ Nd	¹⁵¹ Eu	²³⁶ U	²⁴¹ Pu
⁹⁹ Tc	¹⁴⁷ Sm	¹⁵³ Eu	²³⁸ U	²⁴² Pu
¹⁰¹ Ru	¹⁴⁹ Sm	¹⁵⁵ Gd	²³⁷ Np	²⁴¹ Am
¹⁰³ Rh	¹⁵⁰ Sm	²³³ U	²³⁸ Pu	^{242m} Am
¹⁰⁹ Ag	¹⁵¹ Sm	²³⁴ U	²³⁹ Pu	²⁴³ Am
¹⁴³ Nd	¹⁵² Sm	²³⁵ U	²⁴⁰ Pu	

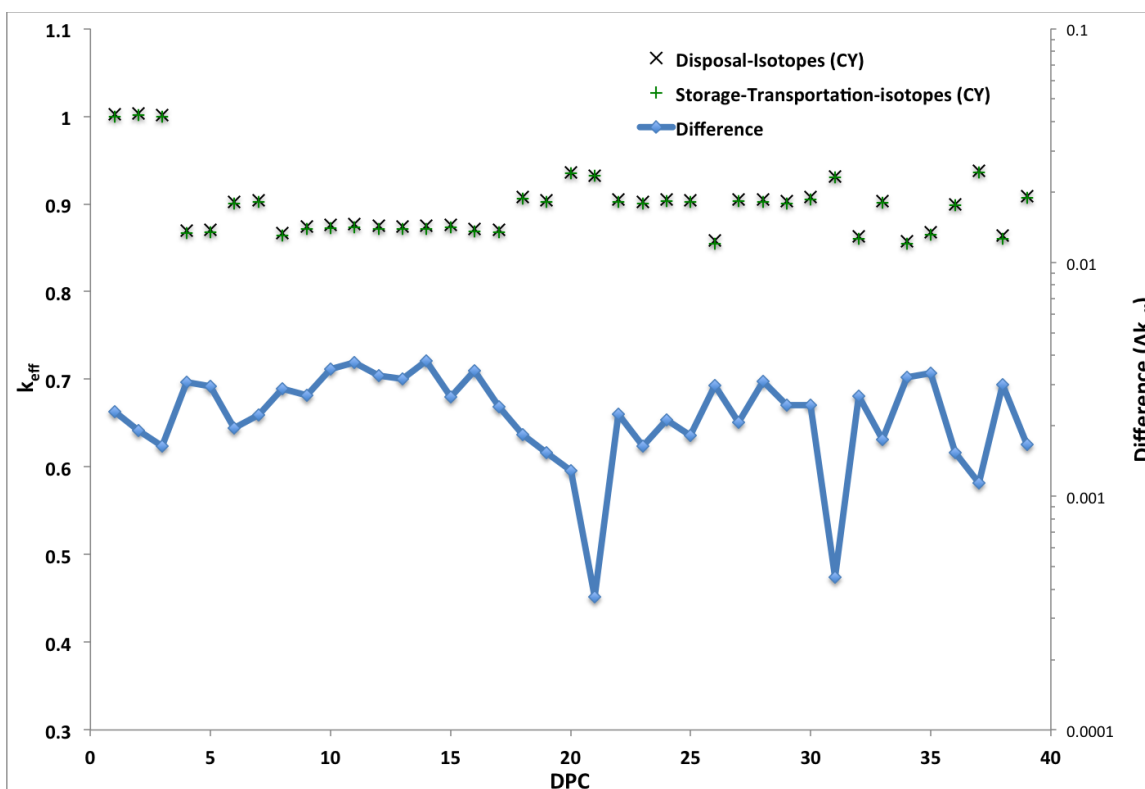


Figure A-1. Comparison (in terms of reactivity) between disposal-isotopes and storage-transportation-isotopes for CY DPCs in the calendar year 9999. .

Figure A-2 presents the as-loaded k_{eff} s for the five sites (Maine Yankee [MY], Connecticut Yankee [CY], Rancho Seco [RS], Trojan [TJ], and Sequoyah [SQ]) analyzed in the main body of this report with disposal-isotopes for the loss-of-neutron-absorber scenario. As discussed in the main body, $k_{eff} < 0.98$ is used in this study as a representative acceptance criterion for as-loaded calculations. However, if analyses like these are used to support future disposal licensing, additional validation and assessment of applicable biases will be required. Similar to the main body of this report, the time-dependent reactivity calculation results are provided for the time range between the calendar years 2001 and 9999 (i.e., approximately 8,000 years). Note that the disposal-isotopes set yielded 25 DPCs above the representative subcritical line in the year 9999, whereas 23 DPCs (as reported in Table 16) were above the representative subcritical limit using the storage-transportation-isotopes set. Two additional DPCs above the subcritical limit using the disposal-isotopes are from SQ site. As mentioned in the main body of this report, the degraded basket analysis was performed only for the RS site, as RS DPCs contain coated carbon steel spacer disks. Figure A-3 presents the RS basket degradation results reevaluated with disposal-isotopes. The disposal-isotopes set yielded 19 RS DPC above the representative subcritical limit (in the year 9999), whereas 18 RS DPCs

(as reported in Table , main body) were above the representative subcritical limit using the storage-transportation-isotopes set. Table A-2 summarizes the number of DPCs above the representative subcritical limit with disposal-isotopes and storage-transportation-isotopes.

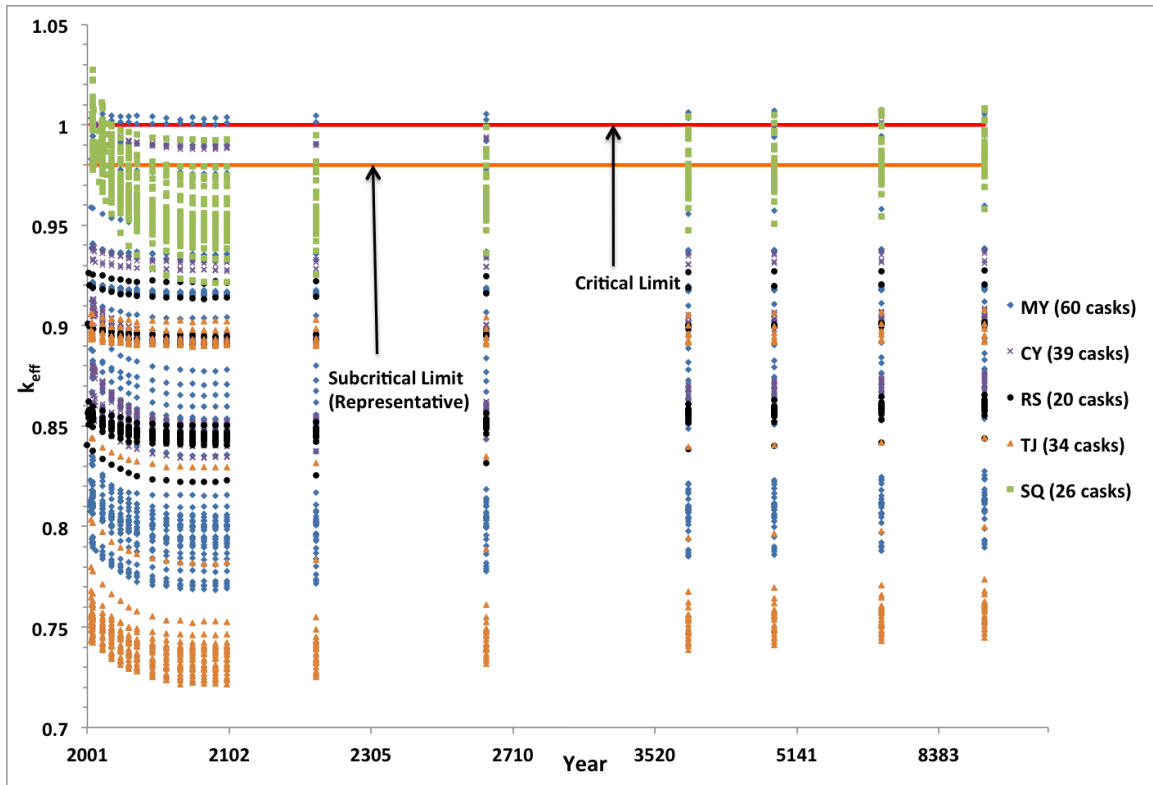


Figure A-2. k_{eff} vs. calendar year for the loss-of-neutron-absorber case based on actual loading and disposal-isotopes.

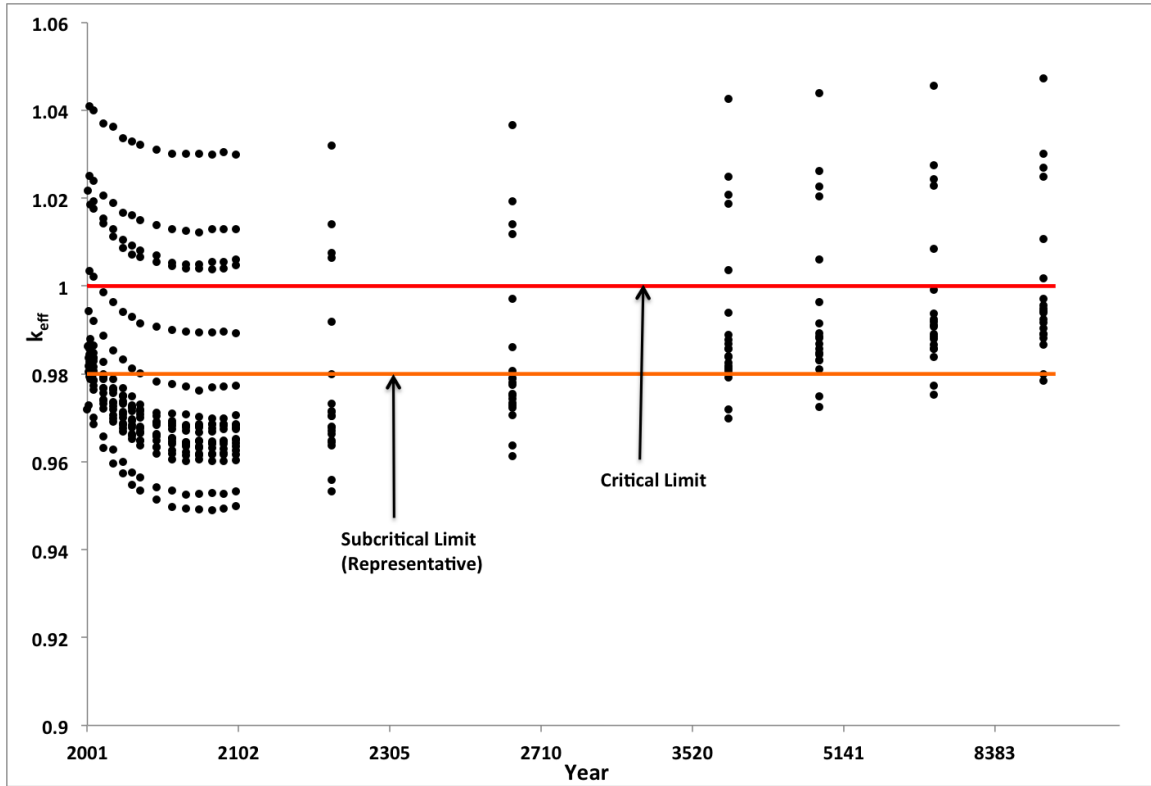


Figure A-3. k_{eff} vs. calendar year for the RS basket degradation case based on actual loading and disposal-isotopes.

Table A-2. Number of DPCs above subcritical limit with disposal-isotopes and storage-transportation-isotopes in the calendar year 9999

Description	Disposal-isotopes (this appendix)	Storage-transportation-isotopes (main body)
Number of DPCs with $k_{eff} > 0.98$ (loss-of absorber case)	25	23
Number of DPCs with $k_{eff} > 0.98$ (degraded basket case)	19	18

A.3. NEW SITES

Three new sites were evaluated in FY15 and results are presented in this appendix including Humboldt Bay site, Catawba nuclear station, and Salem nuclear power plant. While Humboldt Bay (HB) is a shutdown BWR site, Catawba (CTB) and Salem (SL) are operating PWR nuclear power stations. The DPCs used in HB, CTB, and SM are briefly described below.

Humboldt Bay (HB)

The HB nuclear power plant, located southeast of Eureka, California, was operated commercially from 1963 to 1976. Produced during HB’s 13 years of service, 390 assemblies [20] are stored in five Holtec’s MPC-HB (DPC) canister. [24] MPC-HB can accommodate 80 fuel assemblies per canister, up to 40 of which may be damaged. The MPC-HB also uses single Metamic™ neutron absorber panels between

storage locations to ensure criticality control. [24] The MPC-HB basket components are stainless steel construction; hence, complete loss of neutron absorber was only considered as the potential degradation scenario. Figure A-4 illustrates the MPC-HB 80-assembly DPC basket without neutron absorber.

The MPC-HB is loaded with 6×6 and 7×7 BWR assembly types. A planar average enrichment of 2.6 w/o ^{235}U was used for licensing calculations. Table A-3 shows the reactivity of the complete loss-of-neutron-absorber scenario with the design basis assembly (6×6 assembly type with 2.6 w/o ^{235}U).

Table A-3. Calculated degraded absorber k_{eff} for the MPC-HB with design basis fuel

Enrichment (w/o ^{235}U)	Burnup (GWd/MTU)	k_{eff}
2.6	0	0.98787 ± 0.00037

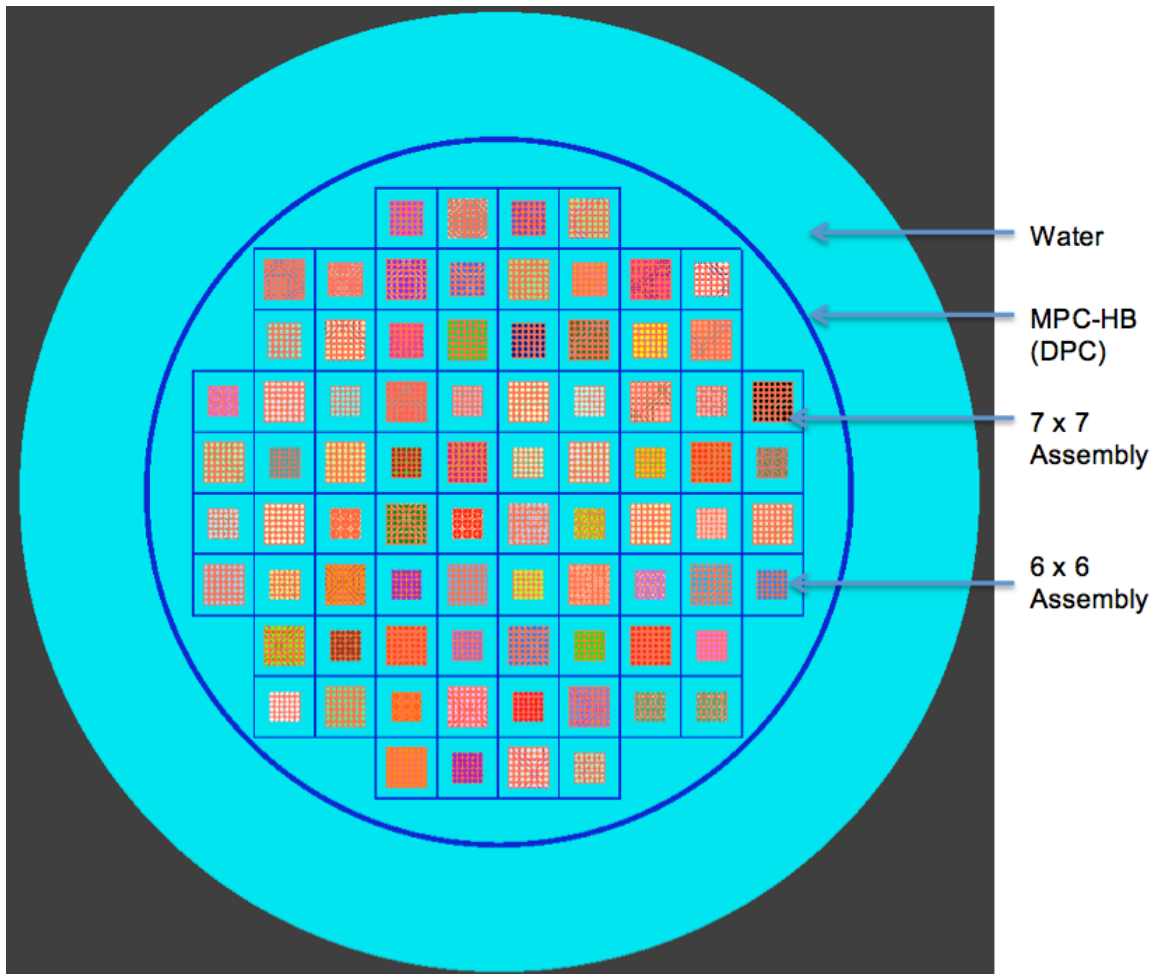


Figure A-4. Holtec’s MPC-HB 80-assembly basket without neutron absorber panels as modeled in KENO VI.

The following assumptions were applied for HB as-loaded calculations:

- Gadolinium (1 wt% Gd_2O_3 in 2 rods) was conservatively ignored in the 6×6 HB assemblies. Control blade insertion was assumed during the depletion period. As stated in Ref. A-2, control blade insertion provides the greatest impact on reactivity. Use of a full-length control blade insertion over an extraordinarily long depletion period is bounding for all anticipated reactor operation scenarios and negates the need to model burnable absorbers.
- Moderator density was assumed to be 0.49 gm/cc for HB fuel assemblies, which corresponds to 35% core average void fraction. [A-3]
- A uniform burnup profile was employed for the BWR fuel assemblies at the HB site. HB irradiated fuel assemblies are low burnup assemblies (~ 1.3 to 23 GWD/MTU). For PWR fuel assemblies, Ref. [10] determined that a uniform axial distribution is typically bounding for low burnup assemblies.
- For the damaged fuel and fuel debris, the bounding model defined in the SAR [24] was adopted for UNF-ST&DARDS HB criticality analysis. Damaged fuel assemblies in the DFCs were modeled with 0.488" pellet diameter and a 7×7 array of bare (without cladding) rods. The pitch of the 7×7 array was determined by the inner DFC width. For the damaged fuel and fuel debris in the DFCs, it was assumed that the fuel was present along the entire length of the DFC, including the areas that were not covered by the poison in the basket.

Catawba (CTB)

CTB unit 1 started its operation in 1985, while unit 2 started producing electricity in 1986. CTB employs the NAC UMS system (described in the main body of this report), which was also used by MY. CTB uses W 17×17 fuel assemblies. Twenty-four as-loaded CTB DPCs were analyzed. The CTB DPC basket components are stainless steel construction; hence, complete loss of neutron absorber was only considered as the potential degradation scenario.

Salem (SL)

SL unit 1 started its operation in 1977, while unit 2 started producing electricity in 1981. SL uses the Holtec International's MPC-32 (described in the main body of this report), which is also being used by SQ. SL uses W 17×17 fuel assemblies. Seven as-loaded SL MPC-32 (DPCs) were assessed. Similar to SQ (Section 5.6, main body), if control components were present, they were considered in the criticality analysis. The MPC-32 is an all stainless steel canister; therefore, loss of neutron absorber was the only degradation scenario considered for the MPC-32.

Figure A-5 presents the as-loaded k_{eff} s of the three new sites (HB, CTB, and SL) analyzed in this appendix for the loss-of-neutron-absorber scenario. These new sites were evaluated using disposal isotopes. All the seven DPCs from SL and two DPCs from HB are above the representative subcritical limit in the calendar year 9999.

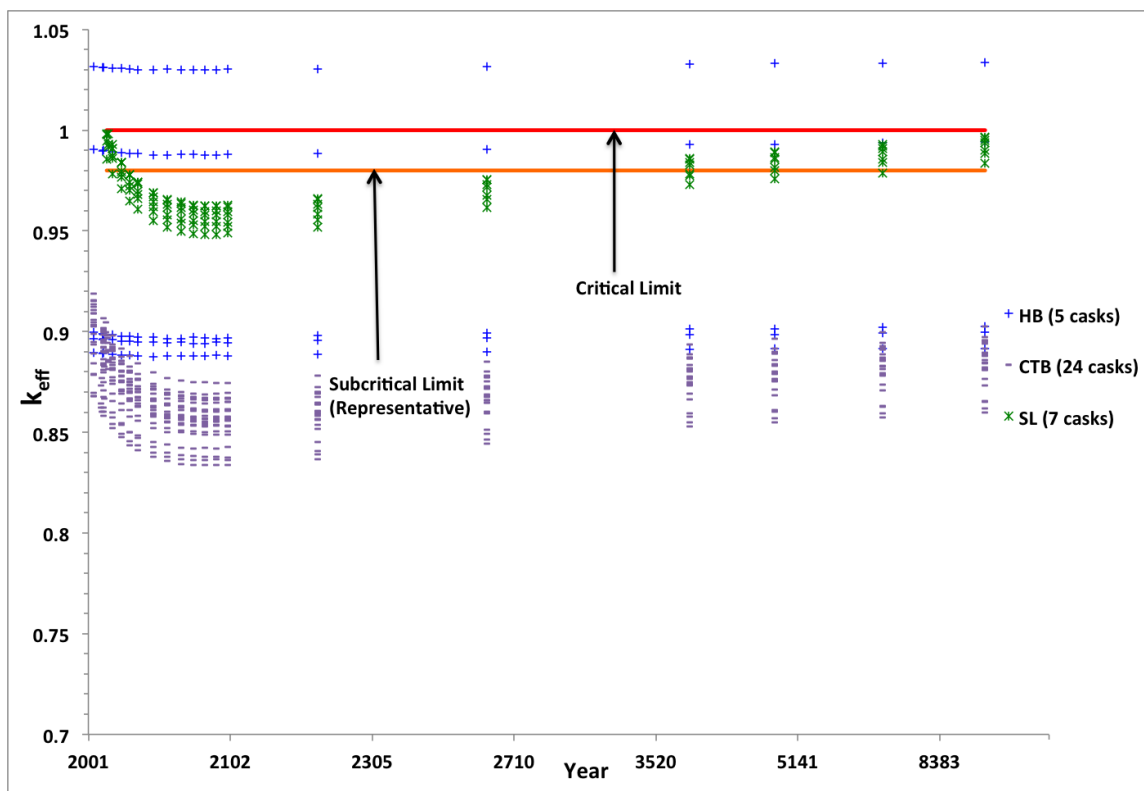


Figure A-5. k_{eff} vs. calendar year for the loss-of-neutron-absorber case, based on actual loading and disposal isotopes.

Table A-4 summarizes the analyses performed for the DPCs stored at the eight selected reactor sites. The summary results are presented for the calendar year 9999. Of the 215 DPCs analyzed, all would exceed the subcritical limit defined in this report ($k_{eff} > 0.98$) with loss of neutron absorbers if they were loaded with the design-basis fuel used for licensing. Using as-loaded fuel characteristics and burnup credit (29 nuclides), only 34 of the 184 (16%) (none from RS site) would exceed the subcritical limit for the loss-of-neutron-absorber scenario. For the RS DPCs, 19 of the 20 DPCs would exceed the subcritical limit with the basket degradation scenario. Therefore, a total of 53 DPCs (25%) would exceed the representative subcriticality limit with a loss-of-neutron-absorber scenario for MY, CY, TJ, SQ, HB, CTB, and SL sites and a loss-of-coated-carbon-steel-spacer-disks scenario for RS.

Table A-4. Summary of DPC As-loaded Criticality Analyses in the Calendar Year 9999

Description	Value
Total DPCs analyzed	215
Total DPCs that fail subcriticality with loss of neutron absorber (design-basis loading)	215 (100%)
Total DPCs that fail subcriticality (as loaded)	
Loss of neutron absorber	34 (16%)
Loss of neutron absorber and carbon steel structures	53 (34+19) (25%)

A.4. AS-LOADED CRITICALITY ANALYSIS WITH CHLORIDES IN GROUNDWATER

As mentioned in the main body report, neutron moderation by water is needed for a waste package to achieve criticality. However, the groundwater (or pore water) that may flood a breached DPC will contain various dissolved aqueous species. Seventeen species were studied in the main body and it was determined that Cl, Li, and B provide the maximum reduction in canister reactivity because of their large neutron absorption cross sections. However, available groundwater data indicate that Cl (as chloride) is the only naturally abundant neutron-absorbing element in groundwater that can provide significant reduction of reactivity and is available in most of the repository concepts under consideration in varying quantity.

In the main body of this report, three uniform canister loadings, namely, 10 GWd/MTU, 20 GWd/MTU, and 30 GWd/MTU were used with a 32-assembly DPC and with different levels of neutron absorber in the basket for the study of reactivity reduction of dissolved aqueous species in groundwater. The objective of this generic study was to identify the most viable species that could be further credited in the as-loaded analysis. Additionally, the generic groundwater study presented in the main body could be used to approximately determine the reactivity impact (Δk_{eff}) for a specified amount of a dissolved element.

In this section, the impact of Cl (in terms of NaCl) concentration in groundwater on the reactivity of as-loaded DPCs is studied. Figure A-6 presents the reactivity as a function of NaCl concentration in the calendar year 9999 for the DPCs at MY, SQ, CY, SL, and HB with loss of neutron absorber and at RS with a degraded basket. DPCs that yielded k_{eff} 0.98 or greater with fresh water were only analyzed with NaCl solution. Figure A-6 indicates that ~0.9 molal (moles of solute per kilograms of solvent) NaCl solution (~31,000 mg/L Cl) would be sufficient to maintain k_{eff} below 0.98 for all the DPCs at MY, CY, RS, SQ, SL, and HB sites. Note that using the generic calculations in the main body it was approximated that 32,500 mg/L Cl would be required to maintain k_{eff} below 0.98 for the analyzed sites (Note that both in the main body and in this appendix a RS DPC yielded the maximum reactivity). In this context, it is also important to note that a saturated NaCl brine has a concentration of approximately 6 molal.

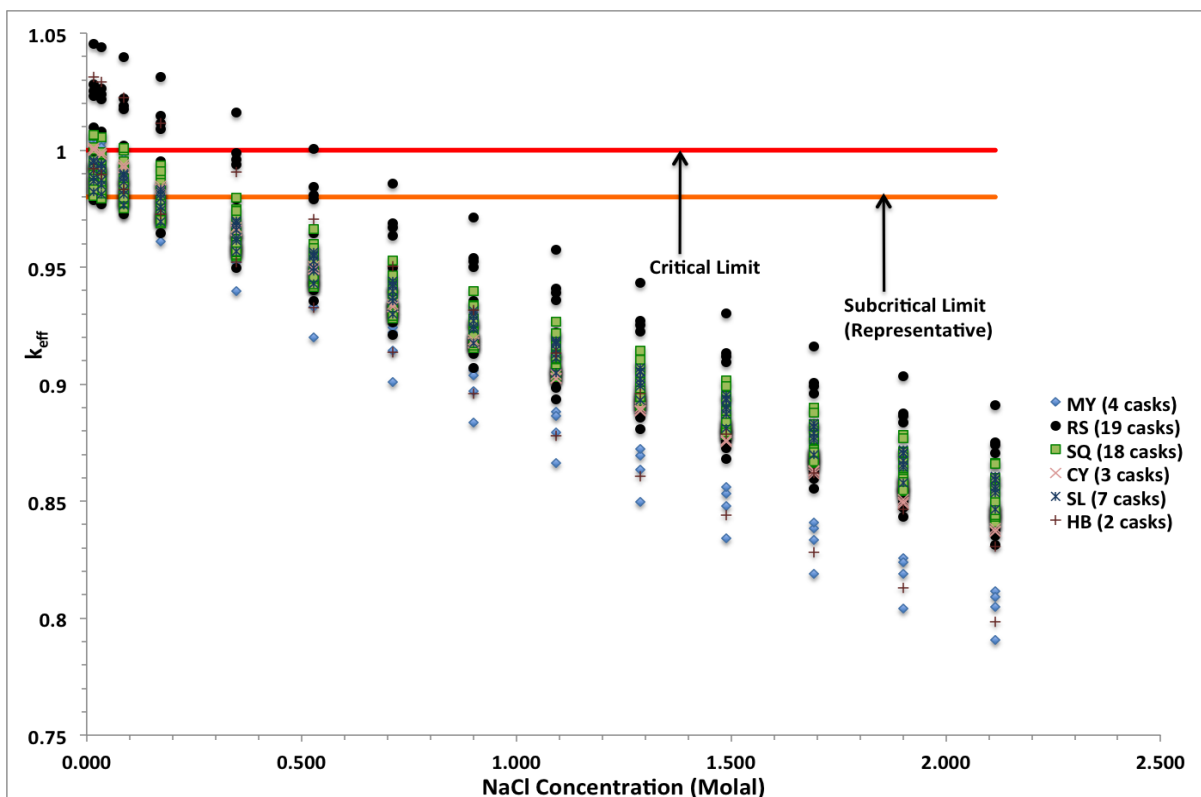


Figure A-6. k_{eff} vs. NaCl concentration for the loss-of-neutron-absorber (MY, SQ, CY, SL, and HB) and degraded basket (RS) cases based on actual loading.

A.5. AS-LOADED CRITICALITY ANALYSIS WITH ENGINEERING FILLER MATERIALS

An engineering option to mitigate the potential for DPC post-closure criticality is to fill the canister cavity with engineering filler materials that can prevent flooding of the DPC (moderator displacement) during the repository time frame. Filler material can also be selected to provide neutron absorption in addition to its moderator displacement functionality. Filler material options for direct disposal of DPCs are discussed in detail in Ref. A-4.

Criticality aspects (moderator displacement and neutron absorption) of filler materials are studied in Ref. A-4 using uniform DPC loading. In this section, the moderator displacement aspect of the filler materials is investigated using as-loaded DPCs at SQ. Aluminum was used as a representative filler material that only provides water displacement. Additionally, gibbsite ($Al(OH)_3$), which is a mineral of aluminum and can potentially form from aluminum in the presence of water over the repository performance period [A-5], was also considered for this study. 58% and 68% volumetric mixtures of filler materials were considered. For example, 58% aluminum was modeled as aluminum slurry, which was a mixture of 58% by volume aluminum powder and 42% by volume water. It is assumed that the filler material for the loss-of-neutron-absorption scenario uniformly fills all the basket cells.

Figure A-7 presents reactivity as a function of filler material volume fraction for the DPCs at SQ (with loss of neutron absorber) for the calendar year 9999. Only SQ DPCs that yielded k_{eff} 0.98 or greater with fresh water were analyzed with filler materials. The volume fraction was calculated by dividing the volume of the filler material in a basket cell by the free volume of that basket cell for the complete loss of neutron absorber case. Figure A-7 shows that about 34% volume (58% volumetric mixture) is required to

be filled (uniformly) by aluminum slurry to maintain k_{eff} below 0.98 for all the DPCs at SQ in the year of 9999. The required filled volume fraction would be slightly lower with a 68% volumetric mixture of aluminum. However, if the aluminum turns into gibbsite (or other similar materials that react with water to form a hydrogenous compound) over the repository performance period, about 72.5% volume would be required to be filled. Any volume change that may occur because of aluminum to gibbsite conversion is not accounted for in this study. Note that aluminum is only used in this study as a representative material. Gibbsite (potential mineral form of aluminum over the repository performance period) is included in this study to show that the eventual mineral product(s) of a filler material and its criticality implication must be considered as a filler material selection criterion. Candidate filler materials and filling methods are discussed in Ref. A-4.

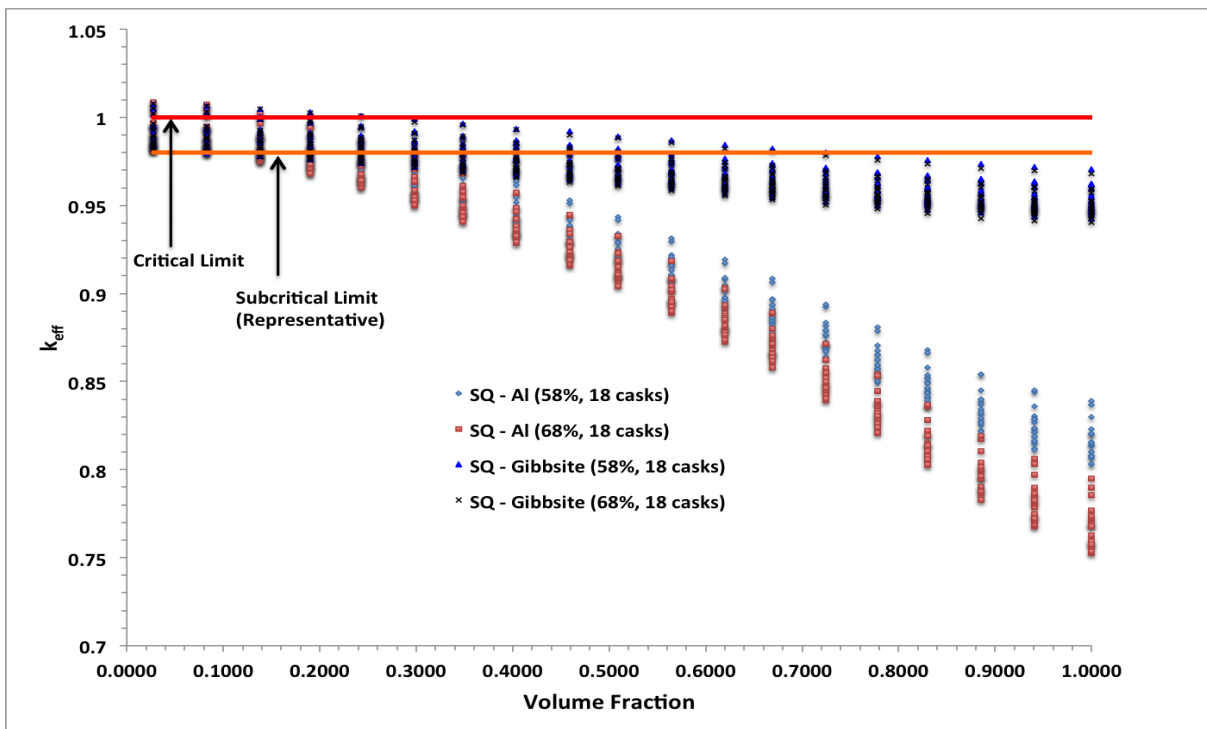


Figure A-7. Reactivity as a function of aluminum and gibbsite volume fraction for DPCs at SQ site.

A.6. REACTIVITY IMPACT OF ^{10}B AREAL DENSITY FOR AS-LOADED DPCS

As mentioned in the main body of this report, the degradation mechanisms for both neutron absorber and basket structure components over repository timeframes are not well understood. However, sufficient information is not currently available to support a basis for assuming neutron absorber's continued presence in the basket to provide criticality control. As such, it is assumed that DPCs will lose their neutron absorber from the basket gradually over time. The reactivity effect of this gradual loss of neutron absorber is studied in this section. Note that only the ^{10}B areal density has been varied for this study keeping the thickness of the absorber plates constant. Figure A-8 presents the reactivity variation of DPCs at SQ as a function of ^{10}B areal density in the neutron absorber panels for the calendar year 9999, assuming the DPC is flooded with fresh water. Only SQ DPCs (with complete loss of absorber) that yielded k_{eff} 0.98 or greater with fresh water were analyzed. Figure A-8 indicates that loss of neutron absorber from the basket up to a certain threshold ^{10}B areal density would not significantly increase reactivity. However, when the loss of neutron absorber from the basket passes the threshold ^{10}B areal

density, significant reactivity increase is expected. Because only ^{10}B areal density was varied for this study (keeping the thickness of the absorber plates constant), some of the DPCs, which were above 0.98 (k_{eff}) with complete loss of neutron absorber, are now slightly below 0.98. This is expected as aluminum in the absorber plates provides some moderator displacement compared to the complete loss-of-absorber case. Note that the reactivity behavior with loss of neutron absorber from the basket is strongly related to the DPC geometry.

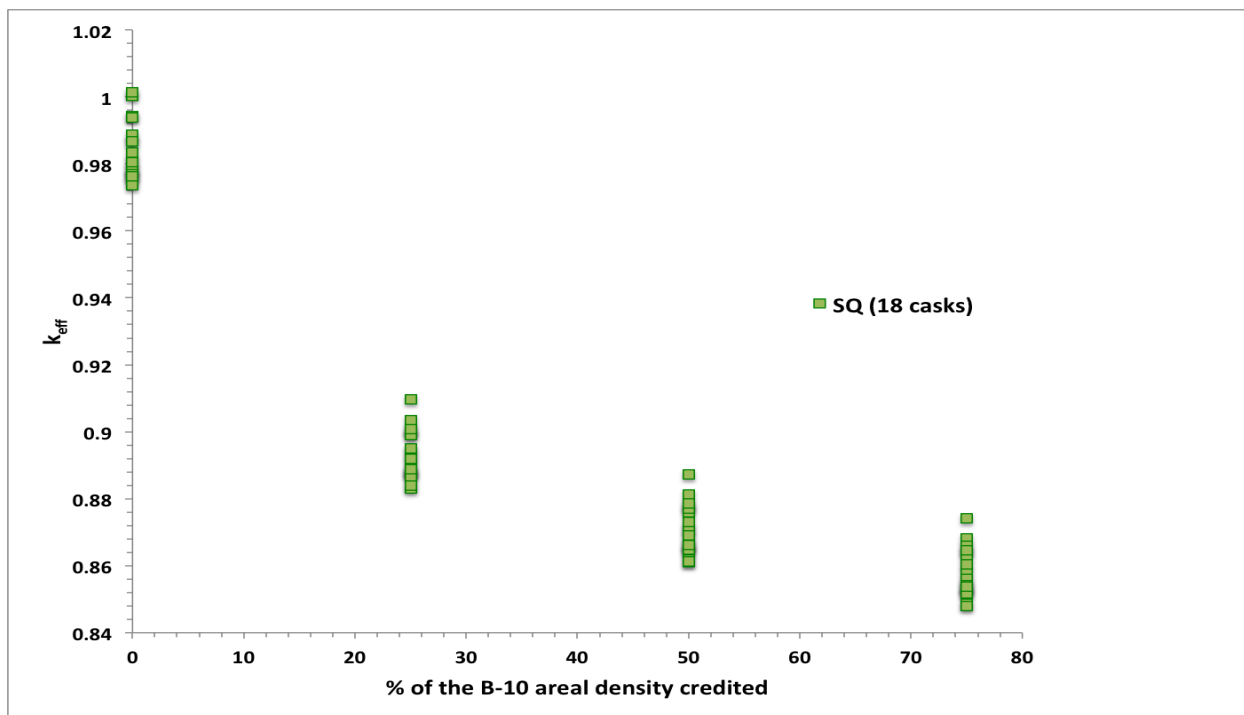


Figure A-8. Reactivity impact of ^{10}B areal density variation for as-loaded SQ DPCs.

A.7. CONCLUSION

In this appendix, criticality analyses were performed using fresh water for six types of DPCs (total 215 DPCs) located at eight sites for two canister degradation scenarios: (1) loss of neutron absorber and (2) basket degradation. Twenty-nine principal isotopes as recommended in Ref. A-1 for post-closure criticality analysis were used. Conservatively, degraded materials (basket or absorber) were not credited in the criticality analysis because their locations within the basket were unknown. The main sources of reactivity margin (relative to licensing design basis analyses) investigated in this paper include:

- burnup credit for 29 actinide and fission product nuclides previously demonstrated to exhibit a significant effect on fuel reactivity, and
- use of actual as-loaded DPCs, crediting actual assembly design, and reactor depletion conditions.

Additional analyses were performed to calculate the amount of CI required to maintain subcriticality (using the representative subcriticality limit) for the as-loaded DPCs at the eight evaluated sites. SQ DPCs were also analyzed with varying volume fractions of filler materials. The analyses performed in this report indicate that demonstrating subcriticality over a repository performance period may be attainable by combining detailed canister-specific analysis with full burnup credit and crediting CI in the repository groundwater composition if it is available in high enough concentrations. Preconditioning measures such

as adding filler materials to fill the canister void region and displace the moderator could be another option to mitigate post-closure criticality.

A.8. REFERENCES

- A-1. US Department of Energy, *Disposal Criticality Analysis Methodology Topical Report*, YMP/TR-004Q, Revision 2, Office of Civilian Radioactive Waste Management, October 2003.
- A-2. J. M. Scaglione and J. C. Wagner, *Review of Yucca Mountain Disposal Criticality Studies*, Proceedings of the 13th International High-Level Radioactive Waste Management Conference (IHLRWM), April 10–14, 2013, Albuquerque, NM.
- A-3. Humboldt Bay site supplied document.
- A-4. R. T. Jubin, K. Banerjee, and T. Severynse, *Potential Dual-Purpose Canister (DPC) Filler Materials*, FCRD-UFD-2014-000521 Rev. 0, US Department of Energy, Used Fuel Disposition R&D Campaign, July 2014.
- A-5. Office of Civilian Radioactive Waste Management Office of Repository Development, *Geochemistry Model Validation Report: Material Degradation and Release Model*, ANL-EBS-GS-000001 REV 02 (September 2007).

**APPENDIX B.
FY16 Criticality Study**

This page is intentionally left blank.

B.1. INTRODUCTION

This appendix documents work performed supporting the US Department of Energy (DOE) Nuclear Energy (NE) Fuel Cycle Technologies Used Fuel Disposition under work breakdown structure element 1.02.08.03.07 - DR, "Disposal of Dual Purpose Canisters." In particular, this appendix fulfills the M4 milestone, M4FT-16OR080307011, "Update of DPC Direct Disposal Criticality Analysis Report" within work package FT-16OR08030701, "Disposal of Dual Purpose Canisters-ORNL."

This appendix presents the dual purpose canister (DPC) criticality evaluations performed in FY16 to support the feasibility determination of direct disposal of DPCs. This appendix extends the work reported in the main body of this report (FY14) and Appendix A (FY15). The main objectives of the FY16 DPC disposal criticality study included (1) development of a rule-based boiling water reactor (BWR) criticality analysis methodology to support as-loaded BWR analysis, (2) as-loaded criticality analysis of new sites, and (3) determination of maximum chlorine requirement to suppress criticality of canisters with potential to form critical configuration in a repository time frame. In FY16, 339 as-loaded canisters were analyzed from 16 sites, which extended the analyzed canister tally from 215 (analyzed over last two years) to 554 (23 sites).

B.2. BWR AS-LOADED CRITICALITY ANALYSIS APPROACH

The detailed justifications of the BWR as-loaded criticality analysis approach as implemented in UNF-ST&DARDS is documented in Ref. B-1. UNF-ST&DARDS uses the declared burnups and enrichments from DOE fuel inventory surveys [B-2] to perform criticality safety calculations that take full burnup credit (actinides and fission products) for BWR fuel bundles loaded in DPCs. Justification for the following features of the criticality analysis approach has been developed in Ref. B-1.

- Selection of axial burnup profiles for BWR fuel from publicly available sources (Selected profiles are meant to be conservative.)
- Justification for applying the selected axial burnup profiles to all types of BWR fuel
- Comparison of the axial features of the fuel from which the profiles were selected with the range of axial features of the population of fuel analyzed
- Justification for modeling the fuel assemblies with a uniform axial and radial enrichment (BWR fuel typically has a number of different enrichments which vary within a single axial segment [also known as a lattice] and as a function of elevation.)
- Justification for modeling the axial void profile as a single nominal value that does not change with elevation or time by using the margin associated with the conservative depletion assumption that control blades are fully inserted throughout the entire irradiation history of the fuel assembly

B.3. SITES ANALYZED

A total of 339 loaded DPCs at 16 sites were analyzed. Table B-1 presents the sites and DPCs analyzed. These 16 sites include three decommissioned sites: Zion, Yankee Rowe, and La Crosse. All the DPCs loaded at these sites were analyzed. The number of DPCs analyzed at each operating site is primarily based on the availability of DPC loading maps. Six DPC types were analyzed, including (1) Holtec International's MPC-32, (2) Holtec International's MPC-24, (3) Holtec International's MPC-68, (4) NAC International's TSC-37 (two variations with intact and damaged fuel assemblies), (5) NAC International's Yankee-MPC (36 assembly capacity), and (6) NAC International's MPC-LACBWR (68 assembly capacity). The criticality models of the DPC variants mentioned above are described in detail in Ref. B-1. Loss-of-neutron-absorber is the only degradation scenario considered in this appendix.

Table B-1. List of sites and number of loaded DPCs assessed for criticality

Site Name	Number of DPCs	Fuel type	DPC type
Vermont Yankee	13	BWR	MPC-68
Grand Gulf	23	BWR	MPC-68
Columbia	27	BWR	MPC-68
Salem	9	PWR	MPC-32
Waterford	9	PWR	MPC-32
Comanche Peak	9	PWR	MPC-32
Browns Ferry	40	BWR	MPC-68
River Bend	19	BWR	MPC-68
Fitzpatrick	21	BWR	MPC-68
Indian Point	18	PWR	MPC-32
Farley	21	PWR	MPC-32
Cook	12	PWR	MPC-32
Arkansas Nuclear One	37	PWR	MPC-24 and MPC-32
Zion	61	PWR	TSC-37
Yankee Rowe	15	PWR	Yankee-MPC
La Crosse	5	BWR	MPC-LACBWR
Total	339		

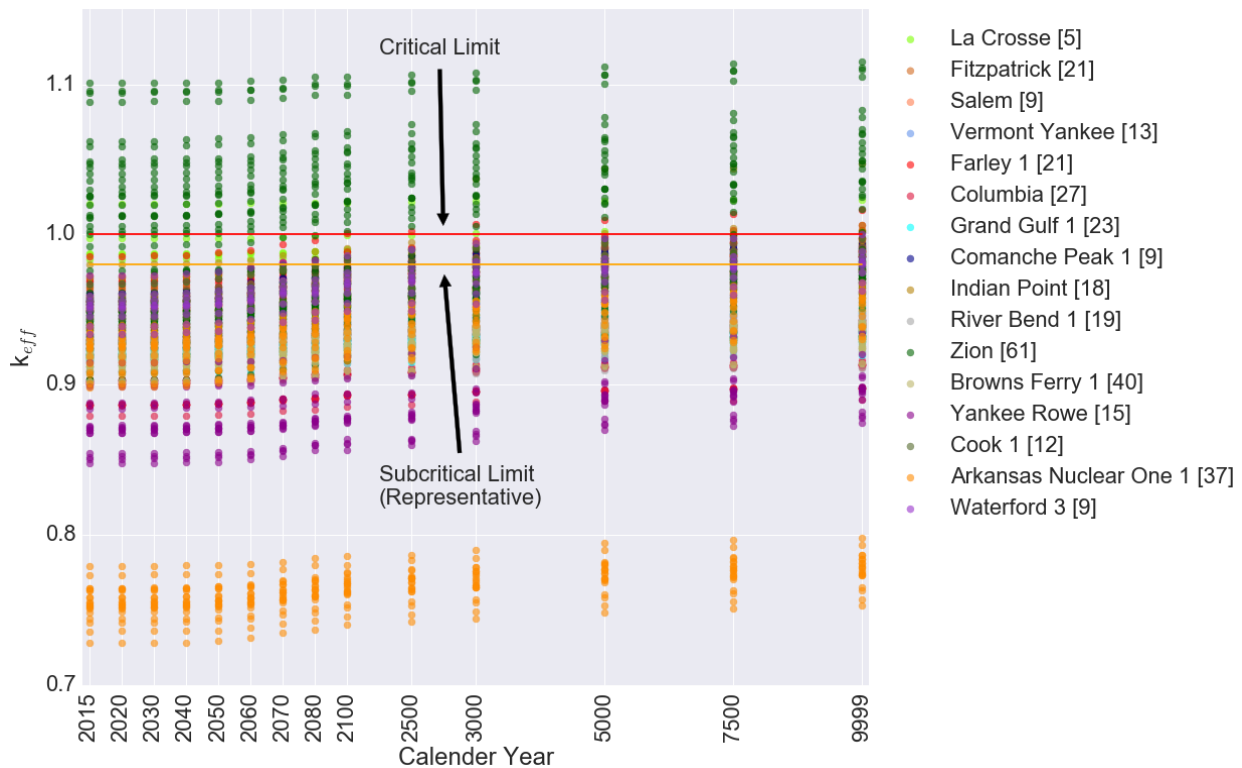


Figure B-1. k_{eff} vs. calendar year for the loss-of-neutron-absorber case, based on actual loading and disposal-isotopes. The number within the bracket indicates number of DPCs.

Figure B-1 presents the as-loaded k_{eff} s of the 16 sites analyzed in this appendix for the loss-of-neutron-absorber scenario. These new sites were evaluated using disposal isotopes (see Table A-1). Out of 339 DPCs, 92 are above the representative subcritical limit in the calendar year 9999.

Table B-2 summarizes the criticality analysis performed for the DPCs to date. The summary results are presented for the calendar year 9999. Of the 554 DPCs (339 new and 215 from FY15) analyzed to date, all would exceed the subcritical limit defined in this report ($k_{eff} > 0.98$) with loss of neutron absorbers if they were loaded with the design-basis fuel used for licensing. Using as-loaded fuel characteristics and burnup credit (29 nuclides), only 126 (92 + 34 from FY15 analysis) of the 554 (23%) would exceed the subcritical limit for the loss-of-neutron-absorber scenario. Of the RS DPCs, 19 of the 20 DPCs would exceed the subcritical limit with the basket degradation scenario. Therefore, a total of 145 DPCs (26%) would exceed the representative subcriticality limit with a loss-of-neutron-absorber scenario for all the analyzed DPCs and a loss-of-coated-carbon-steel-spacer-disks scenario for the RS site.

Table B-2. Summary of DPC as-loaded criticality analyses in calendar year 9999

Description	Value
Total DPCs analyzed	514
Total DPCs that fail subcriticality with loss of neutron absorber (design-basis loading)	215 (100%)
Total DPCs that fail subcriticality (as loaded)	
Loss of neutron absorber	126 (~23%)
Loss of neutron absorber and carbon steel structures (RS only)	145 (126 + 19) (~26%)

B.4. AS-LOADED CRITICALITY ANALYSIS WITH CHLORIDES IN GROUNDWATER

In this section, the impact of Cl (in terms of NaCl) concentration in groundwater on the reactivity of as-loaded DPCs is studied. Figure B-2 presents the reactivity as a function of NaCl concentration in the calendar year 9999 for the DPCs at Farley, Indian Point, Cook, Salem, Waterford, Zion, La Crosse, and Comanche Peak with loss of neutron absorber. DPCs that yielded k_{eff} 0.98 or greater with fresh water and loss of neutron absorber were only analyzed with NaCl solution. Figure B-2 indicates that ~1.8 molal (moles of solute per kilograms of solvent) NaCl solution (~64,000 mg/L Cl) would be sufficient to maintain k_{eff} below 0.98 for the analyzed DPCs at the 16 sites. In this context, it is also important to note that a saturated NaCl brine has a concentration of approximately 6 molal.

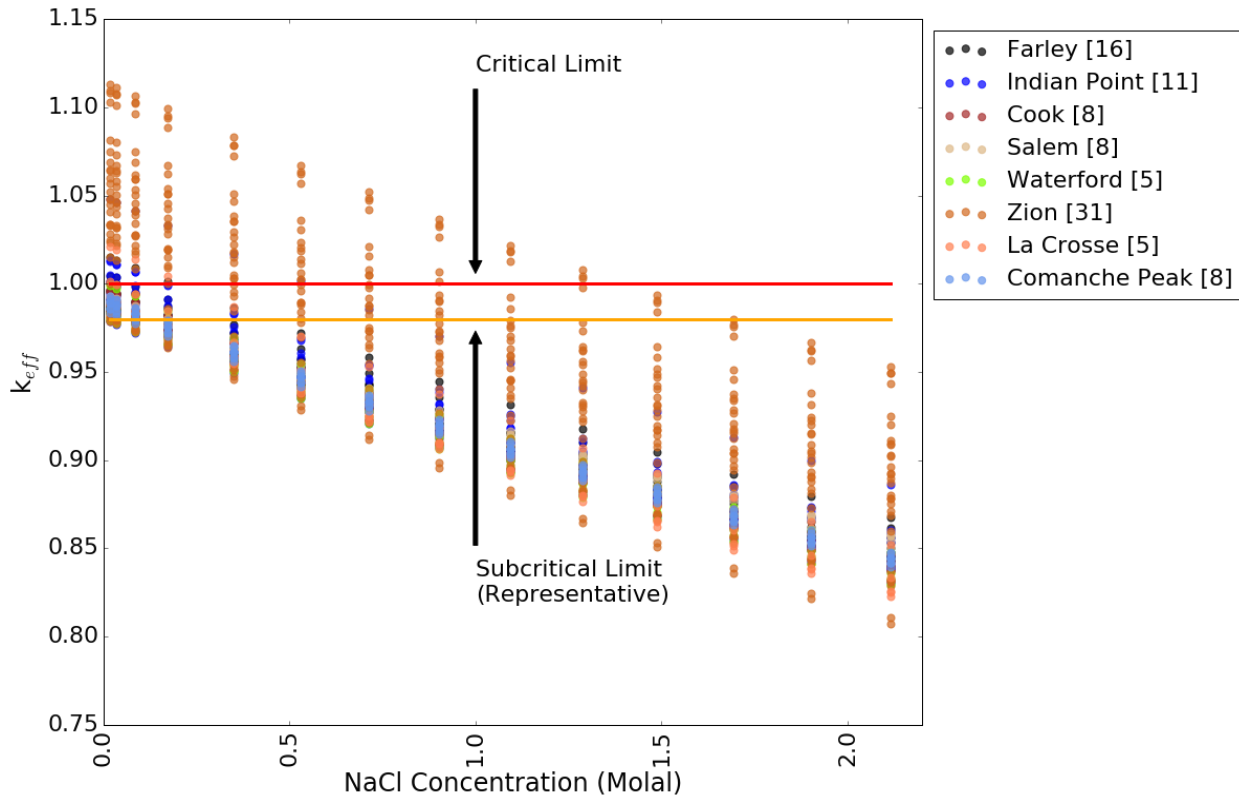


Figure B-2. k_{eff} vs. NaCl concentration for the DPCs with $k_{eff} > 0.98$ for the loss-of-neutron-absorber scenario. (Numbers in brackets = number of DPCs).

B.5. CONCLUSION

This appendix presents criticality analyses that were performed using fresh water for six types of DPCs (total 339 DPCs) located at 16 sites for loss-of-neutron-absorber degradation scenarios. Twenty-nine principal isotopes were used as recommended in Ref. A-1 for post-closure criticality analysis. Conservatively, degraded materials (basket or absorber) were not credited in the criticality analysis because their locations within the basket were unknown. Figure B-3 presents the updated criticality roadmap from Figure 25 in the main body of this report. As noted above, this year an approach has been developed for as-loaded BWR criticality analysis. Although the BWR burnup credit methodology development box is marked as green in Figure B-3, the BWR analysis approach developed in FY16 may require some minor refinements to support all BWR fuel types.

Additional analyses were performed to calculate the amount of Cl required to maintain subcriticality (using the representative subcriticality limit) for the as-loaded DPCs at the 16 evaluated sites. Analyses performed as discussed in this appendix for the 339 as-loaded DPCs show that ~1.8 molal NaCl would be sufficient to maintain subcriticality in all the analyzed DPCs, while ~0.9 molal NaCl requirement were determined for the 215 DPCs analyzed and presented in Appendix A. The increase in reactivity and corresponding NaCl requirement are mainly due to the Zion canisters loaded with damaged fuel assemblies, which were modelled as unirradiated. Damaged fuel modeling approach needs to be refined for improved reactivity evaluation of loaded canisters with damaged fuels. Therefore, for all the analyzed DPCs (554), current maximum NaCl requirement would be ~1.8 molal. The analyses performed in this report indicate that demonstrating subcriticality over a repository performance period may require both detailed canister-specific analysis with full burnup credit and crediting Cl in the repository groundwater composition if it is available in high enough concentrations. Studies presented in Appendix A also show

that preconditioning measures—such as adding filler materials to fill the canister void region and displace the moderator—could be another option to mitigate post-closure criticality. The next step in support of the filler material approach would be to conduct an experiment to determine the viability of filling a DPC up to a predetermined volume and using various filling options conceptualized in Ref. A-4.

Criticality Analysis Roadmap					
Feasibility Assessment	Identify sources of water and potential for pooling in DPC by host media				
	Perform DPC model development to establish baseline	Develop and apply misload analysis methodology	Assess radiolysis rates required for significant impact to in-package chemistry	Groundwater analyses for different geologies	Identify performance assessment parameters directly influenced by criticality consequence
	Review neutron absorber and basket material performance data for existing DPCs	Development of BWR burnup credit methodology	Evaluation of chemistry ranges inside DPCs and corrosion rates on primary components	Develop probability based sampling framework for generic distributions	
	Perform envelope analysis on key parameters that lead to criticality	Evaluate probability of criticality	Develop geochemistry models accounting for in-package chemistry effects	Establish model for evaluating reaction kinetics and impacts on PA parameters	
	Evaluate envelope parameters against geochemistry model results to refine credible range	Evaluate criticality consequence effects on repository distributions	Generate risk curves per influence parameter		
Licensing Determination	Criticality validation (e.g., experiments with Cf in solution, relevant configurations)	Justify and incorporate site-specific parameter distributions	Justify use of non-bounding assumptions	Validate site-specific geochemistry models	

Figure B-3. DPC criticality analyses roadmap as described in Ref. [4] with the completion status; Yellow: work in progress and Green: completed.

B.6. REFERENCES

- B-1. J. B. Clarity, H. Liljenfeldt, and K. Banerjee, *Criticality Process, Modeling and Status for UNF-ST&DARDS*, FCRD-NFST-2015-000440, Rev. 1, US Department of Energy, Nuclear Fuel Storage and Transportation Planning Projects (July 2016).
- B-2. “Nuclear Fuel Data Survey,” Form GC-859, EIA, Washington, DC (July 2012).

This page is intentionally left blank.

**APPENDIX C.
FY17 Criticality Study**

This page is intentionally left blank.

C.1. INTRODUCTION

This appendix documents work performed supporting the US Department of Energy (DOE) Nuclear Energy (NE) Spent Fuel and Waste Disposition (SFWD) Spent Fuel and Waste Science and Technology under work breakdown structure element 1.08.01.03.05 “Direct Disposal of Dual Purpose Canisters.” In particular, this appendix fulfills the M4 milestone, M4SF-17OR010305022, “Initial development of a misload analysis methodology” within work package SF-17OR01030502, “Direct Disposal of Dual Purpose Canisters - ORNL.”

This appendix presents the assembly misload analysis methodology developed in FY17 to support the feasibility determination of the direct disposal of DPCs from a criticality perspective. The main objective was to develop a misload analysis methodology to support as-loaded criticality analysis of the loaded DPCs. The misload analysis has been applied to 99 loaded DPCs at three sites. The analyzed sites include both PWR and BWR reactors and three canister variants—MPC-32, TSC-37 and MPC-68.

C.2. MISLOAD DEFINITION AND REGULATORY GUIDANCE

In 2002, the US Nuclear Regulatory Commission issued the revision 2 to Interim Staff Guidance 8, “Burnup Credit in the Criticality Safety Analyses of PWR Spent Fuel in Transportation and Storage Casks” (ISG 8 rev. 2). This document provides guidance for taking burnup credit for storage and transportation casks. If the wrong assembly is placed in the right position, or if the right assembly is placed in the wrong position, it is considered a misload and requires analysis for any storage or transportation system that uses burnup credit. The ISG 8 rev. 2 only mentioned pool-side burnup measurements as an acceptable method to prevent misloads.

In 2012 the revision 3 of the Interim Staff Guidance 8 “Burnup Credit in the Criticality Safety Analyses of PWR Spent Fuel in Transportation and Storage Casks” (ISG 8 rev. 3), Reference C-1, was issued with updated guidance for misload analyses, stating that

Misload analyses may be performed in lieu of a burnup measurement. A misload analysis should address potential events involving the placement of assemblies into a SNF storage or transportation system that do not meet the proposed loading criteria. . . .

A misload analysis should consider:

- *misloading of a single severely underburned assembly and,*
- *misloading of multiple moderately underburned assemblies.*

ISG 8 rev. 3 continues, defining a single severely underburned assembly:

The severely underburned assembly for the single misload analysis should be chosen such that the misloaded assembly reactivity bounds 95% of the discharged PWR fuel population considered unacceptable for loading in a particular storage or transportation system with 95% confidence.

It also defines the moderately underburned assemblies:

The multiple moderately underburned assemblies for this analysis should be assumed to make up at least 50% of the system payload, and should be chosen such that the misloaded assemblies’ reactivity bounds 90% of the total discharged PWR fuel population.

Finally, it designates the location in the cask where the misloaded assembly should be placed:

“The misload analysis should also consider the effects of placing the underburned assemblies in the most reactive positions within the loaded system (e.g., middle of the fuel basket).”

ISG 8 rev. 3 was written to support the current standard practice of design basis criticality analysis that uses uniform or symmetric zone loading with bounding fuel characteristics (e.g., fuel type, enrichment, burnup) to accommodate loading of discharged assemblies with diverse characteristics. For uniform and

symmetric loading, it is straight forward to determine the most reactive position(s) in the canisters. On the other hand, the determination of the most reactive position(s) in an actual loaded canister for as-loaded criticality analysis being used for direct disposal of DPCs is more involved mainly due to the non-symmetric reactivity distribution.

C.3. ASSEMBLY MISLOAD METHODOLOGY

This section describes a misload analysis methodology to support as-loaded criticality analysis for a given site and a given canister. The methodology is based on the ISG 8 rev. 3 but is extended to include BWR assemblies supported by the BWR burnup credit methodology described in Reference C-2 and also cover the scenario where the right assemblies are being placed in the wrong position. The placement of the right assembly in the wrong position is a more likely misload scenario to go undetected in the disposal scenario since taking the wrong assembly would be discovered in subsequent canister loadings.

The methodology has been fully implemented and automated in UNF-ST&DARDS by using and extending the existing criticality analysis capabilities described in Reference C-2 including doing the analysis for year 9999 and using the assumptions for loss of neutron absorbers and degradation of carbon steel baskets. The misload analysis methodology is described below:

1. Select a site and canister.
2. Determine what discharged assemblies were in the pool (and any connected pool) during canister loading.
3. Determine the individual reactivity of each assembly available in the pool, as well as the assemblies in the loaded cask.
4. Identify the single severely underburned assembly and the multiple moderately underburned assemblies as described in Section C.3.1.
5. Generate a criticality importance map (i.e. how important is a canister position in terms of its contribution to the total criticality of the canister) for the canister model from fission densities using a uniform fuel loading as described in Section C.3.2.
6. Perform a criticality calculation using two approaches for a single assembly misload as described in Section C.3.3.
7. Perform a criticality calculation of the multiple assembly misload as described in Section C.3.4.
8. Perform a criticality calculation for the worst possible configuration assuming right assemblies were placed in wrong positions as described in Section C.3.5.
9. The highest k_{eff} from steps 5–7 above is the misload analysis result.

The methodology also assumes that damaged fuel loaded in damaged fuel cans has not been misloaded as the damaged fuel cans in general only fits in certain oversized positions inside the canister. It also assumes that no prior misloads have changed the inventory of the pools at the time of loading the analyzed canister.

C.3.1. Identification of Underburned Assemblies

To determine which underburned assemblies are to be considered for misload analysis, the Unified Database (UDB) within UNF-ST&DARDS is queried for assemblies that were present in the pool at the time the canister was loaded. A criticality calculation is performed on each of those assemblies using UNF-ST&DARDS and assuming one centimeter of water around the assembly, reflecting boundary conditions, a cooling time approximately the same as the analysis date (in our disposal case 7500 years) n , and using the disposal burnup credit isotopes presented in table 2. The result is a distribution of k_{inf} (see Figure C-1) that can be used to rank the assemblies in the pool according to reactivity.

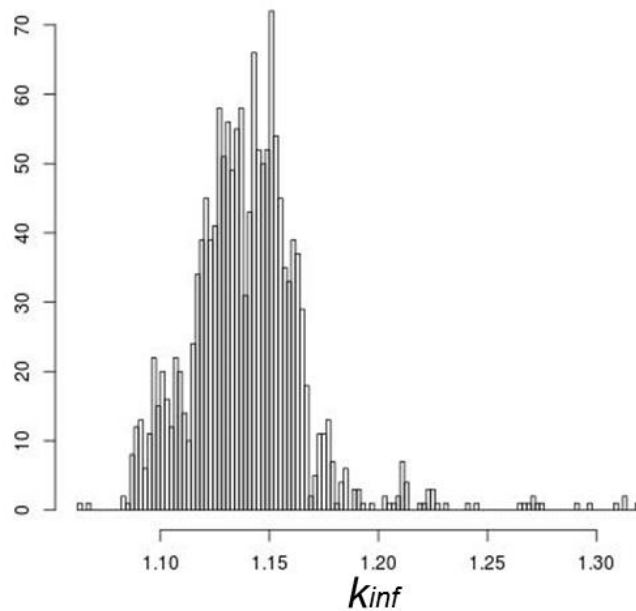


Figure C-1. Example distribution of k_{inf} for all assemblies in a pool at the time of loading a specific canister at a specific site. Y-axis shows number of assemblies in each bin.

For the analysis of the single severely underburned assembly, the most reactive assembly available is used as shown in Figure C-2 (left figure). For the moderately underburned assemblies, the first step is to identify the assembly that bounds 90% of the available discharged inventory. The assemblies corresponding to 50% of the analyzed cask (e.g., 16 for MPC-32, 19 for TSC-37) are selected as the moderately underburned assemblies in ascending reactivity order from the assembly that bounds 90% of the discharged inventory (Figure C-2, right figure).

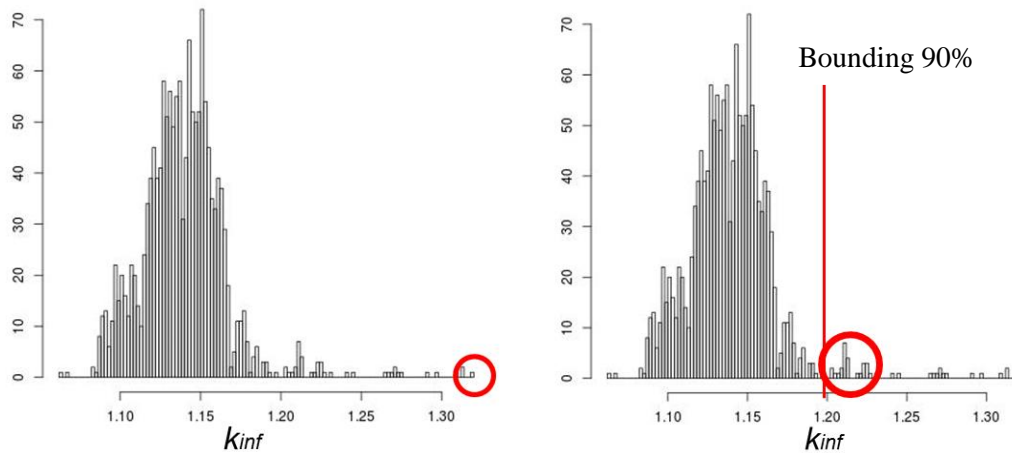


Figure C-2. The single severely underburned assembly (circled in red in the left plot) is the assembly with the highest k_{inf} . The multiple moderately underburned assemblies (circled in red in the right plot) are selected as the number of assemblies corresponding to 50% of the cask payload with the lowest available reactivity that bounds 90% (red line in right plot) of the assemblies available in the pool. Y-axis shows number of assemblies in each bin.

C.3.2. Generation of Criticality Importance Map Independent of

A criticality calculation is run to determine the most reactive region in a uniformly loaded canister. Based on the fission reaction rates in each position (canister cell), a zoned criticality importance map can be derived independent of actual loading (Figure C-3) for an MPC-32 cask design.

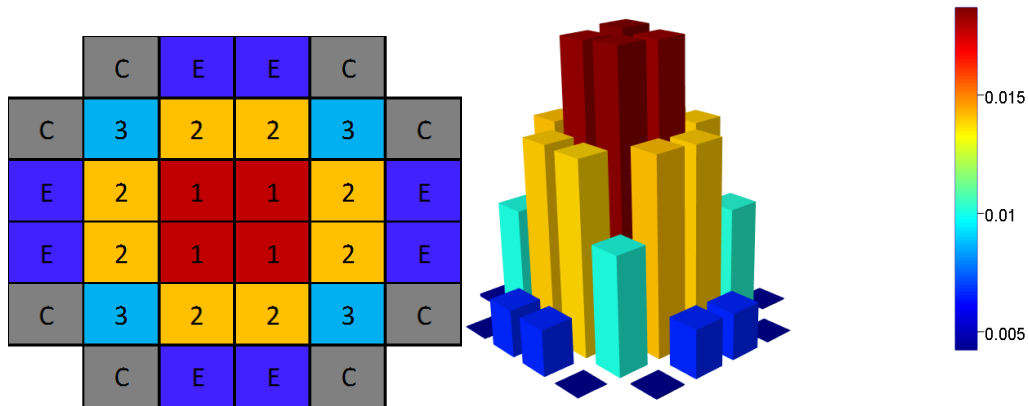


Figure C-3. A loading independent criticality importance map (left) generated by ranking the highest (indicated by 1) to lowest number of fissions generated in each position (canister cell) of a uniformly loaded MPC-32 canister. Both E (edge) and C (corner) are excluded from misloads due to high leakage. The right figure shows the fission reaction rate at each cell location.

This criticality importance map is similar to the map used in a regular uniform misload analysis in accordance to ISG-8, rev3. However, this importance map based on uniform loading is not suitable to be directly used in the as-loaded analysis.

C.3.3. Single Assembly Misload Analysis for As-Loaded Canister

Since each position in the cask for the as-loaded analysis is unique when it comes to reactivity, the most reactive position in the cask depends heavily on the loading of the canister and the reactivity of the selected assembly for misload. For the three sites evaluated in this work, two approaches were used to determine the most reactive single assembly misload.

The first approach includes analysis of the cask-specific fission density map that is automatically acquired by performing a regular as-loaded criticality analysis in UNF-ST&DARDS (Figure C-4). ISG 8 rev. 3 recommends that the assembly be placed in the most reactive position, which corresponds to the position with the highest number of fissions. The assembly in the position with the highest number of fissions is replaced by the severely underburned assembly identified previously.

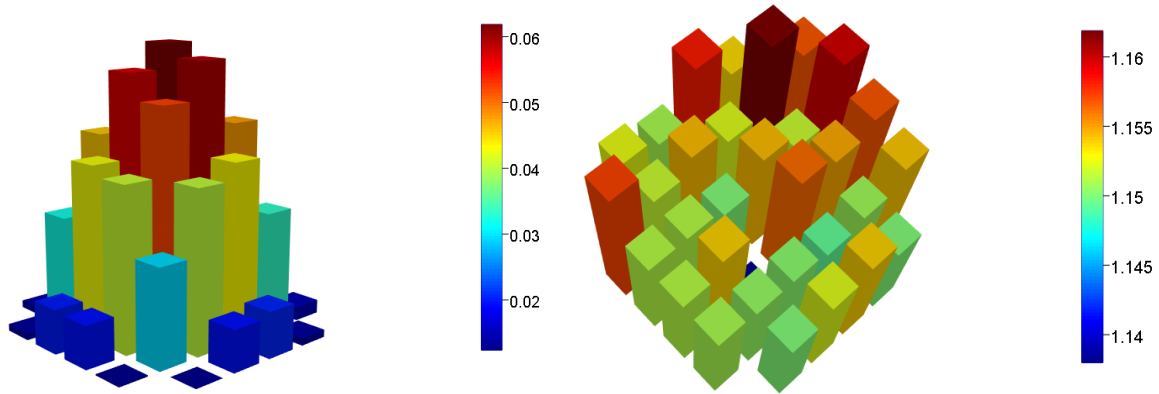


Figure C-4. Number of fissions (left) and individual assembly reactivity (right) for each position of an as-loaded MPC-32 cask.

For most as-loaded analysis cases, this approach takes out the most reactive assembly from the center region of the canister, which, depending on the loading, could actually lower the cask reactivity. A better approach for those cases would be to replace one of the assemblies neighboring the highly reactive one to drive up the system’s reactivity.

The second approach is therefore to determine which of the neighboring positions would drive the system reactivity the most if misloaded with a highly reactive assembly from the pool. The neighbors are filtered based on the importance map shown in Figure C-3 to find the neighbor closest to the center and compare the individual assembly reactivity (Figure C-4) to select the one with the lowest individual assembly reactivity value. This assembly is the one assembly impacting the most reactive position in the most significant negative direction.

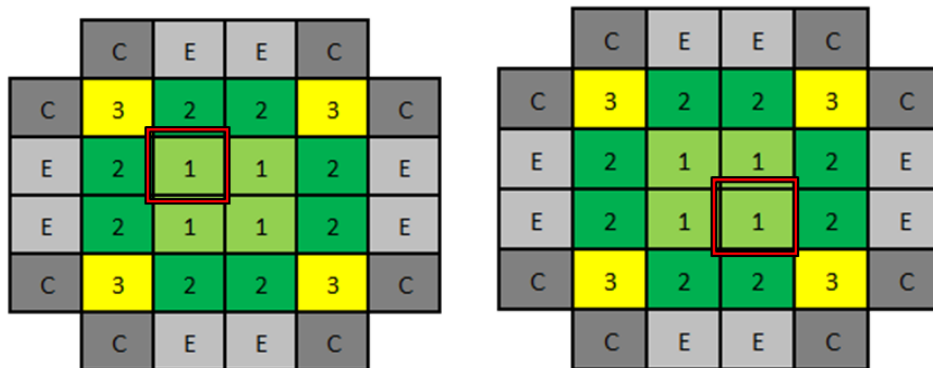


Figure C-5. Identified position for single assembly misload using highest reactivity approach (left) and neighbor nearest center with lowest reactivity approach (right)

These two approaches were used for the three sites analyzed to determine the highest reactivity increase in case of a misload. This methodology is expected to be consistent for all other designs and loadings. For the example cask shown in Figure C-4, the misloaded positions are shown in Figure C-5 and are both located at different locations in the center of the cask. The reactivity increase from placing the single severely underburned assembly in a position is shown in Figure C-6. In this example, the two positions with the highest reactivity increase were identified using the two approaches.

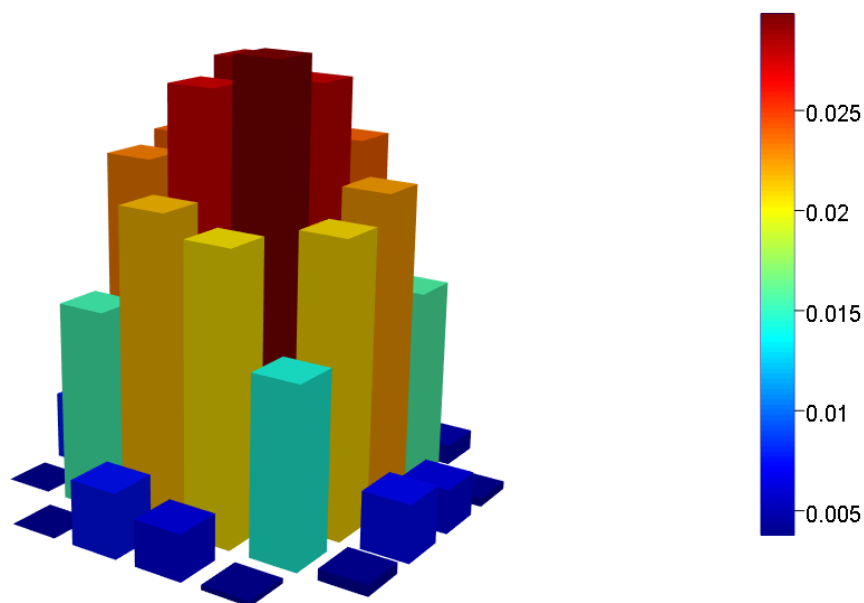


Figure C-6. Increase in reactivity from misloading the position with the single severely underburned assembly.

C.3.4. Multiple Assembly Misload

ISG 8 rev. 3 suggests that the analysis of multiple moderately underburned assemblies assumes that at least 50% of the payload is misloaded. The approach used to determine the multiple assembly misload is similar to the single position approach, but the position with the highest number of fissions does not need to be identified. Instead, the most reactive of the identified moderately underburned assemblies will be placed in the most center position according to the importance map in Figure C-3. If several positions have the same importance, the position with the lowest cell position number will be loaded. The resulting misload order for an MPC-32 canister is shown in Figure C-7.

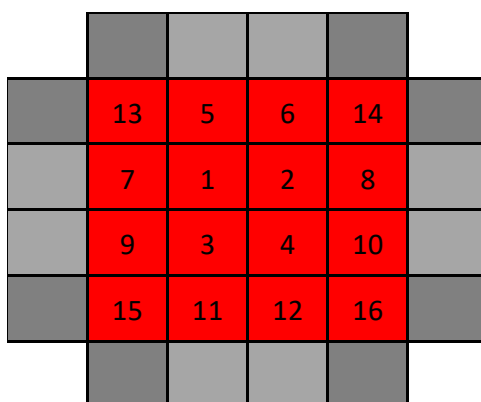


Figure C-7. Loading priority for an example as-loaded canister with multiple moderately underburned assembly misload based on the importance map and position cell number. The red positions indicate misloaded positions, while the others are still the as-loaded positions.

C.3.5. Worst and Optimal Configuration in an As-Loaded Canister

For as-loaded analysis, a third misload must be considered that is not applicable for the regular bounding analysis. The third misload is for the case in which the correct assemblies have been loaded into the canister in the wrong order. This scenario is the most likely scenario for disposal, as the previously mentioned, single severely underburned assembly and multiple moderately underburned assembly misloads are likely to be identified long before disposal.

The approach to account for this misload scenario is to rank all assemblies by their individual reactivities and then place them in the canister with the most reactive assembly closest to the center according to the importance map.

By reversing the order as discussed above, the lowest reactive optimal configuration is achieved. This is not a misload analysis scenario, but it can be used as a measure of how reactive the actual loading is compared to the optimal and worst configuration using the same assemblies. It may also be used for planning future loading campaigns to reduce reactivity of each loaded canister to support direct disposal of DPCs.

C.4. RESULTS

The misload methodology described above was used to evaluate three different sites with three different canister designs. All canister criticality calculations presented in this section have been performed using the UNF-ST&DARDS criticality process described in Reference C-2 for the loss-of-neutron-absorber degradation scenarios in year 9999. This is the same process used in the previous analyses in this report described in Appendix A and Appendix B.

C.4.1. Sequoyah (operating reactor site), 27 MPC-32 Canisters

Figure C-8 shows the result from the individual assembly reactivity calculations from the pool inventory at Sequoyah. Most assemblies have k_{inf} values distributed between 1.05 and 1.20, although a few assemblies have reactivity up to approximately 1.31. This suggests that the impact of a single severely underburned assembly misload could have a significant impact on the canister reactivity.

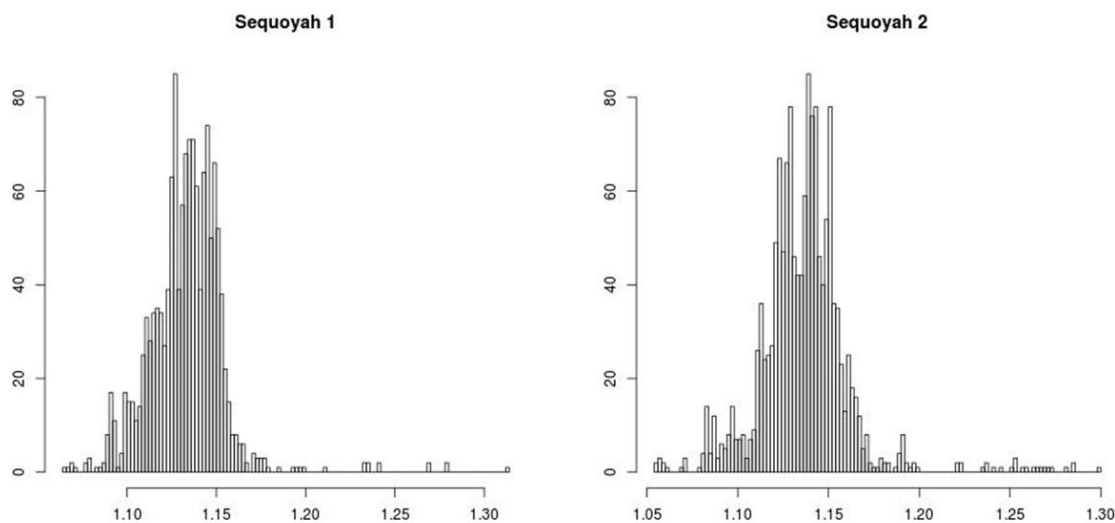


Figure C-8. Individual assembly reactivity distribution for the pool inventory at Sequoyah 1 and 2. Y-axis shows number of assemblies in each bin.

Figure C-9 depicts the as-loaded reactivity (presented by red dots) along with the reactivity variation between worst and optimal configurations (presented by vertical line). A large range indicates that the inventory is diverse, with some highly reactive assemblies and some low reactive assemblies, while a short range indicates a very uniform loading. An as-loaded reactivity high in the range usually indicates that the canister was loaded based on decay heat since high burnup assemblies (high decay heat and low reactivity) were placed in the outer part of the canister to limit the peak cladding temperature. An as-loaded reactivity that is low in the range can indicate that the canister is loaded for low dose since it warrants placing high burnup assemblies in the inner part of the canister to be shielded by the less active (but more reactive) assemblies on the edge. In the case for Sequoyah, no clear trend can be seen.

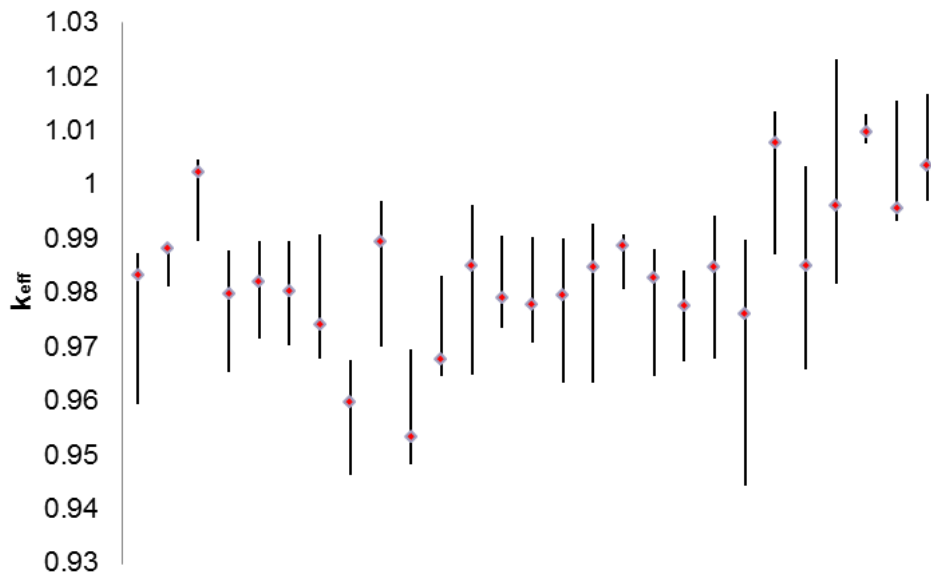


Figure C-9. The red markers indicate the reactivity of the loaded canisters at Sequoyah, and the black lines are the ranges between optimum and worst possible loading for reactivity using the same canister inventory.

Figure C-10 presents an increase in reactivity between misload and as-loaded canister in pcm for (1) two-different single severely underburned assembly misload approaches, (2) the multiple moderately underburned assembly misload and, (3) the worst configuration misload. It can be seen that any of the four different misload scenarios can yield highest reactivity increase, with

- single misload using highest fission density is most reactive 10 times,
- single misload using lowest reactive neighbor in the center is most reactive 12 times,
- multiple misload is most reactive 4 times, and
- worst configuration is most reactive 1 time.

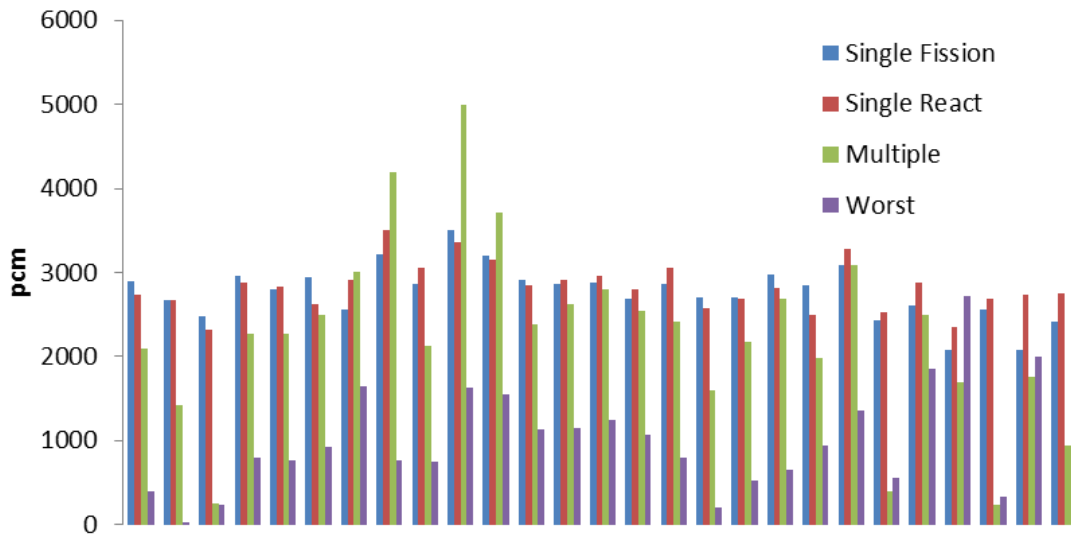


Figure C-10. Reactivity increase in pcm for each misload type and canister loaded at Sequoyah. Single Fission is the single assembly misload method misloading the position with the highest fission density, Single React is the single assembly misload method misloading the neighbor with lowest reactivity closest to the center, multiple is the multiple moderately underburned assembly misload and worst is the worst configuration misload.

The bounding misload case compared to the as-loaded calculation is presented in Figure C-11, where the average increase of reactivity from the misload analysis is 3,007 pcm with a range of 2,487–5,000 pcm.

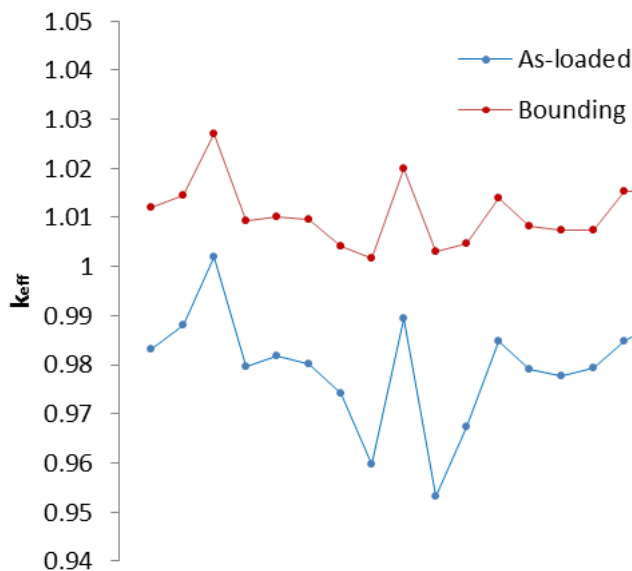


Figure C-11. The as-loaded reactivity and the most bounding of the misload types.

C.4.2. Zion (shutdown reactor site), 32 TSC-37 Canisters

Figure C-12 shows the results from the individual assembly reactivity calculations from the pool inventory at Zion. Most assemblies are distributed between 1.05–1.20, and in this case, there are also

groups of assemblies with reactivities up to 1.30 due to high enrichments and low burnup assemblies that were in the last cycle of the reactors before shutdown. This suggests that the impact of multiple moderately underburned assembly misload could yield most impact on canister reactivity.

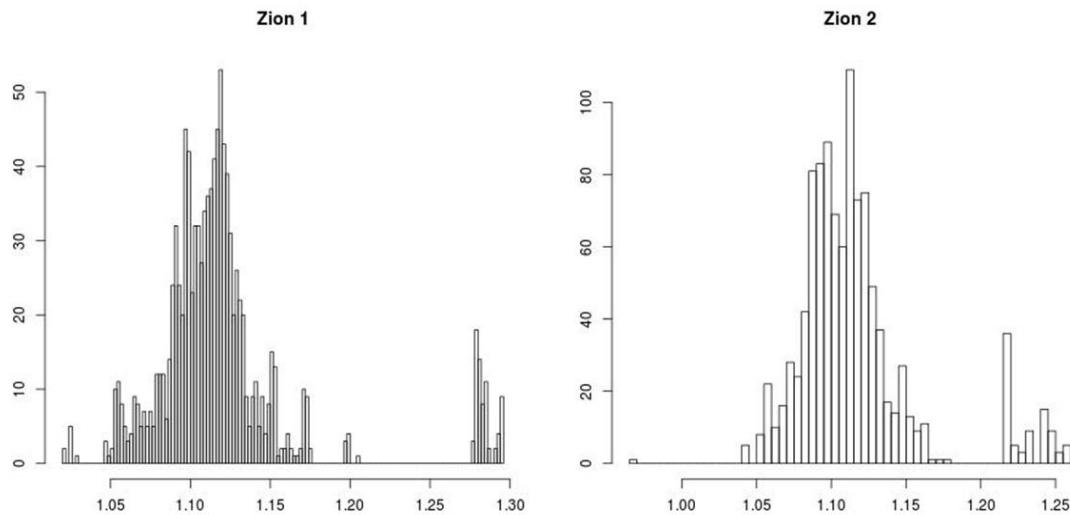


Figure C-12. Individual assembly reactivity distribution for the pool inventory at Zion 1 and 2. Y-axis shows number of assemblies in each bin.

The difference between optimal and worst loading shown in Figure C-13 is minimal for most canisters. The as-loaded k_{eff} is typically low for most of those canisters, indicating they may have been loaded based on low dose effects. The less uniformly loaded canisters containing fuel from the last cycle indicate that loading might have been designed for low temperatures.

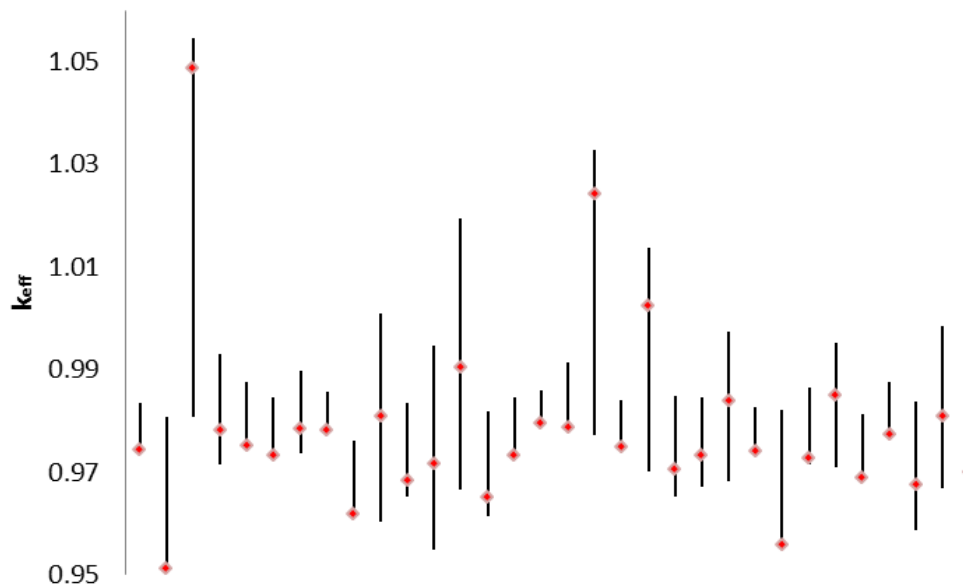


Figure C-13. Red markers indicate the reactivity of the loaded canisters at Zion, and the black lines are the ranges between optimized and worst possible loading for reactivity using the same canister inventory.

For the two different single, severely underburned assembly misloads—the multiple moderately underburned assembly misload and the worst configuration misload—the results are shown in Figure C-14 in pcm with an increase of reactivity compared to the as-loaded canister. For Zion, the multiple moderately underburned assembly misload dominate for most canisters except for those with the highest as-loaded reactivity, and those likely already had more reactive assemblies in the center locations. The figure shows the following:

- single misload using highest fission density is most reactive 1 time,
- single misload using lowest reactive neighbor in the center is most reactive 3 times,
- multiple misload is most reactive 28 times and,
- worst configuration never is most reactive.

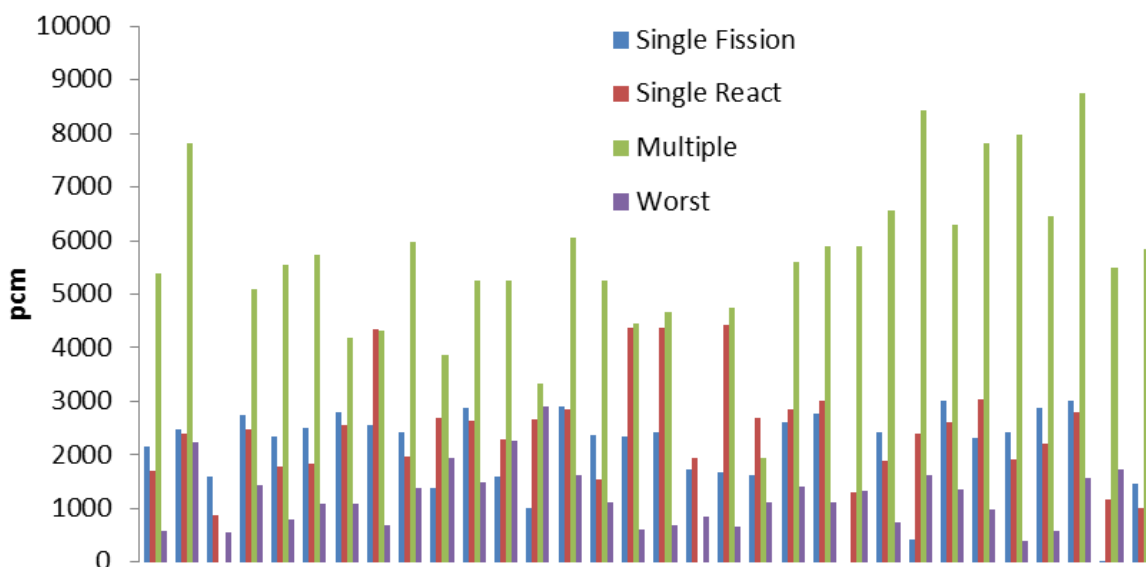


Figure C-14. Reactivity increase in pcm for each misload type and canister loaded at Zion. Single Fission is the single assembly misload method misloading the position with the highest fission density, Single React is the single assembly misload method misloading the neighbor with lowest reactivity closest to the center, multiple is the multiple moderately underburned assembly misload and worst is the worst configuration misload.

The bounding misload case compared to the as-loaded calculation is presented in Figure C-15, where the average increase of reactivity from the misload analysis is 5,444 pcm with a range from 1,585–8,747 pcm.

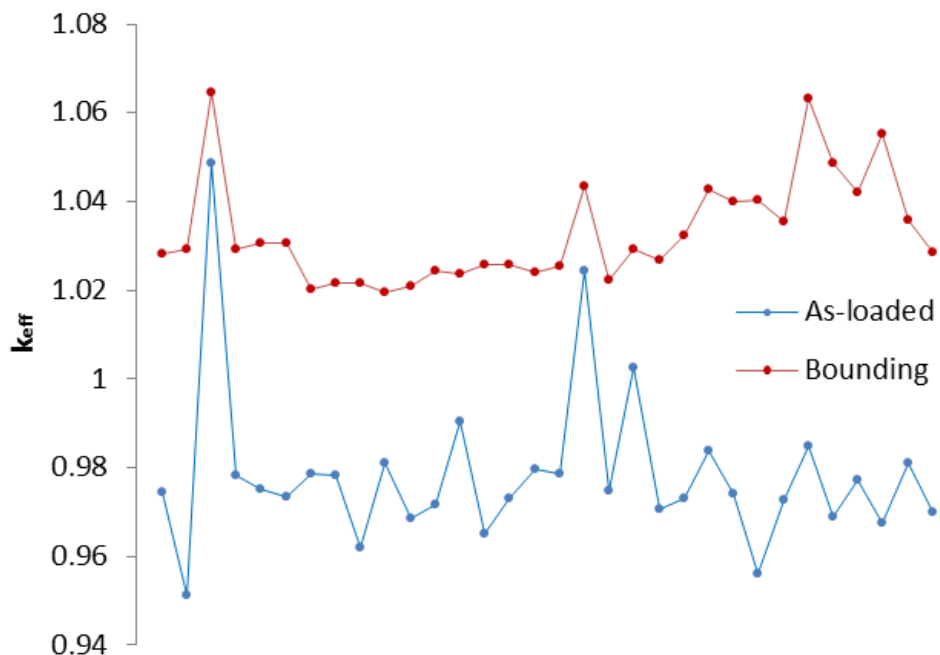


Figure C-15. The as-loaded reactivity and the most bounding of the misload types.

C.4.3. Browns Ferry, 40 MPC-68 Canisters

Figure C-16 shows the result from the individual assembly reactivity calculations from the pool inventory at Browns Ferry. Most assemblies are distributed between 1–1.10, and no assemblies with exceptionally high reactivity are available in the pools. This suggests that the impact of multiple moderately underburned assembly misload could have the highest impact on the canister reactivity.

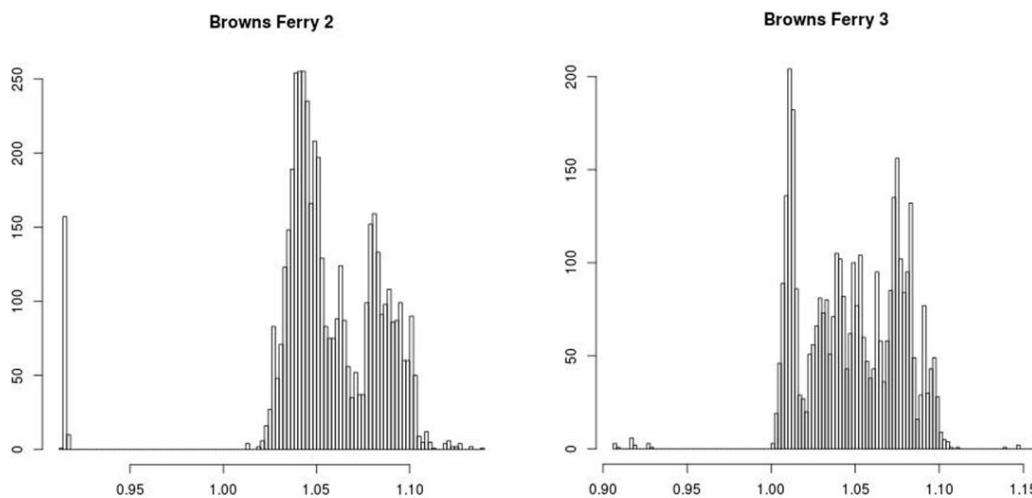


Figure C-16. Individual assembly reactivity distribution for the pool inventory at Browns Ferry 2 and 3. Y-axis shows number of assemblies in each bin.

The reactivity difference between the worst and optimal configuration is relatively small for all canisters, indicating a uniform loading and no particular bias toward being closer to worst or optimal configuration.

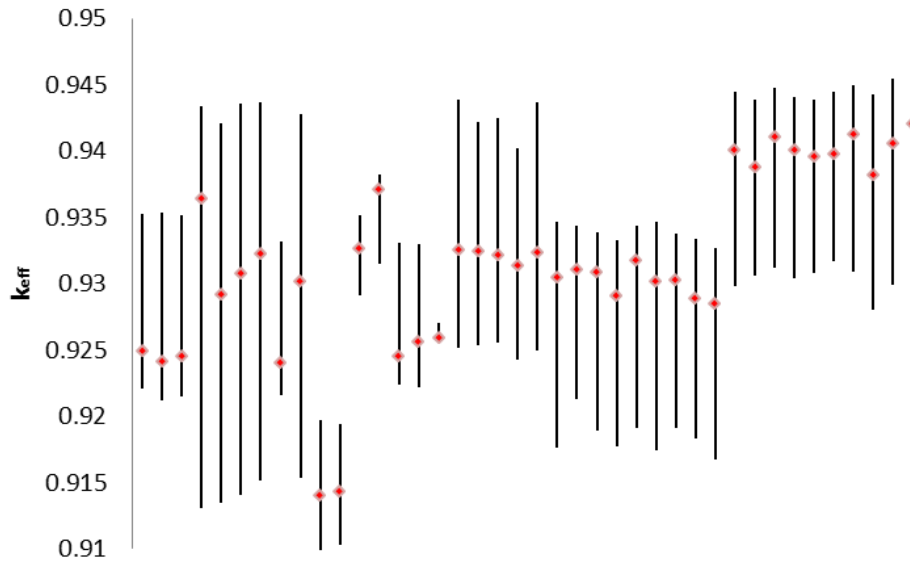


Figure C-17. Red markers indicate the reactivity of the loaded canisters at Browns Ferry, and black lines are the range between optimized and worst possible loading for reactivity using the same canister inventory. Notice that the range in k_{eff} is much smaller than for Sequoyah and Zion.

For the two different single, severely underburned assembly misloads—the multiple moderately underburned assembly misload and the worst configuration misload—the results are shown in Figure C-18 in pcm, with an increase of reactivity compared to the as-loaded canister. For Browns Ferry, the multiple moderately underburned assembly misload dominates all canisters due to the lack of assemblies with very high reactivity available in the pool and mostly uniformly loaded canisters.

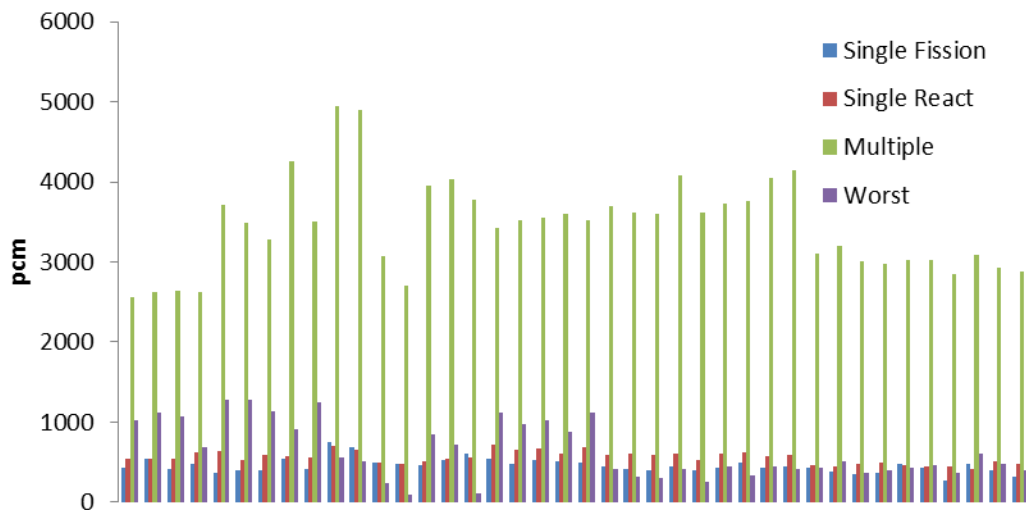


Figure C-18. Reactivity increase in pcm for each misload type and canister loaded at Browns Ferry. Single Fission is the single assembly misload method misloading the position with the highest fission density, Single React is the single assembly misload method misloading the neighbor with lowest

reactivity closest to the center, multiple is the multiple moderately underburned assembly misload and worst is the worst configuration misload.

The bounding misload case compared to the as-loaded calculation is presented in Figure C-19, where the average increase of reactivity from the misload analysis is 3,451 pcm with a range from 2,567–4,943 pcm.

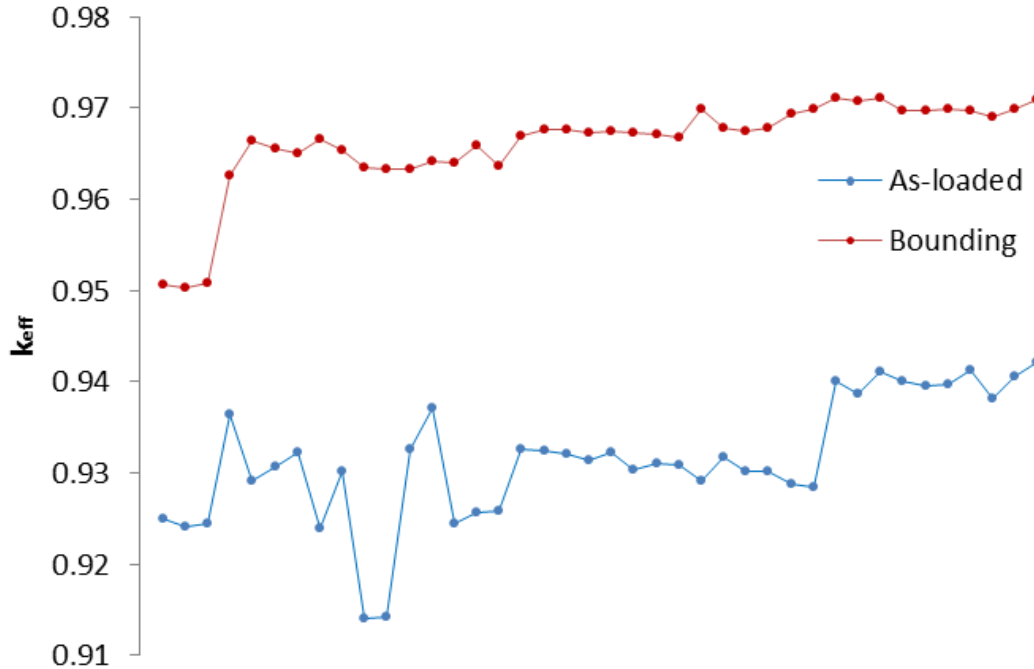


Figure C-19. The as-loaded reactivity and the most bounding of the misload types.

C.5. CONCLUSION

This appendix presents a misload methodology for as-loaded criticality analysis for a disposal scenario that includes loss-of-neutron-absorbers. The misload methodology has been applied to evaluate 99 DPCs stored at three sites. In addition to the suggested misload types in ISG 8 rev. 3, an additional type (worst case configuration) was implemented to specifically address the as-loaded criticality analysis approach, where the correct inventory was assumed to be incorrectly loaded in the most reactive configuration. This worst-case configuration is considered the most likely misload scenario for disposal as the other misload scenarios involving selection of incorrect assemblies should be detected during the subsequent loadings. If no misload has been identified for a site that completed loading of all discharged assemblies in DPCs, worst case scenario should be used to support as-loaded criticality analysis for that site. The bounding misload type and increase in reactivity is highly dependent on both the canister inventory and the spent fuel pool inventory available at the time of the loading. The selected sites have a wide range of characteristics covering PWR and BWR reactors, the most commonly used DPCs, and different assembly reactivity distributions in the spent fuel pool. The evaluation indicates that the proposed methodology is applicable to other sites and DPC models as well.

The methodology has also been implemented in UNF-ST&DARDS for automated misload analysis for all canisters where loading maps and canister criticality models are available.

Figure C-20 presents the updated criticality roadmap from Figure 25 in the main body of this report. The development of the misload analysis methodology is considered complete, but the box will remain yellow

until the approach has been applied to all canisters. An automated analysis will be possible as the new canister models are implemented.

Criticality Analysis Roadmap					
Feasibility Assessment	Identify sources of water and potential for pooling in DPC by host media				
	Perform DPC model development to establish baseline	Develop and apply misload analysis methodology	Assess radiolysis rates required for significant impact to in-package chemistry	Groundwater analyses for different geologies	Identify performance assessment parameters directly influenced by criticality consequence
	Review neutron absorber and basket material performance data for existing DPCs	Development of BWR burnup credit methodology	Evaluation of chemistry ranges inside DPCs and corrosion rates on primary components	Develop probability based sampling framework for generic distributions	
	Perform envelope analysis on key parameters that lead to criticality	Evaluate probability of criticality	Develop geochemistry models accounting for in-package chemistry effects	Establish model for evaluating reaction kinetics and impacts on PA parameters	
	Evaluate envelope parameters against geochemistry model results to refine credible range	Evaluate criticality consequence effects on repository distributions		Generate risk curves per influence parameter	
Licensing Determination	Criticality validation (e.g., experiments with Cl in solution, relevant configurations)	Justify and incorporate site-specific parameter distributions	Justify use of non-bounding assumptions	Validate site-specific geochemistry models	

Figure C-20. DPC criticality analyses roadmap as described in Ref. [4], with the color yellow indicating a work in progress and green indicating completion.

C.6. REFERENCES

- C-1. Division of Spent Fuel Storage and Transportation, Interim Staff Guidance – 8, Revision 3, Burnup Credit in the Criticality Safety Analyses of PWR Spent Fuel in Transportation and Storage Casks, U.S. Nuclear Regulatory Commission, September 26, 2012.
- C-2. J. B. Clarity, H. Liljenfeldt, and K. Banerjee, *Criticality Process, Modeling and Status for UNF-ST&DARDS*, FCRD-NFST-2015-000440, Rev. 1, US Department of Energy, Nuclear Fuel Storage and Transportation Planning Projects (July 2016).

This page is intentionally left blank.

**APPENDIX D.
FY 2018 Criticality Study**

This page is intentionally left blank.

D.1. INTRODUCTION

This appendix documents work performed supporting the US Department of Energy (DOE) Office of Nuclear Energy (NE) Spent Fuel and Waste Disposition (SFWD) under work breakdown structure element 1.08.01.03.05 “Direct Disposal of Dual Purpose Canisters.” In particular, this appendix fulfills the M4 milestone, M4SF-18OR010305013, “Update of DPC Direct Disposal Criticality Analysis Report” within work package SF-18OR01030501, “Direct Disposal of Dual Purpose Canisters - ORNL.”

This appendix presents the dual-purpose canister (DPC) criticality evaluations performed in FY 2018 to support the feasibility determination of direct disposal of DPCs and extends the work reported in the main body of this report. The main objectives of the FY 2018 DPC disposal criticality study were to develop criticality calculation templates for the NUHOMS[®] 24PT1 [D-1] and NUHOMS[®] 32PT [D-2] dry shielded canisters (DSCs) and to perform as-loaded criticality analyses for sites using these two canister types and the loading maps of which are currently available in the database. A total of 60 as-loaded canisters from five sites were analyzed over the time interval between calendar years 2015 and 22,000 using the burnup credit methodology described in the previous sections of this report. The analyzed sites were San Onofre (17 canisters), Palisades (11 canisters), Millstone (18 canisters), Ginna (6 canisters), and Kewanee (8 canisters).

Criticality analyses models were developed for the intact canister configuration, applicable to normal conditions of transport and storage, and for degraded material configurations, applicable to canister repository time frame. The degraded material configurations assume two scenarios: (1) complete loss of the fixed neutron absorber (i.e., ¹⁰B) without fuel basket geometry changes and (2) complete degradation and loss of basket materials, including neutron absorber plates and carbon steel basket components (e.g., basket support discs). The effect of canister material degradation and neutron absorber loss is a significant increase in k_{eff} . The intact canister configurations were analyzed for 9 analysis dates between 2015 and 2100. The degraded material configurations were analyzed for 17 analysis dates between 2015 and 22,000.

As mentioned in the main report, neutron moderation by water is needed for a waste package to achieve criticality. However, the groundwater (or pore water) that may flood a breached DPC will contain various dissolved aqueous species. Seventeen species were studied in the main report, and it was determined that Cl, Li, and B provide the maximum reduction in canister reactivity because of their large neutron absorption cross sections. However, available groundwater data indicate that chlorine (as chloride) is the only naturally abundant neutron-absorbing element in groundwater that can provide a significant reduction in reactivity and is available in most of the repository concepts under consideration in varying quantity. Analyses were performed to determine the maximum chlorine requirement to suppress criticality of canisters with the potential to form critical configuration in a repository time frame. The impact of chlorine (in terms of NaCl) concentration in groundwater on the reactivity of as-loaded DPCs exceeding a k_{eff} value of 0.98 was evaluated for the calendar year 22,000. Previous chlorine concentration effects on k_{eff} documented in this report were evaluated for the calendar year 9,999. The impacted DPCs will be reevaluated for the calendar year 22,000 in the future. Note that within the time interval between the calendar years 2015 and 22,000, canister k_{eff} initially decreases with increasing decay time, reaches a minimum value, and then increases with increasing decay time. Hence the k_{eff} value for the calendar year 22,000 is slightly higher than that for the calendar year 9,999.

Canister misload analyses were performed for a worst-canister-misload configuration scenario, which is described in Sect. C.3.5. The assumption for this scenario is that the correct assemblies have been loaded into a canister but in the wrong order. The worst-misload configuration is obtained by placing fuel assemblies in the canister with the most reactive assembly closest to the canister center. The approach to misloaded assembly selection is to rank all assemblies by their individual reactivities, i.e., k_{inf} values. Currently, misload k_{eff} values are determined assuming all fuel assemblies in the canister have a decay time of 9,500 years. The misload analysis was performed for a total of 49 canisters containing intact fuel

assemblies and loaded to full capacity. The 11 San Onofre Unit 1 canisters not analyzed, which contain damaged fuel and/or empty locations, will be analyzed in the future.

Filler material may be used to maintain canister subcriticality during disposal. A nonhydrogenous filler material can reduce k_{eff} by displacing the pure water moderator assumed to flood a canister over the repository time frame. The height of a filler material, consisting of 68% aluminum and 32% pure water by volume, required to maintain canister subcriticality was determined for a representative canister predicted to have a k_{eff} value greater than 0.98 in 22,000 assuming complete loss of neutron absorber.

Criticality models and criticality analysis results for sites using the NUHOMS[®] 24PT1-DSC are presented in Sect. D.2. Criticality models and criticality analysis results for sites using the NUHOMS[®] 32PT-DSC are presented in Sect. D.3. The filler height calculation is presented in Sect. D.4.

D.2. NUHOMS[®] 24PT1-DSC

The NUHOMS[®] 24PT1-DSC is dedicated to storage and transportation of irradiated Westinghouse (W) 14×14 pressurized water reactor (PWR) fuel assemblies and non-fuel components. This canister is a component of the NUHOMS[®] MP187 transportation system [D-1]. San Onofre Nuclear Generation Station (SONGS) Unit 1 (SONGS1) was a Westinghouse three-loop PWR using the W 14×14 fuel type. The power reactor was permanently shut down on November 3, 1992, and the nuclear facility is undergoing decommissioning currently. Fuel assemblies discharged from the power reactor are stored at the SONGS independent spent fuel storage installation (ISFSI) in 17 NUHOMS[®] 24PT1-DSCs. These canisters contain 395 SONGS1 spent nuclear fuel (SNF) assemblies.

The NUHOMS[®] 24PT1-DSC consists of a stainless steel cylindrical shell with top and bottom carbon steel shield plugs, inner and outer bottom stainless steel closure plates, and outer top stainless steel closure plate.

The fuel basket defines 24 fuel locations and includes 26 spacer discs made of carbon steel and four support rods made of precipitation-hardened steel. The fuel tubes are made of stainless steel. The fuel basket utilizes fixed neutron absorbers to maintain subcriticality with optimum neutron moderation. The neutron absorber panel material is Boral[®]. A bottom spacer was installed underneath each W 14×14 fuel assembly to center the fuel in the DSC.

D.2.1. Criticality Model for the Intact XSO14W Fuel Assembly Type

The fuel assemblies irradiated in SONGS1 power reactor were W 14×14 fuel assemblies with stainless steel cladding identified in the nuclear fuel database [D-3] as XSO14W. Four W 14×14 zirconium-clad mixed oxide (MOX) fuel assemblies, identified as the XSO14WM type in the database, were also irradiated in the SONGS1 power reactor. A XSO14W fuel assembly has 180 fuel rods, 16 stainless steel guide tubes, and 7 spacer grids made of Inconel-718. Only the active fuel region of a fuel assembly is explicitly modeled. A horizontal cross-sectional view of the model for the fuel assembly type XSO14W through the active fuel region is shown in Figure D-1. Fuel compositions in the intact XSO14W fuel assembly model consist of oxygen and the set of isotopes reported in Table , which is recommended for SNF storage and transportation burnup credit criticality analyses. The active fuel region of an intact XSO14W fuel assembly is modeled as 18 uniform axial zones with nuclide concentrations based on assembly average burnup and the PWR 18-zone axial burnup profiles currently used in UNF-ST&DARDS neutronics calculations (see Sect. 3.1).

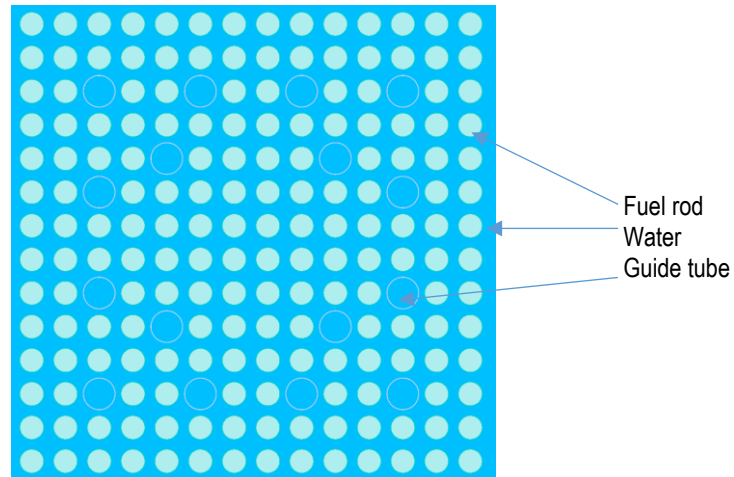


Figure D-1. Horizontal cross-sectional view of the XSO14W fuel assembly model.

D.2.2. Criticality Model for Damaged UO₂ Fuel Assemblies

Nine NUHOMS® 24PT1-DSCs contain damaged UO₂ fuel assemblies. The damaged fuel assemblies were placed in failed fuel cans. A NUHOMS® 24PT1-DSC may contain up to four failed fuel cans loaded in designated locations. Burnup is not credited for damaged fuel in damaged fuel cans. A damaged fuel assembly is represented as the design basis UO₂ fresh fuel assembly with an initial enrichment of 4.0 wt% ²³⁵U used in the criticality safety analysis [D-4].

D.2.3. Criticality Model for Intact MOX Fuel Assemblies

Two NUHOMS® 24PT1-DSCs contain a total of four intact MOX fuel assemblies. The intact MOX fuel assemblies were placed in failed fuel cans. A MOX fuel assembly is represented as the design-basis MOX fuel assembly used in the criticality safety analysis [D-5]. A horizontal cross-sectional view of the design-basis MOX fuel assembly and assembly plutonium loading are shown in Figure D-2.

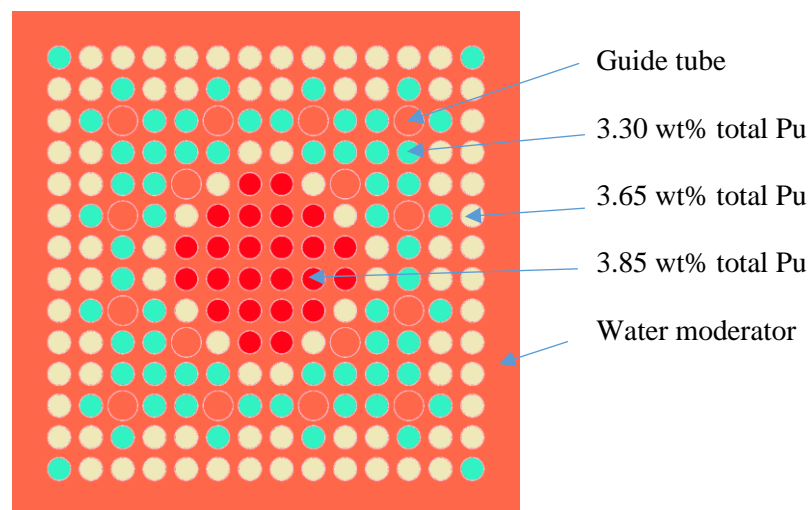


Figure D-2. Horizontal cross-sectional view of the MOX fuel assembly model.

D.2.4. SONGS1 Unit 1 Irradiated Non-Fuel Hardware

Non-fuel components include thimble assemblies, reactor control cluster assembly, and secondary neutron source assemblies. A fuel assembly may contain one of the three different non-fuel components inserted into its guide tubes. No credit is taken for the presence of non-fuel hardware within a fuel assembly. Moderator water is modeled in place of non-fuel components, which is conservative with respect to criticality.

D.2.5. Dummy Assembly

One NUHOMS® 24PT1-DSC contains a dummy assembly in basket cell number 9. A dummy assembly is an unirradiated stainless steel-encased structure that approximates the weight and center of gravity of a fuel assembly [D-4]. Hence, the dummy fuel assembly was modeled as a typical XSO14W fuel assembly with 179 UO₂ fuel rods being replaced with solid stainless steel rods with a radius of approximately 0.526 cm. This radius was deduced based on the assembly rod length of the W 14×14 steel clad fuel, 377.47 cm (148.61 in.), and weight per rod, 2.64 kg (5.82 lb) [D-6].

D.2.6. Criticality Model for Intact Canister Configurations

A criticality analysis model was developed for the intact (regular) canister configuration based on the criticality safety analysis reports used by the vendor to demonstrate compliance with both 10 CFR 71 [D-4] and 10 CFR 72 requirements [D-7]. The regular canister model is intended for use in criticality analyses of canisters under normal conditions of transport/dry storage. The fuel basket is intact, fuel assemblies are centered, and the mass density of water moderator and reflector is 1 g/cm³ in this model. Fuel compositions consist of oxygen and the set of isotopes reported in Table .

Verification of the regular canister model was performed by comparison to a reference k_{eff} value provided in the Safety Analysis Report (SAR) (Ref. [D-7]) for an infinite array of transportation packages under normal conditions of transport. The package model consists of the NUHOMS® 24PT1-DSC surrounded by a packaging structural shell, gamma shield, and neutron shield. Mirror reflective conditions were specified for the package X and Y sides to simulate an infinite array of packages. The reference k_{eff} value for the infinite array of packages containing W 14×14 steel-clad fuel assemblies centered in each guidesleeve is 0.8581 ± 0.0013 (one sigma) [D-7, Table 6.4-1]. The reference k_{eff} value was obtained with the KENO-Va Monte Carlo criticality code and the 44-neutron group library based on ENDF-B/5 in the SCALE 4.4 code package [D-3]. A similar model was developed for an infinite array of packages, and the k_{eff} value for this model was calculated with KENO-VI and the continuous cross-section library ce_v7 based on ENDF/B-VII in the SCALE 6.2.2 code package. The SCALE 6.2.2 k_{eff} value is 0.85517 ± 0.00019 . The difference of $\Delta k_{eff} = 0.003$ between SAR and current calculations may be attributed to differences between the SCALE code versions and cross-section libraries used in those calculations. A criticality validation of the SCALE 4.4 code package was provided in the criticality safety analysis [D-7]. That validation determined an upper subcritical limit (USL) of 0.9401 from the trending analysis of the benchmark calculations and an administrative margin of 0.05. By using a similar trending analysis, the USL value would be 0.9464 for criticality benchmark calculations using SCALE 6.2 and the ENDF/B-VII data [D-9]. Hence, these validation studies indicate an approximately 600 pcm difference between expected k_{eff} bias and bias uncertainty values for SCALE 4.4 and SCALE 6.2 criticality calculations.

D.2.7. Criticality Models for Material Degradation Scenarios

Models were developed for two degradation scenarios because the fuel basket in this canister design contains neutron absorber panels and carbon steel disc plates: (1) complete loss of neutron absorber and (2) complete loss and degradation of the neutron absorber panels and support disc plates. The former scenario is referred to as the loss-of-neutron-absorber scenario, and the latter scenario is referred to as the degraded basket material scenario. The model for the loss-of-neutron-absorber scenario uses pure water in place of basket aluminum and absorber plates. A horizontal cross-sectional view of the canister model

assuming a loss-of-neutron absorber is shown in Figure D-3. The basket material degradation scenario has the potential of producing a compact fuel assembly geometry configuration. Figure D-4 shows a horizontal cross-sectional view of the canister model for the degraded basket material scenario. In this configuration, the spacing between fuel tubes was eliminated and fuel assemblies were displaced inward to produce the most reactive fuel configuration. Fuel compositions in these models consist of oxygen and the set of isotopes reported in Table A-1, which is recommended for post-closure burnup credit criticality analyses.

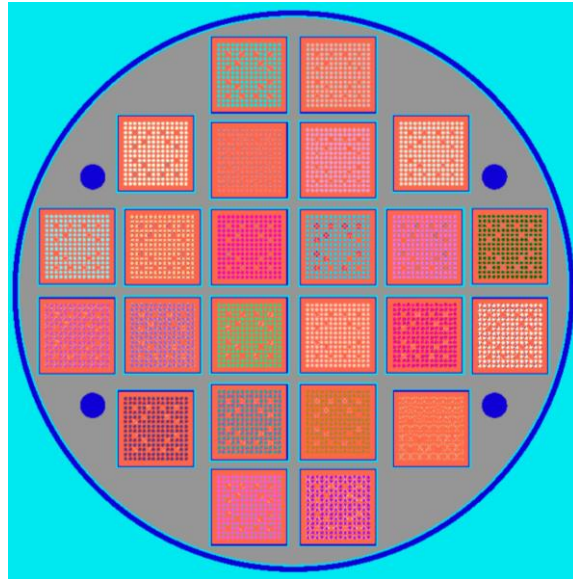


Figure D-3. Horizontal cross-sectional view of the NUHOMS® 24PT1-DSC model through a disc plate for the loss-of-neutron-absorber scenario.

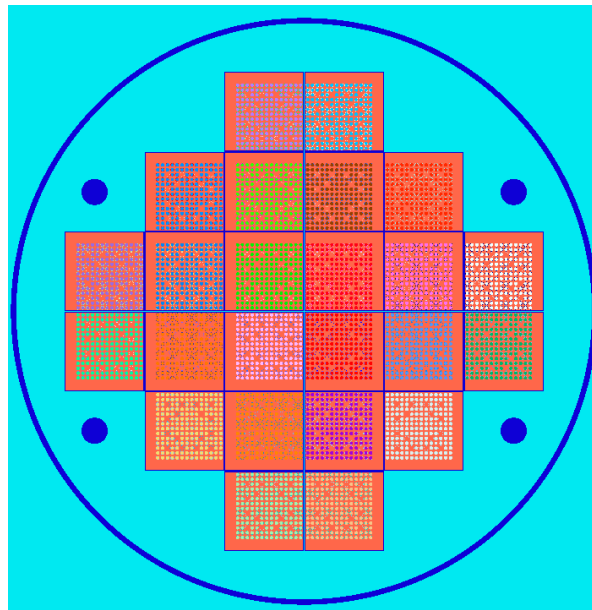


Figure D-4. Horizontal cross-sectional view of the NUHOMS® 24PT1-DSC model for the degraded basket scenario.

D.2.8. Criticality Model for Misload Calculations

A misload criticality analysis was performed for six SONGS1 SNF canisters containing intact fuel assemblies and loaded to full capacity. A total of 11 SONGS1 SNF canisters containing damaged fuel and/or empty locations were not analyzed. The canister misload model is based on the assumption that the correct assemblies have been loaded into the canister but in the most reactive configuration. This configuration is referred to as the worst-misload configuration in Sect. C.3.5. Fuel assembly placement for the worst-misload configuration is illustrated in Figure D-5. The numbers on the figure indicate the rank of an individual fuel assembly based on assembly k_{inf} values at a decay time of 9,500 years. The fuel composition for the misload model includes oxygen and the degradation disposal nuclides presented in Table A-1. The neutron absorber is neglected in this model (i.e., loss-of-neutron-absorber scenario).

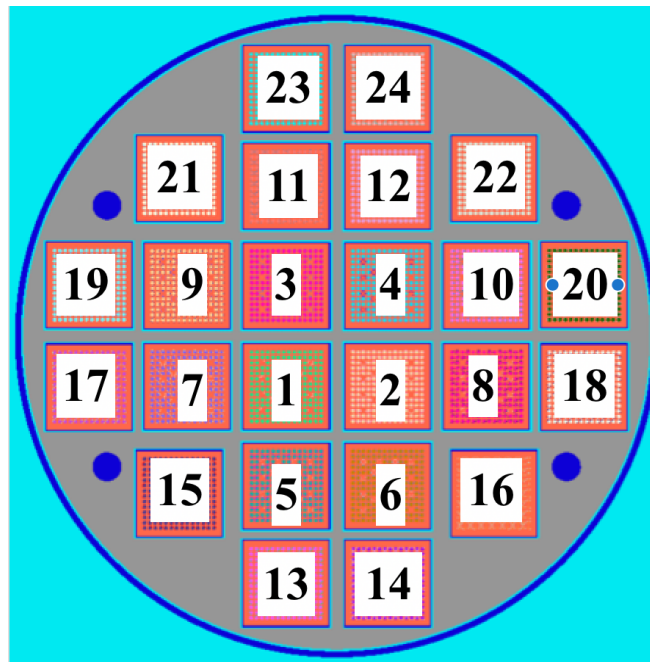


Figure D-5. Illustration of fuel assembly ranking for the worst-misload configuration of the NUHOMS® 24PT1-DSC.

D.2.9. Criticality Calculations Results for SONGS1 SNF Canisters

Criticality calculations were performed for decay times within the time interval between calendar years 2015 and 22,000 using the canister models developed for the as-loaded disposal criticality analysis of the SONGS1 SNF under three scenarios: (1) intact (or regular) fuel basket configuration, (2) loss-of-neutron absorber, and (3) degraded basket materials. Figure D-6 shows k_{eff} variation as a function of calendar year. The one sigma statistical uncertainty for all k_{eff} values is 0.0003 or less. In the figure, time variation between 2000 and 2100 is shown on a linear scale and time variation between 2100 and 22,000 is shown on a logarithmic scale.

The estimated k_{eff} values for the 17 canisters with an intact fuel basket configuration vary between 0.6766 and 0.7985 over the time interval between calendar years 2015 and 2100; that is, all k_{eff} values are below the 0.98 subcritical limit. For the loss-of-absorber scenario, the k_{eff} values for the 17 canisters vary between 0.7630 and 0.8786 over the time interval between calendar years 2015 and 22,000; that is, all estimated k_{eff} values are below the 0.98 subcritical limit for repository time frame. For the material

degradation scenario, the estimated k_{eff} values for the 17 canisters vary between 0.8855 and 1.0589 over the time interval between calendar years 2015 and 22,000. Out of 17 DPCs, five canisters are above the representative subcritical limit of 0.98 throughout the time interval analyzed.

For the five canisters the k_{eff} values of which are predicted to exceed the k_{eff} subcriticality limit of 0.98 assuming material degradation scenario, the pure water was replaced with groundwater compositions of various NaCl concentrations and the models thus modified were used to determine k_{eff} as a function of NaCl concentration. Figure D-7 presents k_{eff} variation as a function of NaCl concentration for those five canisters in the calendar year 22,000. A minimum required chlorine concentration in the groundwater of 1.092 mol/kg H₂O is determined to maintain a subcritical state. In this context, it is also important to note that a saturated NaCl brine has a concentration of approximately 6 molal.

Figure D-8 shows a k_{eff} increase between the worst-misload scenario and the as-loaded configuration for the six SONGS1 SNF canisters fully loaded with intact fuel assemblies. This increase varies between approximately 500 and 2000 pcm.

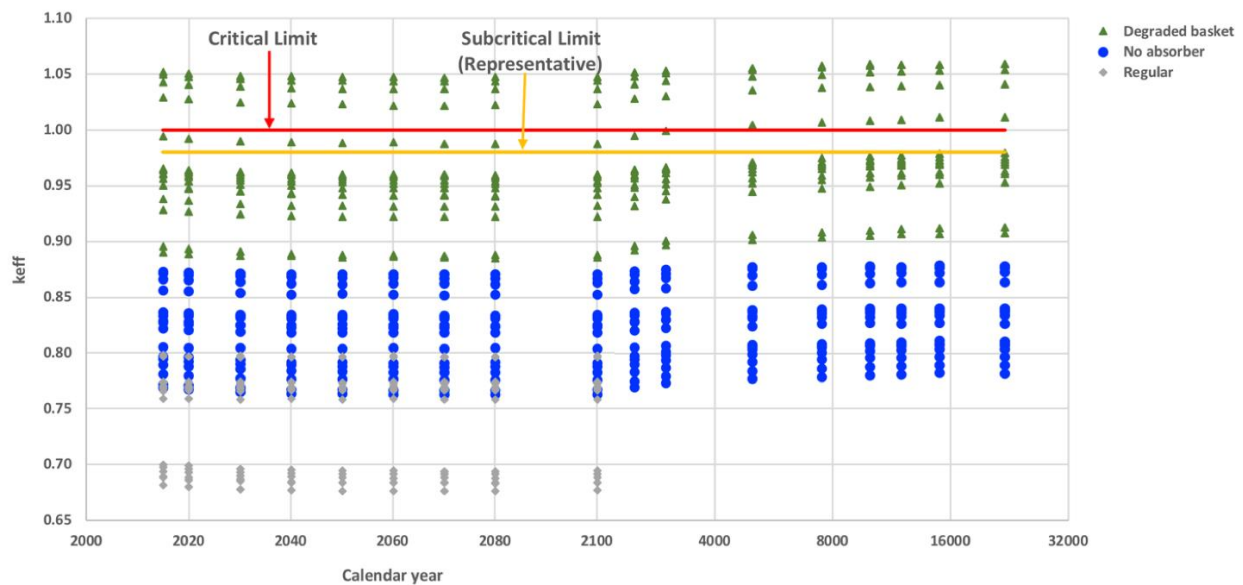


Figure D-6. k_{eff} vs. calendar year for the SONGS1 SNF canisters with degraded basket materials, no neutron absorber, and regular configurations.

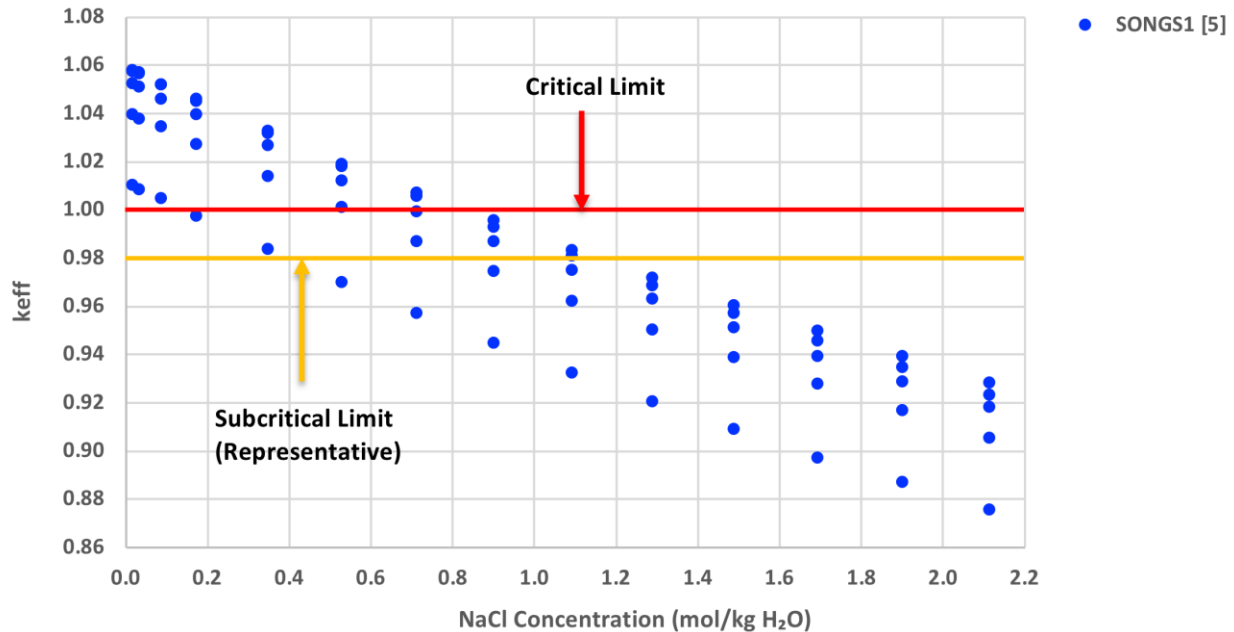


Figure D-7. k_{eff} vs. NaCl concentration for SONGS1 SNF canisters with $k_{eff} > 0.98$ for the degraded basket scenario (numbers in brackets = number of DPCs).

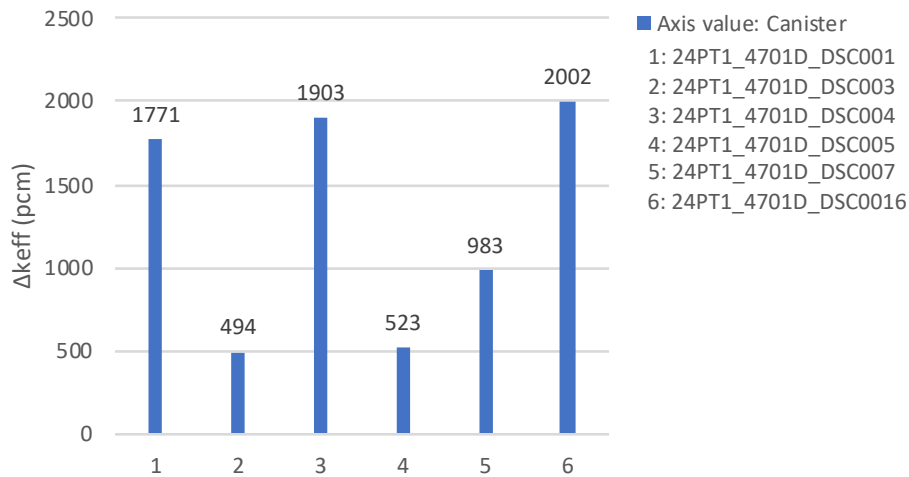


Figure D-8. k_{eff} increase between the worst-misload scenario and the as-loaded configuration for six SONGS1 SNF canisters.

D.3. NUHOMS® 32PT-DSC

The fuel classes authorized for loading in the NUHOMS® 32PT-DSC include intact B&W 15×15, Combustion Engineering (CE) 14×14, CE 15×15, W 17×17, W 15×15, and W 14×14 fuel assemblies (with or without control components) [D-10]. Damaged fuel assemblies are not authorized for loading in this canister. Intact fuel assemblies may contain control components (CCs), including burnable poison rod assemblies, thimble plug assemblies, control rod assemblies, control element assemblies, rod control assemblies, axial power shaping rod assemblies, orifice rod assemblies, vibration suppression inserts, neutron source assemblies, and neutron sources. Up to 32 CCs are authorized for storage in a canister.

The NUHOMS® 32PT-DSC consists of a stainless steel cylindrical shell with top and bottom carbon steel shield plugs, inner and outer bottom stainless steel closure plates, and outer top stainless steel closure plate. This canister has four subtypes: 32PT-S100, 32PT-S125, 32PT-L100, and 32PT-L125 defining a short canister, which has a length of 472.948 cm (186.2 in.), and a long canister, which has a length of 488.188 cm (192.2 in). The fuel basket consists of a grid assembly of welded stainless steel plates or tubes that form 32 fuel compartments.

Aluminum and/or neutron absorber plates (which are made of either borated aluminum or metal matrix) are placed within each fuel compartment. Depending on fuel assembly design, 0, 4, 8, or 16 poison rod assemblies (PRAs) may be used for criticality control. Based on the number of PRAs, a fuel basket is designated as either Type A, A1, or A2 (no PRAs), Type B (4 PRAs), Type C (8 PRAs), or Type D (16 PRAs). Types A1 and A2 have higher ¹⁰B loading for metallic plates than the other types. Within each fuel cell, either two Al plates (no poison) or two Al plates and two poison plates are installed, depending on the required number of PRAs. A DSC may contain either 16, 20, or 24 poison plates. Fuel assemblies containing PRAs are not authorized in the fuel basket with 16 poison plates. Information about the basket type and basket poison plate configuration of each as-loaded canister is currently unavailable in the database.

The NUHOMS® 32PT-DSC is used at the Palisades (11 canisters), Millstone (18 canisters), Ginna (6 canisters), and Kewanee (8 canisters) ISFSIs to store SNF assemblies. The fuel assemblies loaded in these canisters are represented by the RW-859 fuel assembly types XPA15C (Palisades), C1414C (Milestone 2), and W1414WL (Ginna and Kewanee). Criticality model templates for the loss-of-neutron absorber scenario were developed for the four NUHOMS® 32PT-DSC subtypes with respect to basket length (i.e., 32PT-S100, 32PT-S125, 32PT-L100, and 32PT-L125). Only the active fuel region of a fuel assembly is explicitly modeled. A model for the XPA15C fuel assembly type, irradiated in the Palisades power reactor only, was also developed. Model templates for the assembly types C1414C and W1414WL were already available in the template repository. No credit was taken for the presence of non-fuel hardware or PRAs. Moderator water is modeled in place of these components, which is conservative with respect to criticality. The models specify water moderator and reflector with a density of 0.998 g/cm³ [D-10].

D.3.1. Criticality Model for the XPA15C Fuel Assembly Type

The fuel assemblies irradiated in the Palisades power reactor were Combustion Engineering or Exxon Nuclear 15×15 fuel assemblies with Zircaloy cladding identified in the RW nuclear fuel database [D-3] as XPA15C. A typical XPA15C fuel assembly has 216 fuel rods, 8 Zircaloy-4 guide bars, and 1 instrument tube [D-11,D-12]. A horizontal cross-sectional view of the model for the fuel assembly type XPA15C through the active fuel region is showed in Figure D-9. The guide bars are modeled as a water moderator, which is conservative with respect to fuel assembly reactivity and consistent with the fuel assembly model used in the SAR.

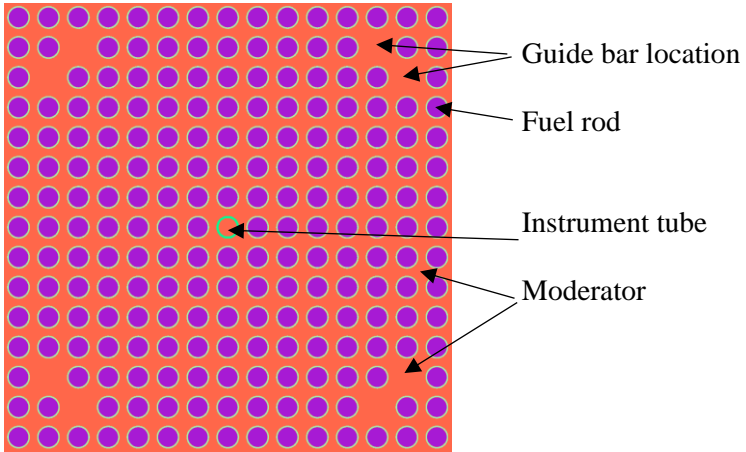


Figure D-9. Horizontal cross-sectional view of the XPA15C fuel assembly model.

D.3.2. Canister Model for the Loss-of-Neutron-Absorber Scenario

A horizontal cross-sectional view of the NUHOMS[®] 32PT-DSC model for the loss-of-neutron-absorber scenario is shown in Figure D-10. In this model, Al and poison plates are replaced by a water moderator and a fuel assembly is centered within its fuel basket cell.

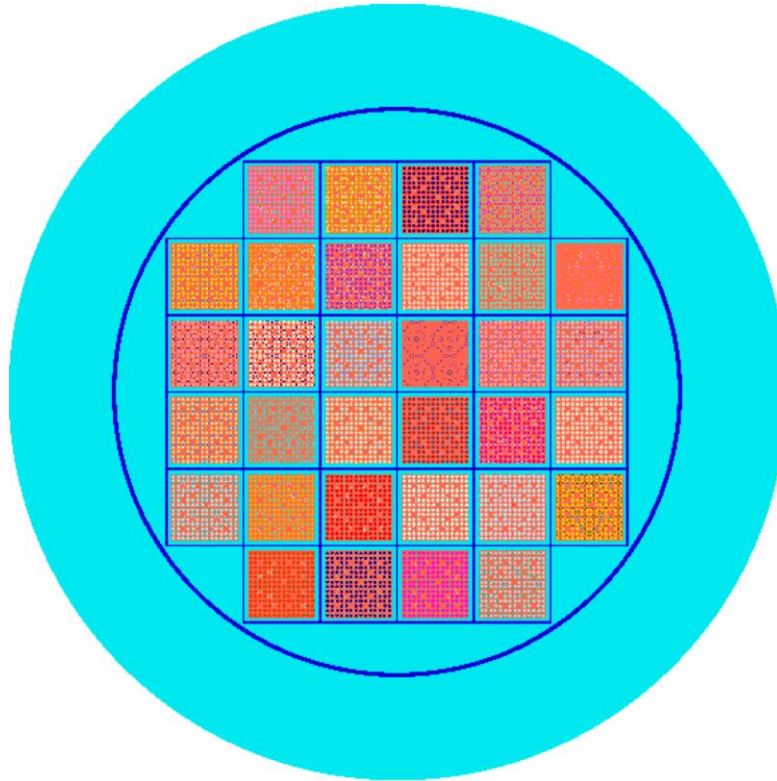


Figure D-10. Horizontal cross-sectional view of the NUHOMS[®] 32PT-DSC model for the loss-of-neutron-absorber scenario.

D.3.3. Criticality Model for Misload Calculations

The canister misload model is based on the assumption that correct assemblies have been loaded into the canister but in the most reactive configuration. This configuration is referred to as a worst-misload configuration in Sect. C.3.5. Fuel assembly placement for the worst-misload configuration is illustrated in Figure D-11. The numbers indicate the rank of an individual fuel assembly based on assembly k_{inf} values at a decay time of 9,500 years. The fuel composition for the misload model includes oxygen and the degradation disposal nuclides presented in Table A-1. The neutron absorber is neglected in this model (i.e., loss-of-neutron-absorber scenario).

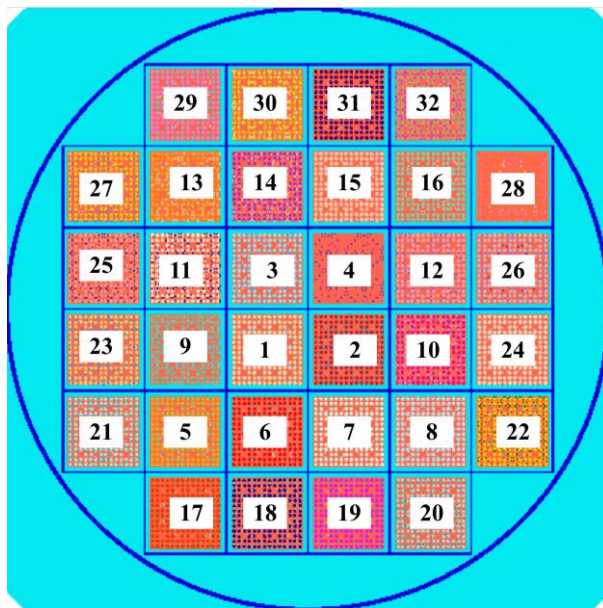


Figure D-11. Illustration of fuel assembly ranking in the worst-misload configuration for the NUHOMS® 32PT-DSC.

D.3.4. Criticality Calculations Results for the NUHOMS® 32PT-DSC

Post-closure disposal criticality calculations were performed as a function of decay time for the NUHOMS® 32PT-DSCs loaded with SNF at the Palisades (11 canisters), Ginna (6 canisters), Kewanee (8 canisters), and Millstone (18 canisters) ISFSIs. Results are provided for the loss-of-neutron-absorber scenario and 17 decay times within the time interval between calendar years 2015 and 22,000. Figure D-12 shows k_{eff} variation as a function of calendar year. The one sigma statistical uncertainty for all k_{eff} values is 0.0003 or less. In the figure, time variation between 2000 and 2100 is shown on a linear scale, and time variation between 2100 and 22,000 is shown on a logarithmic scale.

The k_{eff} values are predicted to vary from 0.9335 to 1.0312 for the Palisades SNF, 0.9063 to 0.9993 for the Ginna SNF, 0.9085 to 0.9572 for the Kewanee SNF, and 0.8722 to 0.9504 for the Millstone SNF canisters. Two canisters loaded with Ginna SNF and 10 canisters loaded with Palisades SNF are predicted to exceed the k_{eff} subcriticality limit of 0.98 assuming a loss-of-neutron-absorber scenario. For these canisters, the pure water was replaced with groundwater compositions of various NaCl concentrations and the models thus modified were used to determine k_{eff} as a function of NaCl concentration for the calendar year 22,000. Figure D-13 presents k_{eff} variation as a function of NaCl concentration for those 12 canisters. The minimum required chlorine concentrations in the groundwater of 0.086 mol/kg H₂O and 0.529 mol/kg H₂O are determined to maintain a subcritical state for canisters loaded with Ginna SNF and Palisades SNF, respectively. In this context, it is also important to note that a saturated NaCl brine has a

concentration of approximately 6 molal. A results summary for this canister in 22,000 is provided in Table D-1.

Figure D-14 shows the k_{eff} increase between the worst-misload scenario and the as-loaded configuration for the analyzed NUHOMS® 32PT-DSCs. This increase varies between 27 and 7565 pcm. The NUHOMS® 32PT-DSCs loaded with Palisades SNF would have a relatively large reactivity increase, from 1341 to 7565 pcm, between the worst-misload scenario and the as-loaded configuration.

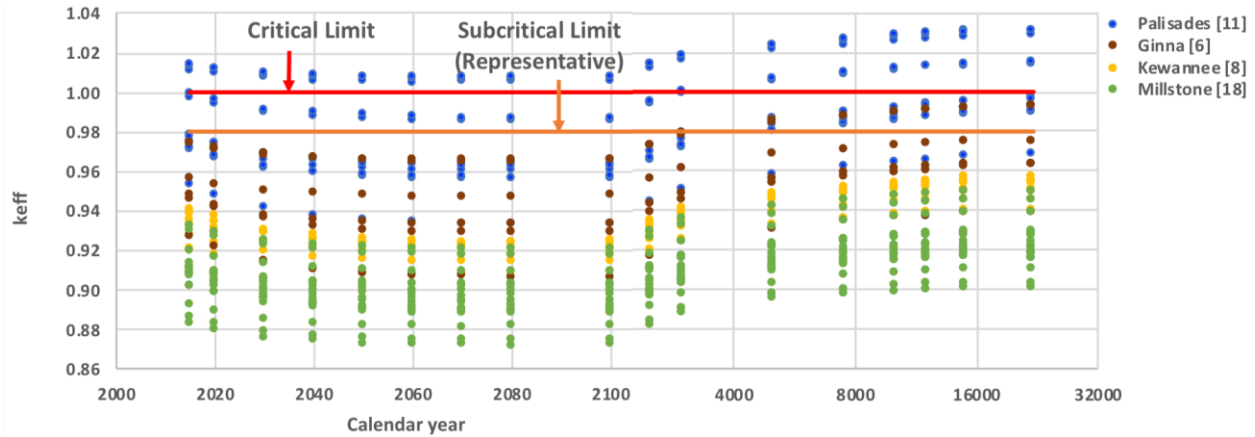


Figure D-12. k_{eff} vs. calendar year for the loss-of-neutron-absorber scenario, based on actual loading and disposal isotopes (numbers in brackets = number of DPCs).

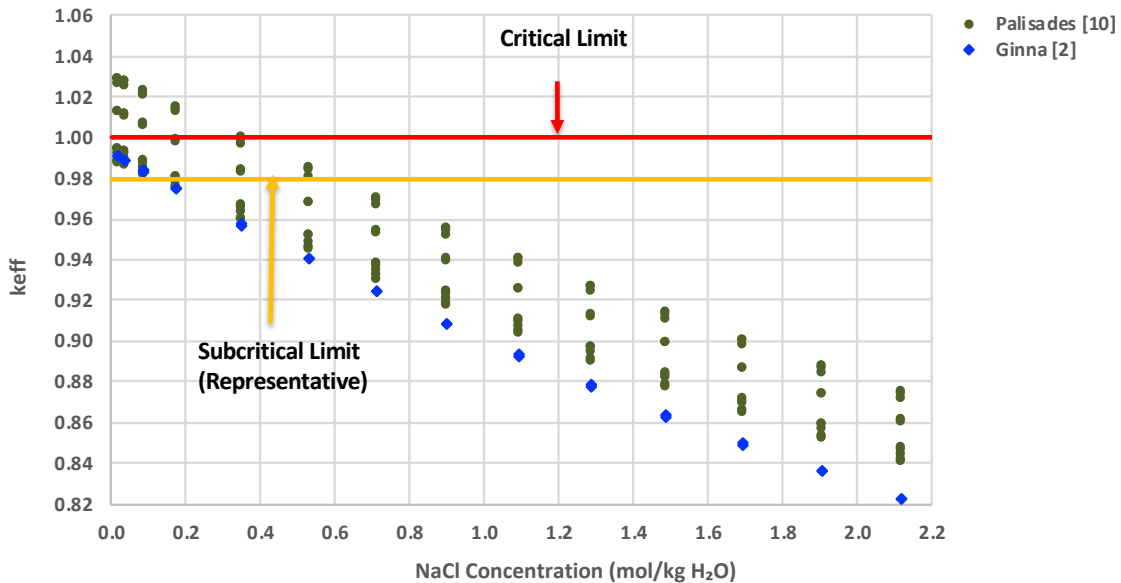


Figure D-13. k_{eff} vs. NaCl concentration for the DPCs with $k_{eff} > 0.98$ for the loss-of-neutron-absorber scenario (numbers in brackets = number of DPCs).

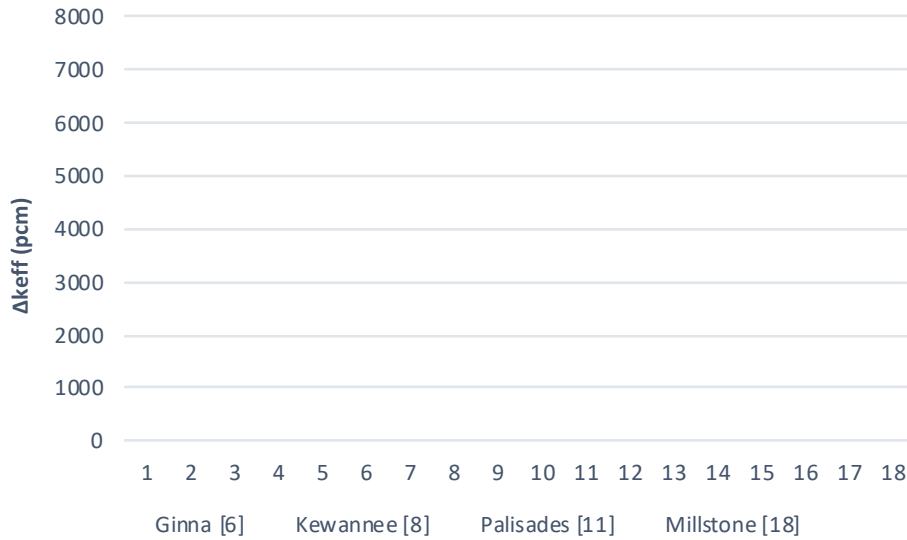


Figure D-14. k_{eff} increase between the worst-misload scenario and the as-loaded configuration (numbers in brackets = number of DPCs).

Table D-1. Final NUHOMS® 32PT-DSC statistics in the year 22,000

Description	Values for loss of neutron absorber
Number of DSCs	43
Number of DSCs with $k_{eff} > 0.98$ (as-loaded analysis)	12
Maximum k_{eff}	1.0312
Chlorine requirement for Palisades SNF canisters	0.529 mol/kg H ₂ O
Chlorine requirement for Ginna SNF canisters	0.086 mol/kg H ₂ O

D.4. FILLER HEIGHT SCOPING CALCULATION

A filler height scoping calculation was performed for a representative DPC: the MPC-32-262 loaded with Farley SNF. This canister is predicted to have a k_{eff} value of 1.0218 ± 0.0003 in the calendar year 22,000 assuming the loss-of-neutron-absorber scenario. The filler material was modeled as 68% Al and 32% H₂O by volume. The disposal criticality model for the MPC-32 design was modified to enable k_{eff} calculations as a function of filler height. Radially, the filler material is assumed to occupy the free space outside fuel pins and guide tubes. The guide tubes and the instrument tube are assumed to contain pure water. Vertical and horizontal cross-sectional views of the model are shown in Figure D-15. Filler height effects on k_{eff} are shown in Table D-2 as a function of fuel pin axial burnup zone. For this canister, a filler height of 367.9825 cm (from basket bottom) is required to maintain canister subcriticality under a loss-of-neutron-absorber scenario.

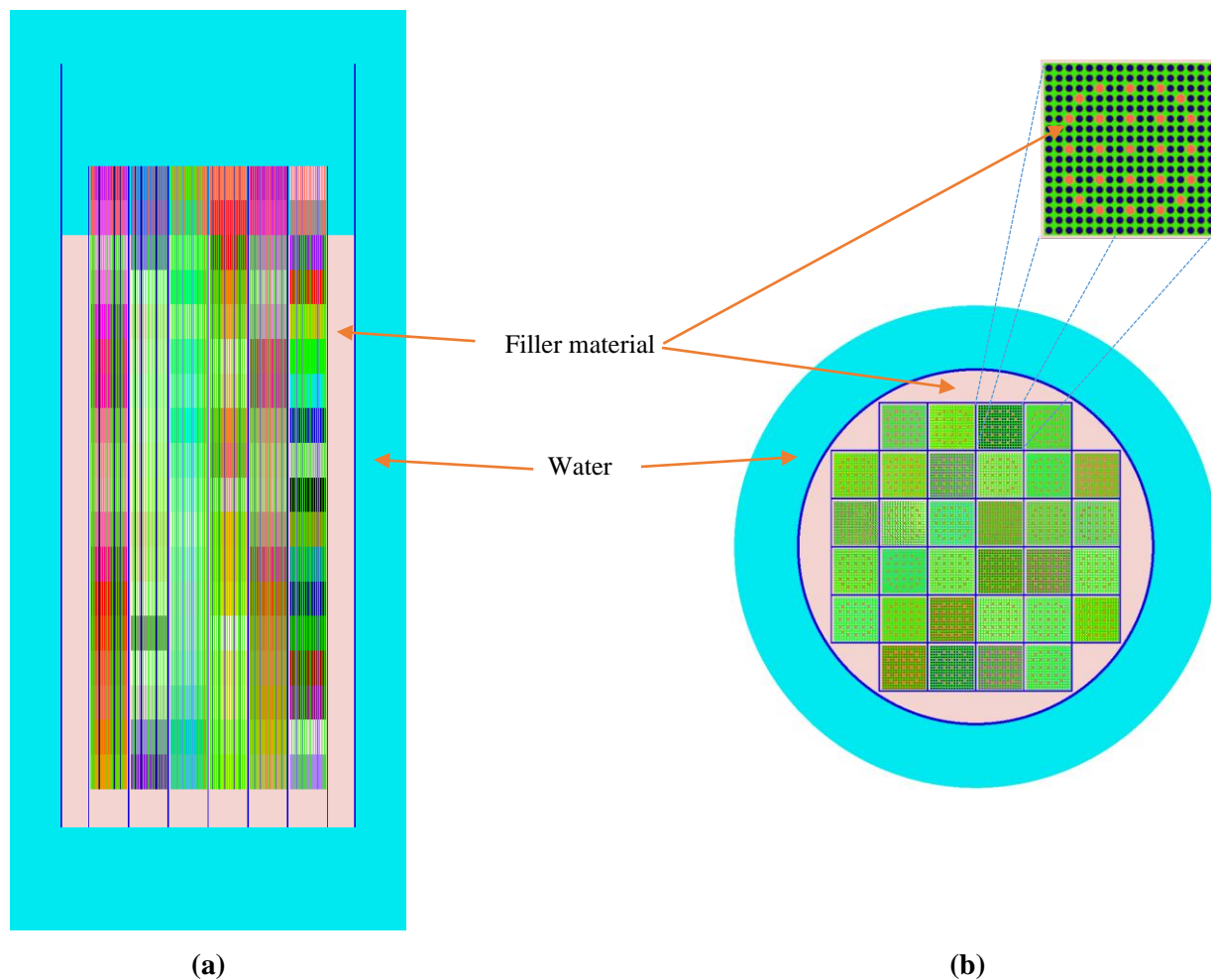


Figure D-15. (a) Vertical cross-sectional view and (b) horizontal cross-section view of the MPC-32 disposal criticality model for filler height studies.

Table D-2. k_{eff} as a function of filler height.

Outermost axial fuel zone	Filler height ^a	k_{eff}	sigma
14	307.0225	1.02292	0.00036
15	327.3425	1.02065	0.00028
16	347.6625	1.01169	0.00027
17	367.9825	0.96016	0.00028
18	388.3025	0.83271	0.00024

^aFrom basket bottom.

D.5. CONCLUSIONS

This appendix presents criticality analysis models for the NUHOMS[®] 24PT1-DSC and NUHOMS[®] 32PT-DSC canister types. A total of 60 as-loaded canisters from five sites were analyzed over the time interval between calendar years 2015 and 22,000 using the burnup credit methodology described in this report. The analyzed sites were San Onofre (17 canisters), Palisades (11 canisters), Millstone (18 canisters), Ginna (6 canisters), and Kewanee (8 canisters).

SONGS1 SNF assemblies are currently stored in 17 NUHOMS[®] 21PT1-DSCs. This canister has a capacity of 24 fuel assemblies and contains 26 carbon steel discs to support the fuel basket cells. Three criticality models were developed describing (1) the regular intact canister configuration; (2) the loss-of-neutron-absorber scenario; and (3) the degraded basket material scenario. The estimated k_{eff} values for the 17 canisters with an intact fuel basket configuration vary between 0.6766 and 0.7985 over the time interval between calendar years 2015 and 2100; that is, all k_{eff} values are below the 0.98 subcritical limit. For the loss-of-neutron-absorber scenario, the k_{eff} values vary between 0.7630 and 0.8786 over the time interval between calendar years 2015 and 22,000; that is, all estimated k_{eff} values are below the 0.98 subcritical limit for repository time frame. For the basket material degradation scenario, the estimated k_{eff} values vary between 0.8855 and 1.0589 over the time interval between calendar years 2015 and 22,000. Out of 17 DPCs, five canisters are predicted to be above the representative subcritical limit of 0.98 throughout the time interval analyzed. For the five canisters, the pure water in the model was replaced with groundwater compositions of various NaCl concentrations and the models thus modified were used to determine k_{eff} as a function of NaCl concentration for the calendar year 22,000. A minimum required chlorine concentration in the groundwater of 1.092 mol/kg H₂O was determined to maintain a subcritical state. The one sigma statistical uncertainty for all k_{eff} values is 0.0003 or less.

Post-closure disposal criticality calculations were performed as a function of decay time for as-loaded NUHOMS[®] 32PT-DSCs at the Palisades (11 canisters), Ginna (6 canisters), Kewanee (8 canisters), and Millstone (18 canisters) ISFSIs. Results are provided for a loss-of-neutron-absorber scenario and 17 decay times within the time interval between calendar years 2015 and 22,000. The one sigma statistical uncertainty for all k_{eff} values is 0.0003 or less. The k_{eff} values are predicted to vary between 0.9335 to 1.0312 for the Palisades SNF, 0.9063 and 0.9993 for the Ginna SNF, 0.9085 and 0.9572 for the Kewanee SNF, and 0.8722 and 0.9504 for the Millstone SNF. Two canisters loaded with Ginna SNF and 10 canisters loaded with Palisades SNF are predicted to exceed the k_{eff} subcriticality limit of 0.98 assuming a loss-of-neutron-absorber scenario. For these canisters, the pure water was replaced with groundwater compositions of various NaCl concentrations and the models thus modified were used to determine k_{eff} as a function of NaCl concentration for the calendar year 22,000. The minimum required molal chlorine concentrations in the groundwater of 0.086 mol/kg H₂O and 0.529 mol/kg H₂O were determined to maintain a subcritical state for canisters loaded with Ginna SNF and Palisades SNF, respectively.

Canister misload criticality analyses were performed assuming a worst configuration in an as-loaded canister, which is based on the assumption that correct assemblies have been loaded into the canister but in the most reactive configuration. k_{eff} values for worst-misload configurations were determined assuming that all fuel assemblies in the canister have a decay time of 9,500 years and the neutron absorber is completely lost. The misload analysis was performed for a total of 49 canisters containing intact fuel assemblies and loaded to full capacity. The 11 canisters not analyzed, which contain San Onofre Unit 1 damaged fuel and/or empty locations, will be analyzed in the future. The k_{eff} increase between the worst-misload scenario and the as-loaded configuration for the six analyzed SONGS1 SNF canisters varies between approximately 500 and 2000 pcm. The k_{eff} increase between the worst-misload scenario and the as-loaded configuration for the analyzed NUHOMS[®] 32PT-DSCs varies between approximately 27 and 7565 pcm.

A filler height scoping calculation was performed for the MPC-32-262 canister loaded with Farley SNF. This canister is predicted to have a k_{eff} value of 1.0218 in the calendar year 22,000 assuming a loss-of-neutron-absorber scenario. The filler material was modeled as 68% Al and 32% H₂O by volume. A filler height of 367.9825 cm (from basket bottom) was evaluated to maintain in a subcritical state ($k_{eff} < 0.98$) under loss-of-neutron-absorber scenario.

D.6. REFERENCES

- D-1. *Certificate of Compliance for Radioactive Material Packages*, Certificate Number 9255, Revision Number 11, US Nuclear Regulatory Commission (2013).
- D-2. *Certificate of Compliance for Radioactive Material Packages*, Certificate Number 9302, Revision Number 7, US Nuclear Regulatory Commission (2014).
- D-3. *RW-859 Nuclear Fuel Data*, Energy Information Administration, US Department of Energy, Washington, D.C. (Oct. 2004).
- D-4. *Safety Analysis Report for the NUHOMS-MP187 Multi-Purpose Cask*, Rev. 11, Document No. NUH-05-151, Transnuclear West Inc. (2001).
- D-5. *Appendix A to Certificate of Compliance No. 1029, Technical Specifications for the Advanced NUHOMS Systems Operating Controls and Limits*, ADAMS Accession Number ML05152013.
- D-6. *Characteristics of Spent Fuel, High-Level Waste, and Other Radioactive Wastes which May Require Long-Term Isolation*, DOE/RW-0184, Volume 3, US Department of Energy (1987).
- D-7. *Advanced NUHOMS System Final Safety Analysis Report Rev. 0*, ADAMS Accession Number: ML031040379 (2003).
- D-8. *SCALE Version 4.4 – A Modular Code System for Performing Standardized Computer Analyses for Licensing Evaluation*, NUREG/CR-0200, Rev. 6, (ORNL/NUREG/CSD-2/R6), Oak Ridge National Laboratory, US Nuclear Regulatory Commission (2000).
- D-9. W.J. Marshall, B.T. Rearden, and E.L. Jones, “Validation of SCALE 6.2 Criticality Calculations Using KENO V.A and KENO-VI,” *Proceedings of International Conference on Nuclear Criticality Safety*, Charlotte, NC (2015).
- D-10. *NUHOMS[®]-MP197 Transportation Cask Safety Analysis Report*, Revision 15, Document No. NUH09.0101, Transnuclear Inc. (2014).
- D-11. *Palisades Final Safety Analysis Report Update*, Revision 31, Chapter 3 – Reactor – Figures, ADAMS Accession Number: ML16120A359 (2016).
- D-12. *Palisades Final Safety Analysis Report Update*, Revision 32, Chapter 3 – Reactor – Tables, ADAMS Accession Number: ML16120A32 (2016).

This page is intentionally left blank.

**APPENDIX E.
FY 2019 Criticality Study**

This page is intentionally left blank.

E.1. INTRODUCTION

This appendix documents work performed supporting the US Department of Energy (DOE) Office of Nuclear Energy (NE) Spent Fuel and Waste Disposition (SFWD) under work breakdown structure element 1.08.01.03.05 “Direct Disposal of Dual Purpose Canisters.” In particular, this appendix fulfills the M3 milestone, M3SF-19OR010305013, “Update of DPC Direct Disposal Criticality Analysis Report” within work package SF-19OR01030501, “Direct Disposal of Dual Purpose Canisters - ORNL.”

This appendix presents the dual-purpose canister (DPC) criticality evaluations performed in FY 2019 to support the feasibility determination of direct disposal of DPCs and extends the work reported in the main body and preceding appendices of this report. The main objectives of the FY 2019 DPC disposal criticality study were to develop degraded canister criticality calculation templates for the NUHOMS[®] 32PTH1 [D-2] and NUHOMS[®] 61BT/BTH [D-2] dry shielded canisters (DSCs) from the intact models documented in the forthcoming *Criticality Process, Modeling and Status for UNF-ST&DARDS* [E-1] and to perform as-loaded criticality analyses for sites using these two canister types, as well as the TSC-37 and the loading maps currently available in the database.

A total of 92 as-loaded canisters from five sites were analyzed for the time interval between calendar years 2020 and 22,000 using the burnup credit methodology described in the previous sections of this report. The analyzed canisters were at the following sites: Nine Mile Point (6 canisters), Cooper (8 canisters), Monticello (10 canisters), Crystal River (38 canisters), and Kewanee (30 canisters beyond those analyzed in Appendix D, for a total of 38 canisters).

Criticality analyses models were developed for (1) the intact canister configuration applicable to normal conditions of transport and storage as described in the UNF-ST&DARDS status report referenced above [E-1] and (2) for degraded material configurations applicable to the canister repository time frame specified in this report. The degraded material configurations assume two scenarios: (1) complete loss of the fixed neutron absorber (i.e., ¹⁰B) without fuel basket geometry changes and (2) complete degradation and loss of basket materials, including neutron absorber plates and aluminum and carbon steel basket components (e.g., insert plates and basket support discs). The effect of canister material degradation and neutron absorber loss is a significant increase in k_{eff} . The degraded material configurations were analyzed for 10 analysis dates between 2020 and 22,000.

As mentioned in the main report, neutron moderation by water is needed for a waste package to achieve criticality. However, the groundwater (or pore water) that may flood a breached DPC will contain various dissolved aqueous species. Seventeen species were studied in the main report, and it was determined that Cl, Li, and B provide the maximum reduction in canister reactivity because of their large neutron absorption cross sections. However, available groundwater data indicate that chlorine (as chloride) is the only naturally abundant neutron-absorbing element in groundwater that can provide a significant reduction in reactivity and is available in most of the repository concepts under consideration in varying quantities. Analyses were performed to determine the chlorine requirement to suppress the reactivity of canisters that have the potential to form critical configuration in a repository time frame. The impact of chlorine (in terms of NaCl) concentration in groundwater on the reactivity of as-loaded DPCs exceeding a k_{eff} value of 0.98 was evaluated for the calendar year 22,000. Previous chlorine concentration effects on k_{eff} documented in this report were evaluated for the calendar year 9,999. The impacted DPCs will be reevaluated for the calendar year 22,000 in the future. Note that within the time interval between calendar years 2020 and 22,000, canister k_{eff} initially decreases with increasing decay time, reaches a minimum value, and then increases with increasing decay time. Hence the k_{eff} value for the calendar year 22,000 is slightly higher than that for the calendar year 9,999.

The remainder of this appendix is organized as follows: Section E.2 describes the NUHOMS[®] 61BT-DSC loss-of-neutron-absorber model, Section E.3 discusses the criticality calculations for Nine Mile Point, Cooper, and Monticello, Section E.4 provides a description of the NUHOMS[®] 32PTH-DSC loss-of-

neutron absorber model, Sections E.5 and E.6 discuss the Crystal River and Kewaunee criticality calculations, Section E.7 contains the conclusions, and E.8 contains the reference.

E.2. NUHOMS® 61BT-DSC LOSS OF NEUTRON ABSORBER MODEL

A horizontal cross-sectional view of the NUHOMS® 61BT-DSC model for the loss-of-neutron-absorber scenario was developed based on the intact model discussed in Section A-13 of the UNF-ST&DARDS criticality modeling status report [E-1] and is shown in Figure E-1. In this model, Al and poison plates are replaced by a full density water moderator, and a fuel assembly is centered within its fuel basket cell. The structural components of the basket are manufactured of stainless steel, so no degraded basket model is necessary.

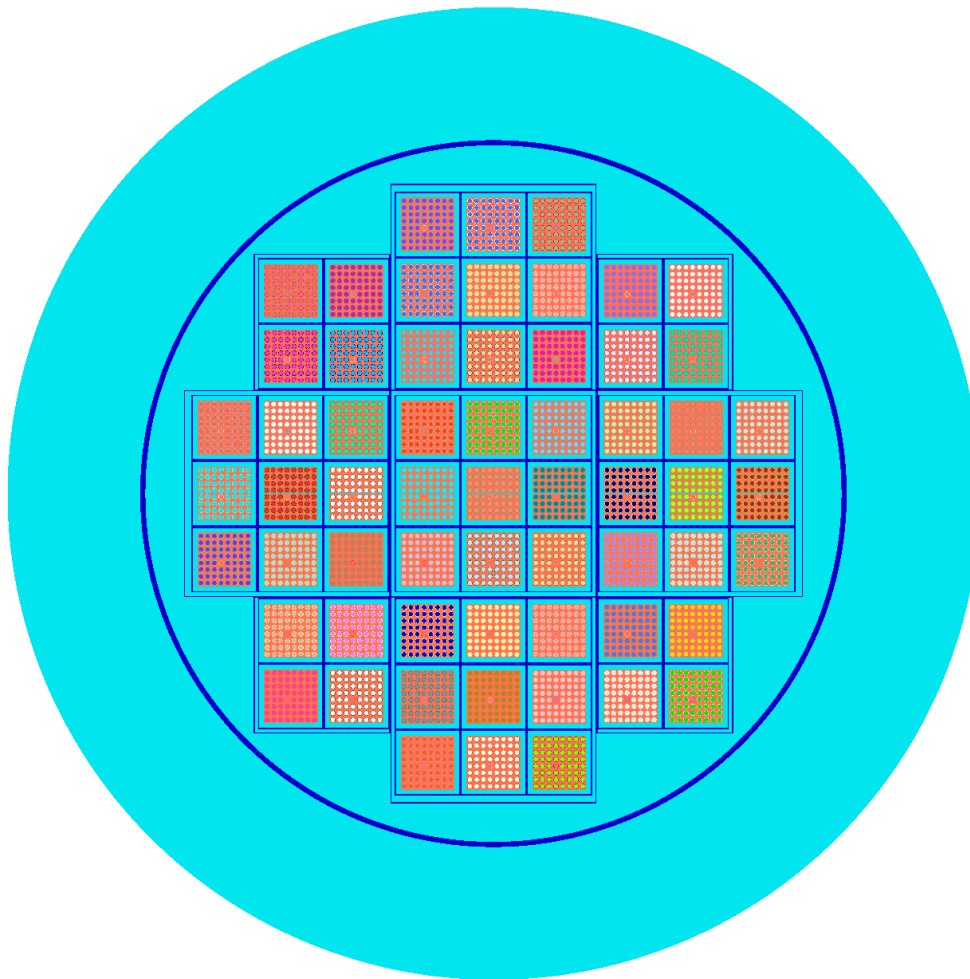


Figure E-1. Horizontal cross-sectional view of the NUHOMS® 61BT-DSC model for the loss-of-neutron-absorber scenario.

E.3. NINE MILE POINT, COOPER, AND MONTICELLO CRITICALITY CALCULATIONS

Post-closure disposal criticality calculations were performed as a function of decay time for the NUHOMS® 61BT-DSCs loaded with SNF at the Nine Mile Point (6 canisters), Cooper (8 canisters), and Monticello (10 canisters) ISFSIs. Results are provided for the loss-of-neutron-absorber scenario for 10

decay times within the time interval between calendar years 2020 and 22,000. Figure E-2 shows k_{eff} variation as a function of calendar year, along with the assumed subcritical limit of 0.98 and the critical limit of 1.0. The one sigma statistical uncertainty for all k_{eff} values is 0.0003 or less for each calculation. The k_{eff} values are predicted to vary from 0.88931 to 0.91339 for the Nine Mile Point SNF canisters, 0.86054 to 0.91567 for the Monticello SNF canisters, and 0.89210 to 0.90822 for the Cooper SNF canisters.

No SNF canisters loaded at the three BWR sites considered here exceeded the 0.98 representative subcritical limit, so no calculations were performed with added NaCl in the moderator.

Figures E-3 through E-5 show the k_{eff} increase between the worst misload scenario and the loss-of-neutron-absorber, as-loaded configuration for the analyzed NUHOMS[®] 61BT-DSCs at Nine Mile Point, Cooper, and Monticello. This increase varies between 830 and 1,525 pcm for the Nine Mile Point canisters, between 407 and 572 pcm for the Cooper SNF canisters, and between 158 and 3,150 pcm for the Monticello SNF canisters.

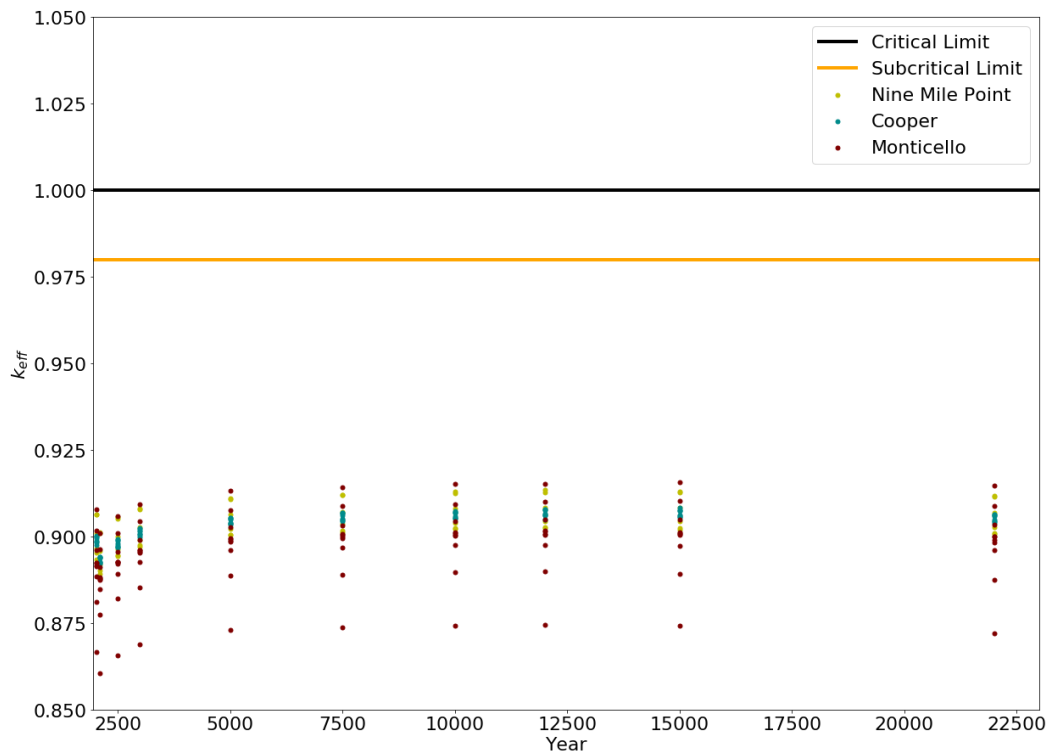


Figure E-2. k_{eff} vs. calendar year for the loss-of-neutron-absorber scenario based on actual loading and disposal isotopes for SNF canisters at Nine Mile Point, Cooper, and Monticello.

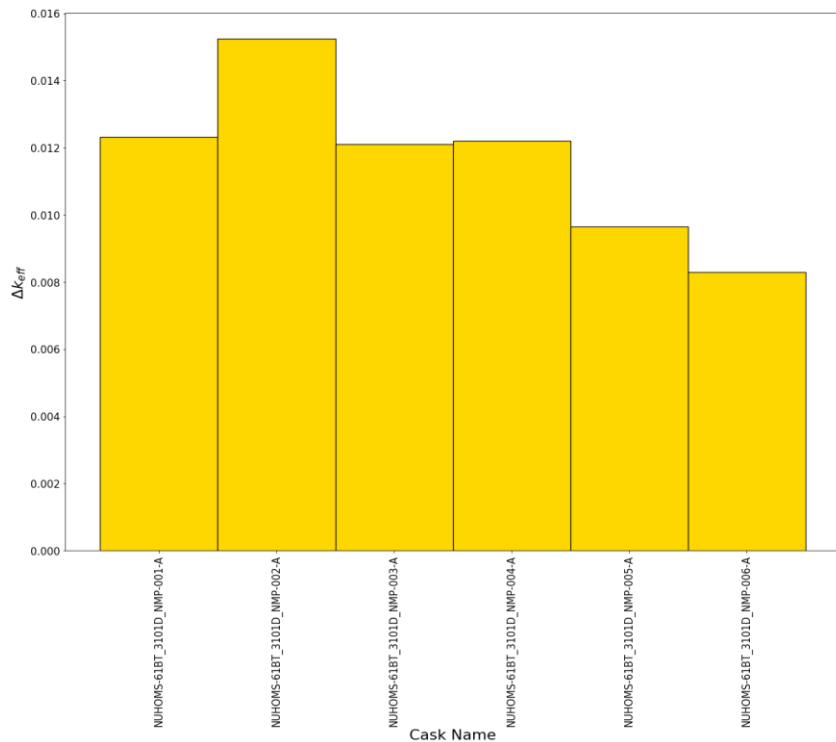


Figure E-3. k_{eff} increase between the worst-misload scenario and the as-loaded configuration for 6 Nine Mile Point SNF canisters.

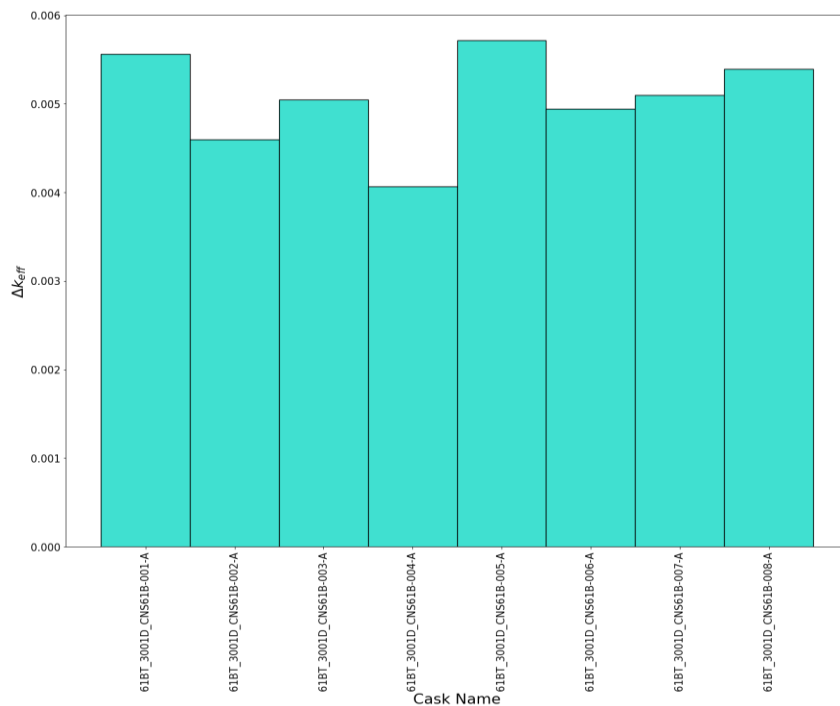


Figure E-4. k_{eff} increase between the worst-misload scenario and the as-loaded configuration for 8 Cooper SNF canisters.

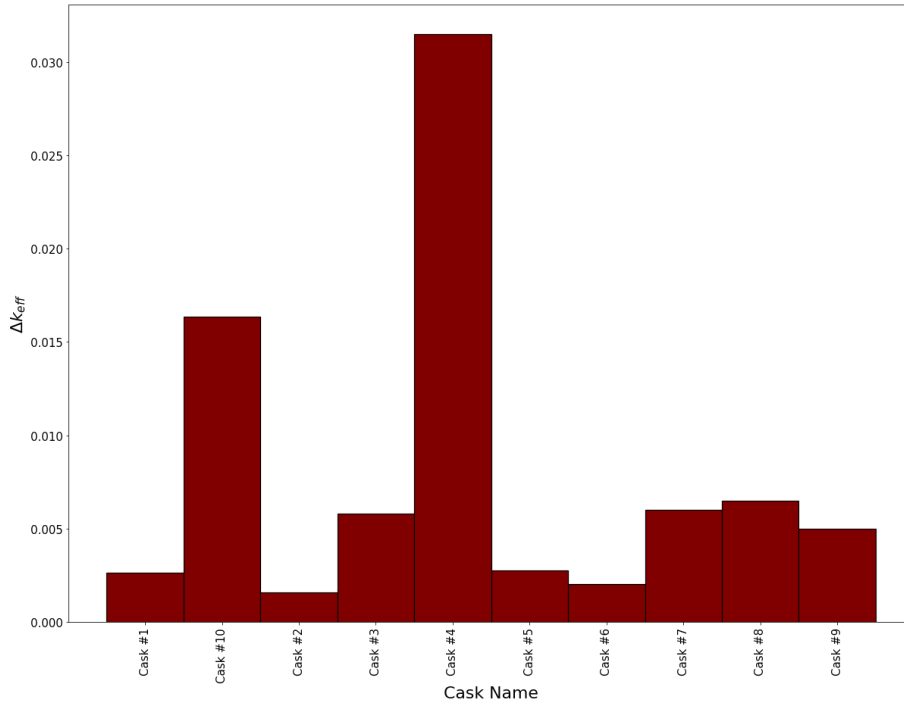


Figure E-5. k_{eff} increase between the worst misload scenario and the as-loaded configuration for 10 Monticello SNF canisters.

E.4. NUHOMS® 32PTH-DSC LOSS OF NEUTRON ABSORBER MODEL

A NUHOMS® 32PTH-DSC model for the loss-of-neutron-absorber scenario was developed based on the intact model discussed in Section A-14 of the UNF-ST&DARDS criticality status report [E-1] and a horizontal cross-sectional view of the model is shown in Figure E-6. In this model, Al and poison plates are replaced by a water moderator, and a fuel assembly is centered within its fuel basket cell. The structural components of the basket are manufactured of stainless steel, so no degraded basket model is necessary.

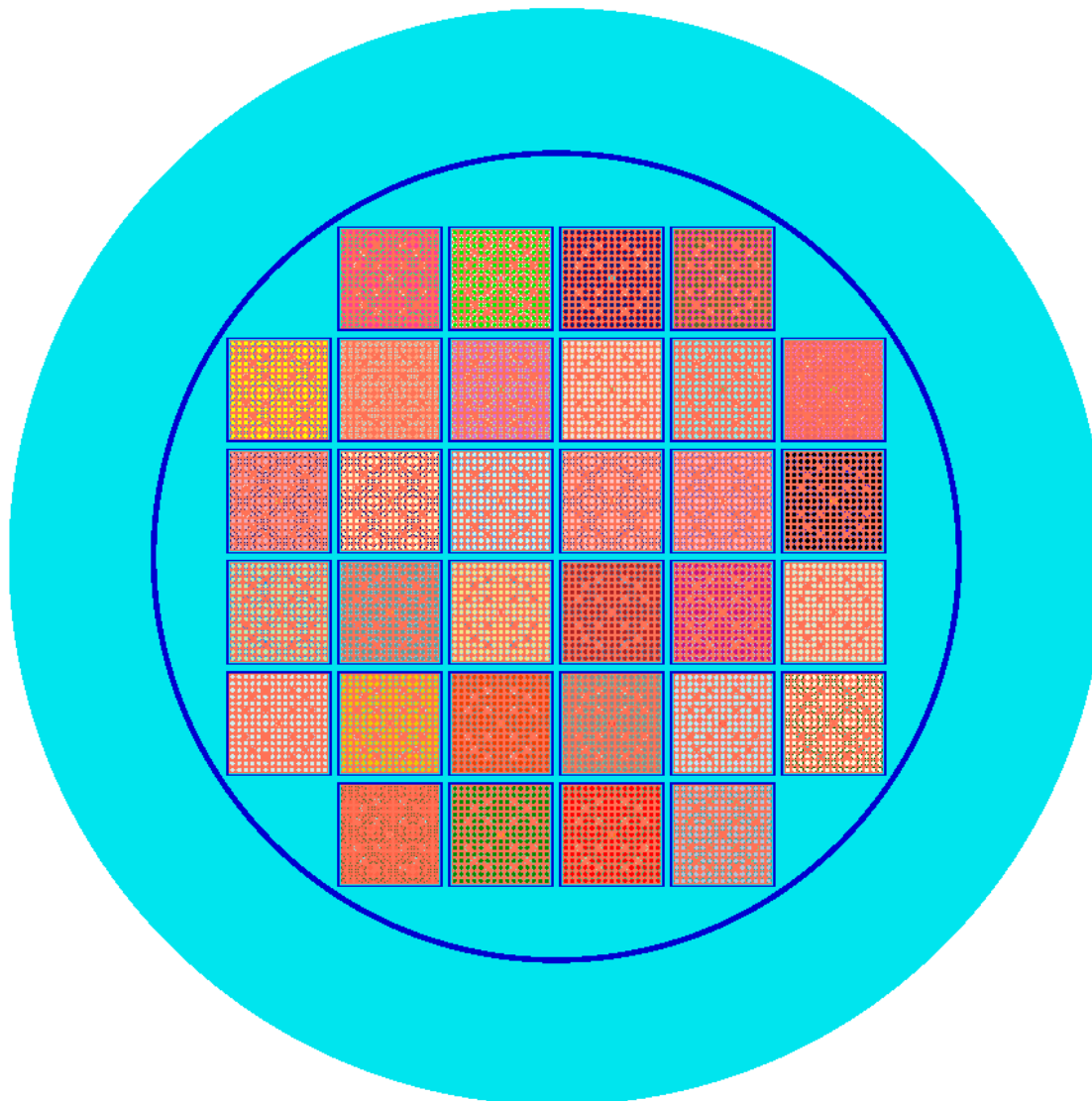


Figure E-6. Horizontal cross-sectional view of the NUHOMS® 32PTH-DSC model for the loss-of-neutron-absorber scenario.

E.5. CRYSTAL RIVER CRITICALITY CALCULATIONS

Post-closure disposal criticality calculations were performed as a function of decay time for the NUHOMS® 32PTH-DSCs loaded with SNF at the Crystal River (38 canisters) ISFSI. Results are provided for the loss-of-neutron-absorber scenario for 10 decay times within the time interval between calendar years 2020 and 22,000. Figure E-7 shows k_{eff} variation as a function of calendar year, along with the assumed representative subcritical limit of 0.98 and the critical limit of 1.0. The one sigma statistical uncertainty for all k_{eff} values is 0.0003 or less for each calculation.

The k_{eff} values are predicted to vary from 0.88026 to 0.97838 for the Crystal River SNF canisters.

No SNF canisters loaded at Crystal River considered here exceeded the 0.98 subcritical limit, so no calculations were performed with added NaCl in the moderator.

Figure E-8 shows the k_{eff} increase between the worst-misload scenario and the as-loaded configuration for 37 of the 38 analyzed NUHOMS® 32PTH-DSCs. One canister was not analyzed because the current

worst-case misload methodology cannot be applied to short loaded canisters. This increase varies between 729 and 9,091 pcm.

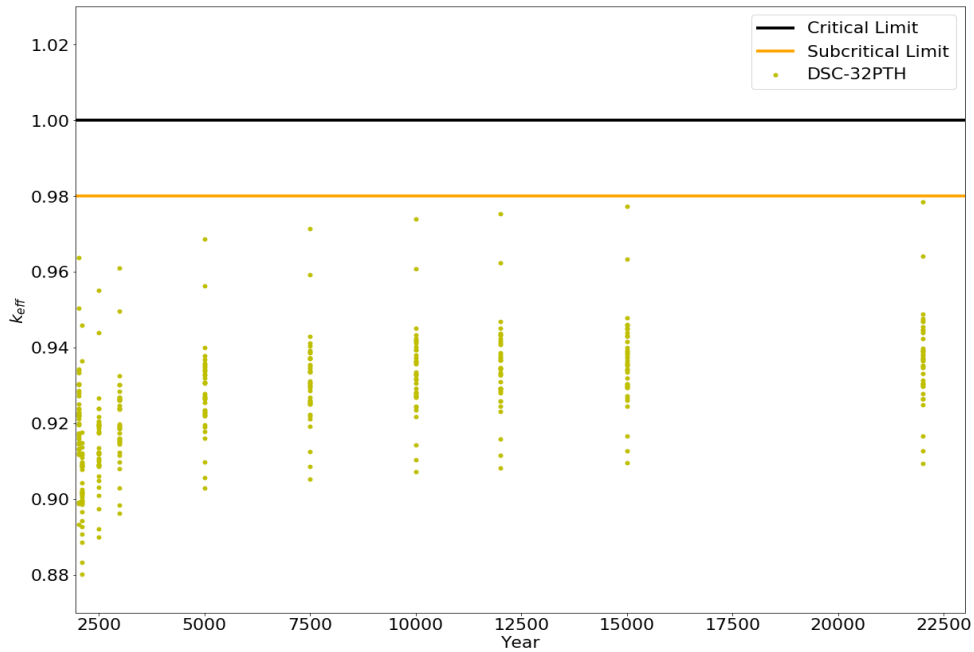


Figure E-7. k_{eff} vs. calendar year for the loss-of-neutron-absorber scenario based on actual loading and disposal isotopes for SNF canisters at Crystal River.

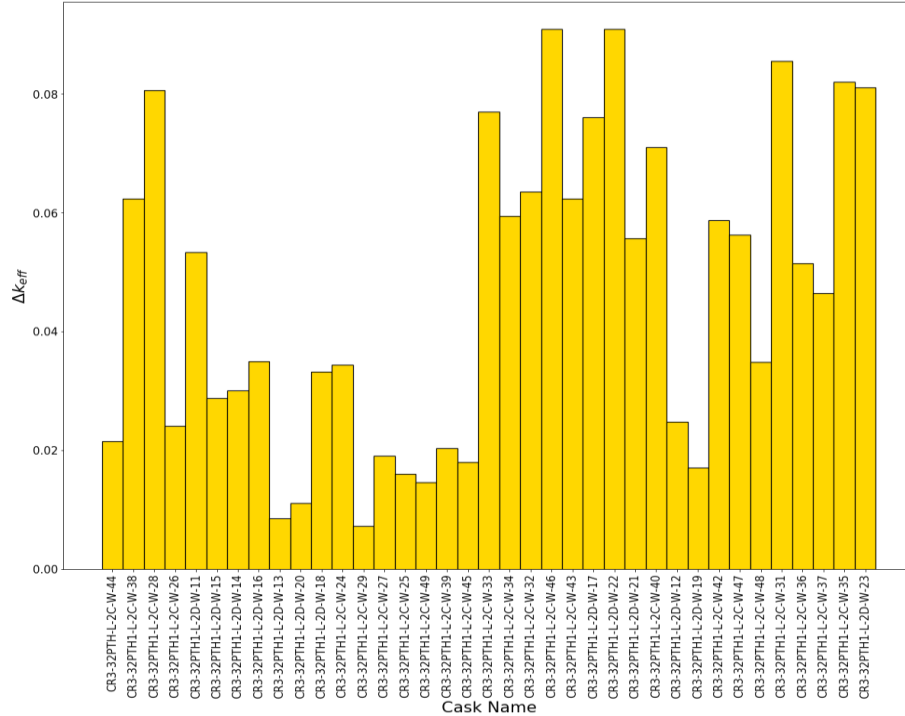


Figure E-8. k_{eff} increase between the worst misload scenario and the as-loaded configuration for Crystal River SNF canisters.

E.6. KEWAUNEE CRITICALITY CALCULATIONS

Post-closure disposal criticality calculations were performed as a function of decay time for the 38 SNF canisters at the Kewaunee ISFSI. Of the 38 SNF canisters, 14 are NUHOMS[®] 32PT-DSCs (including the 8 canisters analyzed in Appendix D, which are included here for completeness), and 24 are TSC-37s. Figure E-9 and Figure E-10 show results for the loss-of-neutron-absorber scenario and the degraded-basket scenario for 10 decay times within the time interval between calendar years 2020 and 22,000. The results in Figure E-9 and Figure E-10 show k_{eff} variation as a function of calendar year. The one sigma statistical uncertainty for all k_{eff} values is 0.0003 or less. The TSC-37 has structural components fabricated from carbon steel, while the NUHOMS[®] 32PT-DSC does not contain any carbon steel structural components. Therefore, only the TSC-37 is evaluated for the degraded basket scenario.

The k_{eff} values are predicted to vary from 0.90962 to 0.97323 for the NUHOMS[®] 32PT-DSCs. The k_{eff} values are predicted to vary from 0.90976 to 0.97352 for the TSC-37s under the loss-of-neutron absorber scenario and from 0.98128 to 1.05163 for the TSC-37s under the degraded-basket scenario. For the TSC-37 canisters in the degraded basket scenario, calculations were performed in which the pure water was replaced with groundwater compositions of various NaCl concentrations, and the models thus modified were used to determine k_{eff} as a function of NaCl concentration for the calendar year 22,000 (most reactive date). Figure E-11 presents k_{eff} variation as a function of NaCl concentration for those 24 canisters. Examining the results presented in Figure E-11, it is clear that 0.50 mol NaCl/ kg H₂O is sufficient to demonstrate subcriticality for all of the Kewaunee canisters. In this context, it is also important to note that a saturated NaCl brine has a concentration of approximately 6 molal.

Figure E-12 shows the k_{eff} increase between the worst misload scenario and the as-loaded configuration for the analyzed NUHOMS[®] 32PT-DSCs under the loss-of-neutron-absorber scenario, and Figure E-13 shows the same information for the TSC-37 canisters. It is noted that misloading calculations are performed for 23 of the 24 TSC-37 because one is short loaded, and the misload methodology does not currently support less-than-full canisters. The increase in k_{eff} varies between -30 and 2,137 pcm for the NUHOMS[®] 32PT-DSCs and between 768 and 11,241 pcm for the TSC-37 canisters. It is observed that canister KPS32PT-S100-A16-HZ013 has a negative change in k_{eff} under the worst case reloading misload configuration. The inputs for both the base line and misloaded cases were checked and found to be correct. It is apparent that the base line loading of KPS32PT-S100-A16-HZ013 has many of the most reactive assembly positioned in a face adjacent orientation with one another, and is not substantially different from the misloaded configuration. It is also noted that the 30 pcm change is an approximately one standard deviation change in k_{eff} and could easily be accounted for due to the calculation-to-calculation variation in Monte Carlo calculations.

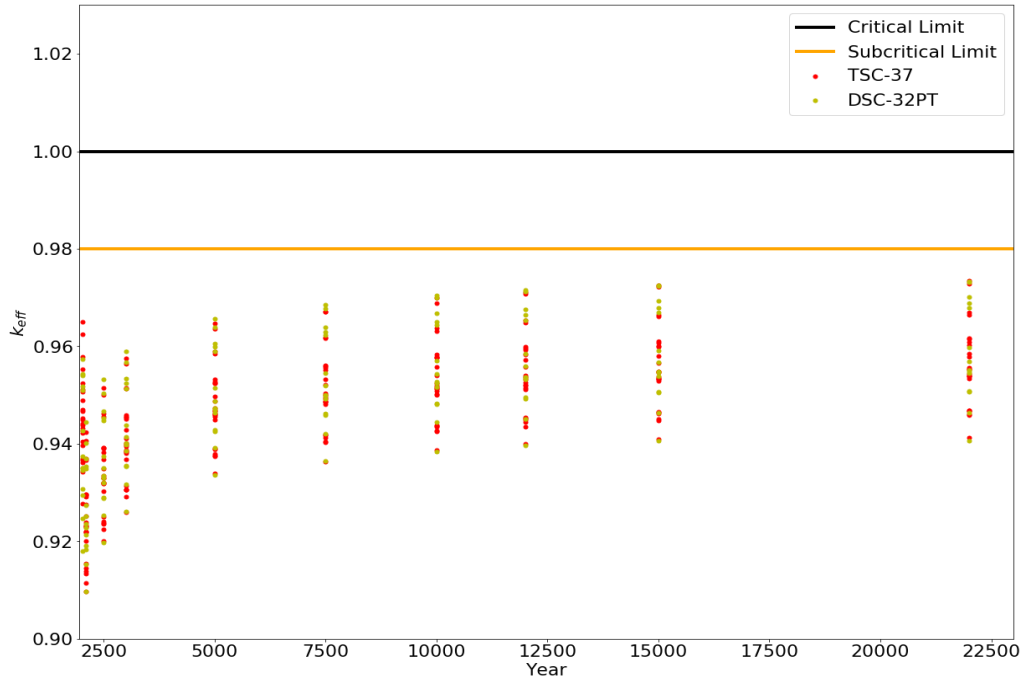


Figure E-9. k_{eff} vs. calendar year for the loss-of-neutron-absorber scenario based on actual loading and disposal isotopes for all SNF canisters at Kewaunee.

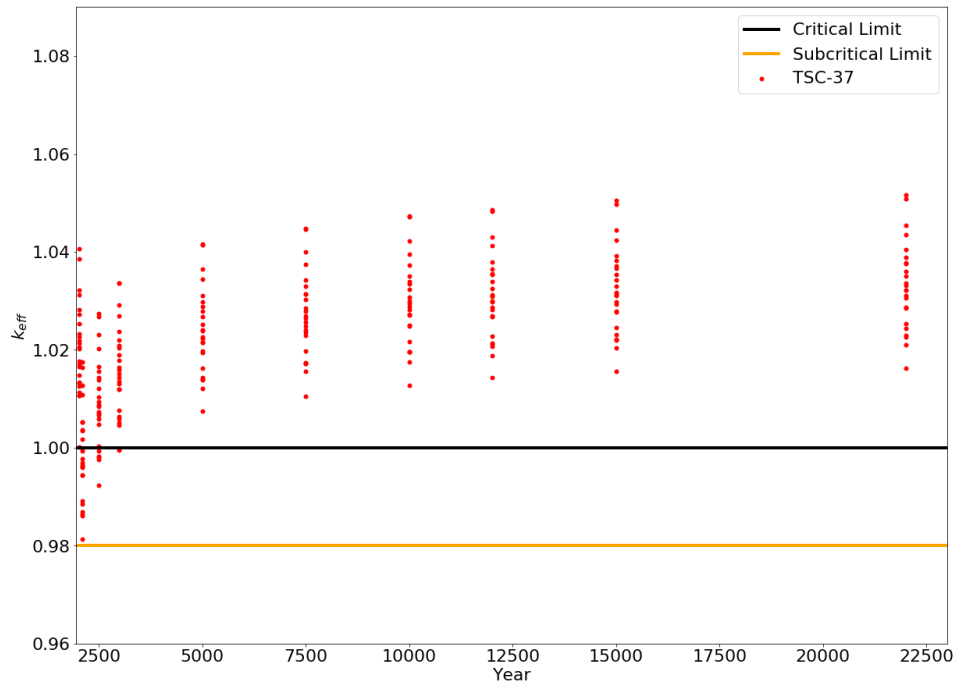


Figure E-10. k_{eff} vs. calendar year for the degraded basket scenario, based on actual loading and disposal isotopes for the TSC-37 canisters at Kewaunee.

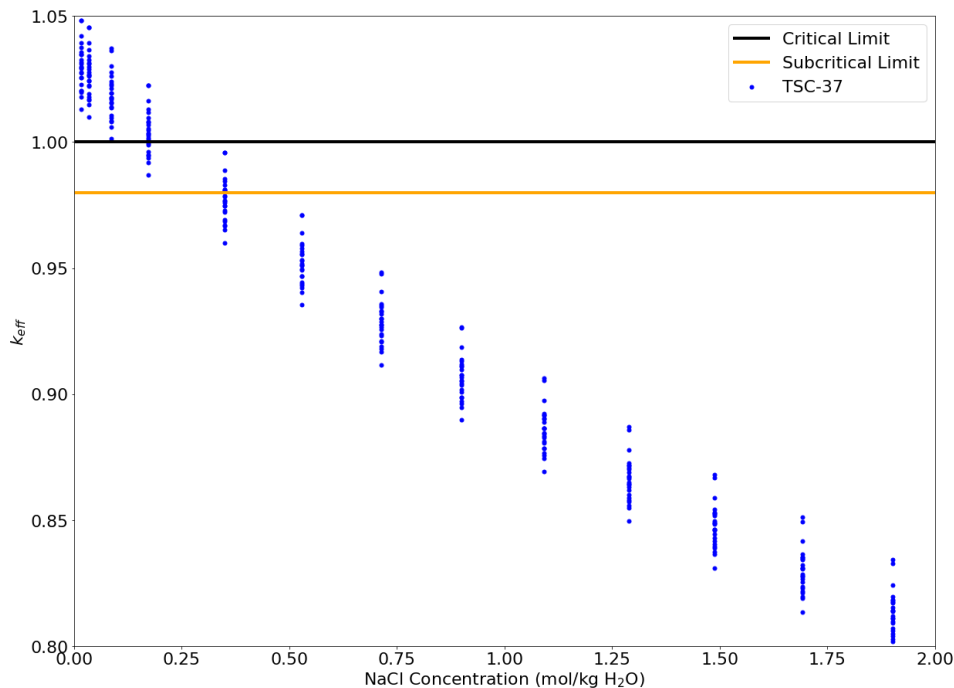


Figure E-11. k_{eff} vs. NaCl concentration for the DPCs with $k_{eff} > 0.98$ for the TSC-37 canisters at Kewaunee under the degraded basket scenario.

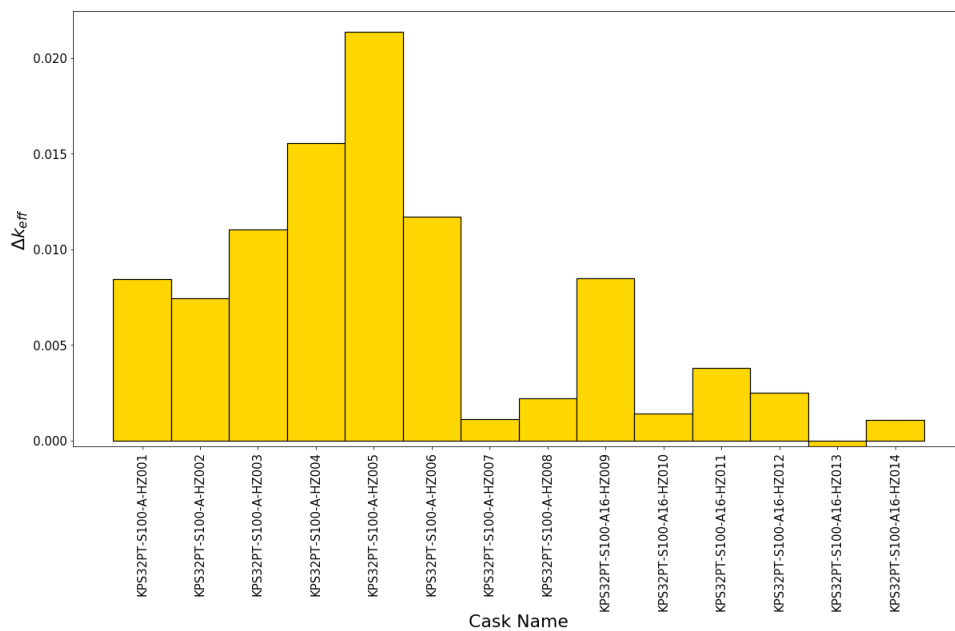


Figure E-12. k_{eff} increase between the worst-misload scenario and the as-loaded configuration for the NUHOMS® 32PTH-DSCs at Kewaunee.

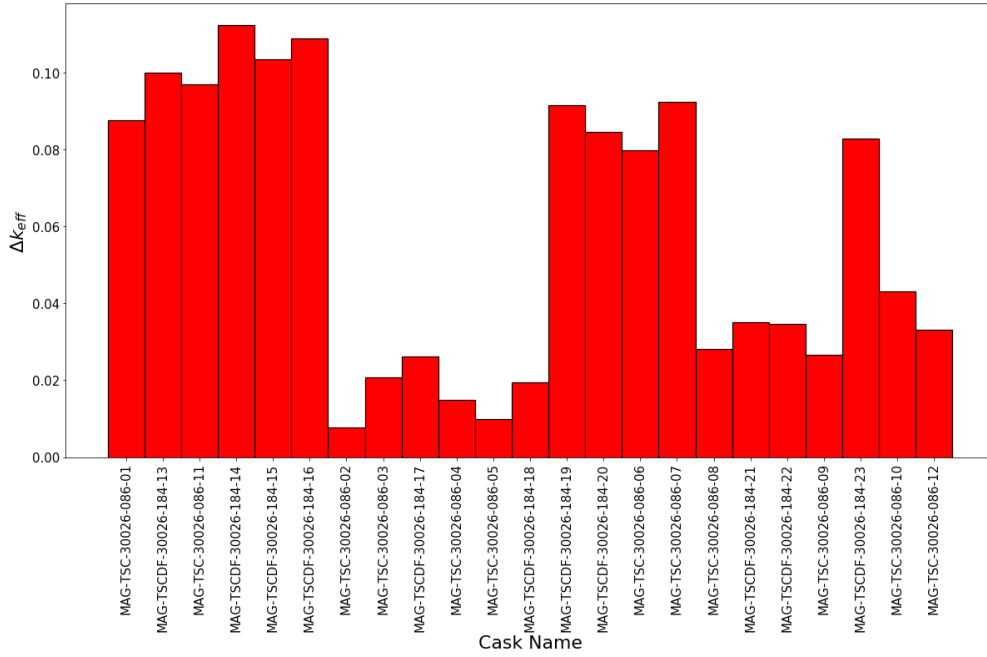


Figure E-13. k_{eff} increase between the worst-misload scenario and the as-loaded configuration for the TSC-37 SNF canisters at Kewaunee.

E.7. CONCLUSIONS

This appendix presents criticality analysis models for the NUHOMS® 61BT-DSC and NUHOMS® 32PTH-DSC canister types. A total of 92 as-loaded canisters from five sites were analyzed over the time interval between calendar years 2020 and 22,000 using the burnup credit methodology described in this report. The analyzed sites were Nine Mile Point (6 canisters), Cooper (8 canisters), Monticello (10 canisters), Crystal River (38 canisters), and Kewaunee (30 canisters beyond those analyzed in Appendix D, for a total of 38 canisters).

The intact configurations of both the NUHOMS® 61BT-DSC and NUHOMS® 32PTH-DSC canister types are described in detail in the UNF-ST&DARDS criticality status report [E-1]. Degraded loss-of-neutron-absorber models are developed from those intact models. Since both canisters contain stainless steel structural components, no additional degraded basket models were needed. A number of canisters at the Kewaunee ISFSI are of the TSC-37 design. Models for the TSC-37 loss-of-neutron-absorber and degraded-basket scenarios that are available from previous years' efforts were used in this work.

Post-closure disposal criticality calculations were performed as a function of decay time for as-loaded canisters at the sites previously discussed. Results are provided for a loss-of-neutron-absorber scenario and for 10 decay times within the time interval between calendar years 2020 and 22,000 for all canisters analyzed. The k_{eff} values are predicted to vary from 0.88931 to 0.91339 for the Nine Mile Point SNF canisters, 0.86054 to 0.91567 for the Monticello SNF canisters, 0.89210 to 0.90822 for the Cooper SNF canisters, 0.88026 to 0.97838 for the Crystal River SNF canisters, 0.90962 to 0.97323 for the NUHOMS® 32PT-DSCs, and from 0.90976 to 0.97352 for the TSC-37s at Kewaunee under the loss of neutron-absorber scenario. The k_{eff} s varied from 0.98128 to 1.05163 for the 24 TSC-37s under the degraded-basket scenario. For all of TSC-37s under the degraded-basket scenario that exceeded the 0.98 subcritical limit, calculations were performed with variable NaCl concentrations in the water, and it was determined that a 0.5 molal concentration was sufficient to demonstrate subcriticality.

Canister misload criticality analyses were performed assuming a worst configuration in an as-loaded canister, which is based on the assumption that correct assemblies have been loaded into the canister, but they are in the most reactive configuration. k_{eff} values for worst misload configurations were determined assuming that all fuel assemblies in the canister have a decay time of 22,000 years, and the neutron absorber is completely lost. The misload analysis was performed for a total of 90 canisters containing intact fuel assemblies that were loaded to full capacity. The 2 canisters not analyzed contain empty locations and will be analyzed in the future. The k_{eff} increase varied between 830 and 1,525 pcm for the Nine Mile Point canisters, between 407 and 572 pcm for the Cooper SNF canisters, between 158 and 3,150 for the Monticello SNF canisters, between 729 and 9,091 pcm for the Crystal River SNF canisters, between -30 and 2,137 pcm for the NUHOMS® 32PT-DSCs, and between 768 and 11,241 pcm for the TSC-37 canisters at Kewaunee.

A summary of the direct disposal criticality calculations is provided in Table E-1. There are 708 canisters that have been analyzed through FY19 for the project. Of the canisters analyzed it was shown that 79% would remain subcritical under the loss-of-neutron-absorber scenario. When considering complete degradation of the baskets of canisters with non-stainless-steel structural components 68% of the canisters are shown to be subcritical. When further considering the potential for the worst-case arrangement of the most reactive fuel assemblies in each canister it is shown that 63% of canisters would remain subcritical.

Table E-1. Summary of the number of canisters meeting the subcritical limit.

Description (Analysis Dates: 2020-22000)	Value
Total DPCs analyzed	708
Total DPCs below subcritical limit with loss of neutron absorber (design-basis loading)	0 (0%)
Total DPCs below subcritical limit with loss of neutron absorber (as-loaded)	556 (~79%)
Total DPCs below subcritical limit with loss of neutron absorber and carbon steel structures (as-loaded)	483 (~68%)
Total DPCs below subcritical limit with loss of neutron absorber and carbon steel structures (as-loaded) considering misload	445 (~63%)

E.8. REFERENCE

E-1. J. B. Clarity, K. Banerjee, and L. P. Miller, *Criticality Process, Modeling and Status for UNF-ST&DARDS*, FCRD-NFST-2015-000440, Rev. 2, US Department of Energy, Nuclear Fuel Storage and Transportation Planning Projects (Forthcoming, September 2019).

**APPENDIX F.
FY 2020 Criticality Study**

F.1. INTRODUCTION

This appendix documents work performed supporting the US Department of Energy (DOE) Office of Nuclear Energy (NE) Spent Fuel and Waste Disposition (SFWD) under work breakdown structure element 1.08.01.03.05 “Direct Disposal of Dual Purpose Canisters.” In particular, this appendix fulfills the M3 milestone, M3SF-20OR010305015, “Update of DPC Direct Disposal Criticality Analysis Report” within work package SF-20OR01030501, “Direct Disposal of Dual Purpose Canisters - ORNL.”

This appendix presents the dual-purpose canister (DPC) criticality evaluations performed in FY 2020 to support the feasibility determination of direct disposal of DPCs and extends the work reported in the main body and preceding appendices of this report. The main objectives of the FY 2020 DPC disposal criticality study were as follows:

- To extend the analysis timeline of the calculations through FY19 for the set of 708 canisters from the year 22,000 to the year 1,100,000.
- To examine the impact of candidate cementitious DPC filler materials on disposal criticality scenarios.
- To analyze an additional 66 as-loaded canisters from four sites for the time interval between calendar years 2020 and 1,100,000 using the burnup credit methodology described in the previous sections of this report. The analyzed canisters were at the following sites: Seabrook (16 canisters), Vogtle (26 canisters), Hope Creek (13 canisters), and Salem (11 canisters).

Criticality analysis models were developed for the intact canister configuration applicable to normal conditions of transport and storage as described in the UNF-ST&DARDS status report [E-2]. The models were then modified for degraded material configurations applicable to the canister repository timeframe specified in this report. The degraded material configurations assume two scenarios: (1) complete loss of the fixed neutron absorber (i.e., ^{10}B) without fuel basket geometry changes, and (2) complete degradation and loss of basket materials, including neutron absorber plates and aluminum and carbon steel basket components (e.g., insert plates and basket support discs). Canister material degradation and neutron absorber loss leads to a significant increase in k_{eff} . The degraded material configurations were analyzed for 27 analysis dates between 2020 and 1,100,000 years.

As mentioned in the main report, neutron moderation by water is needed for a waste package to achieve criticality. However, the groundwater (or pore water) that may flood a breached DPC will contain various dissolved aqueous species. Seventeen species were studied as described in the main report, and it was determined that Cl, Li, and B provide the maximum reduction in canister reactivity because of their large neutron absorption cross sections. However, available groundwater data indicate that chlorine (as chloride) is the only naturally abundant neutron-absorbing element in groundwater that can provide a significant reduction in reactivity and is available in most of the repository concepts under consideration in varying quantities. Analyses were performed to determine the chlorine requirement to suppress the reactivity of canisters with the potential to form a critical configuration in a repository timeframe. The impact of chlorine (in terms of NaCl) concentration in groundwater on the reactivity of as-loaded DPCs exceeding a k_{eff} value of 0.98 was evaluated for calendar year 22,000. Previous chlorine concentration effects on k_{eff} documented in this report were evaluated for calendar year 9,999. The impacted DPCs will be reevaluated for calendar year 22,000, the year of maximum reactivity, in the future.

The remainder of this appendix is organized as follows: Section F.2 describes the work performed to extend the analytical time line from the year 22,000 to the year 1,100,000, Section F.3 discusses the criticality calculations that evaluate cementitious filler materials, Section F.4 documents the calculations for Seabrook, Section F.5 documents the calculations for Vogtle, Section F.6 documents the calculations for Hope Creek, Section F.7 documents the calculations for Salem, Section F.8 contains the conclusions, and F.9 contains the references.

F.2. EXTENSION OF DPC CALCULATIONS TO BEYOND 1,000,000 YEARS

Analyses increasing the period of time over which the k_{eff} of the canisters was assessed from the calendar year 22,000 until the calendar year 1,100,000 were documented earlier this year in [F-1] and are included in this work to consolidate all of the work performed on this project in FY20. This work will allow for the assessment of criticality implications for a longer postclosure period.

The degraded absorber condition was modeled for all canisters in the database, and the degraded basket scenario was modeled for canisters that have non–stainless steel structural components. The disposal isotope set was used for all calculations. The times at which the reactivity of the DPCs was assessed was increased to add evaluation dates of July 1 of the years 25,000, 50,000, 75,000, 100,000, 200,000, 300,000, 500,000, 700,000, 900,000, 1,000,000, and 1,100,000.

The results of the degraded absorber calculations are presented in Figure F-1 for pressurized water reactor (PWR) DPCs and in Figure F-2 for boiling water reactor (BWR) DPCs, and the degraded basket calculations are presented in Figure F-3 for PWR DPCs (there are no BWR DPCs that have non–stainless steel structural components). The results in Figures F-1 through F-3 show that the reactivity for each of the canisters follows a similar trajectory with time. The reactivity initially starts off at a local maximum and decreases over the first 100 years as a result of the decay of fissile ^{241}Pu to absorbing ^{241}Am . The reactivity then rises to its peak for all of the canisters between 10,000 and 25,000 years because of the decay of the ^{241}Am and ^{240}Pu . Following the peak, the reactivity of the canisters declines, reaching a minimum at about 200,000 years because of decay of ^{239}Pu . Following the minimum, there is a gradual rise for the remainder of the time period considered due to the ingrowth of ^{233}U .

To more clearly show the reactivity evolution that a canister experiences during the disposal period, a representative canister's reactivity was plotted as a function of time using the same dates that are used in Figures F.1–F.3. Canister MAG-TSC-30026086-004 from Kewaunee was selected to show this effect. The reactivity trajectory of MAG-TSC-30026086-004 is plotted in F-4 for the degraded absorber case and F-5 for the degraded basket case. By examining the results in Figures F-4 and F-5, it can be seen that the initial drop in reactivity to the global minimum over the first 100 years is $0.025 \Delta k_{eff}$ for the degraded absorber case and $0.026 \Delta k_{eff}$ for the degraded basket case. The rise from the global minimum at the year 2100 to the global maximum at 22,000 years is $0.034 \Delta k_{eff}$ for the degraded absorber case and $0.038 \Delta k_{eff}$ for the degraded basket case. The reactivity then drops $0.028 \Delta k_{eff}$ for both the degraded absorber and degraded basket cases to a local minimum in the year 200,000. The rise from the local minimum to the end of the period analyzed is approximately $0.007 \Delta k_{eff}$ for both cases.

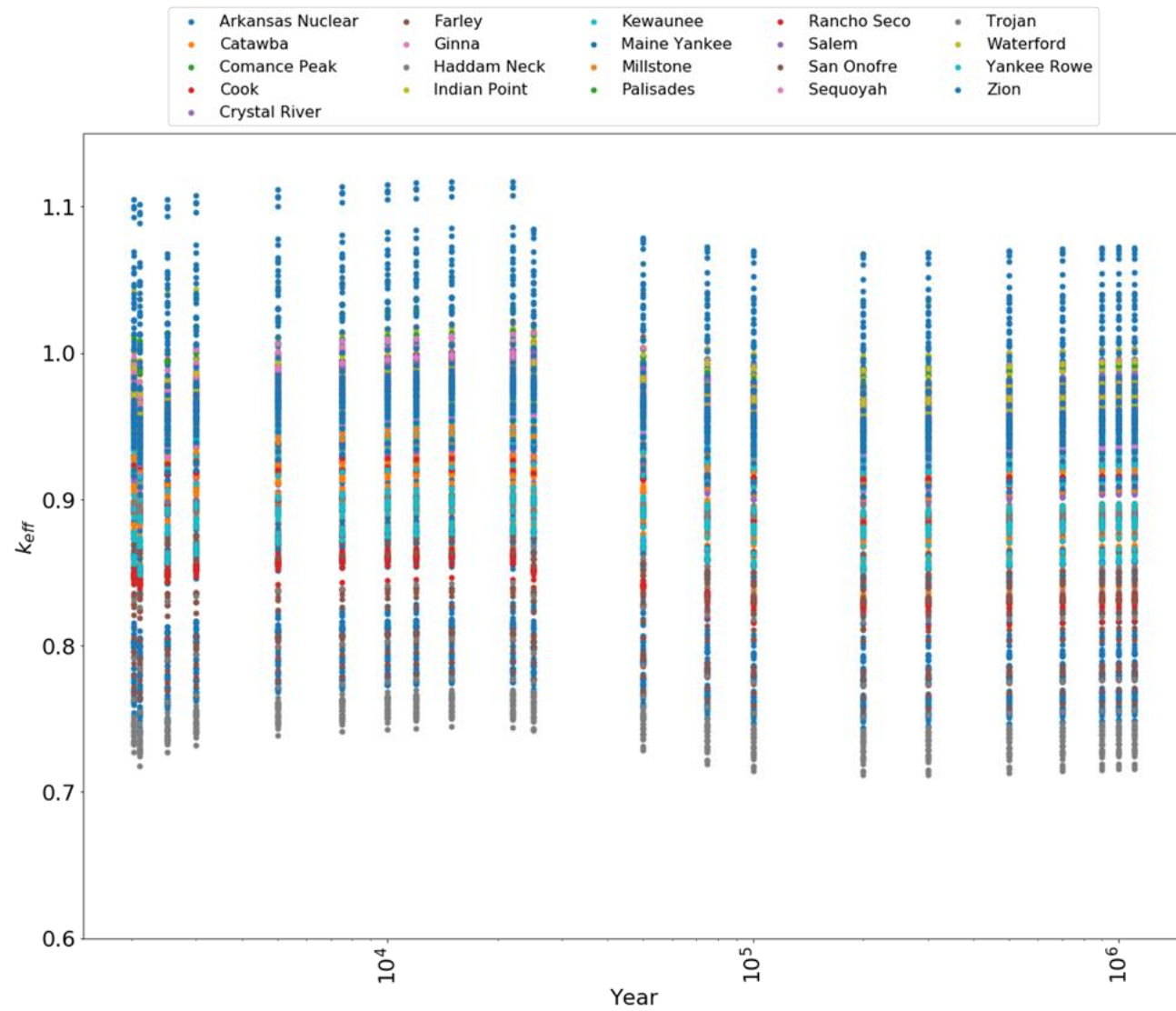


Figure F-1. Degraded absorber calculations for PWR DPCs.

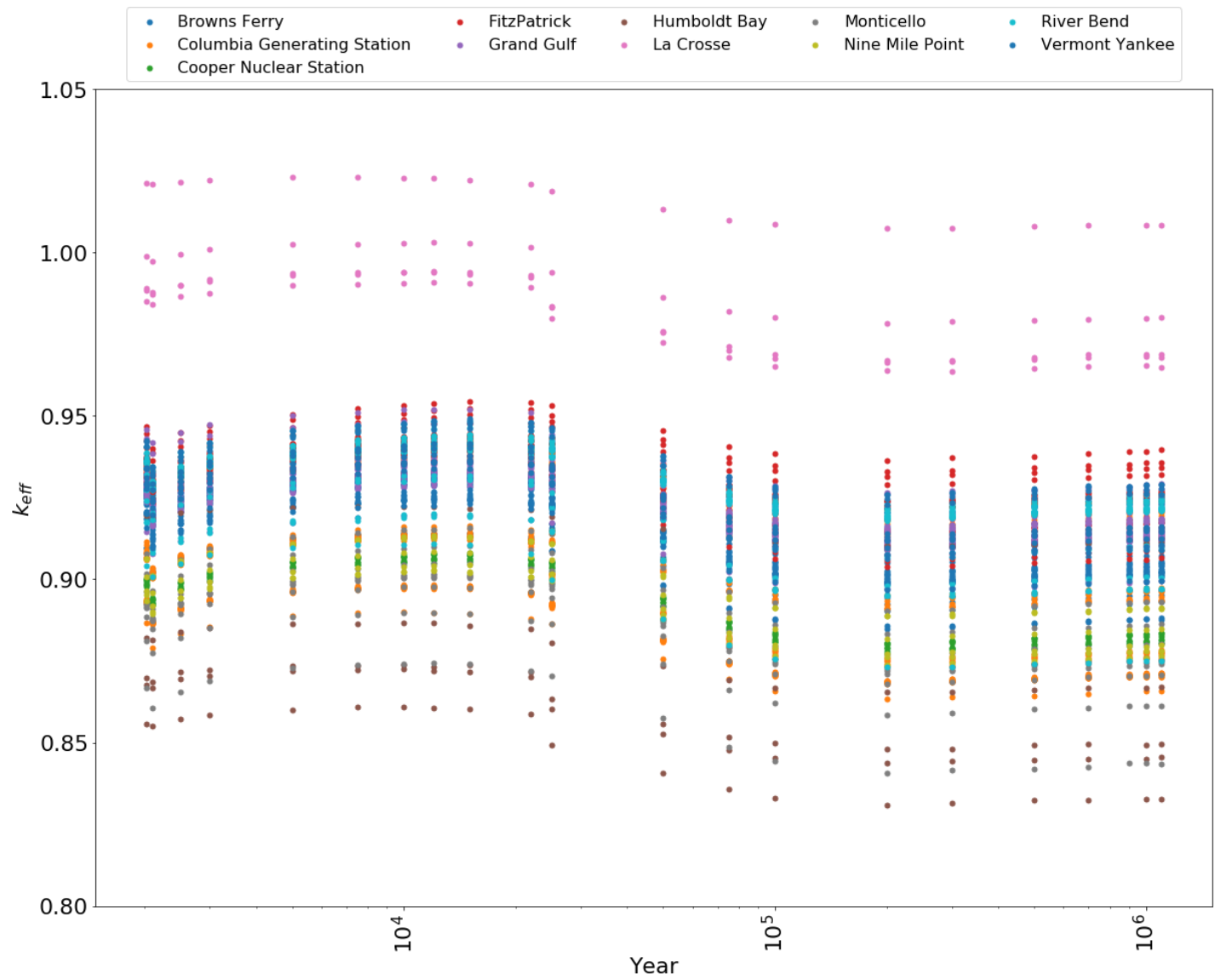


Figure F-2. Degraded absorber calculations for BWR DPCs.

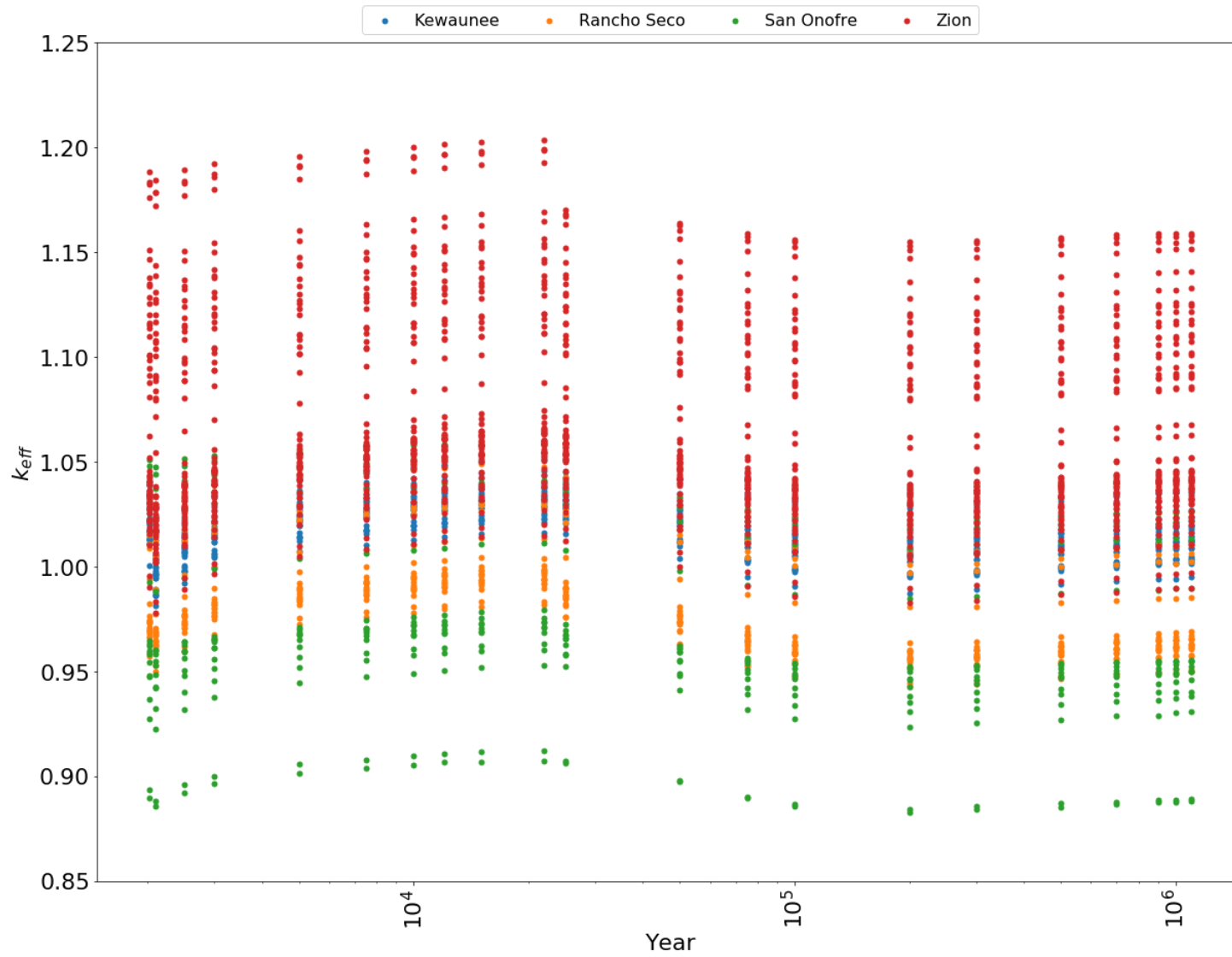


Figure F-3. Degraded basket calculations for PWR DPCs.

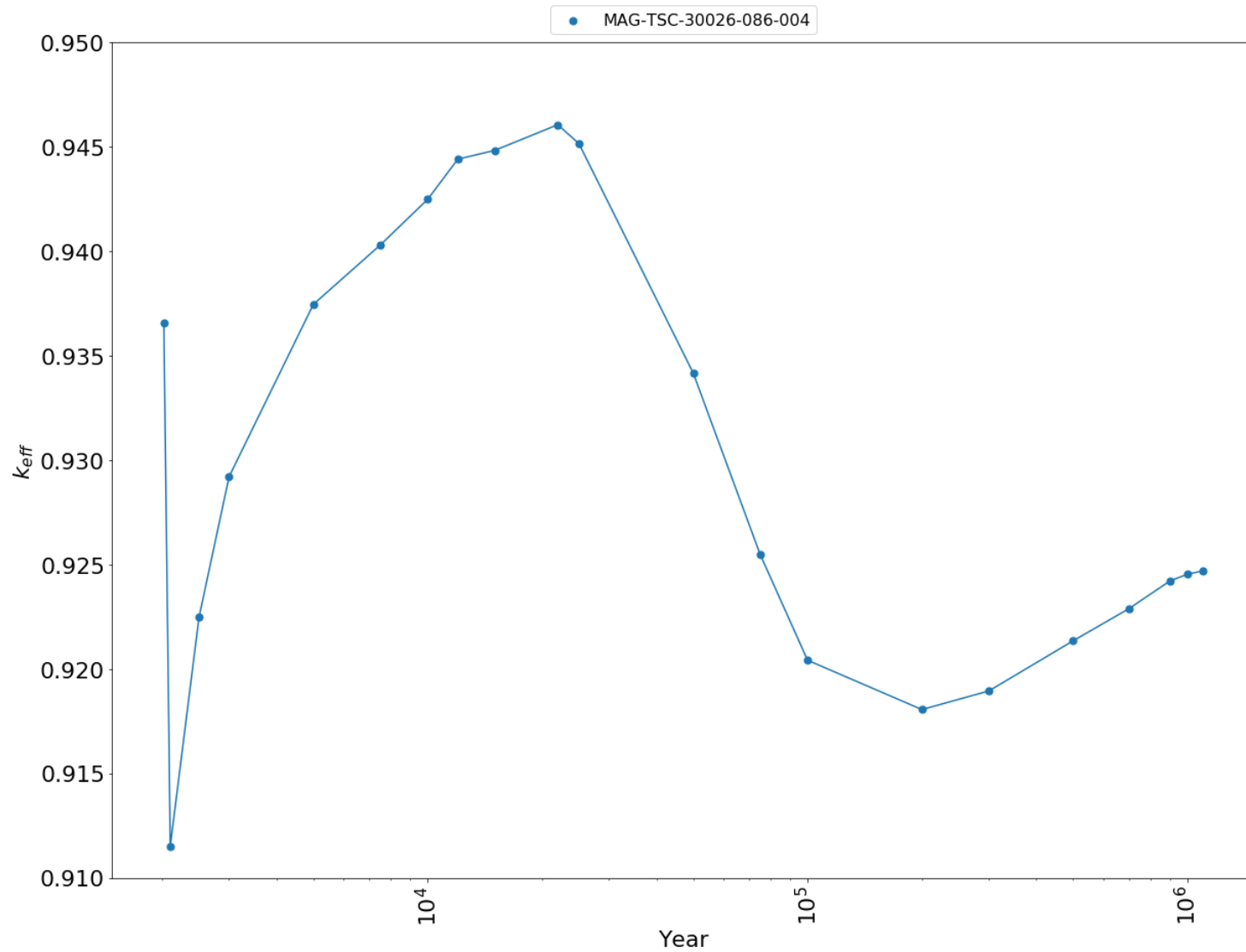


Figure F-4. Degraded absorber reactivity trajectory for TSC-37 canister MAG-TSC-30026086-004 at Kewaunee.

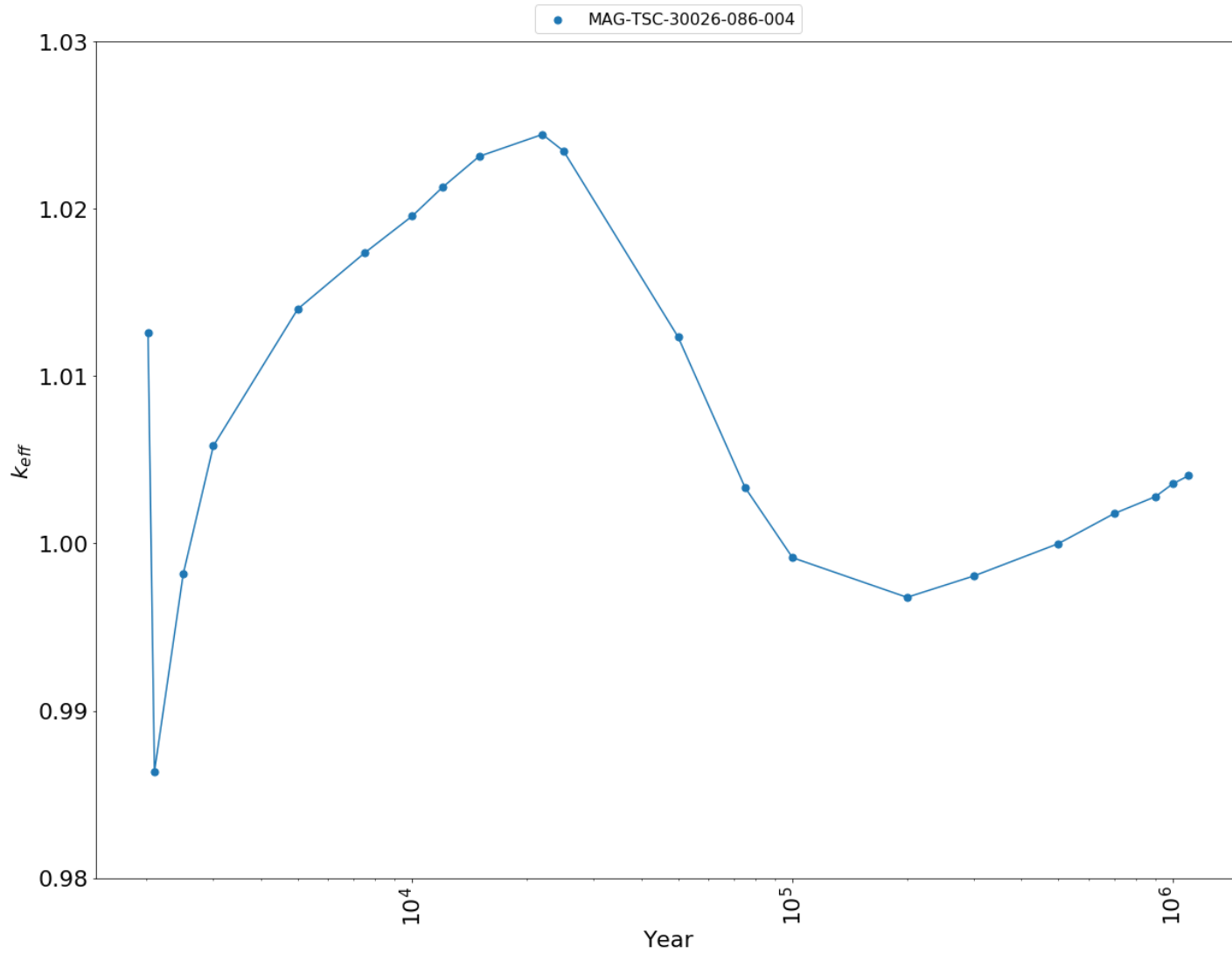


Figure F-5. Degraded basket reactivity trajectory for TSC-37 canister MAG-TSC-30026086-004 at Kewaunee.

F.3. EVALUATION OF CEMENTITIOUS FILLER MATERIALS FOR CRITICALITY CONTROL

This section documents calculations performed to assess the impact of the addition of cementitious filler materials on post closure criticality safety for a single canister from the Zion site. The filler materials considered in this analysis have been provided by Sandia National laboratories and include (1) a mixture of wollastonite and calcium phosphate, (2) a mixture of aluminum oxide and aluminum phosphate, (3) a hydroxide-based calcium phosphate cement, and (4) a chloride-based calcium phosphate cement. A summary of the chemical composition of the filler materials used is provided in Table F-1.

Table F-1. Chemical composition of filler materials.

Filler material	Component	Weight percentage of component
Wollastonite / calcium phosphate	CaSiO ₃	40%
	Ca ₁₀ (PO ₄) ₆ (OH) ₂	60%
Aluminum oxide / aluminum phosphate	Al ₂ O ₃	86.4%
	AlPO ₄ (H ₂ O) ₂	13.6%
Calcium phosphate cement (OH)	Ca ₁₀ (PO ₄) ₆ (OH) ₂	100%
Calcium phosphate cement (Cl)	Ca ₁₀ (PO ₄) ₆ (Cl) ₂	100%

F.3.1. Calculations

The canister used to perform this assessment (TSCD-37-TSCDF-015) was selected because it was the highest reactivity canister of those analyzed to date. Further, it was determined that the canister decay date of July 1, 22,000, represented the peak reactivity over the first 1.1 million years of its life, so the fuel isotopic compositions from this date were used in the calculations.

Each set of calculations was performed with two basket configurations, the degraded neutron absorber (NA) model and the degraded basket (DB) model. The NA model considers the intact basket structure while removing the neutron absorber material that is placed in the basket for criticality control during storage and transportation. The DB model removes the basket structural material and replaces it with water to simulate the corrosion of the basket following emplacement.

Calculations performed for this assessment can be subdivided into four categories based on the amount of coverage of the canister by the filler material. The first set of calculations simulates a complete filling of the basket with filler material so that the entire inner volume of the canister that is not occupied by the fuel or structural material is modeled as being comprised of filler material. The second set of calculations assumes that it will not be possible to place filler material in the damaged fuel cans located in the oversized cells at the four corners on the minor axes of the basket, but filler is otherwise able to fill the basket. The third set of calculations analyzes filler exclusion from the guide tubes and instrumentation tubes of the fuel assemblies. If the basket is filled from the bottom to the top, then the dashpot entry ways for guide tubes may be too small to allow for filler ingress. The fourth set of calculations analyzes the incomplete axial filling of each fuel tube. These calculations assume that there is no filler material the entire length of the guide tubes and instrumentation tube and that a variable portion of the top part of the assembly is unable to be filled.

SCALE-generated renderings of the scenarios modeled are shown in Figures F-6 through F-9. In each figure, light blue represents the portion of the canister with filler material, pink represents portions of the canister occupied by fresh water, and red represents the basket's structural material. Figure F-6 shows the radial views of the NA and DB models for the complete filling case, Figure F-7 shows the NA and DB models for the damaged fuel filler exclusion case, Figure F-8 shows the NA and DB models for the guide tube filler exclusion case, and Figure F-9 shows an axial depiction of the incomplete axial filling case.

For the complete filling and damaged fuel filler exclusion cases, calculations were performed using each of the four filler materials and varying the porosity of the material in 5% increments, from 0 to 100%. In this work, the term *porosity* means the volume fraction of the filler material that is occupied by water. Based on the results of those calculations, it was determined that the behavior of wollastonite / calcium phosphate, aluminum oxide / aluminum phosphate, and calcium phosphate cement (OH) was so similar that it was only necessary to perform calculations for the guide tube exclusion cases and the incomplete axial filling cases with one of those fillers and the calcium phosphate cement (Cl) material. The incomplete axial filling case used calculations which assumed that the filler material present in the remainder of basket had a porosity of 50%, since SNL staff stated this porosity level was likely obtainable.

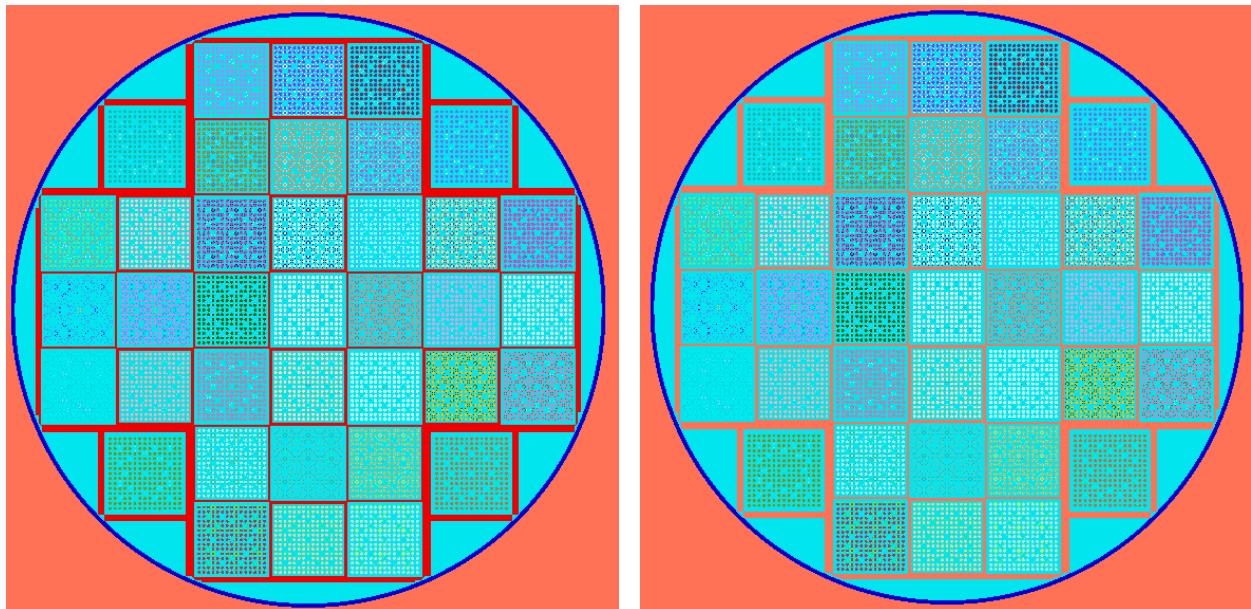


Figure F-6. Radial view of the complete filling models for the NA case (left) and the DB case (right).

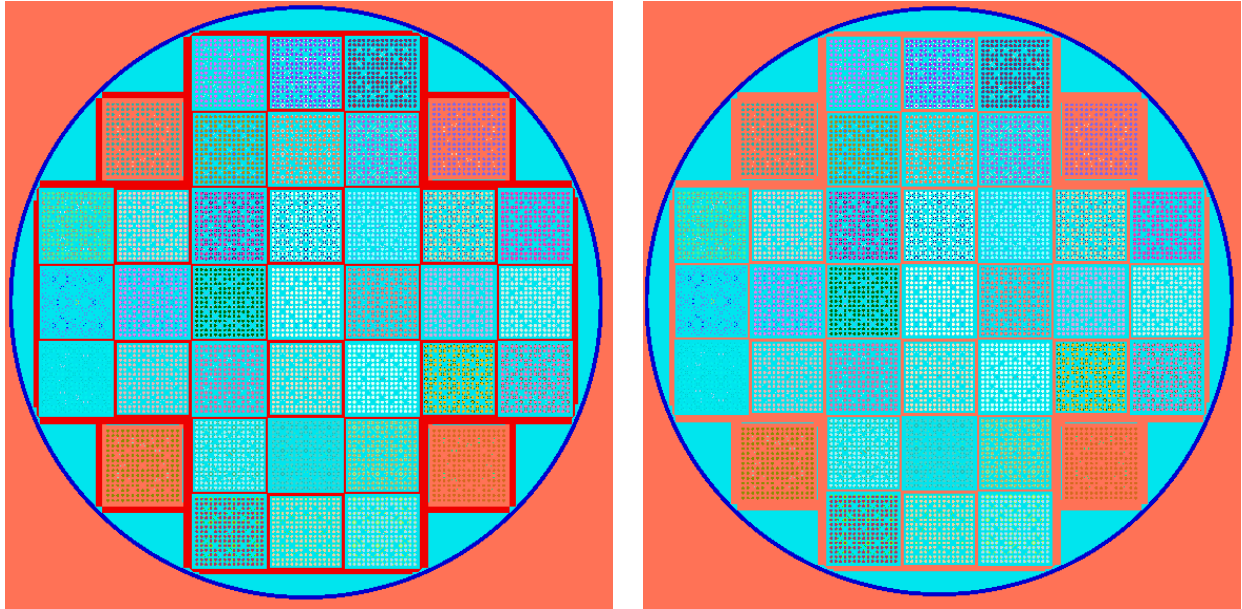


Figure F-7. Radial view of the damaged fuel filler exclusion models for the NA case (left) and the DB case (right).

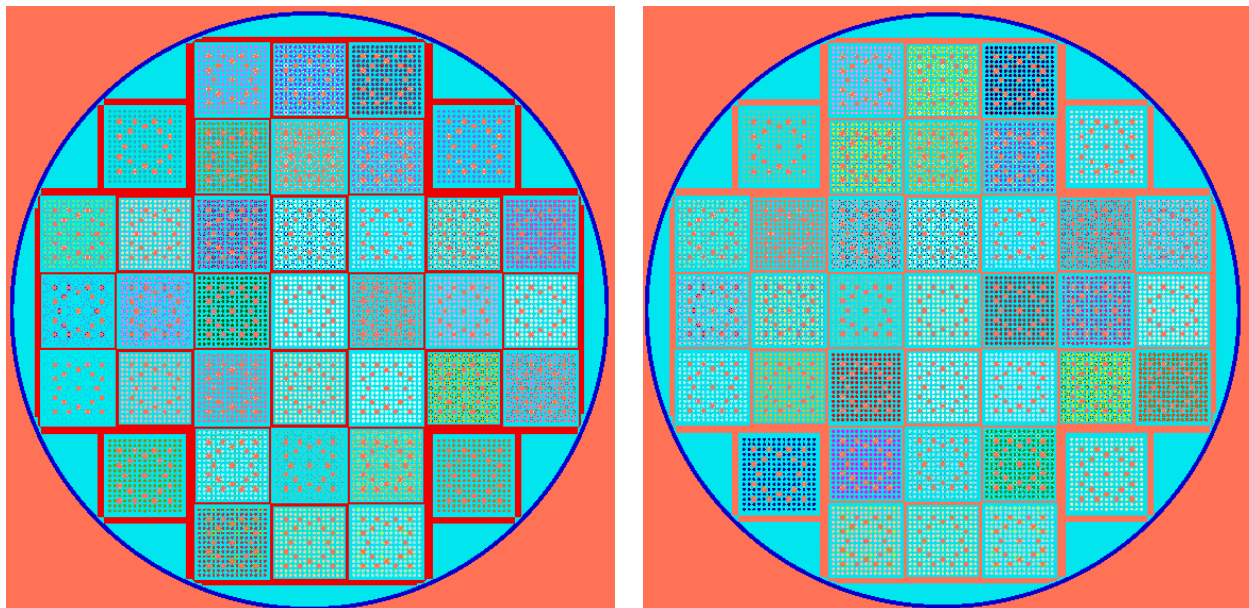


Figure F-8. Radial view of the guide tube filler exclusion models for the NA case (left) and the DB case (right).

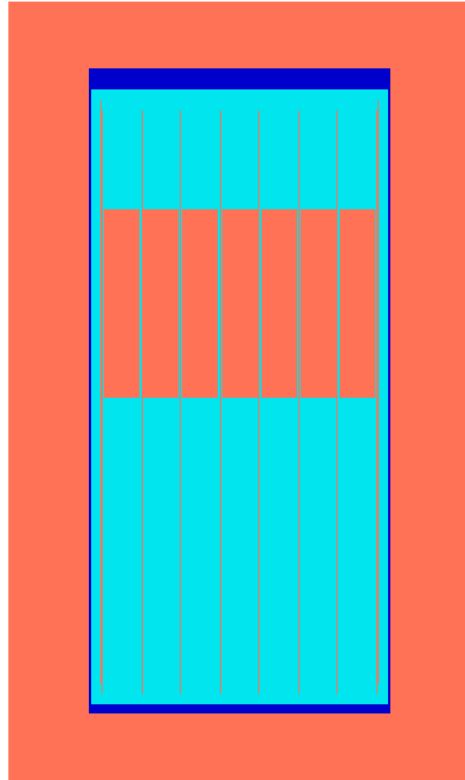


Figure F-9. Axial view of the incomplete axial filling model showing the top seven of 18 nodes unfilled.

F.3.2. Results

The results for the complete filling and damaged fuel exclusion models are presented in Figure F-10 for the NA case and in Figure F-11 for the DB case. An estimated subcritical 0.98 is used for comparison. A few observations may be made based on the results shown in Figures F-10 and F-11. The first observation is that all of the filler types except the calcium phosphate cement (C1) perform similarly to one another across the full porosity range (except perhaps at <10%, which does not appear to be achievable). The chloride-based calcium phosphate cement provides better criticality control over all porosities because ^{35}Cl is a neutron absorber. The second observation is that excluding the filler material from the damaged fuel locations results in the canister's reactivity plateauing below 70% porosity for the chloride-based cement and below somewhere between 40 and 50% porosity for the other filler materials. The plateauing occurs because the k_{eff} of the system switches away from being driven by the center of the canister where additional filler material is added and is driven by the damaged fuel locations, which do not have any filler material. The third observation is that for the NA case, the porosity required to meet a hypothetical k_{eff} limit of 0.98 is approximately 85% or less for the chloride-based cement and 65% or less for the other filler materials. For the DB case, a porosity of less than 75% would be required for the chloride-based cement, and a porosity of less than 45% would be required for the other filler materials.

In order to assess the impact of not being able to fill the guide tubes and instrumentation tubes with filler material, additional calculations were performed using the wollastonite/calcium phosphate and chloride-based cement for the NA and DB cases. The results of these calculations, along with the corresponding complete filling cases for comparison, are presented in Figure F-12 for the NA case and Figure F-13 for the DB case. The results of these calculations show that the increase in k_{eff} associated with having water rather than filler material in the guide tubes is largest at the lowest values of porosity, and it decreases as the porosity of the filler material increases. This due to the relative scarcity of other sources of ^1H as a

neutron moderator at lower porosity levels and relative abundance at higher porosity levels. The 0.98 hypothetical k_{eff} limit decreases the allowable porosity values 7–10% for the wollastonite/calcium phosphate filler materials, and it decreases the allowable porosity about 5% for the chloride-based cement necessary to meet this value.

The final set of calculations aimed to determine how important it is to completely fill the axial extent of the fuel basket. This calculation removed the filler material from each node of the cases that excluded filler material from the guide tubes and instrument tubes. The filler material in the remainder of the basket was taken to be 50% porosity. The results of these calculations are presented in Figure F-14, and they show that regardless of the filler material or basket configuration, the k_{eff} of the canister rises quickly with the decrease in filler height to the point that virtually all impact of the filler material is lost after about 15 inches.

F.3.3. Cementitious Filler Conclusions

In this work, a series of calculations using the TSCDF-37-TSCDF-15 cask from the Zion site were performed to determine the impact of adding filler material to canisters on post-closure criticality. The analysis presented here includes both the NA and DB cases and considers four separate filler materials, which are presented in Table F-1. Of the four filler materials, the chloride-based calcium phosphate cement provided superior criticality control to the other filler materials at the same porosity level. It was also shown that almost the entire canister must be filled in order to achieve criticality control. Having approximately 15 inches of uncovered fuel returns canister reactivity to levels very close to baseline k_{eff} values.

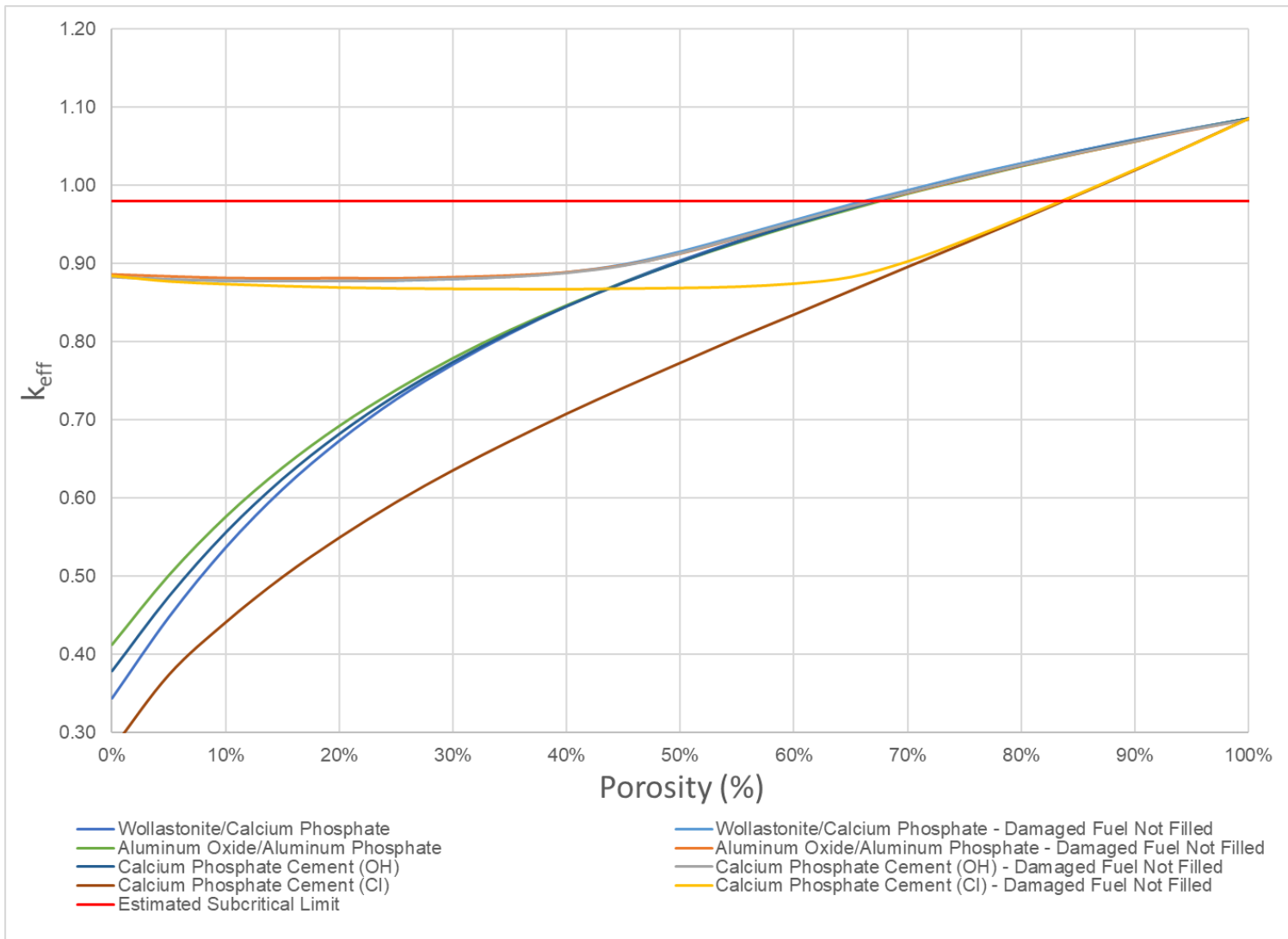


Figure F-10. Canister reactivity vs. porosity for the complete filling and damaged fuel exclusion NA cases.

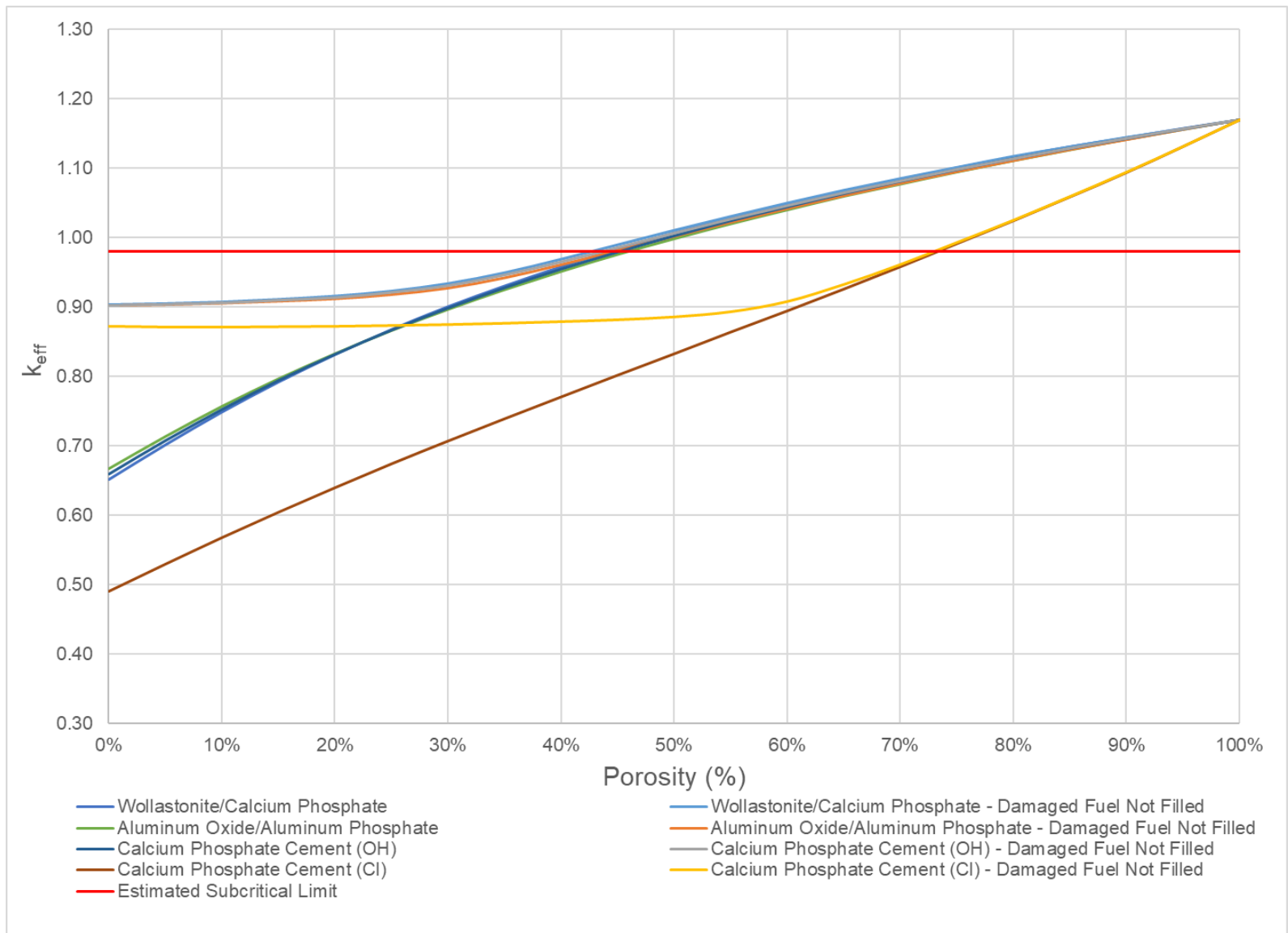


Figure F-11. Canister reactivity vs. porosity for the complete filling and damaged fuel exclusion DB cases.

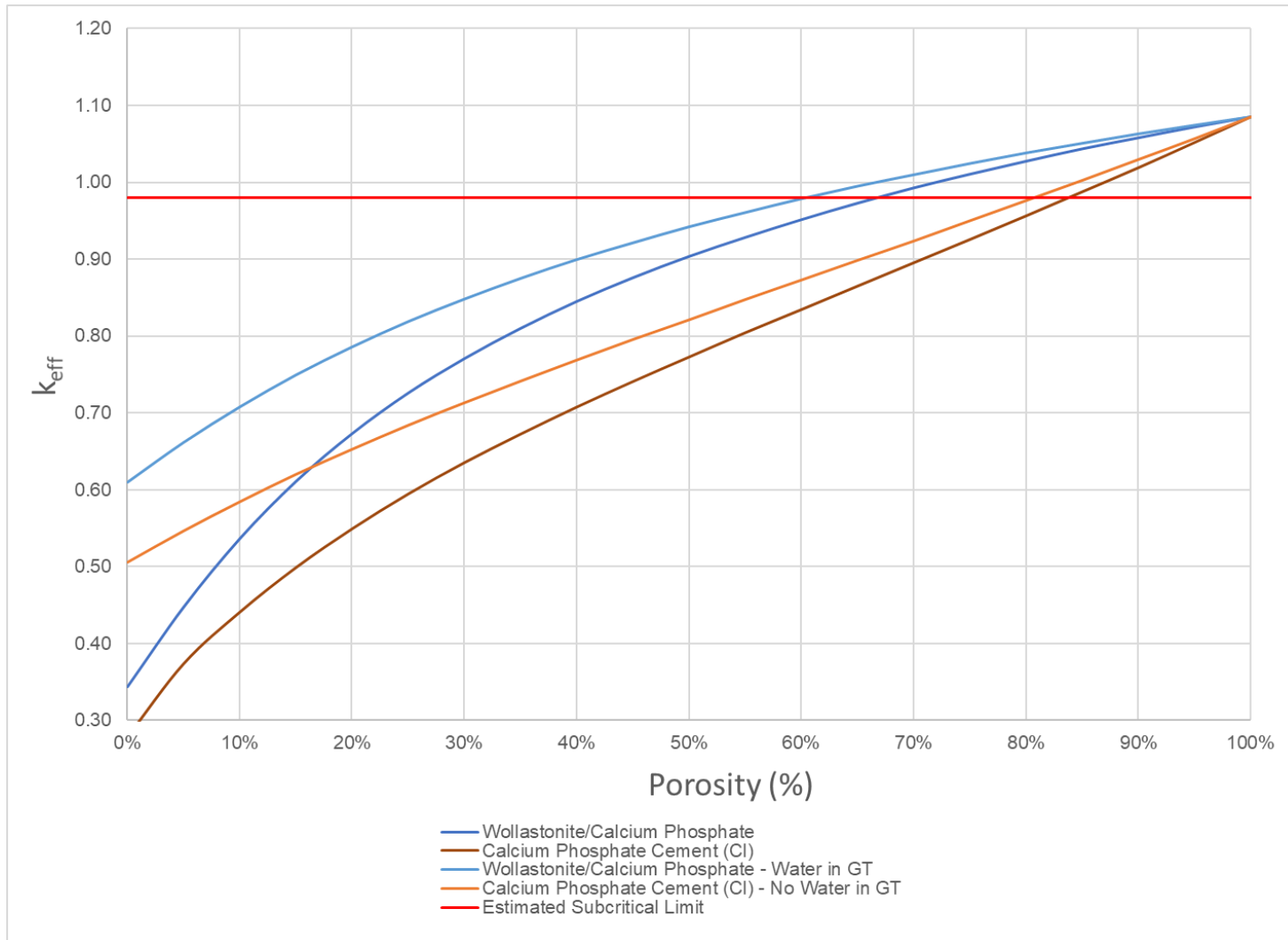


Figure F-12. Canister reactivity vs. porosity for the guide tube filler exclusion NA case.

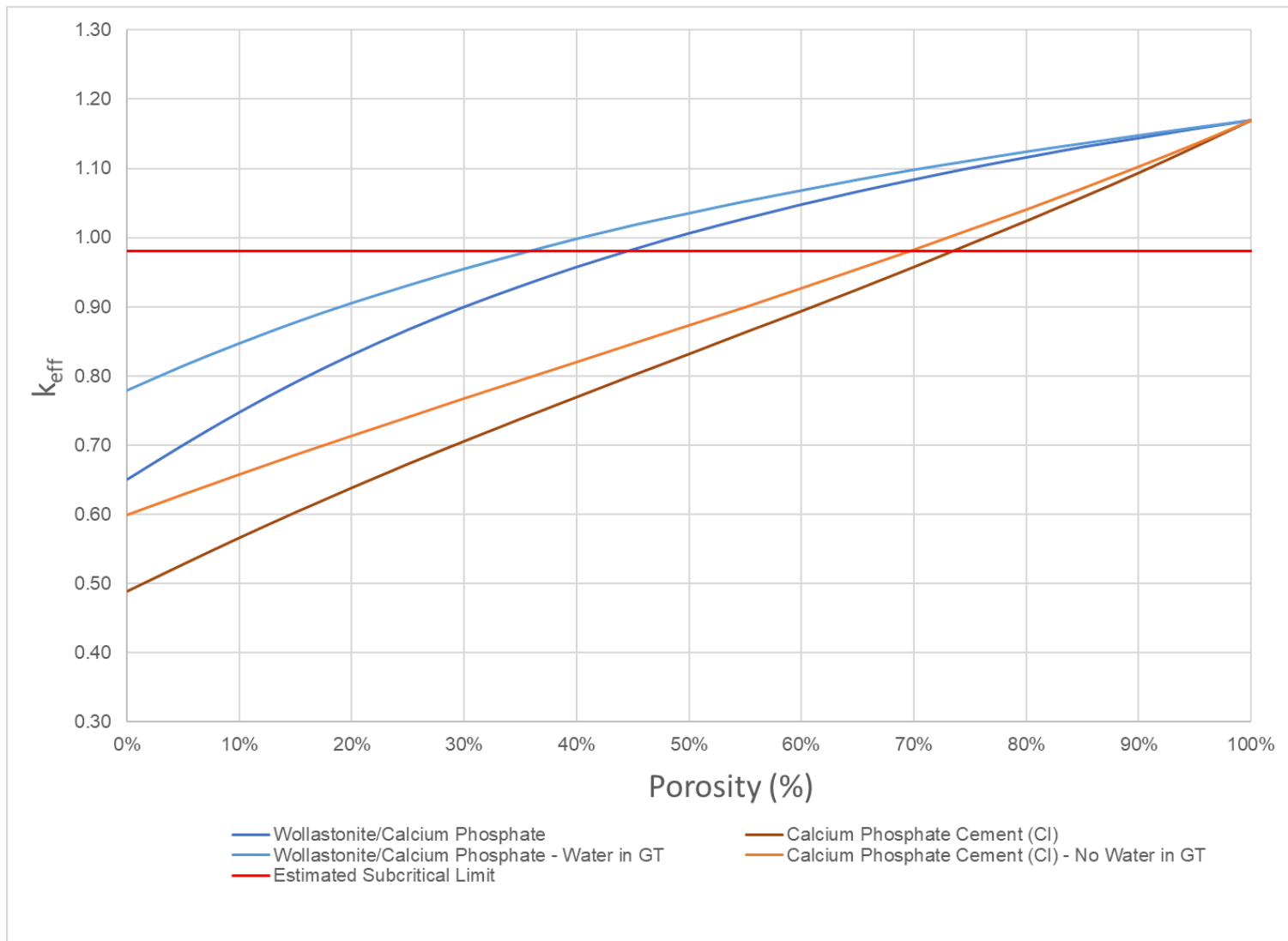


Figure F-13. Canister reactivity vs. porosity for the guide tube filler exclusion DB case.

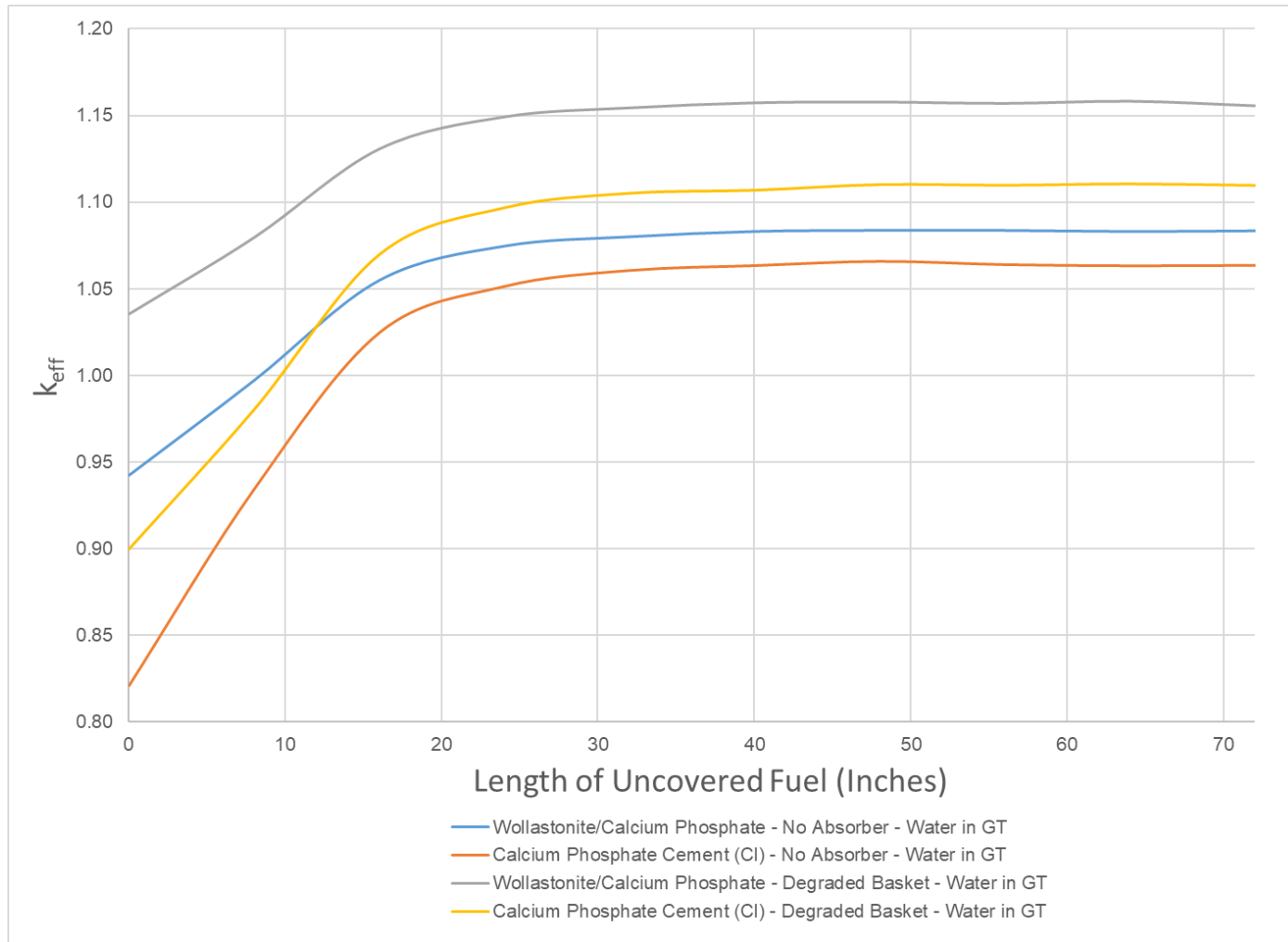


Figure F-14. Canister reactivity vs. length of top portion of assembly uncovered for NA and DB cases (guide tubes water filled, 50% porosity elsewhere).

F.4. SEABROOK CRITICALITY CALCULATIONS

Post-closure disposal criticality calculations were performed as a function of decay time for the 16 SNF canisters at the Seabrook independent spent fuel storage installation (ISFSI). All of the 16 SNF canisters are NUHOMS® 32PTH-DSCs. The NUHOMS® 32PTH-DSC does not contain any carbon steel structural components, so only the loss-of-neutron-absorber scenario is analyzed. Figure F-15 shows results for the loss-of-neutron-absorber scenario for 27 decay times within the time interval between calendar years 2020 and 1,100,000. The results in Figure F-15 show k_{eff} variation as a function of calendar year. The one sigma statistical uncertainty for all k_{eff} values is 0.0003 or less for all cases.

The k_{eff} values are predicted to vary from 0.8915 to 1.0570 for the NUHOMS® 32PTH-DSCs under the loss-of-absorber scenario. For canisters which had k_{eff} values greater than 0.98 under the loss-of-neutron-absorber scenario, calculations were performed in which the pure water was replaced with groundwater compositions of various NaCl concentrations, and the models thus modified were used to determine k_{eff} as a function of NaCl concentration for the calendar year 22,000 (most reactive date). Figure F-16 presents k_{eff} variation as a function of NaCl concentration for those 7 canisters. Examining the results presented in Figure F-16, it is clear that 1.1 mol NaCl/ kg H₂O is sufficient to demonstrate subcriticality ($k_{eff} < 0.98$) for all of the Seabrook canisters. In this context, it is also important to note that a saturated NaCl brine has a concentration of approximately 6 molal.

Figure F-17 shows the k_{eff} increase between the worst misload scenario and the as-loaded configuration for the 16 analyzed Seabrook canisters at the calendar year 22,000. The increase in k_{eff} varies between 498 and 3,309 pcm for Seabrook canisters.

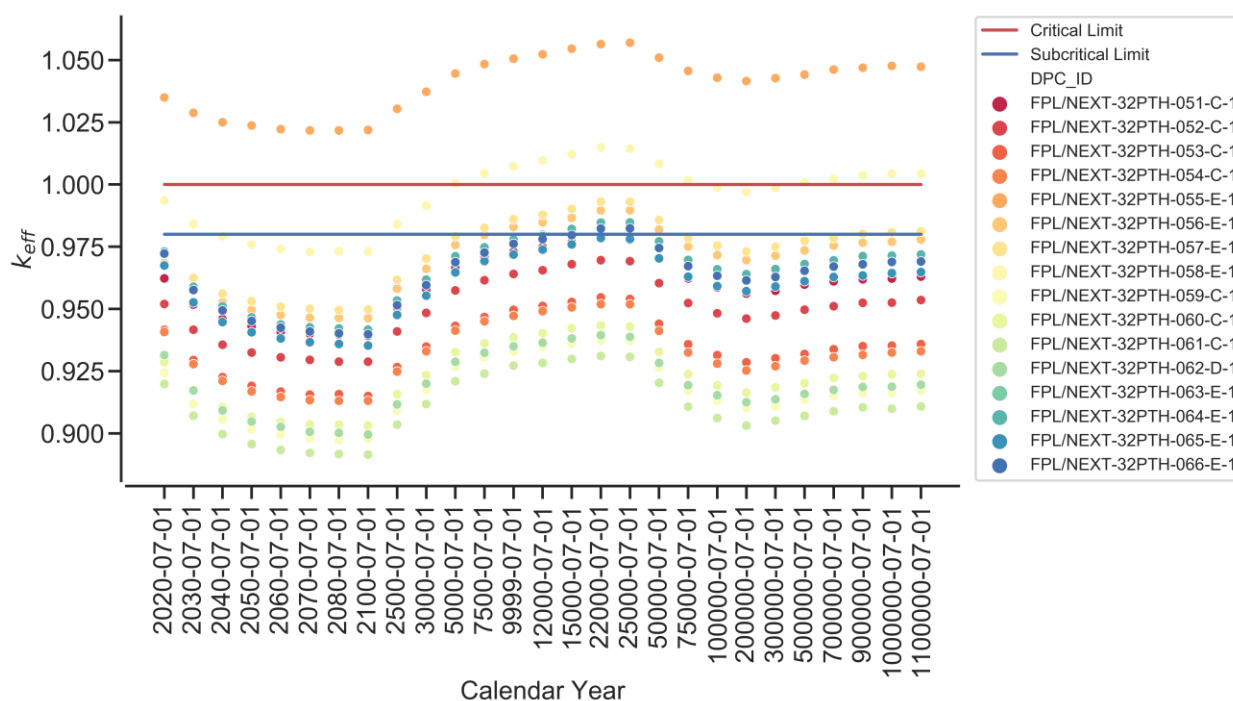


Figure F-15. k_{eff} vs. calendar year for the loss-of-neutron-absorber scenario based on actual loading and disposal isotopes for the SNF canisters at Seabrook.

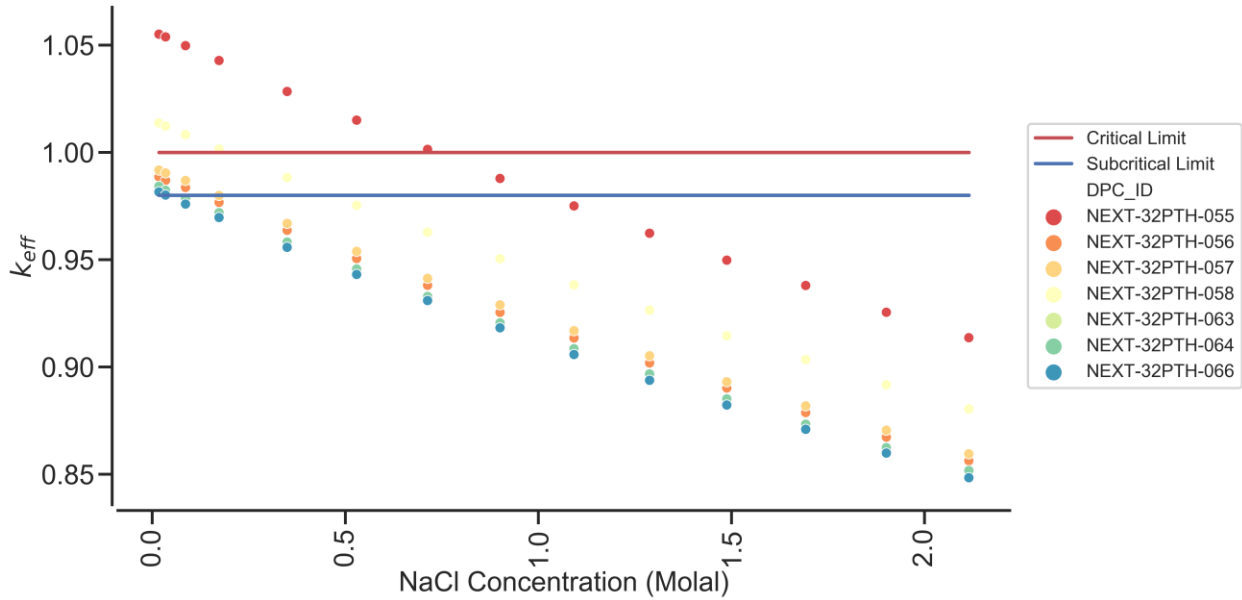


Figure F-16. k_{eff} vs. NaCl concentration for the DPCs with $k_{eff} > 0.98$ for the canisters at Seabrook under the loss-of-neutron-absorber scenario (calendar year 22,000).

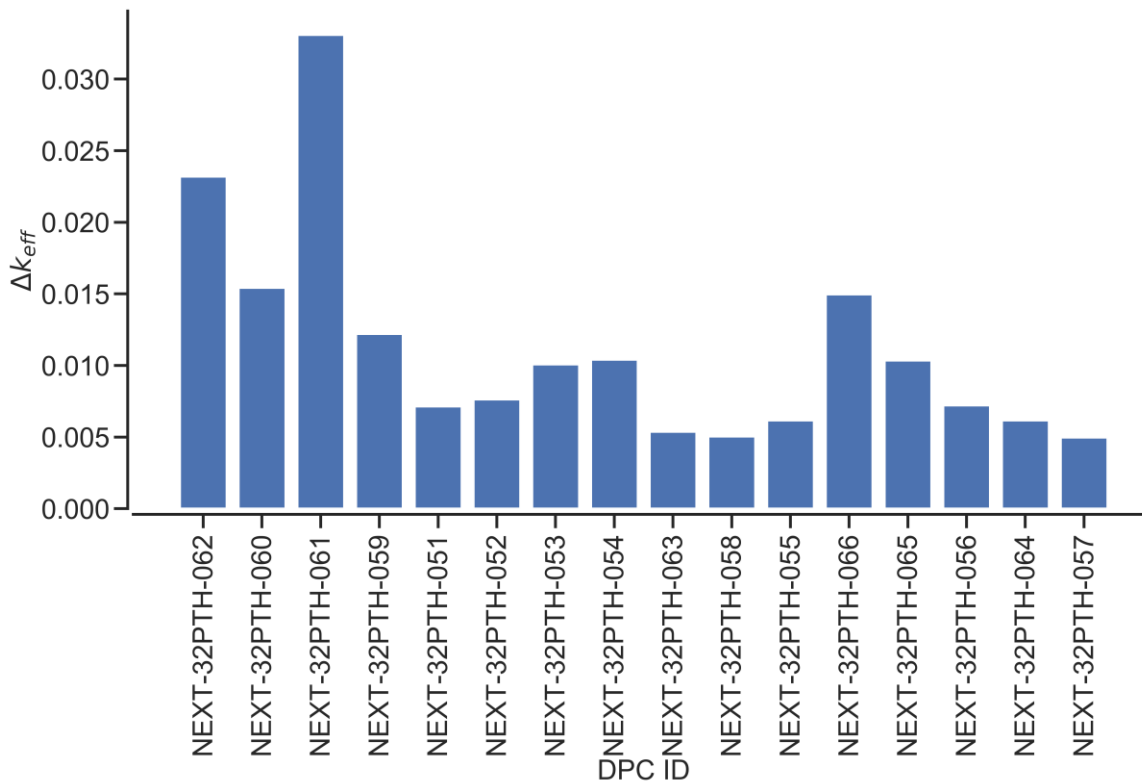


Figure F-17. k_{eff} increase between the worst-misload scenario and the as-loaded configuration for the NUHOMS® 32PTH-DSCs at Seabrook (calendar year 22,000).

F.5. VOGTLE CRITICALITY CALCULATIONS

Post-closure disposal criticality calculations were performed as a function of decay time for the 26 SNF canisters at the Vogtle ISFSI. All of the 26 SNF canisters are of the Holtec MPC-32 design. The MPC-32 does not contain any carbon steel structural components, so only the loss-of-neutron-absorber scenario is analyzed. Figure F-18 shows results for the loss-of-neutron-absorber scenario for 27 decay times within the time interval between calendar years 2020 and 1,100,000. The results in Figure F-18 show k_{eff} variation as a function of calendar year. The one sigma statistical uncertainty for all k_{eff} values is 0.0003 or less for all cases.

The k_{eff} values are predicted to vary from 0.9112 to 1.0105 for the MPC-32 under the loss-of-absorber scenario. For canisters which had k_{eff} values greater than 0.98 under the loss-of-neutron-absorber scenario, calculations were performed in which the pure water was replaced with groundwater compositions of various NaCl concentrations, and the models thus modified were used to determine k_{eff} as a function of NaCl concentration for the calendar year 22,000 (most reactive date). Figure F-19 presents k_{eff} variation as a function of NaCl concentration for those 7 canisters. Examining the results presented in Figure F-19, it is clear that 0.5 mol NaCl/ kg H₂O is sufficient to demonstrate subcriticality ($k_{eff} < 0.98$) for all of the Vogtle canisters. In this context, it is also important to note that a saturated NaCl brine has a concentration of approximately 6 molal.

Figure F-17 shows the k_{eff} increase between the worst misload scenario and the as-loaded configuration for the 26 analyzed Vogtle canisters at the calendar year 22,000. The increase in k_{eff} varies between 579 and 3,808 pcm for Vogtle canisters.

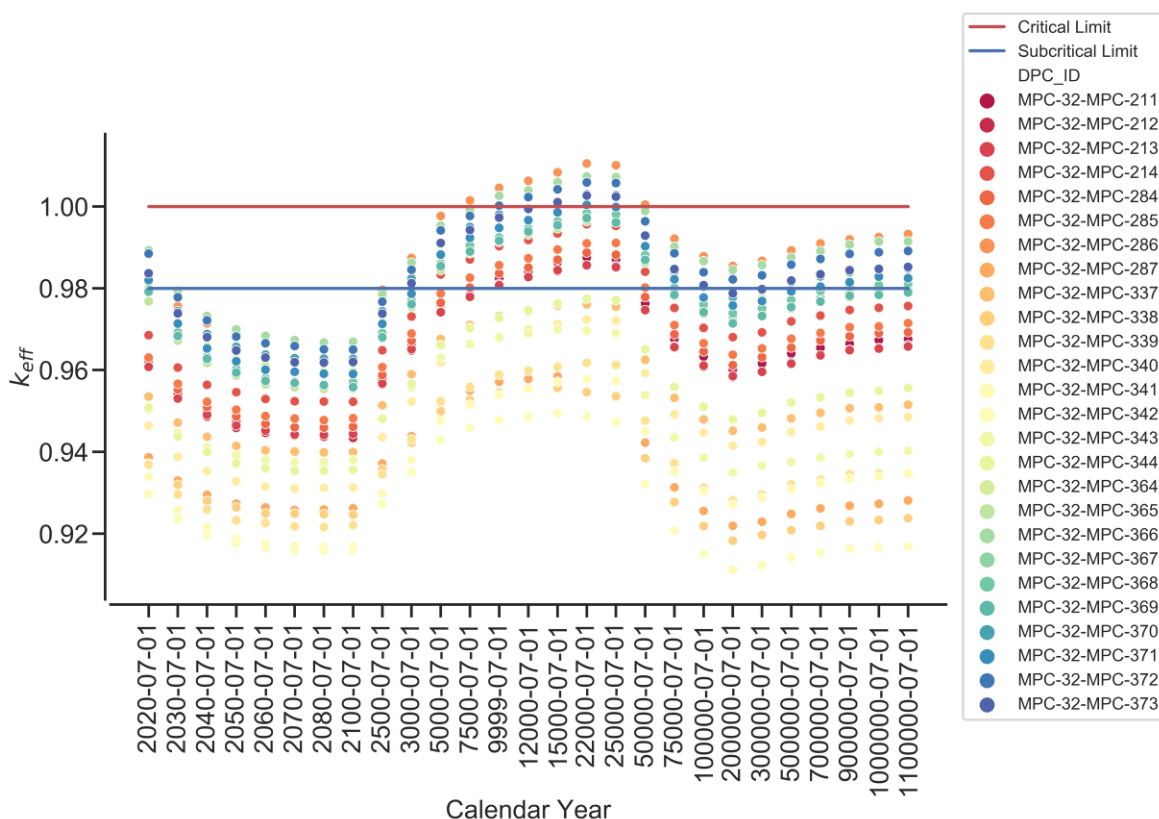


Figure F-18. k_{eff} vs. calendar year for the loss-of-neutron-absorber scenario based on actual loading and disposal isotopes for the SNF canisters at Vogtle.

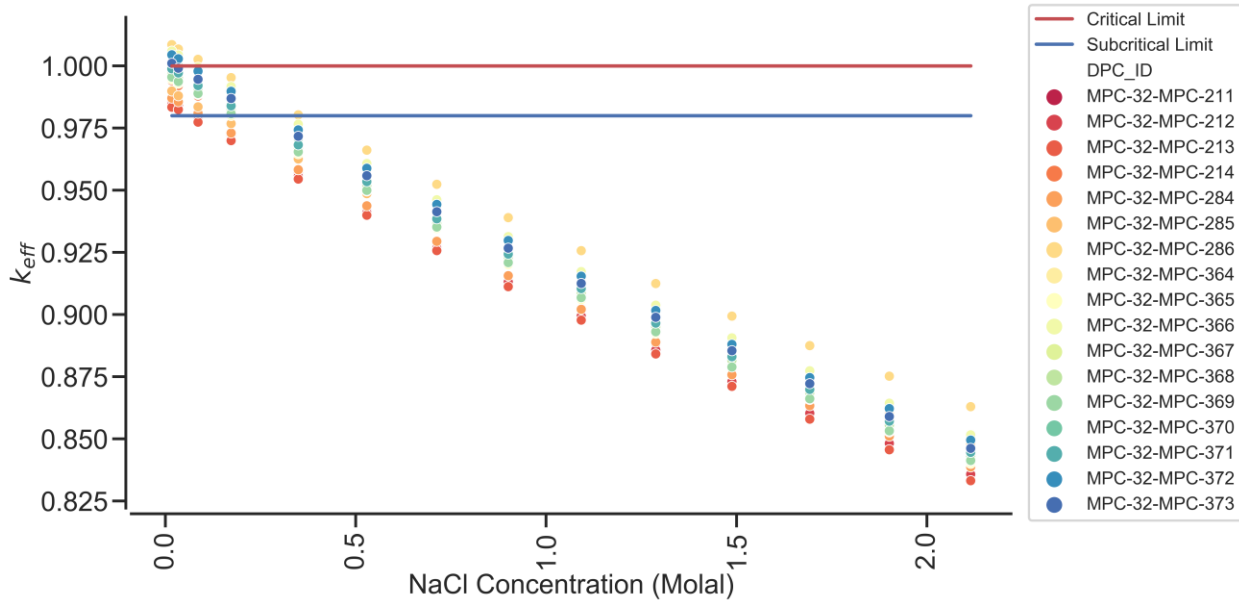


Figure F-19. k_{eff} vs. NaCl concentration for the DPCs with $k_{eff} > 0.98$ for the canisters at Vogtle under the loss-of-neutron-absorber scenario (calendar year 22,000).

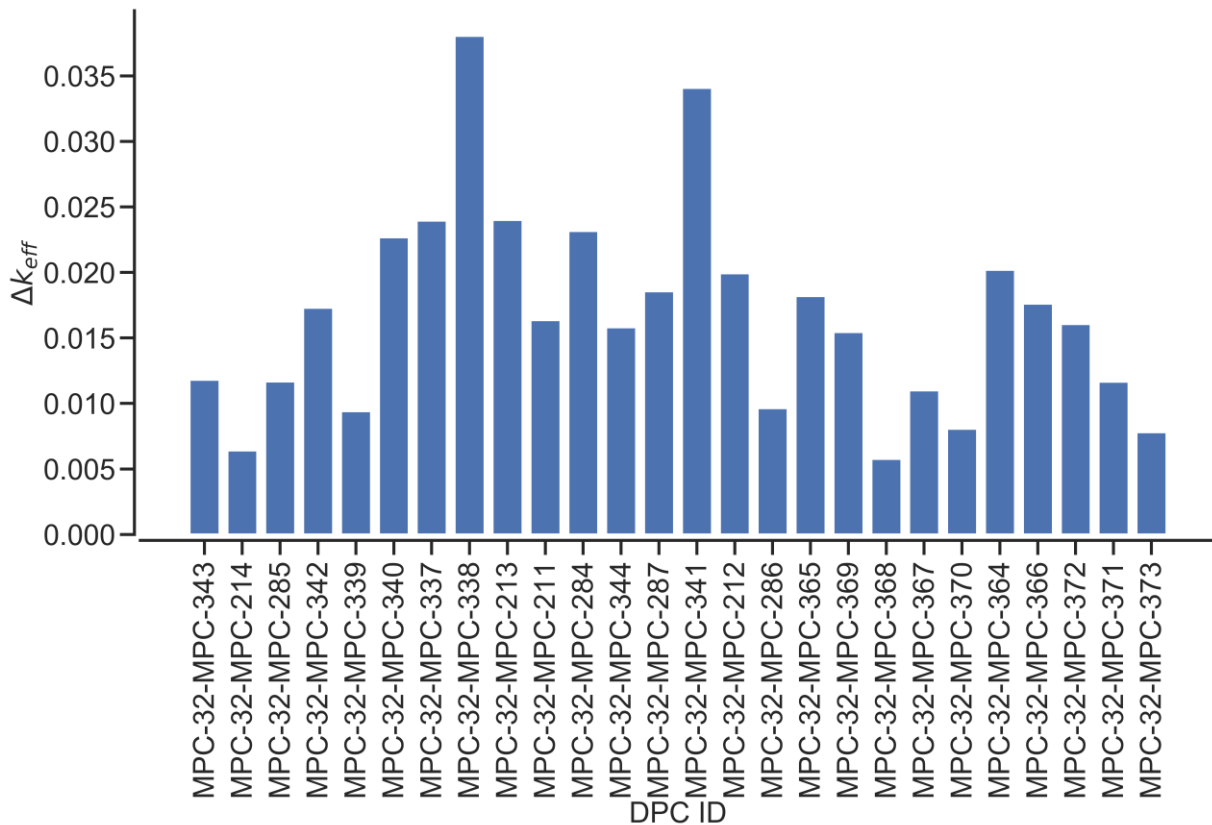


Figure F-20. k_{eff} increase between the worst-misload scenario and the as-loaded configuration for the MPC-32s at Vogtle (calendar year 22,000).

F.6. HOPE CREEK CRITICALITY CALCULATIONS

Post-closure disposal criticality calculations were performed as a function of decay time for the 13 SNF canisters at the Hope Creek ISFSI. All of the 13 SNF canisters are of the Holtec MPC-68 design. The MPC-68 does not contain any carbon steel structural components, so only the loss-of-neutron-absorber scenario is analyzed. Figure F-21 shows results for the loss-of-neutron-absorber scenario for 27 decay times within the time interval between calendar years 2020 and 1,100,000. The results in Figure F-21 show k_{eff} variation as a function of calendar year. The one sigma statistical uncertainty for all k_{eff} values is 0.0003 or less for all cases.

The k_{eff} values are predicted to vary from 0.9004 to 0.9366 for the MPC-68 under the loss-of-absorber scenario. No canisters had k_{eff} values greater than 0.98 under the loss-of-neutron-absorber scenario, so no NaCl calculations were performed for Hope Creek.

Figure F-22 shows the k_{eff} increase between the worst misload scenario and the as-loaded configuration for the 13 analyzed Hope Creek canisters at calendar year 22,000. The increase in k_{eff} varies between 520 and 1,331 pcm for the Hope Creek canisters.

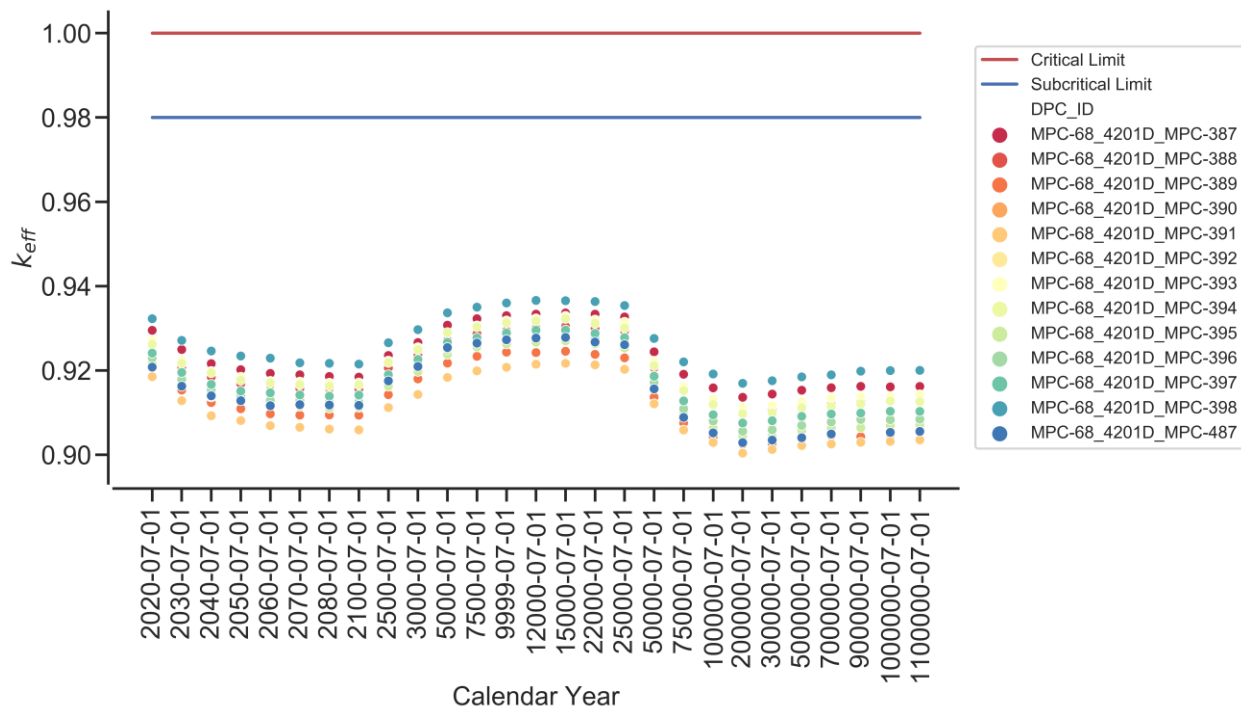


Figure F-21. k_{eff} vs. calendar year for the loss-of-neutron-absorber scenario based on actual loading and disposal isotopes for the SNF canisters at Hope Creek.

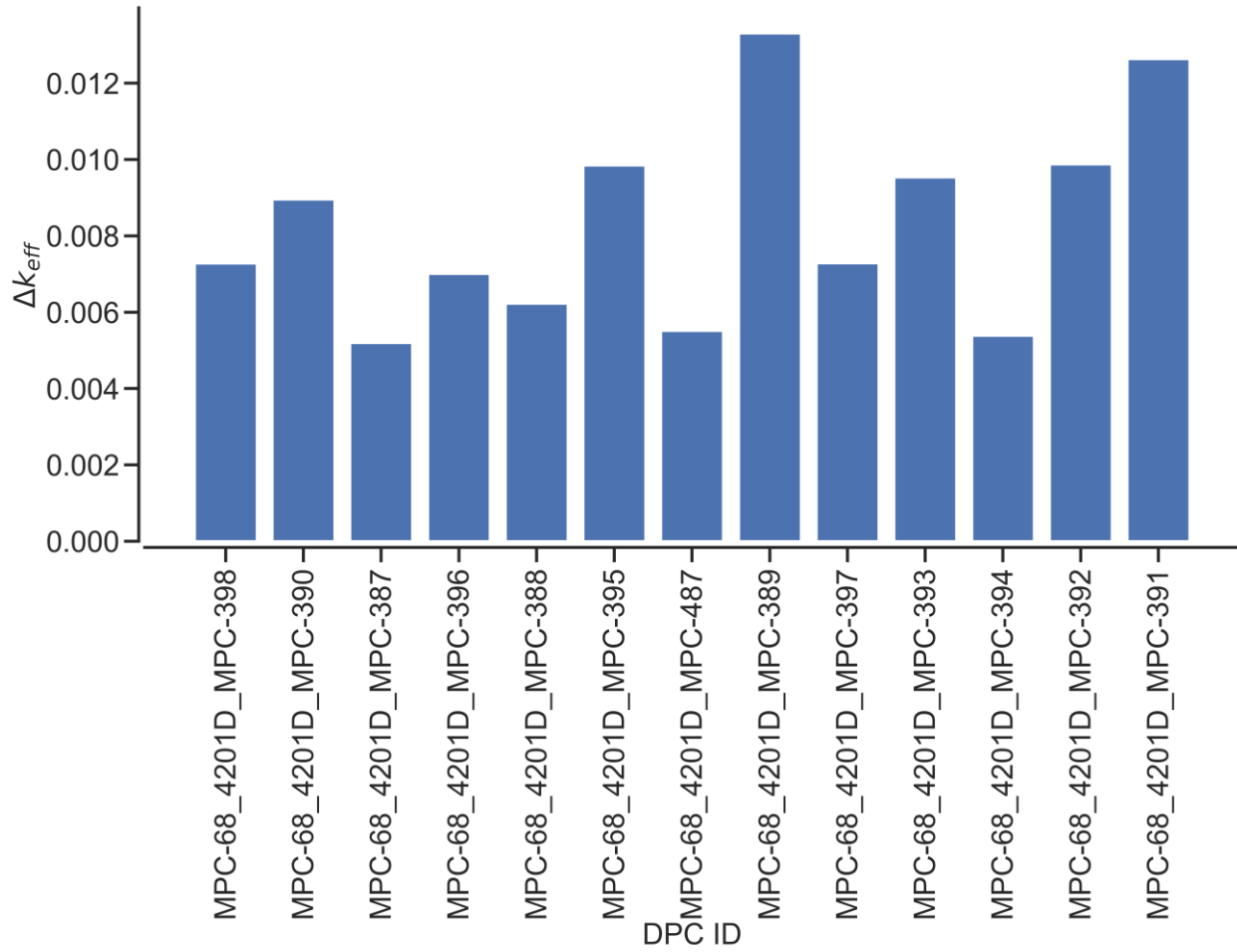


Figure F-22. k_{eff} increase between the worst-misload scenario and the as-loaded configuration for the MPC-68s at Hope Creek (calendar year 22,000).

F.7. SALEM CRITICALITY CALCULATIONS

Post-closure disposal criticality calculations were performed as a function of decay time for the 11 SNF canisters at the Salem ISFSI. All of the 11 SNF canisters are of the Holtec MPC-32 design. The MPC-32 does not contain any carbon steel structural components, so only the loss-of-neutron-absorber scenario is analyzed. Figure F-23 shows results for the loss-of-neutron-absorber scenario for 27 decay times within the time interval between calendar years 2020 and 1,100,000. The results in Figure F-23 show k_{eff} variation as a function of calendar year. The one sigma statistical uncertainty for all k_{eff} values is 0.0003 or less for all cases.

The k_{eff} values are predicted to vary from 0.9486 to 1.0101 for the MPC-32 under the loss-of-absorber scenario. For canisters which had k_{eff} values greater than 0.98 under the loss-of-neutron-absorber scenario, calculations were performed in which the pure water was replaced with groundwater compositions of various NaCl concentrations, and the models thus modified were used to determine k_{eff} as a function of NaCl concentration for the calendar year 22,000 (most reactive date). Figure F-24 presents k_{eff} variation as a function of NaCl concentration for those 11 canisters. Examining the results presented in Figure F-24, it is clear that 0.5 mol NaCl/ kg H₂O is sufficient to demonstrate subcriticality ($k_{eff} < 0.98$) for all of the Salem canisters. In this context, it is also important to note that a saturated NaCl brine has a concentration of approximately 6 molal.

Figure F-25 shows the k_{eff} increase between the worst misload scenario and the as-loaded configuration for the 11 analyzed Salem canisters at calendar year 22,000. The increase in k_{eff} varies between 542 and 2,573 pcm for the Salem canisters.

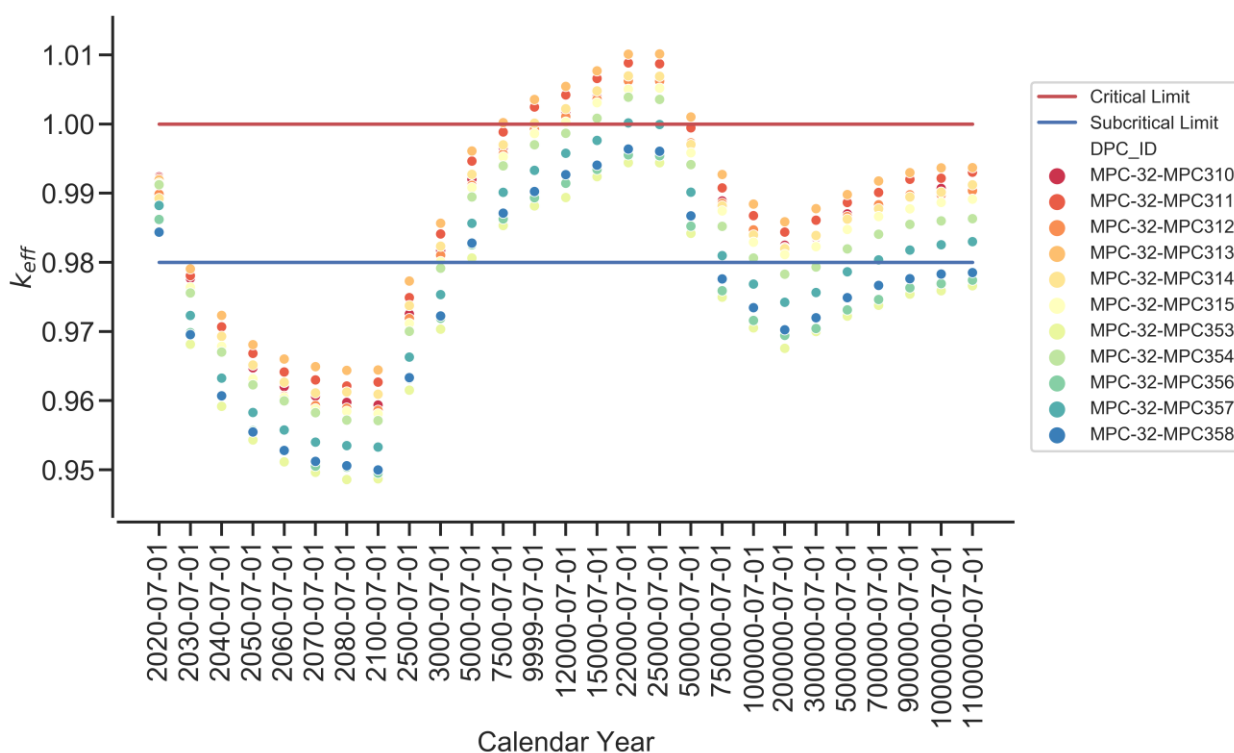


Figure F-23. k_{eff} vs. calendar year for the loss-of-neutron-absorber scenario based on actual loading and disposal isotopes for the SNF canisters at Salem.

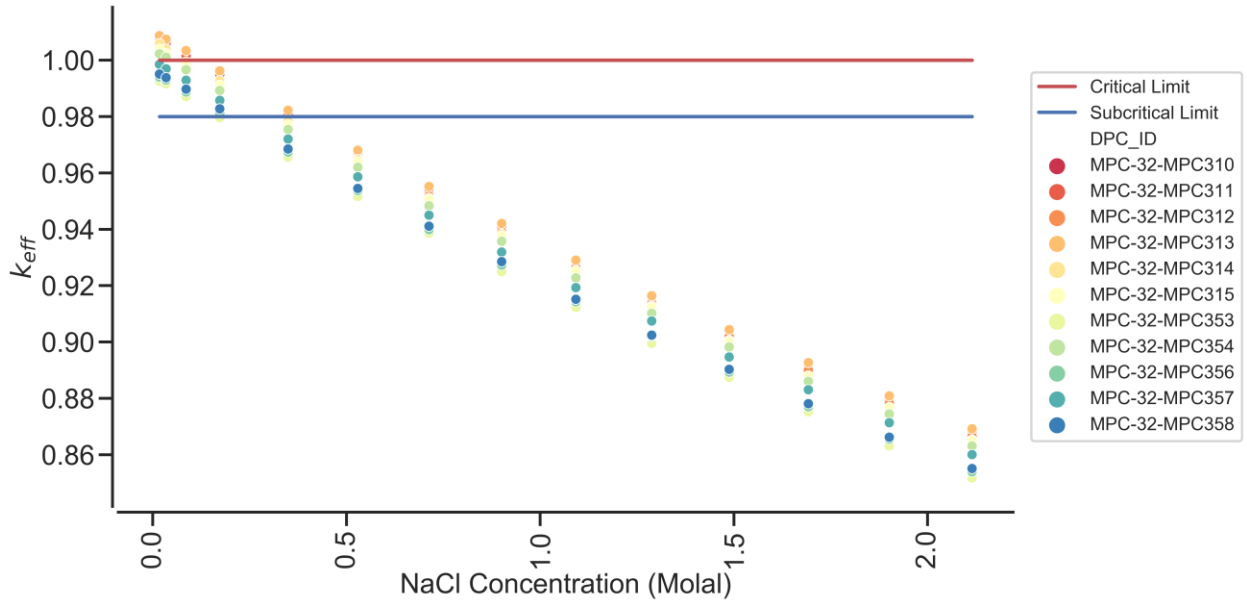


Figure F-24. k_{eff} vs. NaCl concentration for the DPCs with $k_{eff} > 0.98$ for the canisters at Salem under the loss-of-neutron-absorber scenario (calendar year 22,000).

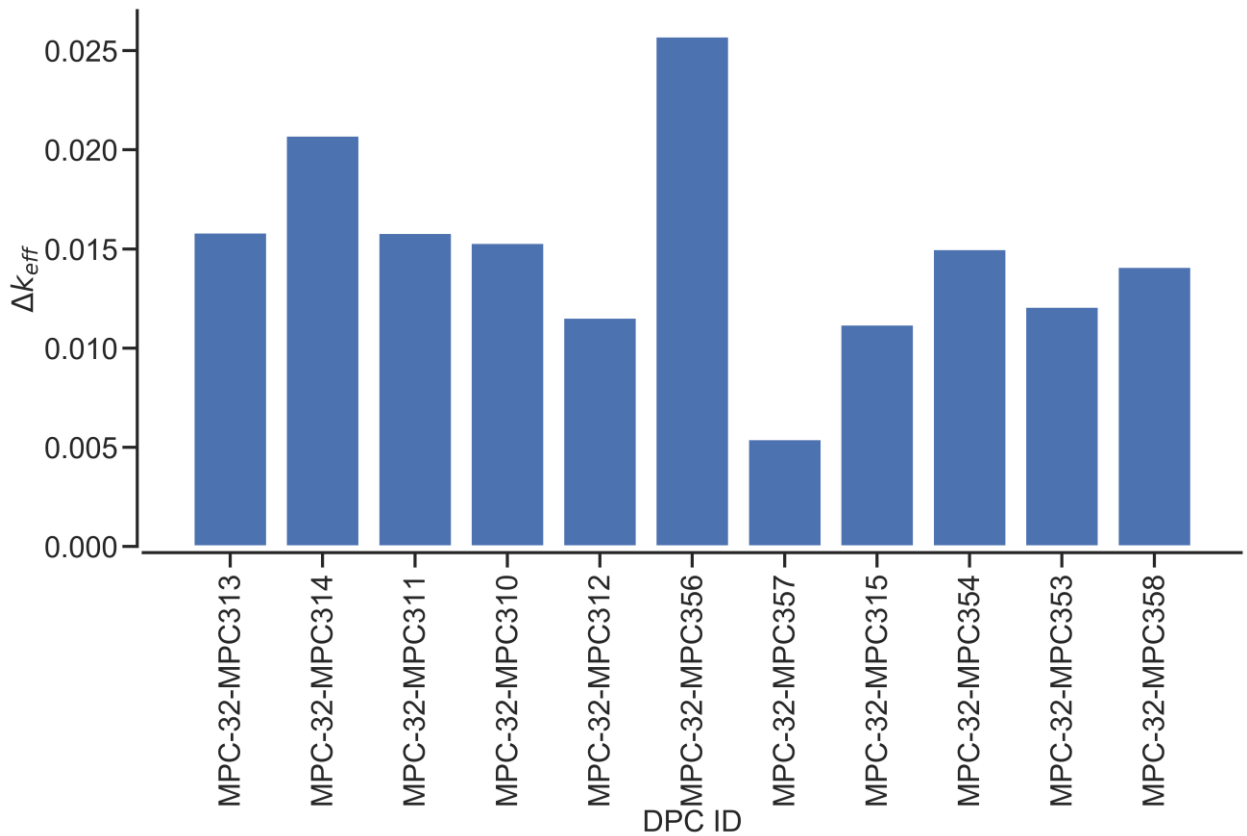


Figure F-25. k_{eff} increase between the worst-misload scenario and the as-loaded configuration for the MPC-32s at Salem (calendar year 22,000).

F.8. CONCLUSIONS

This appendix presents criticality analysis models for the extension of the 708 canisters modeled through FY19 from the year 22,000 out to the year 1,100,000 and the evaluation of cementitious filler materials for criticality control. Post closure criticality analysis was performed for a total of 66 new as-loaded canisters from four sites over the time interval between calendar years 2020 and 1,100,000 using the burnup credit methodology described in this report. The analyzed canisters were at the following sites: Seabrook (16 canisters), Vogtle (26 canisters), Hope Creek (13 canisters), and Salem (11 canisters).

The work performed to extend the analytical timeline of the post closure criticality calculations from previous years' work from 22,000 years to 1,100,000 years showed that the reactivity of the canisters peaked at 22,000 years then dropped to a minimum at approximately 200,000 years, and then increased throughout the remainder of the period analyzed, but not to the level obtained at 22,000 years.

The cementitious filler work included a series of calculations using the TSCDF-37-TSCDF-15 cask from the Zion site to determine the impact on post closure criticality of adding filler material to canisters. The analysis presented here includes both the NA and DB cases and considers four separate filler materials, which are presented in Table F-1. Of the four filler materials, the chloride-based calcium phosphate cement provided superior criticality control compared to the other filler materials at the same porosity level. It was also shown that almost the entire canister must be filled in order to achieve criticality control. Approximately 15 inches of uncovered fuel returns the canister's reactivity to levels very close to baseline k_{eff} values.

Post-closure disposal criticality calculations were performed as a function of decay time for as-loaded canisters at the sites previously discussed. Results are provided for a loss-of-neutron-absorber scenario at 27 decay times within the time interval between calendar years 2020 and 1,100,000 for all canisters analyzed. The k_{eff} values are predicted to vary from 0.89146 to 1.0570 for the Seabrook SNF canisters, 0.9112 to 1.0105 for the Vogtle SNF canisters, 0.9004 to 0.9366 for the Hope Creek SNF canisters, and 0.9486 to 1.0101 for the Salem SNF canisters under the loss of neutron-absorber scenario. None of the canisters modeled for this year's effort had carbon steel structural components, and none were analyzed under the degraded-basket scenario. All canisters that were shown to exceed the 0.98 subcritical limit were analyzed to determine the groundwater NaCl concentrations necessary to show subcriticality. The NaCl concentrations necessary to demonstrate subcriticality were determined to be a maximum of 0.5 molal for the Vogtle and Salem canisters and 1.1 molal for the Seabrook canisters.

Canister misload criticality analyses were performed assuming a worst configuration in an as-loaded canister, which is based on the assumption that correct assemblies have been loaded into the canister, but they are loaded in the most reactive configuration. k_{eff} values for worst misload configurations were determined assuming that all fuel assemblies in the canister have a decay time of 22,000 years, and the neutron absorber is completely lost. The misload analysis was performed for a total of 66 new canisters containing intact fuel assemblies that were loaded to full capacity. The k_{eff} increase varied between 498 and 3,309 pcm for the Seabrook canisters, between 579 and 3,808 pcm for the Vogtle SNF canisters, between 520 and 1,331 for the Hope Creek SNF canisters, and between 542 and 2,573 pcm for the Salem SNF.

A plot of the canisters analyzed this year, along with the remainder of the canisters at Salem, is shown in Figure F-26. The loss-of-neutron-absorber case is shown as a gray line, and the best- and worst-case misload calculations are shown as a pink band around the gray line. Figure F-26 shows that a DPC loading strategy by taking criticality aspect into account can improve the disposability of loaded DPCs. A summary of the direct disposal criticality calculations is provided in Table F-2. For this project, 774 canisters have been analyzed through FY20. Of the canisters analyzed, it was shown that 76% would remain subcritical under the loss-of-neutron-absorber scenario. When considering complete degradation of the baskets of canisters with non-stainless-steel structural components, 66% of the canisters are shown

to be subcritical. When further considering the potential for the worst-case arrangement of the most reactive fuel assemblies in each canister, it is show that 65% of canisters would remain subcritical.

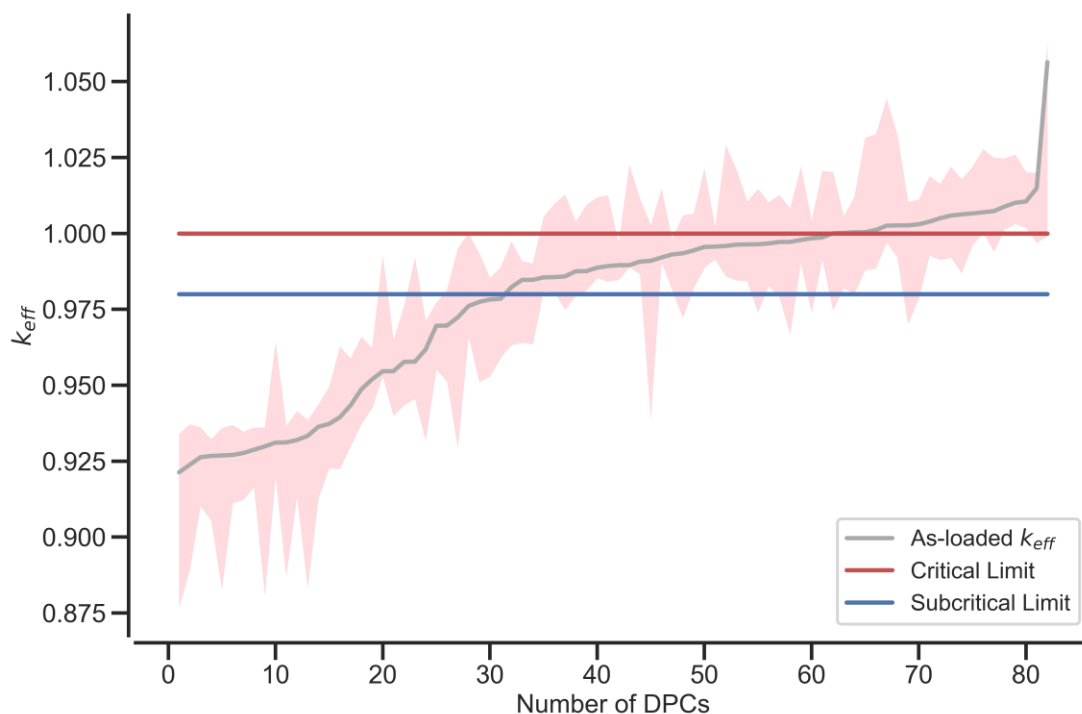


Figure F-26. Summary plot of the post closure criticality calculations performed this year (66 DPCs + other canisters at Salem) including as-loaded (gray line) and best- and worst-case misload (pink band) scenarios.

Table F-2. Summary of the number of canisters meeting the subcritical limit.

Description (analysis dates: 2020–1,100,000)	Value
Total DPCs analyzed	774
Total DPCs below subcritical limit with loss of neutron absorber (design-basis loading)	0 (0%)
Total DPCs below subcritical limit with loss of neutron absorber (as-loaded)	591 (~76%)
Total DPCs below subcritical limit with loss of neutron absorber and carbon steel structures (as-loaded)	514 (~66%)
Total DPCs below subcritical limit with loss of neutron absorber and carbon steel structures (as-loaded) considering misload	503 (~65%)

F.9. REFERENCE

- F-1. J. B. Clarity, K. Banerjee, and L. P. Miller, *Extension of Direct Disposal Criticality Calculations to 1,000,000 Years*, M5SF-20OR0103050123, US Department of Energy, Spent Fuel and Waste Disposition, June 2020.

APPENDIX G. FY 2021 Criticality Study

G.1. INTRODUCTION

This appendix documents work performed supporting the US Department of Energy (DOE) Office of Nuclear Energy (NE) Spent Fuel and Waste Disposition (SFWD) under work breakdown structure element 1.08.01.03.05, “Direct Disposal of Dual Purpose Canisters.” In particular, this appendix fulfills the M3 milestone, M3SF-21OR010305127, “Update of DPC Direct Disposal Criticality Analysis Report” within work package SF-21OR01030512, “Direct Disposal of Dual Purpose Canisters - ORNL.”

This appendix presents the dual-purpose canister (DPC) criticality evaluations performed in FY 2021 to support the feasibility determination of direct disposal of DPCs and extends the work reported in the main body and preceding appendices of this report. The main objectives of the FY 2021 DPC disposal criticality study were as follows:

- Summarize and provide references for other work supporting direct disposal reactivity assessment of DPCs this year at ORNL, and
- Analyze an additional 155 as-loaded canisters from ten sites for the time interval between calendar years 2030 and 1,100,000 using the burnup credit methodology described in the previous sections of this report. The analyzed canisters are organized by site in Table G-1.

Table G-1. Summary of Sites Analyzed in FY21.

Site	DPC Type	Section
Braidwood	MPC-32	G.3
Diablo Canyon	MPC-32	G.4
Byron	MPC-32	G.5
La Salle	MPC-68, MPC-68M	G.6
North Anna	NUHOMS® 32PTH-DSC	G.7
Sequoyah	MPC-32, MPC-37	G.8
Surry	NUHOMS® 32PTH-DSC	G.9
Callaway	MPC-37	G.10
Watts Bar	MPC-37	G.11
Browns Ferry	MPC-89	G.12

Criticality analysis models were developed for the intact canister configuration applicable to normal conditions of transport and storage as described in the UNF-ST&DARDS status report [G-1]. The models were then modified for degraded material configurations applicable to the canister repository timeframe specified in this report. The degraded material configurations assume two scenarios: (1) complete loss of the fixed neutron absorber (i.e., ¹⁰B) without fuel basket geometry changes, and (2) complete degradation and loss of basket materials, including neutron absorber plates and aluminum and carbon steel basket components (e.g., insert plates and basket support discs). This year, a new investigation was performed of baskets composed entirely of Metamic-HT poison material whose degradation and thus neutron absorber loss leads to a significant increase in k_{eff} . The degraded material configurations were analyzed for 23 analysis dates between 2030 and 1,100,000 years.

As mentioned in the main report, neutron moderation by water must occur for a waste package to achieve criticality. However, the groundwater (or pore water) that may flood a breached DPC will contain various dissolved aqueous species. Seventeen species were studied as described in the main report, and it was determined that Cl, Li, and B provide the maximum reduction in canister reactivity because of their large neutron absorption cross sections. However, available groundwater data indicate that chlorine (as chloride) is the only naturally abundant neutron-absorbing element in groundwater that can provide a significant reduction in reactivity; chlorine is available in most of the repository concepts under consideration in varying quantities. Analyses were performed to determine the chlorine requirement to suppress the reactivity of canisters that have the potential to form a critical configuration in a repository timeframe. The impact of chlorine (in terms of NaCl) concentration in groundwater on the reactivity of as-loaded DPCs exceeding a k_{eff} value of 0.98 was evaluated for calendar year 22,000. Previous chlorine concentration effects on k_{eff} documented in this report were evaluated for calendar year 9,999. The impacted DPCs will be reevaluated for calendar year 22,000, the year of maximum reactivity, in the future.

G.2. OTHER DIRECT DISPOSAL OF DPCS ACTIVITIES IN FY2021

In addition to reactivity assessment of new DPCs under the neutron absorber (NA) and degraded basket (DB) configurations, other reactivity-related work was performed this year. This section includes a brief description of this work to serve as a general reference for reactivity modeling efforts this year. Section G.2.1 summarizes the work performed to examine the reactivity impact of basket modification technologies, and Section G.2.2 summarizes the loading pattern optimization work.

G.2.1. Reactivity Effect of Basket Modification Technology

Proposed DPC basket and fuel assembly modification technologies were explored for their post-closure criticality suppression potential in Clarity et al. [G-2]. The three assembly and basket modification technologies considered were the disposal control rodlet assembly (DCRA), and the advanced neutron absorber (ANA) chevron insert, and BWR fuel channel replacement absorbers. The DCRA is similar to a standard guide tube-based absorber, such as a control rod or burnable absorber that would typically be used for power distribution and excess reactivity control during normal PWR operation. The DCRA uses B_4C as a poison material. The second concept is the chevron neutron absorber that would be mounted to the canister basket or the assembly's top nozzles. The neutron absorber would need to be more durable in a repository environment than the aluminum-based absorber technology that is typically installed in DPCs. The ANA materials discussed in Hardin and Donovan's report [G-3], may be appropriate for the purpose and are described as Hastelloy-based alloys similar to Alloy C-4 or Alloy C-22, with natural gadolinium loaded into the material. The third concept is an ANA fuel channel replacement that would replace the currently installed fuel channels. SCALE-generated renderings of the three basket/fuel assembly modification technologies are shown in Figure G-1: the DCRA concept is shown in the upper left, the ANA chevron insert is shown in the upper right, and the ANA fuel channel replacement is shown at the bottom.

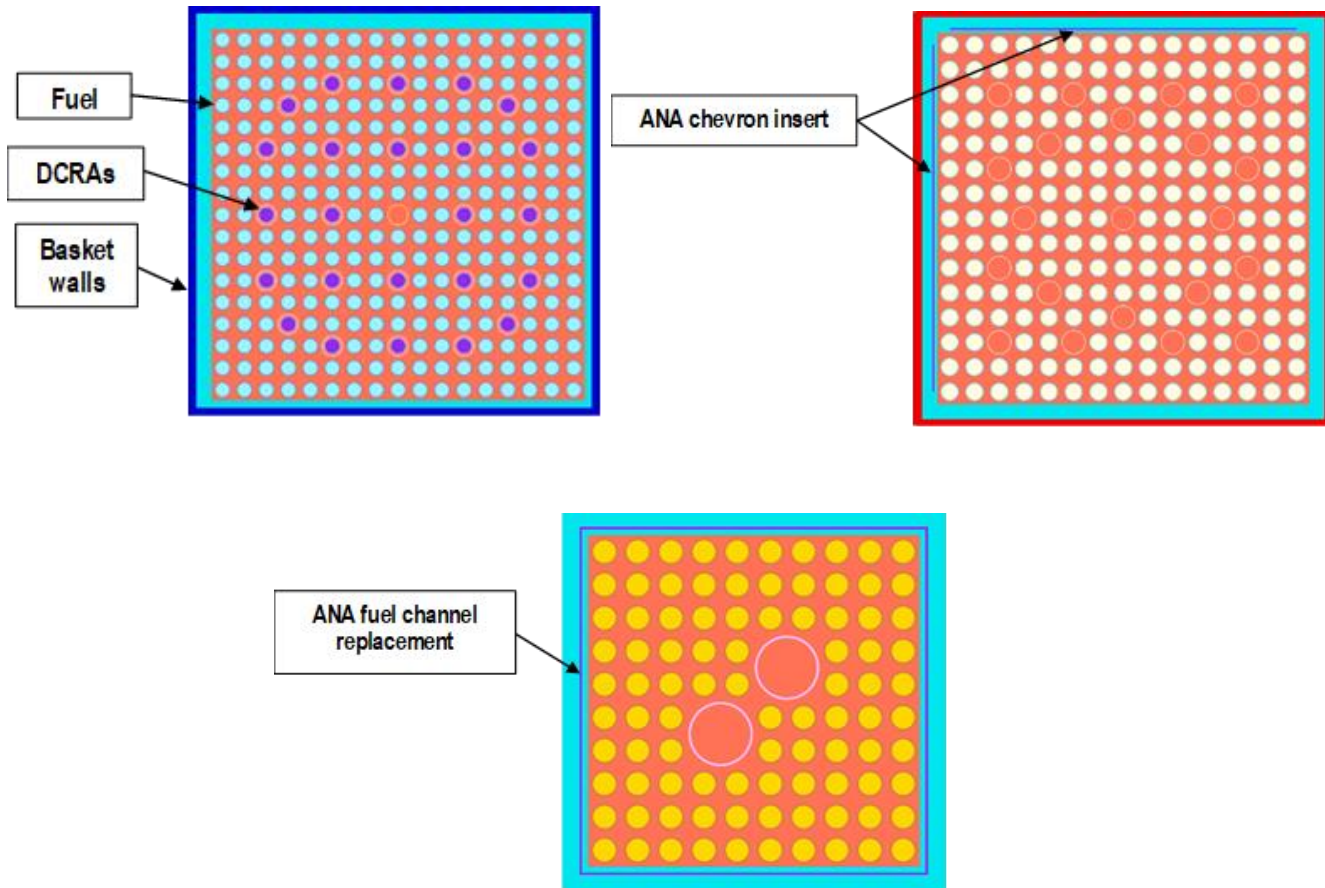


Figure G-1. SCALE-generated renderings of the DCRA (upper left), ANA chevron insert (upper right), and ANA fuel channel replacement (lower) concepts.

The analysis of the basket/fuel assembly modification concepts used three of the most reactive canisters that have been analyzed to date using UNF-ST&DARDS to examine the performance of three potential reactivity suppression technologies under post-closure conditions. The canisters used were limiting loadings for the TSC-37 (highly reactive) and MPC-32 (more moderately reactive) PWR DPCs and the MPC-89 BWR DPC. The reactivity suppression technologies considered were (1) the B₄C-filled DCRA, (2) the ANA-based chevron insert for the PWR canisters, and (3) the ANA-based fuel channel replacement absorber for the MPC-89. For each combination of absorber concept and DPC, various insert patterns and absorber material concentrations were considered.

The results of TSC-37 calculations for the DCRA concept in Ref. [G-2] show that it may be possible to overcome the reactivity increase associated with the NA cases by using between 5 and 9 DCRAs, but the DB condition would require a minimum of 21 DCRAs. The results of the MPC-32 DCRA calculations show that between 4 and 12 DCRAs would be required to offset the reactivity increase associated with the NA case. In all cases, a B₄C concentration of 25% of the theoretical density was sufficient to achieve maximum absorber effectiveness, and densities above that value did not improve performance significantly in cases that were not already deeply subcritical.

The results of the calculations supporting the ANA chevron absorber insert do not show the ability to offset the reactivity of either NA or DB conditions for the TSC-37 calculations. The results from the MPC-32 calculations show that subcriticality could be demonstrated using at least 12 chevron inserts. It is also noted that there is a loss of sensitivity of k_{eff} to increased Gd loading beyond 2 wt.%. It is unlikely that increased Gd loading or in-repository absorber thickness would improve the results.

The results of the calculations supporting the ANA channel replacement insert show that it is possible to offset the loss of neutron absorber and basket structure with 49 or more channels. As with the chevron inserts composed of ANA, there was an apparent decrease in sensitivity to increased Gd loading beyond 2 wt.%, indicating that justifying additional Gd concentration or thickness of the absorber material would not improve the results beyond that point.

It may be advantageous to explore a wider variety of canisters, canisters loading, and absorber patterns in future work. Doing this would allow for a better understanding of the total number of each type of device necessary to meet fleetwide disposal needs. Additionally, it may be beneficial to examine combining the basket modification strategies with optimization of assembly loadings for disposal criticality.

G.2.2. Optimization of Canister Loading Patterns in DPCs for Criticality Suppression

A preliminary investigation of potential reactivity management strategies that can be used to reduce the number of canisters susceptible to criticality over the repository's performance assessment period was performed [G-4]. The investigations included reloading the assemblies in the canisters at the Zion site using the individual assembly reactivity approach and an initial development of an artificial neural network (ANN)-based approach for rapid estimation of canister reactivity that can be applied for an optimum loadings search. These approaches will allow criticality analysis to be incorporated into the decision-making process for canister loading.

To gain an understanding of the potential reactivity reduction obtainable by optimizing canister loadings, the assemblies at Zion were reorganized into new canisters. Zion was selected for this analysis because it was identified in previous versions of this report as having several canisters with k_{eff} values in excess of the hypothetical 0.98 subcritical limit. The Zion site has 61 canisters that contain 2,226 assemblies. Of the assemblies present at Zion, 2,166 are intact, and 60 have been declared as damaged fuel. The damaged fuel assemblies are eligible for storage in the four peripheral locations along the minor axes of the canister. The damaged fuel assemblies are modeled with the fresh fuel assumption, with an expanded pitch to conservatively account for uncertainties in assembly geometry.

To determine the potential reactivity reduction associated with reorganizing the contents of each canister, the assemblies in the Zion casks were reloaded with the algorithm described in Section 2.3 of the report by Clarity et al. [G-4]. The reloading algorithm was run using loading schemes that divided the population of available intact fuel assemblies into one, two, three, and four bins, to determine the impact of distributing the highly reactive fuel across a range of DPCs. In the one-bin case, assemblies were sequentially drawn from the top and bottom of the distribution, so that half of the first canister was filled with the most reactive fuel, and the other half was filled with the least reactive fuel. The increasing number of bins resulted in a more uniform distribution of high reactivity, low reactivity, and intermediate reactivity assemblies across all of the canisters. The results of the calculations are shown in the box plots in Figure G-2. The as-loaded configuration is presented as the first entry in Figure G-2. The other entries correspond to loading schemes with increasing numbers of bins in the assembly selection algorithm. The results show that even a single bin provides significant reduction compared to the as-loaded condition. However, the most reactive canister still has a k_{eff} of ~1.03. A two-bin assembly selection results in a reduction in both the average canister reactivity and the peak canister reactivity to a k_{eff} of approximately 0.99. Therefore, a two-bin selection approach would make all DPCs loaded at the Zion site disposable

without a criticality concern. Increasing the number of bins used beyond two did not result in substantial canister reactivity reduction.

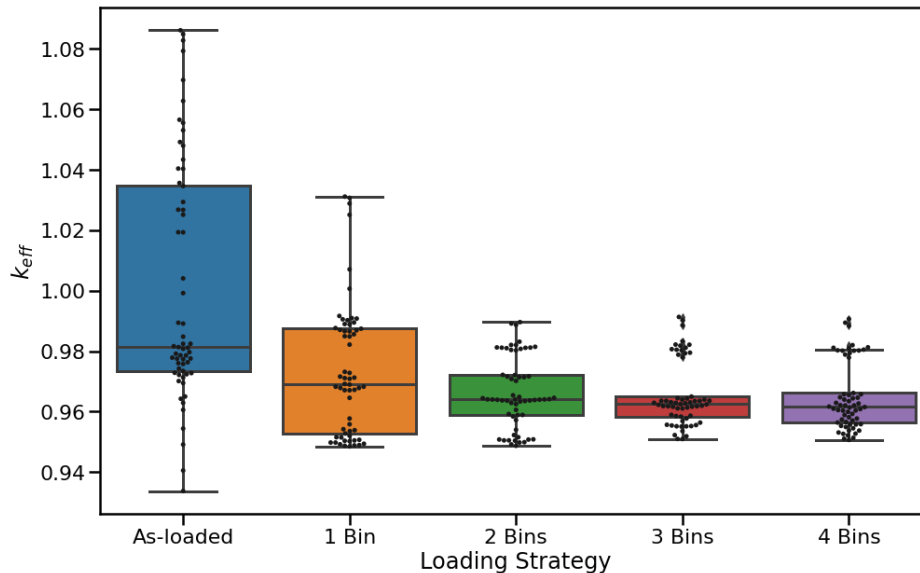


Figure G-2. Box plots for the single-site reloading analysis.

The Zion reloading analysis represents an idealized case in which the loadings were optimized while only considering criticality. Ultimately, the goal is to develop a tool that will allow for the consideration of disposal criticality in a more holistic optimization scheme that would also meet loading constraints associated with on-site storage, such as decay heat and dose. Optimization techniques require that multiple loading patterns be considered before a solution is chosen that meets all constraints. Criticality assessment is typically performed using Monte Carlo eigenvalue calculations. The durations of these calculations for the highly heterogeneous models considered in as-loaded analysis typically spans several hours to a few days per configuration. The time required to run these calculations makes them ill-suited for the rapid criticality assessment desired when considering multiple design constraints.

An initial ANN to predict the k_{eff} of a canister given its contents has been developed [G-4]. ANNs are mathematical constructs that are loosely modeled after the neurological pathways in the brain. ANNs are composed of a series of neurons or units that perform mathematical functions. Units within a neural network are organized in layers which fall into three broad classifications: the input layer, the hidden layers, and the output layer. The input layer accepts input variable values. The first hidden layer receives a weighted sum of the inputs and applies an activation function to the sum, and each subsequent layer takes the weighted sum of the outputs of the units in the preceding layer and applies an activation function to the sum. The output layer applies an activation function to the weighted sum of the last hidden layer. Tunable parameters that are used in developing a neural network include the activation functions used, the number of hidden layers, and the number of units per hidden layer.

ANNs are developed or trained by feeding a number of known input and output sets so that the appropriate weights for each variable at each unit can be determined. For the development of the canister k_{eff} ANN, the values input into the ANN are the assembly reactivities, and the output values are the Monte Carlo-calculated canister k_{eff} values. A diagram showing five input nodes, three hidden layers of ten units, and an output unit is provided in Figure G-3.

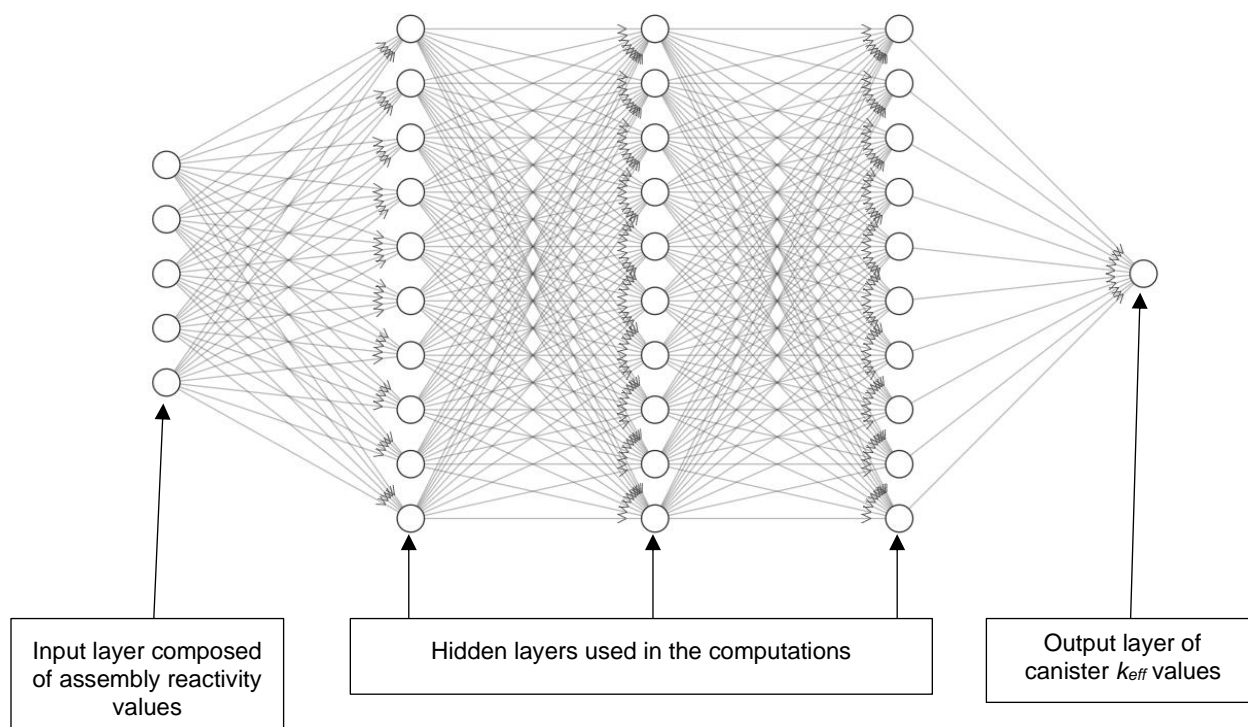


Figure G-3. Diagram of the canister k_{eff} predicting neural network used with the input, output and hidden layers labeled.

To generate training data for the preliminary version of the ANN, 1,000 randomly loaded canisters were analyzed. The fuel assembly used for this purpose was the Westinghouse 17×17 Standard fuel assembly (GC-859, designation W1717WL). The canister used for this analysis was the MPC-32. The first step in this process was to generate a random inventory of fuel assemblies representative of those currently being stored. A 2D kernel density estimator (KDE) was developed using the enrichments and burnups of 105,139 PWR fuel assemblies in the UDB. Assembly reactivity calculations were run for each of the 32,000 assemblies at 9,500 years of cooling time, and 1,000 canister criticality calculations were run in the year 22,000—which represents the peak reactivity time for most canisters—using the loss of NA hypothetical disposal scenario.

The ANN was trained using the assembly reactivity values as inputs and the canister k_{eff} values as outputs. The data were initially divided so that 700 canisters were used as the training data, and 200 canisters were held back as testing data. Reserving the testing data allows for independent quantification of algorithm performance once the ANN has been fully trained. Furthermore, 100 canisters were withheld to serve as a validation data set. The validation data set is used to perform preliminary assessments of the algorithm's accuracy and to decide the number of passes to be made through the training process, or the epochs to be used. Once the validation error has converged to a stable value, then additional epochs are no longer needed. Canisters were randomly assigned to the training, testing, and validation data sets.

The ANN model that provided the best results was a three-hidden-layer network with 64 units per layer. The input layer comprised 32 units corresponding to the assembly reactivity of each storage location in the canister, and the output layer comprised a single unit corresponding to the canister k_{eff} . The data were divided into the training data with 700 casks, the validation data with 100 casks, and the testing data with 200 casks. The training data were fed to the neural network for a series of 4,000 epochs, using the scaled exponential linear unit as the activation function for all units. Figure G-4 shows the training loss (blue) and the validation loss (orange). The validation error served as a metric to determine when enough epochs

had been used to maximize the accuracy of the model. The data in Figure G-4 indicate that the model appears to be fully converged at about 2,500 epochs. The average training error over the last 500 generations was 0.0014, and the average validation error over the last 500 epochs was 0.0030.

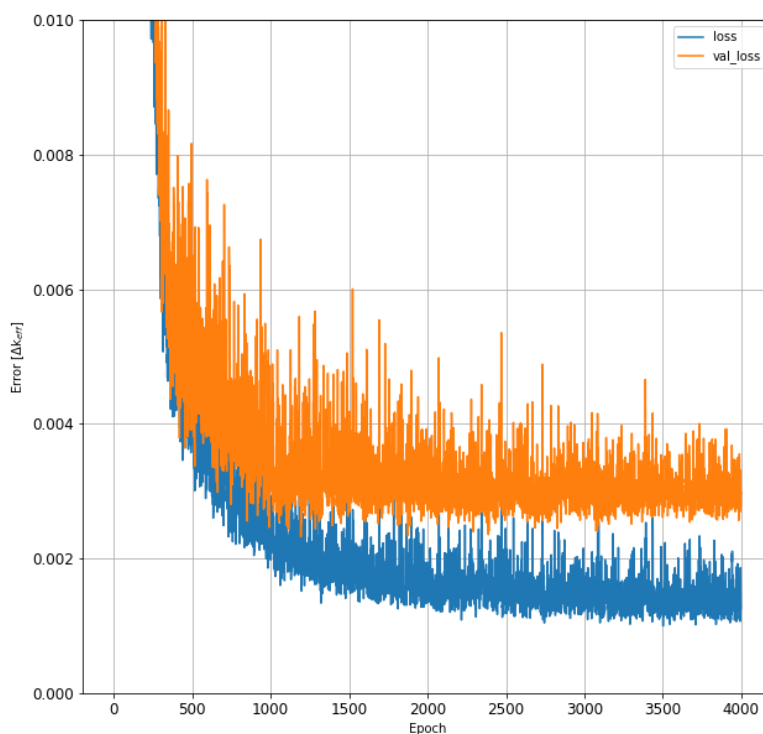


Figure G-4. Training and validation errors for the neural network.

G.3. BRAIDWOOD CRITICALITY CALCULATIONS

Post-closure disposal criticality calculations were performed as a function of decay time for the 17 SNF canisters at the Braidwood ISFSI. All 17 SNF canisters are MPC-32s. The MPC-32 does not contain any carbon steel structural components, so only the loss-of-neutron-absorber scenario was analyzed. Figure G-5 shows results for the loss-of-neutron-absorber scenario for 23 decay times within the time interval between calendar years 2020 and 1,100,000. The results in Figure G-5 show k_{eff} variation as a function of calendar year. The one sigma statistical uncertainty for all k_{eff} values is 0.0004 or less for all cases.

The k_{eff} values are predicted to vary from 0.9218 to 1.0064 for the MPC-32s under the loss-of-absorber scenario. For canisters which had k_{eff} values greater than 0.98 under the loss-of-neutron-absorber scenario, calculations were performed in which the pure water was replaced with groundwater compositions of various NaCl concentrations, and the models thus modified were used to determine k_{eff} as a function of NaCl concentration for the calendar year 22,000 (most reactive date). Figure G-6 presents k_{eff} variation as a function of NaCl concentration for those 16 canisters. Analysis of the results presented in Figure G-6 clearly shows that 0.4 mol NaCl/ kg H₂O is sufficient to demonstrate subcriticality ($k_{eff} < 0.98$) for all Braidwood canisters. In this context, it is also important to note that a saturated NaCl brine has a concentration of approximately 6 molal.

Figure G-7 shows the k_{eff} increase between the worst-misload scenario and the as-loaded configuration for the 17 analyzed Braidwood canisters at the calendar year 22,000. The increase in k_{eff} varies between 671 and 3,221 pcm for Braidwood canisters.

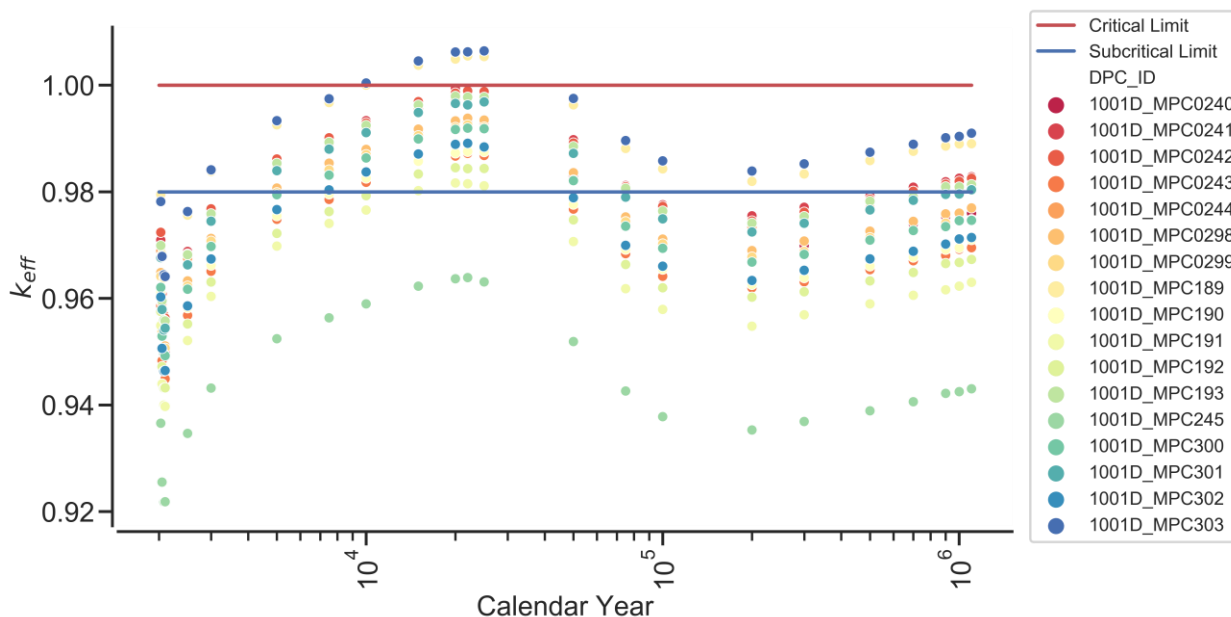


Figure G-5. k_{eff} vs. calendar year for the loss-of-neutron-absorber scenario based on actual loading and disposal isotopes for the SNF canisters at Braidwood.

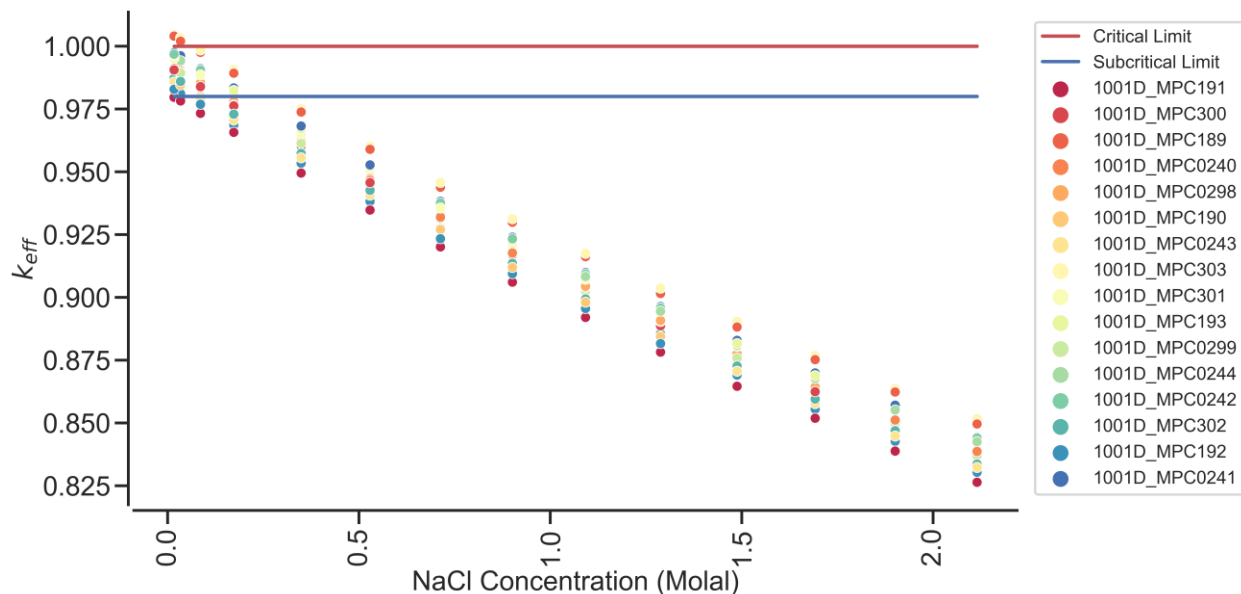


Figure G-6. k_{eff} vs. NaCl concentration for the DPCs with $k_{eff} > 0.98$ for the canisters at Braidwood under the loss-of-neutron-absorber scenario (calendar year 22,000).

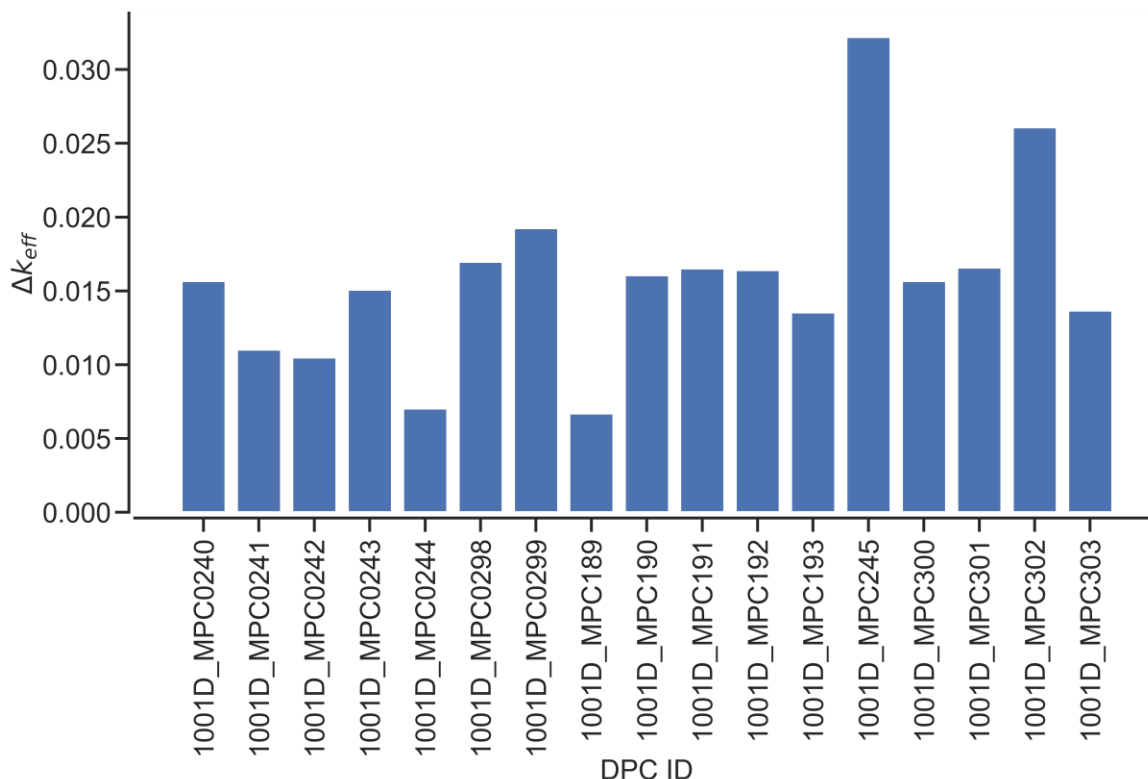


Figure G-7. k_{eff} increase between the worst-misload scenario and the as-loaded configuration for the MPC-32s at Braidwood (calendar year 22,000).

G.4. DIABLO CANYON CRITICALITY CALCULATIONS

Post-closure disposal criticality calculations were performed as a function of decay time for the 26 SNF canisters at the Diablo Canyon ISFSI. All 26 SNF canisters are MPC-32s. The MPC-32 does not contain any carbon steel structural components, so only the loss-of-neutron-absorber scenario is analyzed. Figure G-8 shows results for the loss-of-neutron-absorber scenario for 23 decay times within the time interval between calendar years 2020 and 1,100,000. The results in Figure G-8 show k_{eff} variation as a function of calendar year. The one sigma statistical uncertainty for all k_{eff} values is 0.0004 or less for all cases.

The k_{eff} values are predicted to vary from 0.9327 to 1.0402 for the MPC-32s under the loss-of-absorber scenario. For canisters which had k_{eff} values greater than 0.98 under the loss-of-neutron-absorber scenario, calculations were performed in which the pure water was replaced with groundwater compositions of various NaCl concentrations, and the models thus modified were used to determine k_{eff} as a function of NaCl concentration for the calendar year 22,000 (most reactive date). Figure G-9 presents k_{eff} variation as a function of NaCl concentration for those 25 canisters. Analysis of the results presented in Figure G-9 clearly shows that 0.9 mol NaCl/ kg H₂O is sufficient to demonstrate subcriticality ($k_{eff} < 0.98$) for all Diablo Canyon canisters. In this context, it is also important to note that a saturated NaCl brine has a concentration of approximately 6 molal.

Figure G-10 shows the k_{eff} increase between the worst-misload scenario and the as-loaded configuration for the 26 analyzed Diablo Canyon canisters at the calendar year 22,000. The increase in k_{eff} varies between 306 and 2,014 pcm for Diablo Canyon canisters.

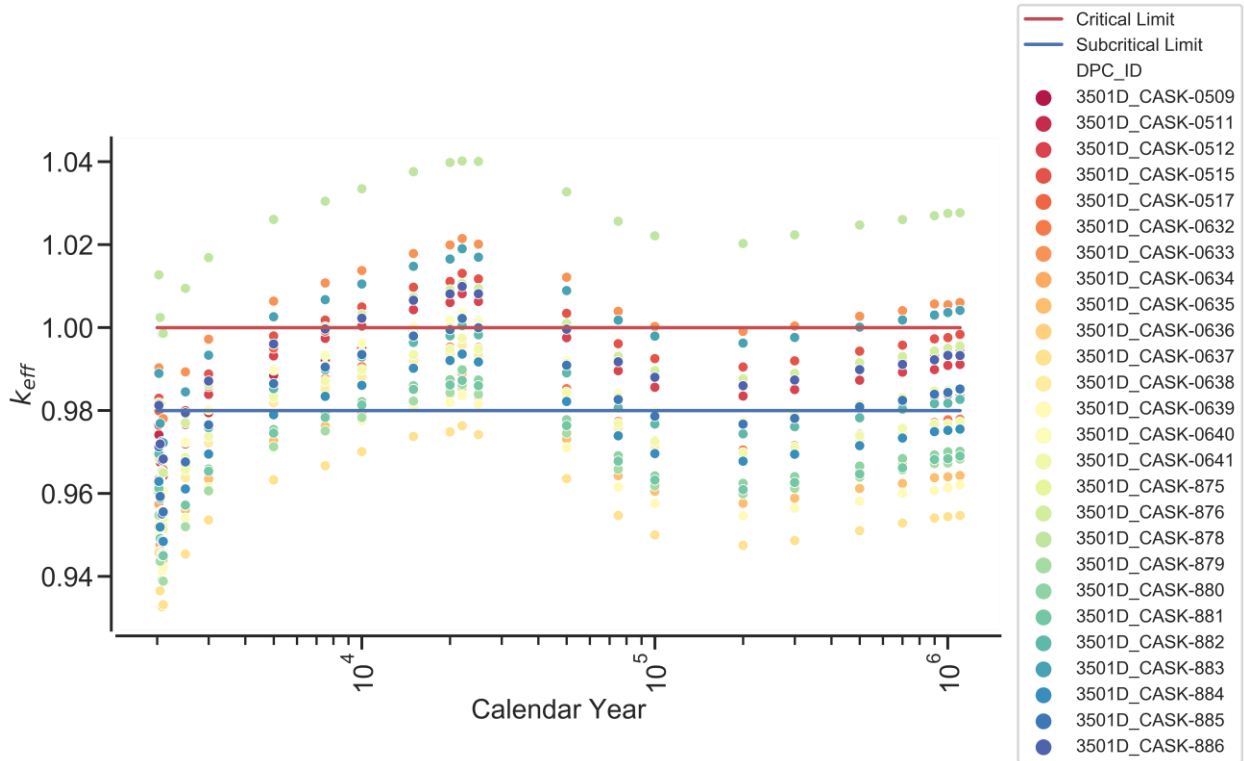


Figure G-8. k_{eff} vs. calendar year for the loss-of-neutron-absorber scenario based on actual loading and disposal isotopes for the SNF canisters at Diablo Canyon.

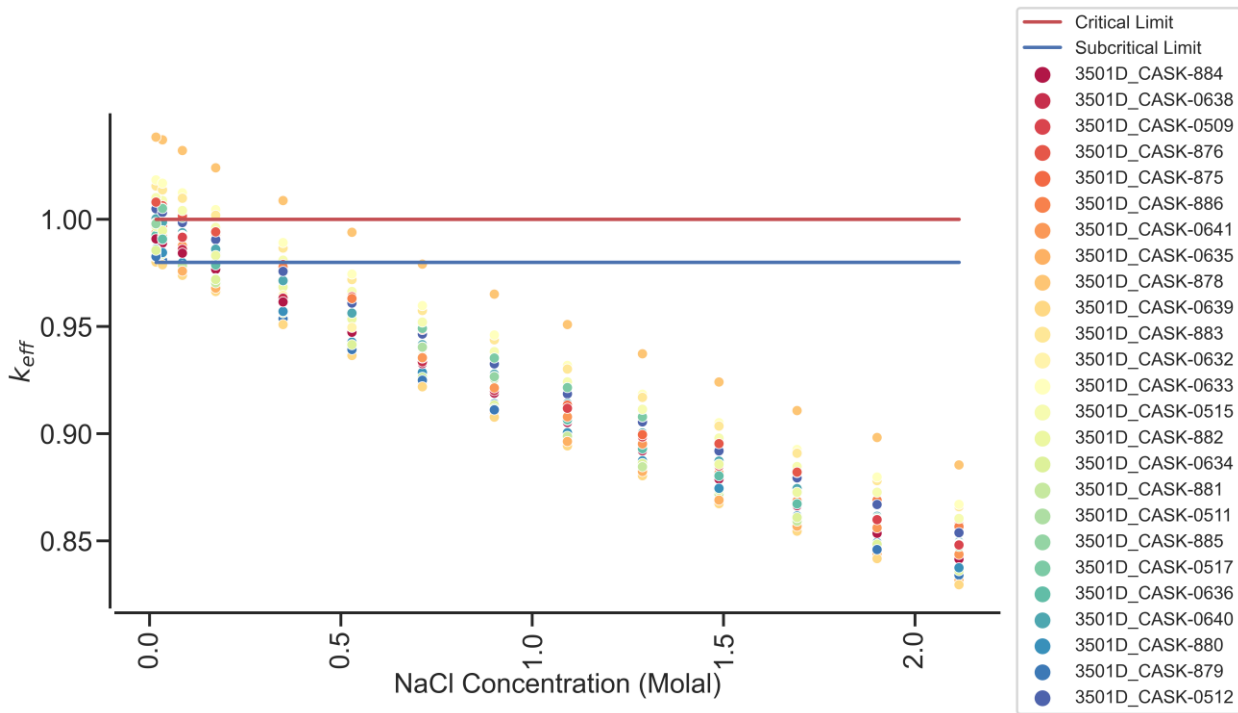


Figure G-9. k_{eff} vs. NaCl concentration for the DPCs with $k_{eff} > 0.98$ for the canisters at Diablo Canyon under the loss-of-neutron-absorber scenario (calendar year 22,000).

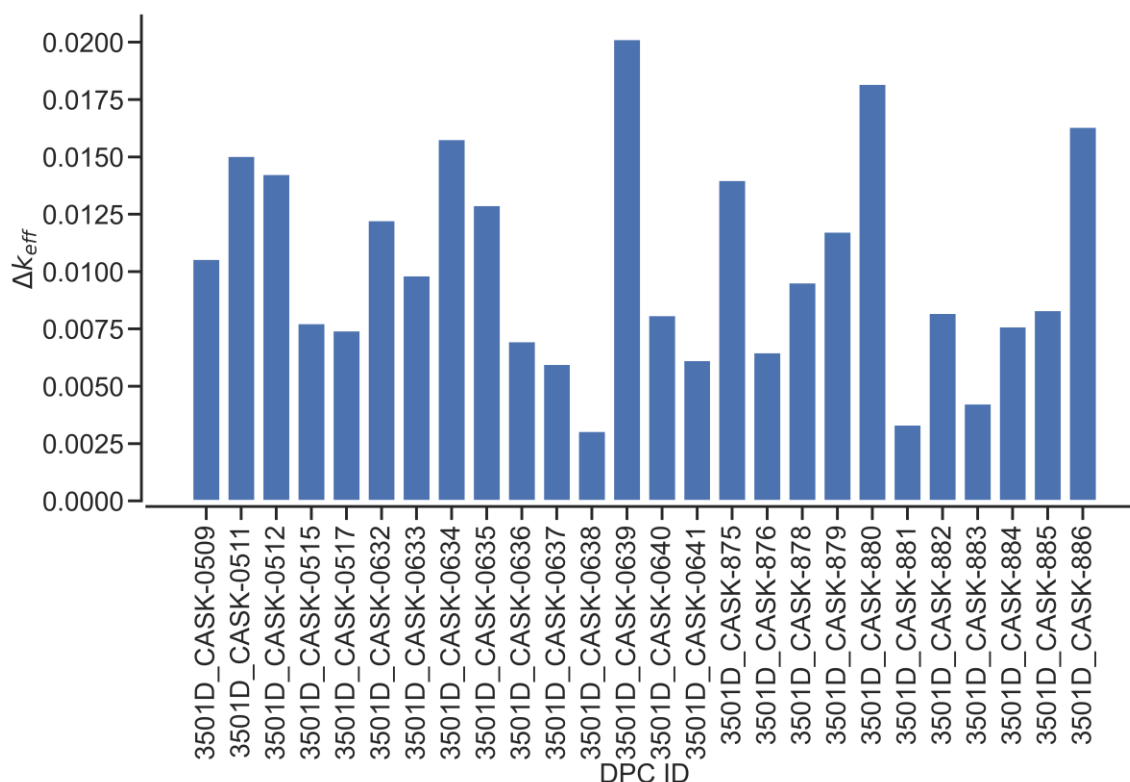


Figure G-10. k_{eff} increase between the worst-misload scenario and the as-loaded configuration for the MPC-32s at Diablo Canyon (calendar year 22,000).

G.5. BYRON CRITICALITY CALCULATIONS

Post-closure disposal criticality calculations were performed as a function of decay time for the 12 SNF canisters at the Byron ISFSI. All 12 SNF canisters are MPC-32s. The MPC-32 does not contain any carbon steel structural components, so only the loss-of-neutron-absorber scenario is analyzed. Figure G-11 shows results for the loss-of-neutron-absorber scenario for 23 decay times within the time interval between calendar years 2020 and 1,100,000. The results in Figure G-11 show k_{eff} variation as a function of calendar year. The one sigma statistical uncertainty for all k_{eff} values is 0.0003 or less for all cases.

The k_{eff} values are predicted to vary from 0.9301 to 0.9967 for the MPC-32s under the loss-of-absorber scenario. For canisters which had k_{eff} values greater than 0.98 under the loss-of-neutron-absorber scenario, calculations were performed in which the pure water was replaced with groundwater compositions of various NaCl concentrations, and the models thus modified were used to determine k_{eff} as a function of NaCl concentration for the calendar year 22,000 (most reactive date). Figure G-12 presents k_{eff} variation as a function of NaCl concentration for those 9 canisters. Examining the results presented in Figure G-12, it is clear that 0.4 mol NaCl/ kg H₂O is sufficient to demonstrate subcriticality ($k_{eff} < 0.98$) for all Byron canisters. In this context, it is also important to note that a saturated NaCl brine has a concentration of approximately 6 molal.

Figure G-13 shows the k_{eff} increase between the worst-misload scenario and the as-loaded configuration for the 12 analyzed Byron canisters at the calendar year 22,000. The increase in k_{eff} varies between 219 and 2,183 pcm for Byron canisters.

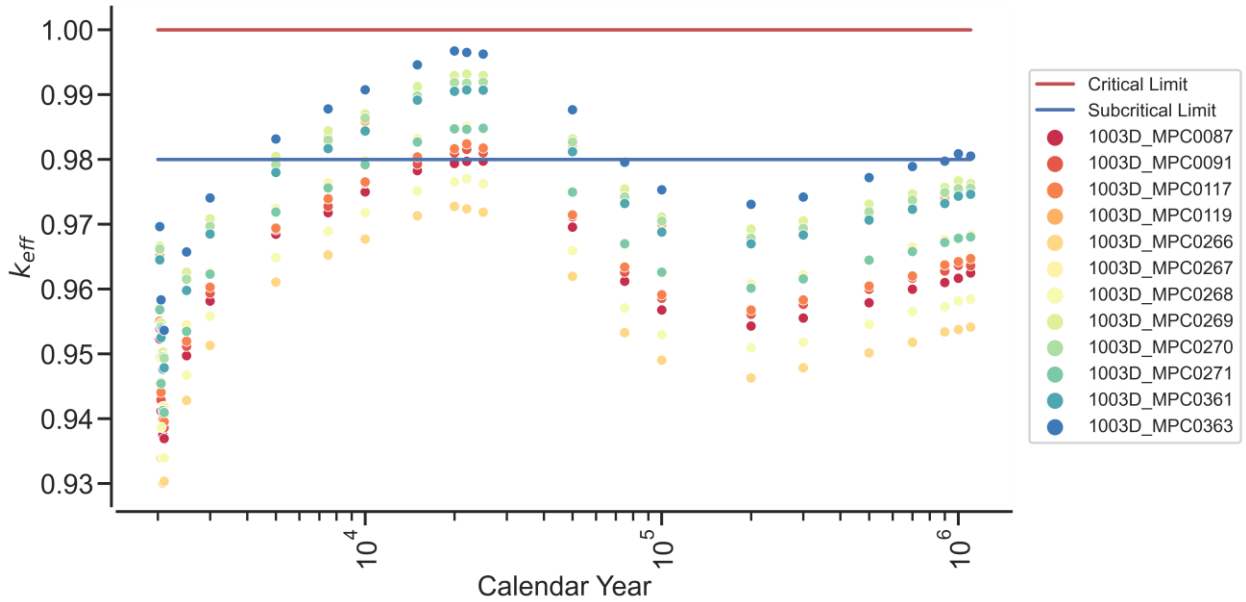


Figure G-11. k_{eff} vs. calendar year for the loss-of-neutron-absorber scenario based on actual loading and disposal isotopes for the SNF canisters at Byron.

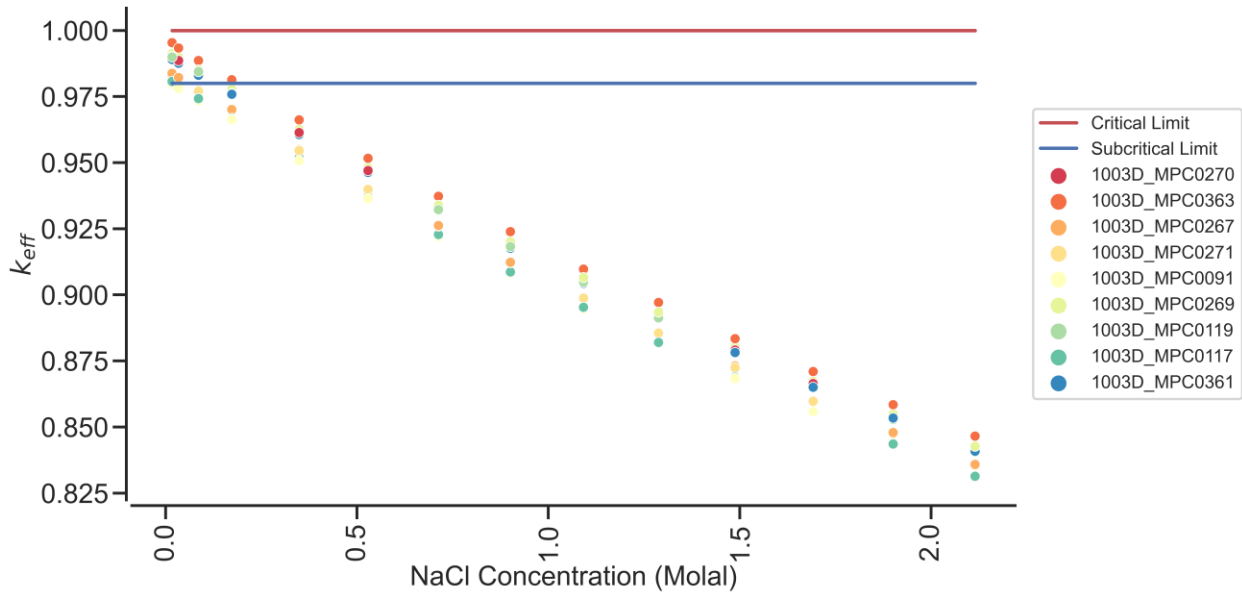


Figure G-12. k_{eff} vs. NaCl concentration for the DPCs with $k_{eff} > 0.98$ for the canisters at Byron under the loss-of-neutron-absorber scenario (calendar year 22,000).

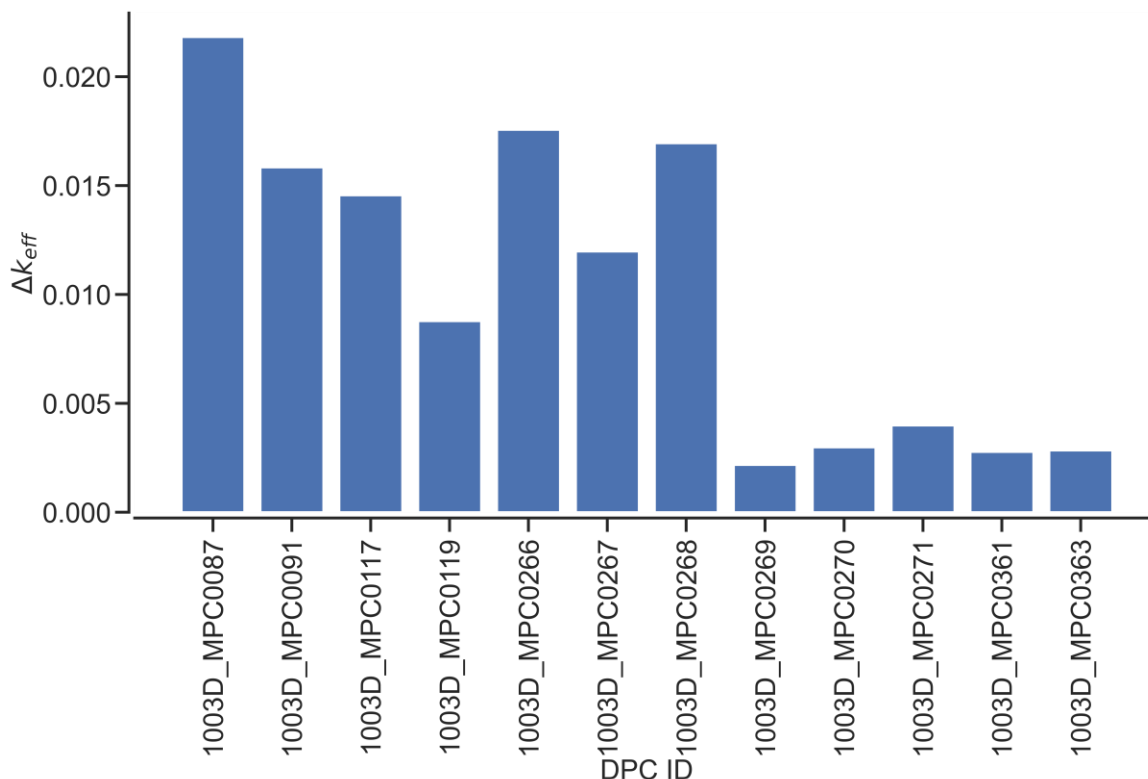


Figure G-13. k_{eff} increase between the worst-misload scenario and the as-loaded configuration for the MPC-32s at Byron (calendar year 22,000).

G.6. LA SALLE CRITICALITY CALCULATIONS

Post-closure disposal criticality calculations were performed as a function of decay time for the 24 SNF canisters at the La Salle independent spent fuel storage installation (ISFSI). Of the 24 SNF canisters, 15 are MPC-68s and 9 are MPC-68Ms. The MPC-68 does not contain any carbon steel or aluminum structural components, so only the loss-of-neutron-absorber scenario is analyzed, whereas the MPC-68M basket is composed of Metamic-HT. For the MPC-68M, the loss of neutron absorber is also the loss of the basket structure; therefore, only the DB condition is modeled. Figure G-14 shows results for the loss-of-neutron-absorber scenario for 23 decay times within the time interval between calendar years 2030 and 1,100,000. The results in Figure G-14 show k_{eff} variation as a function of calendar year. Figure G-15 shows results for the DB scenario for 23 decay times within the time interval between calendar years 2030 and 1,100,000. The results in Figure G-15 show k_{eff} variation as a function of calendar year. The one sigma statistical uncertainty for all k_{eff} values is 0.0003 or less for all cases.

The k_{eff} values are predicted to vary from 0.9014 to 0.9371 for the MPC-68s under the loss-of-absorber scenario. The k_{eff} values are predicted to vary from 1.1335 to 1.1692 for the MPC-68Ms under the DB scenario. No canisters had k_{eff} values greater than 0.98 under the loss-of-neutron-absorber scenario, but all 9 MPC-68M canisters under the DB scenario were above 0.98, and thus, calculations were performed for MPC-68M canisters in which the pure water was replaced with groundwater compositions of various NaCl concentrations. Models thus modified were used to determine k_{eff} as a function of NaCl concentration for the calendar year 22,000 (most reactive date). Figure G-16 presents k_{eff} variation as a function of NaCl concentration for those 9 canisters. Examining the results presented in Figure G-16, it is clear that 1.7 mol NaCl/ kg H₂O is sufficient to demonstrate subcriticality ($k_{eff} < 0.98$) for all La Salle

canisters. In this context, it is also important to note that a saturated NaCl brine has a concentration of approximately 6 molal.

Figure G-17 shows the k_{eff} increase between the worst-misload scenario and the as-loaded configuration for the 15 analyzed La Salle MPC-68 canisters at the calendar year 22,000. Figure G-18 shows the k_{eff} increase between the worst-misload scenario and the as-loaded configuration for the 9 analyzed La Salle MPC-68M canisters at the calendar year 22,000. The increase in k_{eff} varies between 550 and 1,887 pcm for La Salle MPC-68 canisters, and 190 and 612 pcm for La Salle MPC-68M canisters.

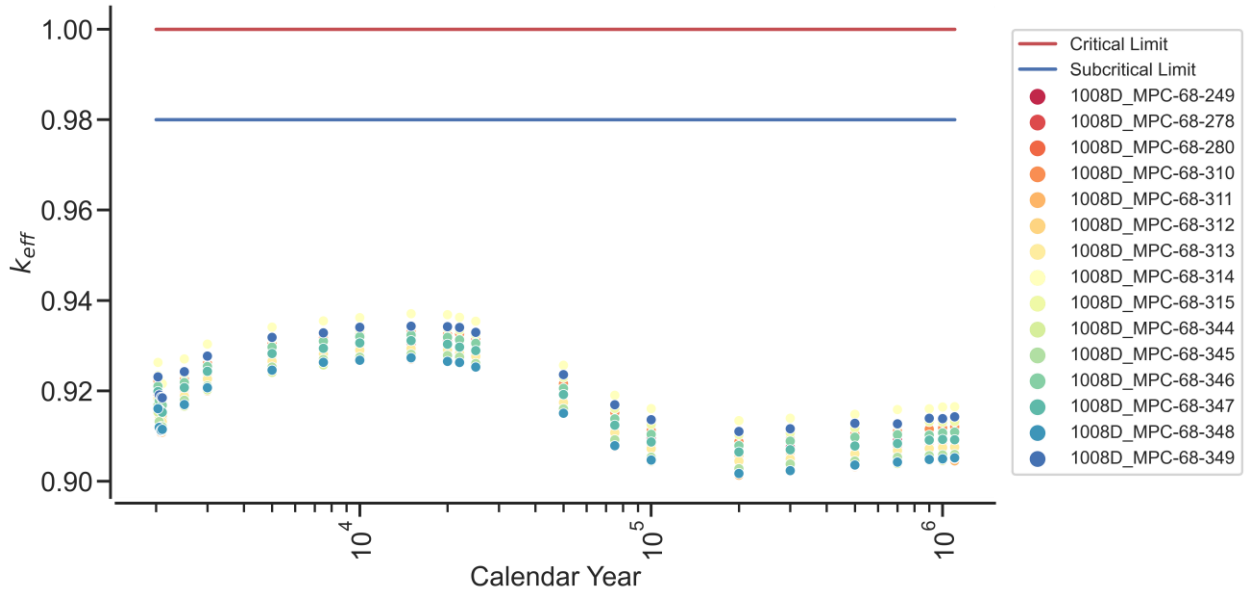


Figure G-14. k_{eff} vs. calendar year for the loss-of-neutron-absorber scenario based on actual loading and disposal isotopes for the MPC-68 SNF canisters at La Salle.

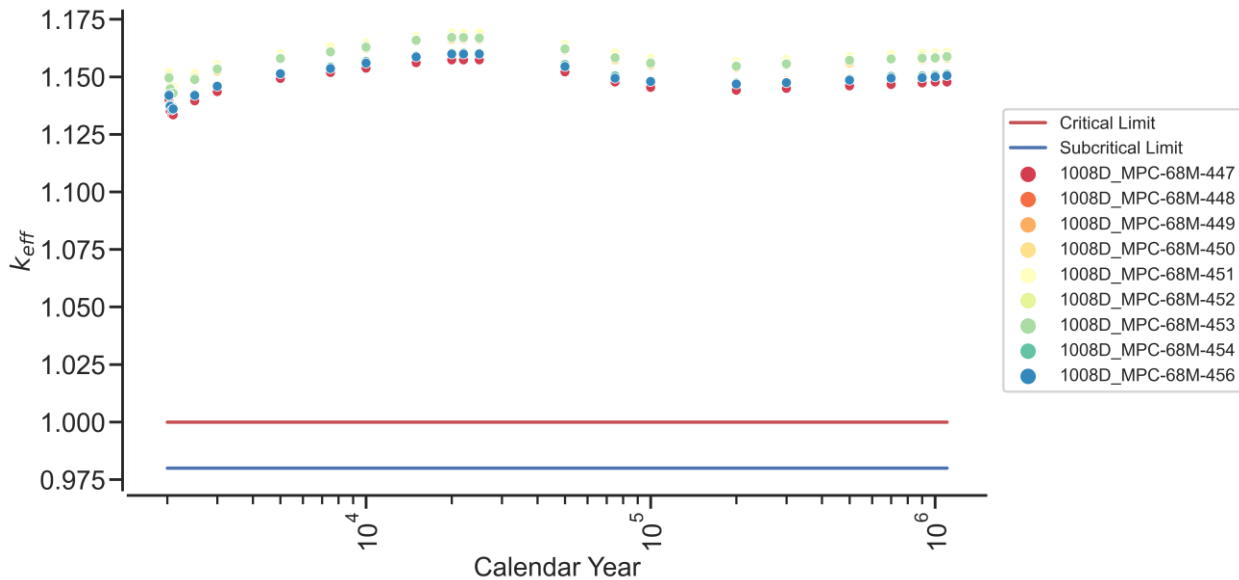


Figure G-15. k_{eff} vs. calendar year for the DB scenario based on actual loading and disposal isotopes for the MPC-68M SNF canisters at La Salle.

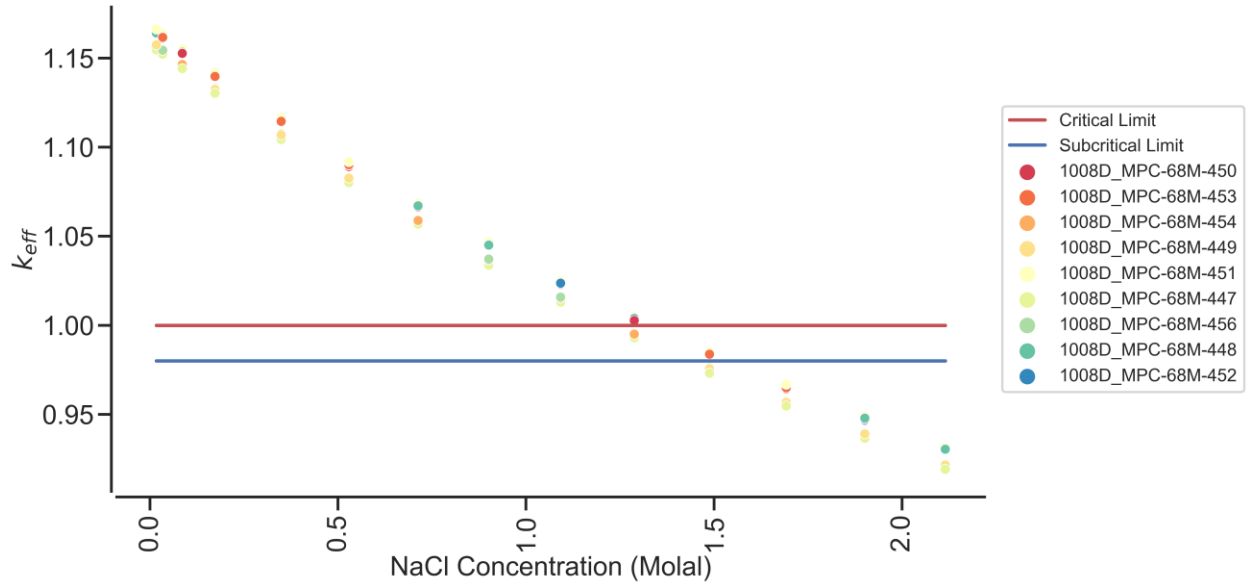


Figure G-16. k_{eff} vs. NaCl concentration for the DPCs with $k_{eff} > 0.98$ for the canisters analyzed in 2021 at La Salle under the DB scenario (calendar year 22,000).

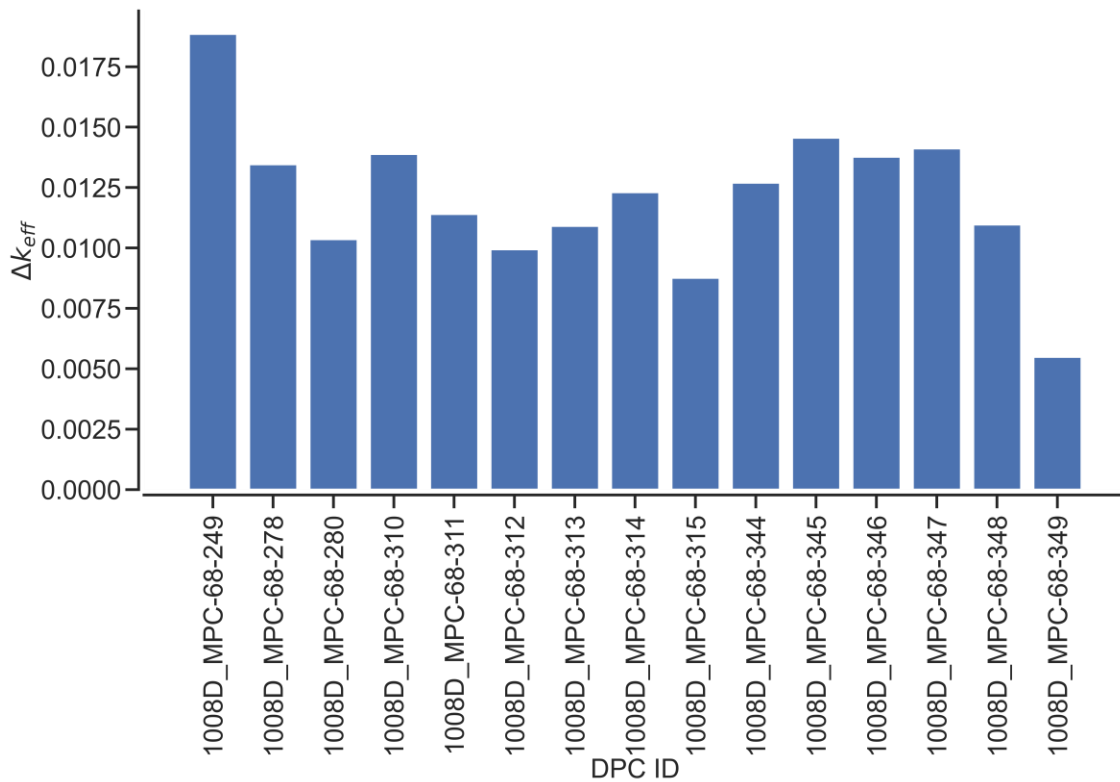


Figure G-17. k_{eff} increase between the worst-misload scenario and the as-loaded configuration for the MPC-68s at La Salle (calendar year 22,000).

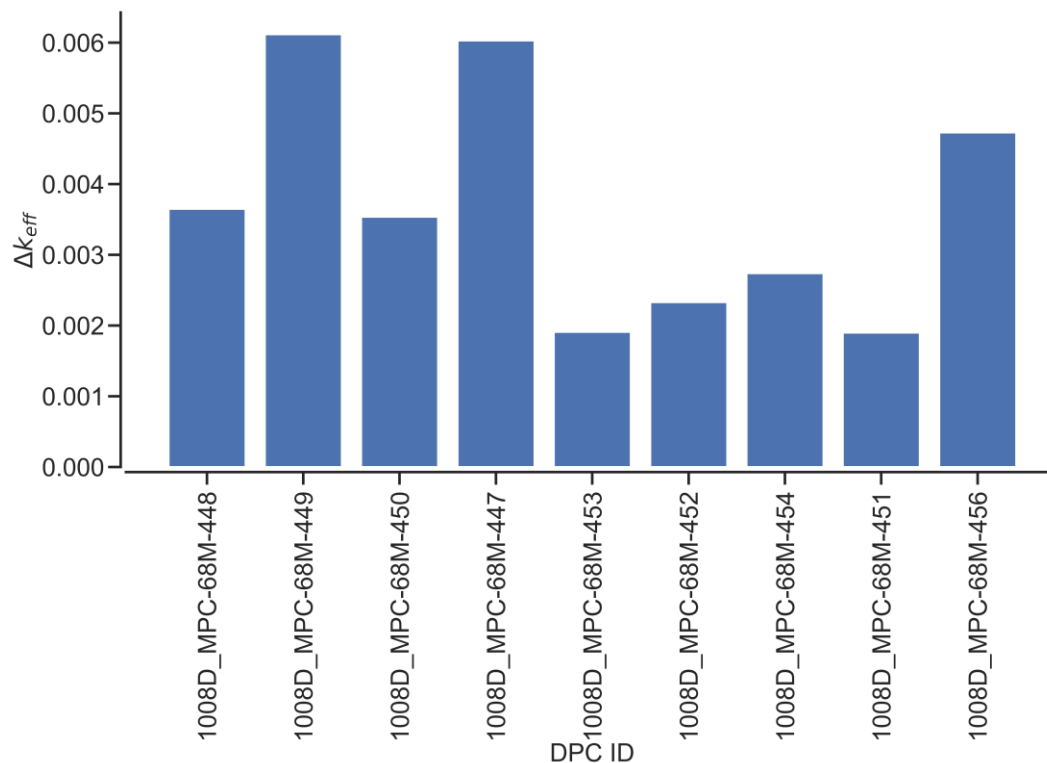


Figure G-18. k_{eff} increase between the worst-misload scenario and the as-loaded configuration for the MPC-68Ms at La Salle (calendar year 22,000).

G.7. NORTH ANNA CRITICALITY CALCULATIONS

Post-closure disposal criticality calculations were performed as a function of decay time for the 13 SNF canisters at the North Anna ISFSI. All 13 SNF canisters are NUHOMS® 32PTH-DSCs. The NUHOMS® 32PTH-DSC does not contain any carbon steel structural components, so only the loss-of-neutron-absorber scenario is analyzed. Figure G-19 shows results for the loss-of-neutron-absorber scenario for 23 decay times within the time interval between calendar years 2030 and 1,100,000. The results in Figure G-19 show k_{eff} variation as a function of calendar year. The one sigma statistical uncertainty for all k_{eff} values is 0.0003 or less for all cases.

The k_{eff} values are predicted to vary from 0.9067 to 0.9718 for the NUHOMS® 32PTH-DSCs under the loss-of-absorber scenario. No canisters had k_{eff} values greater than 0.98 under the loss-of-neutron-absorber scenario, and thus no calculations were performed in which the pure water was replaced with groundwater compositions of various NaCl concentrations.

Figure G-20 shows the k_{eff} increase between the worst-misload scenario and the as-loaded configuration for the 13 analyzed North Anna canisters at the calendar year 22,000. The increase in k_{eff} varies between 325 and 2,456 pcm for North Anna canisters.

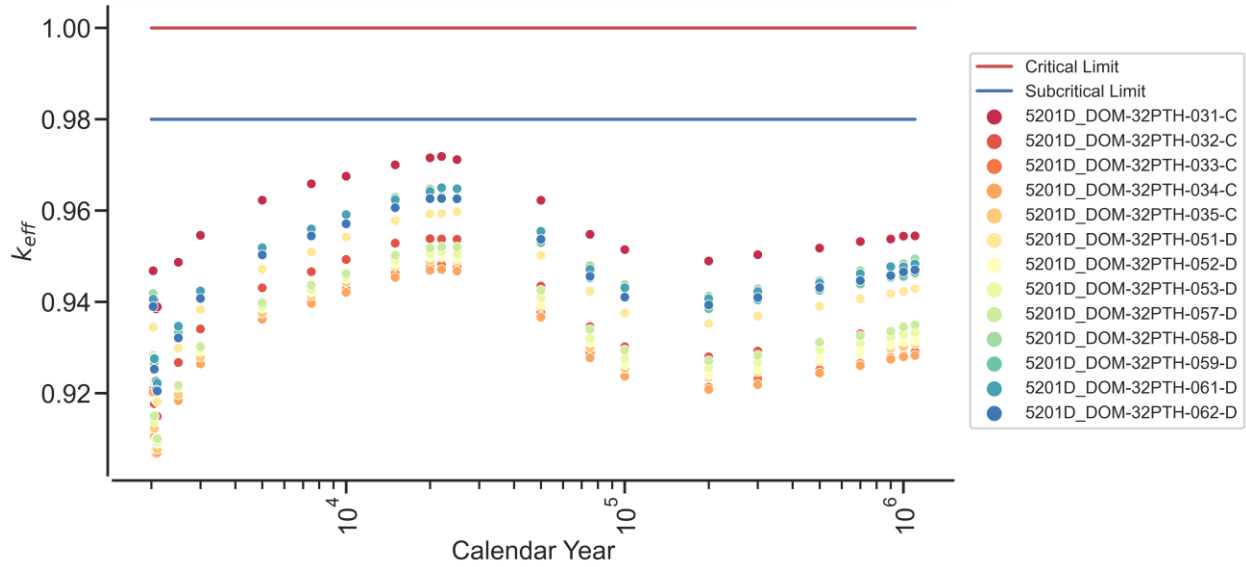


Figure G-19. k_{eff} vs. calendar year for the loss-of-neutron-absorber scenario based on actual loading and disposal isotopes for the SNF canisters at North Anna.

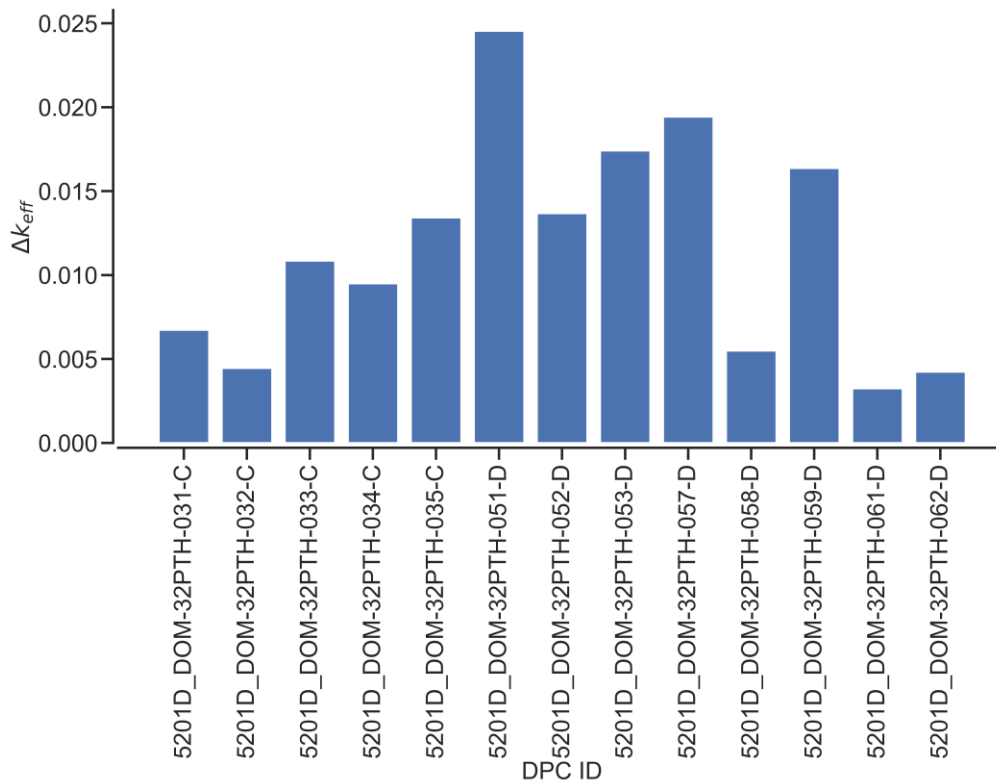


Figure G-20. k_{eff} increase between the worst-misload scenario and the as-loaded configuration for the NUHOMS® 32PTH-DSCs at North Anna (calendar year 22,000).

G.8. SEQUOYAH CRITICALITY CALCULATIONS

Post-closure disposal criticality calculations were performed as a function of decay time for the 14 SNF canisters at the Sequoyah ISFSI. Ten of the SNF canisters are MPC-37s, and four are MPC-32s. The MPC-32s do not contain any carbon steel structural components, so only the loss-of-neutron-absorber scenario was analyzed. The MPC-37 basket is composed entirely of Metamic-HT, so for the MPC-37, the loss of neutron absorber is also the loss of the basket structure; therefore only the DB condition is modeled. Figure G-21 shows results for the MPC-32 loss-of-neutron-absorber scenario for 23 decay times within the time interval between calendar years 2030 and 1,100,000. The results in Figure G-21 show k_{eff} variation as a function of calendar year. Figure G-22 shows results for the MPC-37 DB scenario for 23 decay times within the time interval between calendar years 2030 and 1,100,000. The results in Figure G-22 show k_{eff} variation as a function of calendar year. The one sigma statistical uncertainty for all k_{eff} values is 0.0003 or less for all cases.

The k_{eff} values are predicted to vary from 0.9457 to 1.0056 for the MPC-32s under the loss-of-absorber scenario, and from 1.0413 to 1.1097 for the MPC-37s under the DB scenario. For canisters which had k_{eff} values greater than 0.98 under the loss-of-neutron-absorber or DB scenario, calculations were performed in which the pure water was replaced with groundwater compositions of various NaCl concentrations, and the models thus modified were used to determine k_{eff} as a function of NaCl concentration for the calendar year 22,000 (most reactive date). Figure G-23 presents k_{eff} variation as a function of NaCl concentration for those 14 canisters. Examining the results presented in Figure G-23, it is clear that 1.5 mol NaCl/ kg H₂O is sufficient to demonstrate subcriticality ($k_{eff} < 0.98$) for all Sequoyah canisters. The maximum necessary concentration is 0.6 mol NaCl/kg H₂O. In this context, it is also important to note that a saturated NaCl brine has a concentration of approximately 6 molal.

Figure G-24 shows the k_{eff} increase between the worst-misload scenario and the as-loaded configuration for the 4 analyzed Sequoyah MPC-32 canisters at the calendar year 22,000. The increase in k_{eff} varies between 455 and 1,438 pcm for MPC-32 Sequoyah canisters. Figure G-25 shows the k_{eff} increase between the worst-misload scenario and the as-loaded configuration for the 10 analyzed Sequoyah MPC-37 canisters at the calendar year 22,000. The increase in k_{eff} varies between 936 and 1,833 pcm for MPC-37 Sequoyah canisters.

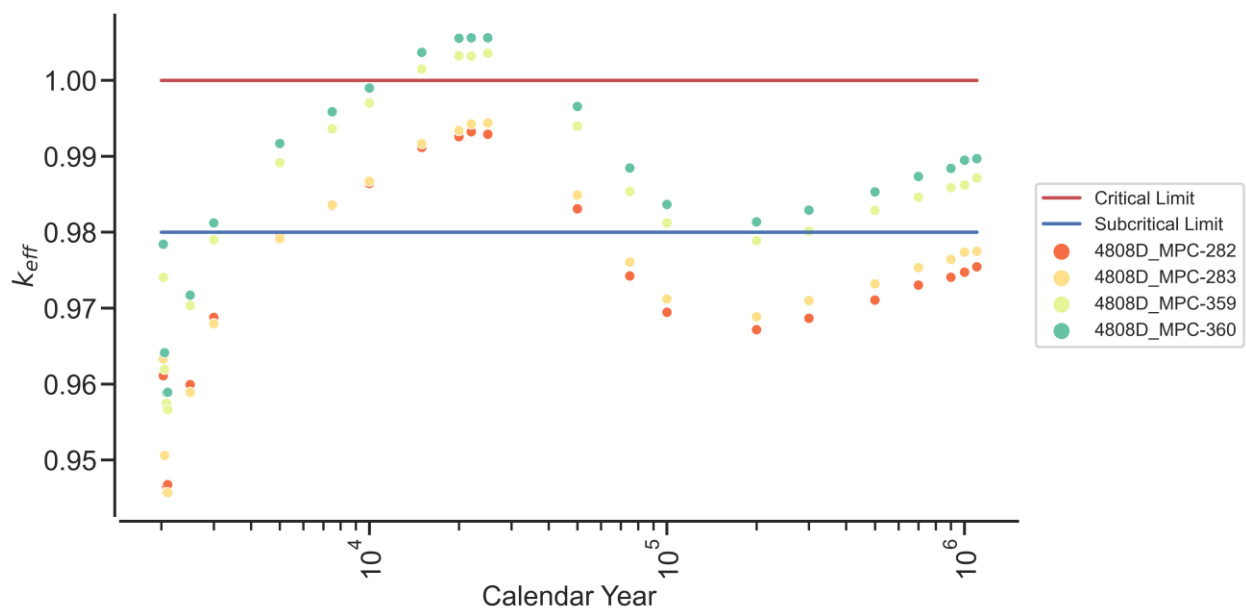


Figure G-21. k_{eff} vs. calendar year for the loss-of-neutron-absorber scenario based on actual loading and disposal isotopes for the MPC-32 SNF canisters at Sequoyah.

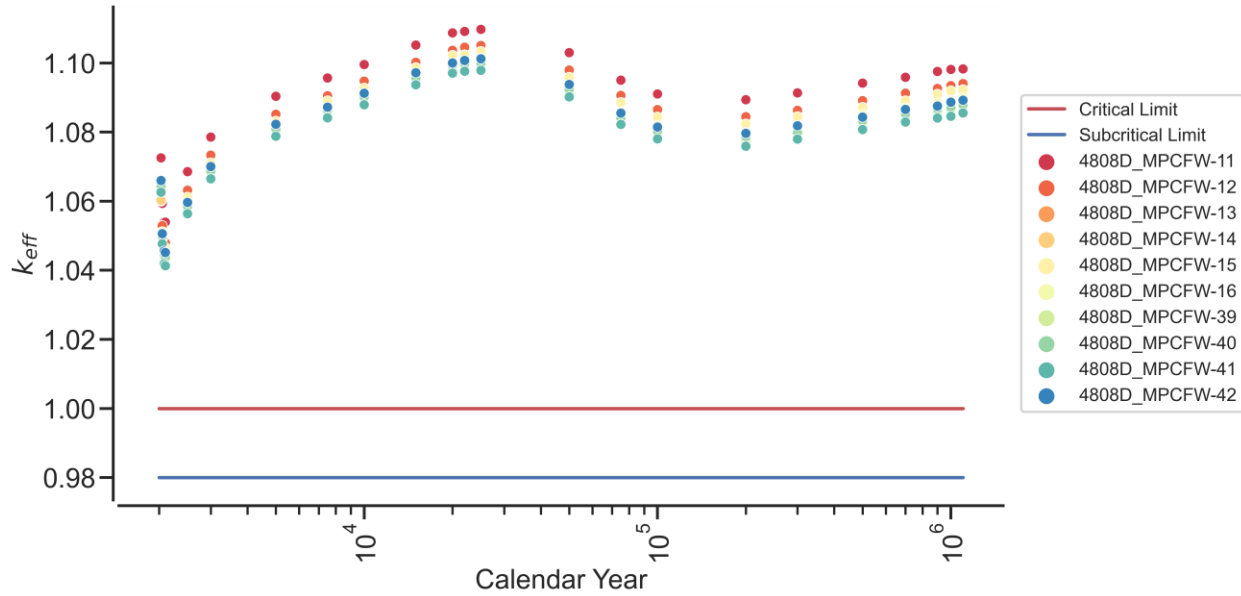


Figure G-22. k_{eff} vs. calendar year for the loss-of-neutron-absorber scenario based on actual loading and disposal isotopes for the MPC-37 SNF canisters at Sequoyah.

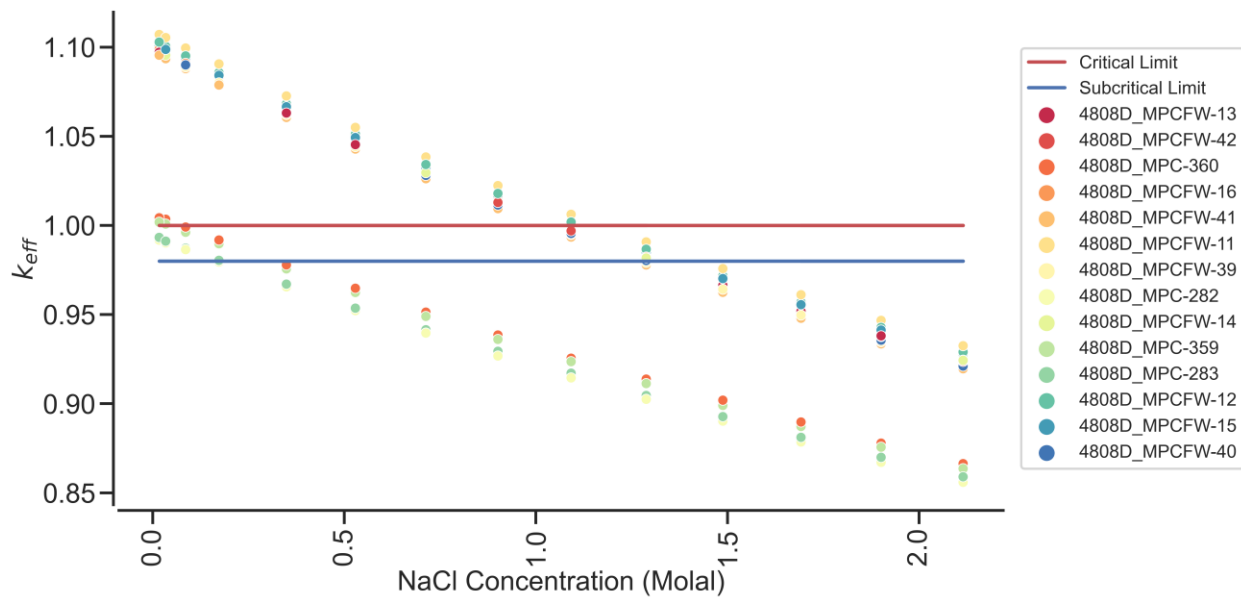


Figure G-23. k_{eff} vs. NaCl concentration for the DPCs with $k_{eff} > 0.98$ for the canisters analyzed in 2021 at Sequoyah under the loss-of-neutron-absorber and DB scenarios (calendar year 22,000).

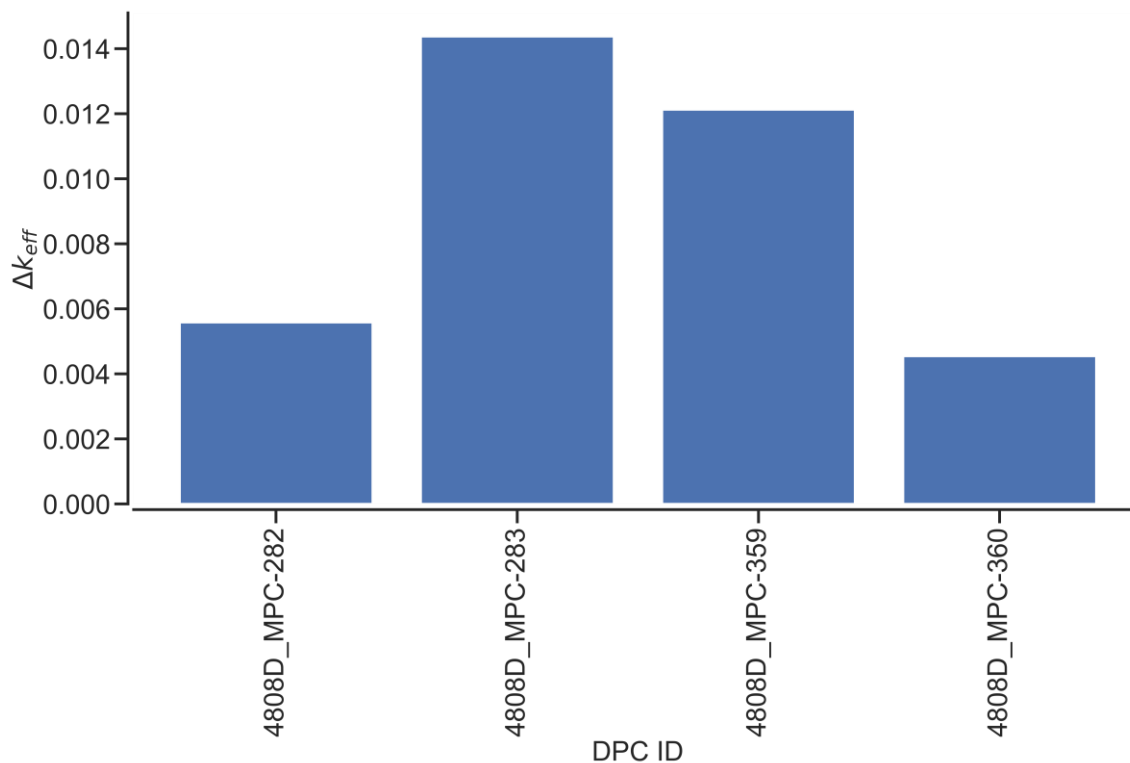


Figure G-24. k_{eff} increase between the worst-misload scenario and the as-loaded configuration for the MPC-32s at Sequoyah (calendar year 22,000).

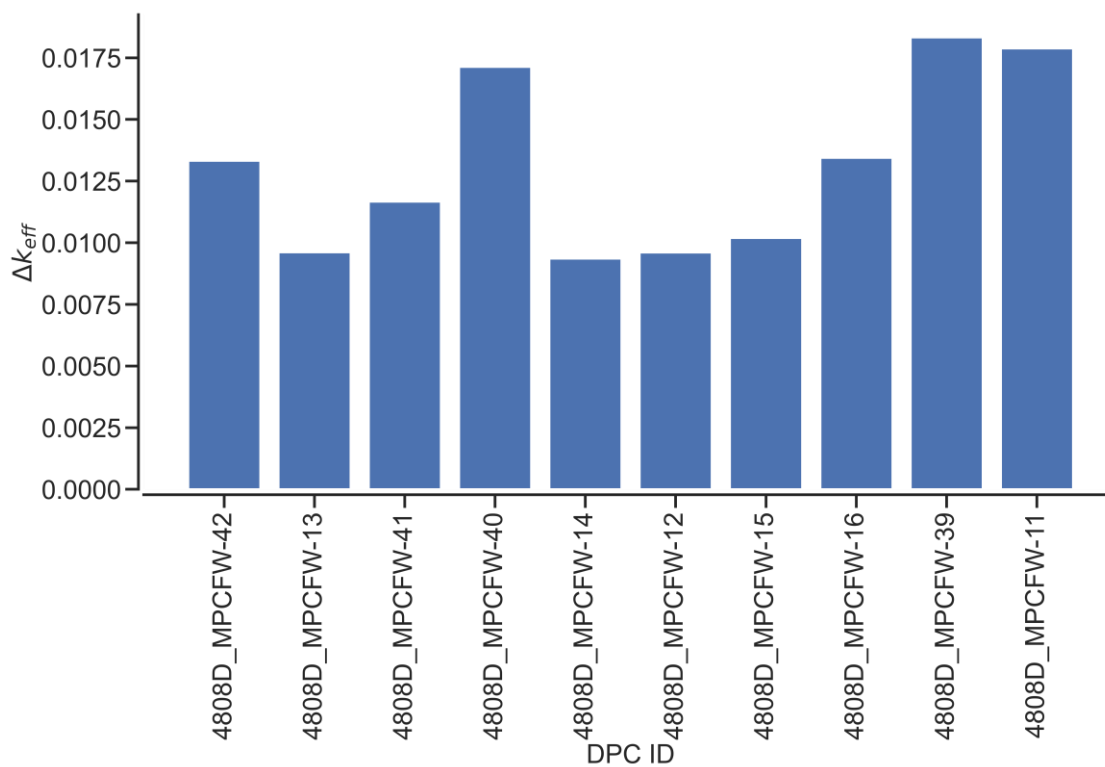


Figure G-25. k_{eff} increase between the worst-misload scenario and the as-loaded configuration for the MPC-37s at Sequoyah (calendar year 22,000).

G.9. SURRY CRITICALITY CALCULATIONS

Post-closure disposal criticality calculations were performed as a function of decay time for the 10 SNF canisters at the Surry ISFSI. All 10 SNF canisters are NUHOMS® 32PTH-DSCs. The NUHOMS® 32PTH-DSC does not contain any carbon steel structural components, so only the loss-of-neutron-absorber scenario is analyzed. Figure G-26 shows results for the loss-of-neutron-absorber scenario for 23 decay times within the time interval between calendar years 2030 and 1,100,000. The results in Figure G-26 show k_{eff} variation as a function of calendar year. The one sigma statistical uncertainty for all k_{eff} values is 0.0003 or less for all cases.

The k_{eff} values are predicted to vary from 0.8916 to 0.9548 for the NUHOMS® 32PTH-DSCs under the loss-of-absorber scenario. No canisters had k_{eff} values greater than 0.98 under the loss-of-neutron-absorber scenario, and thus no calculations were performed in which the pure water was replaced with groundwater compositions of various NaCl concentrations.

Figure G-27 shows the k_{eff} increase between the worst-misload scenario and the as-loaded configuration for the 10 analyzed Surry canisters at the calendar year 22,000. The increase in k_{eff} varies between 288 and 1,856 pcm for Surry canisters.

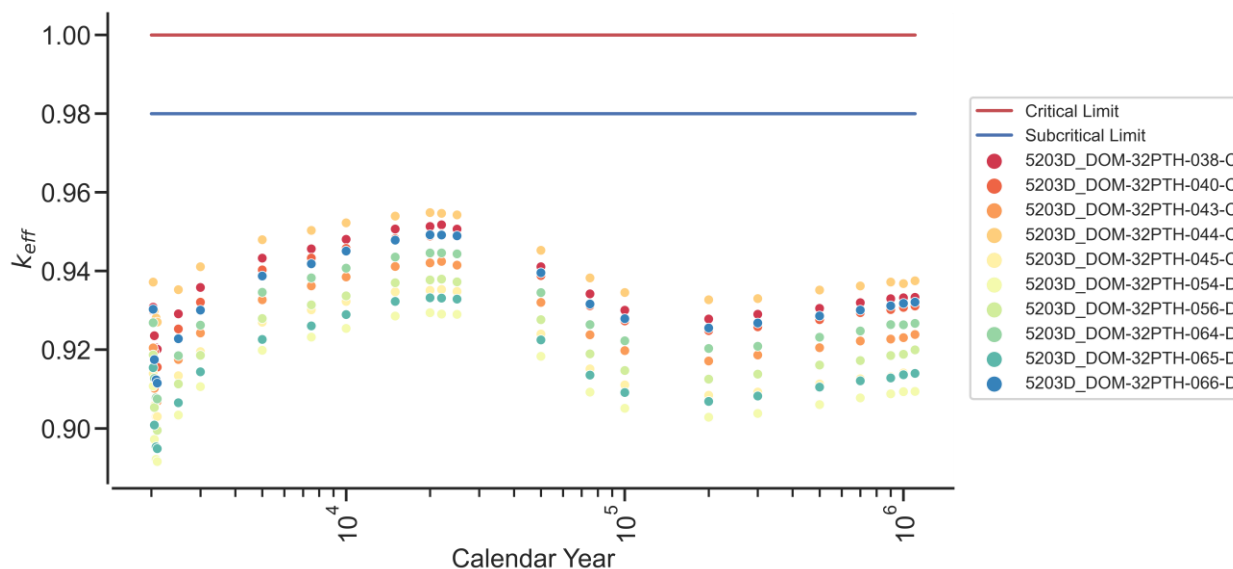


Figure G-26. k_{eff} vs. calendar year for the loss-of-neutron-absorber scenario based on actual loading and disposal isotopes for the SNF canisters at Surry.

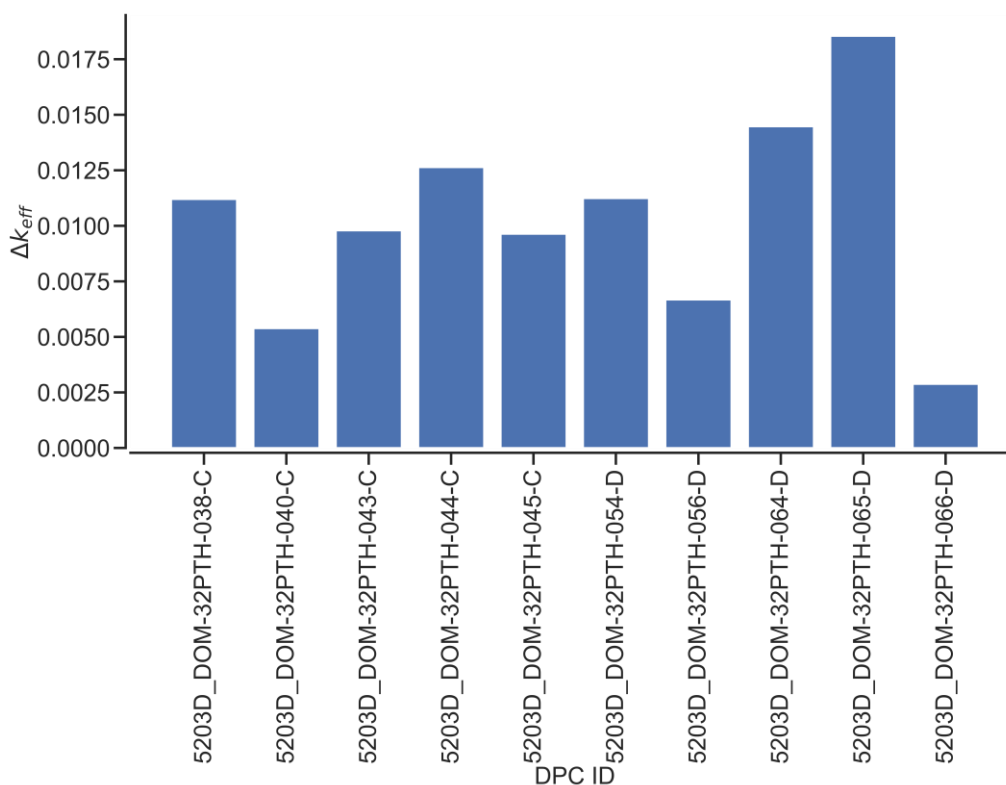


Figure G-27. k_{eff} increase between the worst-misload scenario and the as-loaded configuration for the NUHOMS® 32PTH-DSCs at Surry (calendar year 22,000).

G.10. CALLAWAY CRITICALITY CALCULATIONS

Post-closure disposal criticality calculations were performed as a function of decay time for the 6 SNF canisters at the Callaway ISFSI. All 6 SNF canisters are MPC-37s. The MPC-37 basket is composed entirely of Metamic-HT, so for the MPC-37, the loss of neutron absorber is also the loss of the basket structure; therefore, only the DB condition is modeled. Figure G-28 shows results for the DB scenario for 23 decay times within the time interval between calendar years 2030 and 1,100,000. The results in Figure G-28 show k_{eff} variation as a function of calendar year. The one sigma statistical uncertainty for all k_{eff} values is 0.0003 or less for all cases.

The k_{eff} values are predicted to vary from 1.0346 to 1.1009 for the MPC-37s under the DB scenario. For canisters which had k_{eff} values greater than 0.98 under the DB scenario, calculations were performed in which the pure water was replaced with groundwater compositions of various NaCl concentrations, and the models thus modified were used to determine k_{eff} as a function of NaCl concentration for the calendar year 22,000 (most reactive date). Figure G-29 presents k_{eff} variation as a function of NaCl concentration for those 6 canisters. Examining the results presented in Figure G-29, it is clear that 1.3 mol NaCl/ kg H₂O is sufficient to demonstrate subcriticality ($k_{eff} < 0.98$) for all Callaway canisters. In this context, it is also important to note that a saturated NaCl brine has a concentration of approximately 6 molal.

Figure G-30 shows the k_{eff} increase between the worst-misload scenario and the as-loaded configuration for the 6 analyzed Callaway canisters at the calendar year 22,000. The increase in k_{eff} varies between 2,746 and 4,510 pcm for Callaway canisters.

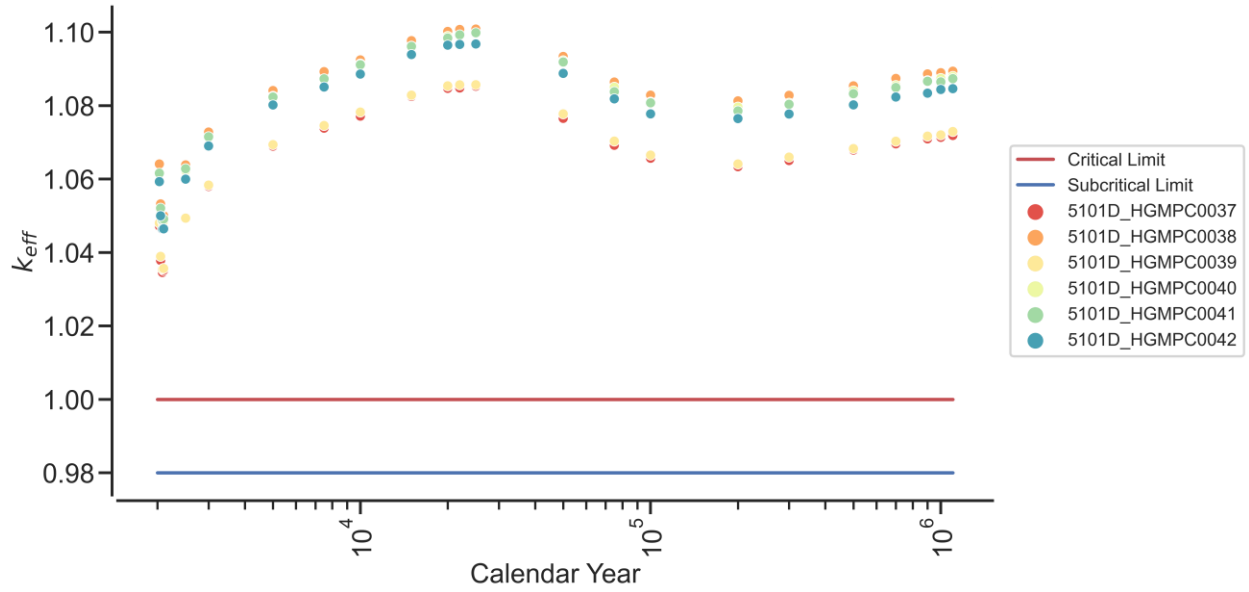


Figure G-28. k_{eff} vs. calendar year for the DB scenario based on actual loading and disposal isotopes for the SNF canisters at Callaway.

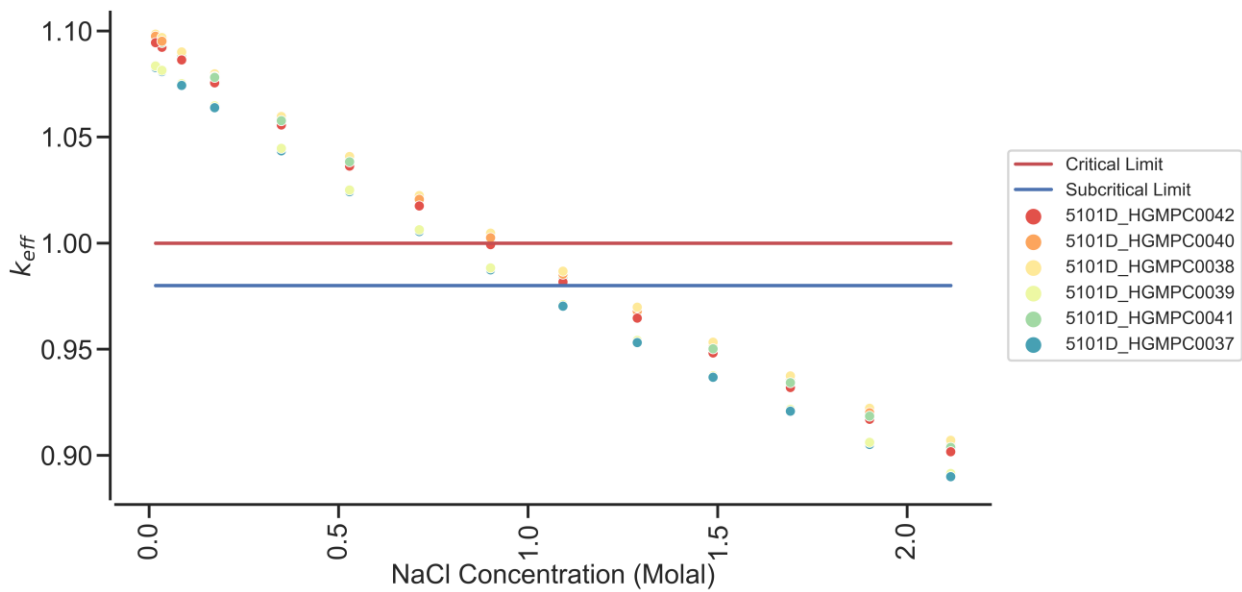


Figure G-29. k_{eff} vs. NaCl concentration for the DPCs with $k_{eff} > 0.98$ for the canisters analyzed at Callaway under the DB scenario (calendar year 22,000).

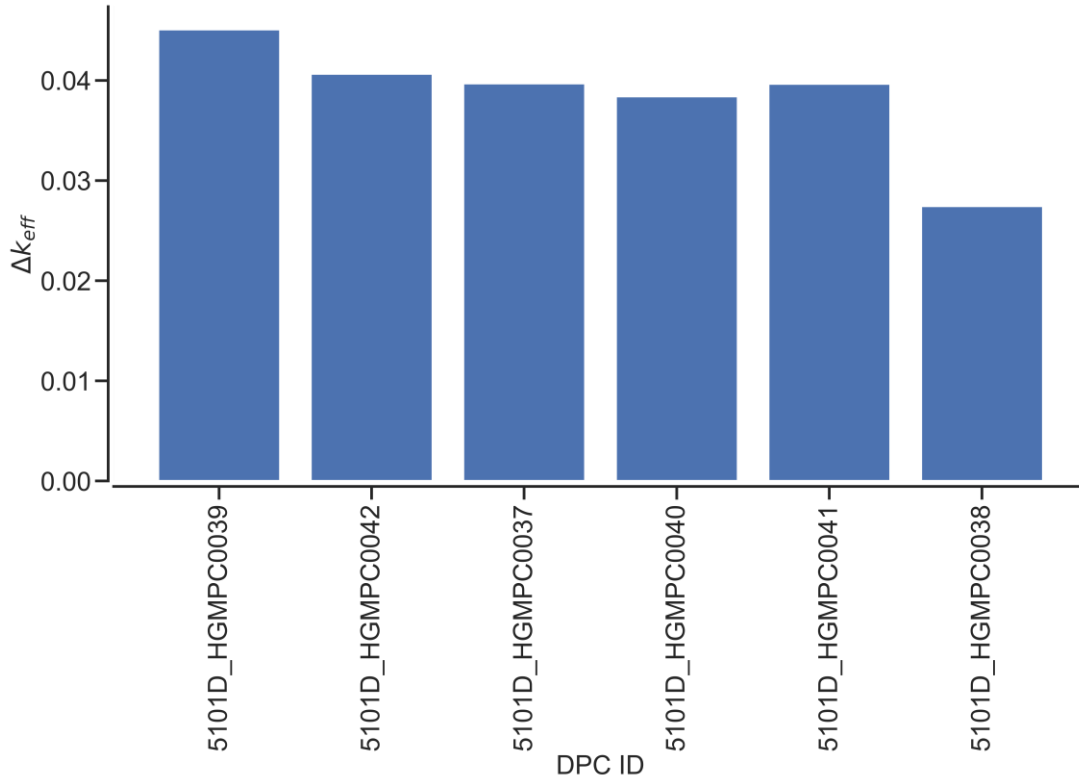


Figure G-30. k_{eff} increase between the worst-misload scenario and the as-loaded configuration for the MPC-37s at Callaway (calendar year 22,000).

G.11. WATTS BAR CRITICALITY CALCULATIONS

Post-closure disposal criticality calculations were performed as a function of decay time for the 6 SNF canisters at the Watts Bar ISFSI. All 6 SNF canisters are MPC-37s. The MPC-37 basket is composed entirely of Metamic-HT, so for the MPC-37 the loss of neutron absorber is also the loss of the basket structure; therefore, only the DB condition is modeled. Figure G-31 shows results for the DB scenario for 23 decay times within the time interval between calendar years 2030 and 1,100,000. The results in Figure G-31 show k_{eff} variation as a function of calendar year. The one sigma statistical uncertainty for all k_{eff} values is 0.0003 or less for all cases.

The k_{eff} values are predicted to vary from 1.0393 to 1.1004 for the MPC-37s under the DB scenario. For canisters which had k_{eff} values greater than 0.98 under the DB scenario, calculations were performed in which the pure water was replaced with groundwater compositions of various NaCl concentrations, and the models thus modified were used to determine k_{eff} as a function of NaCl concentration for the calendar year 22,000 (most reactive date). Figure G-32 presents k_{eff} variation as a function of NaCl concentration for those 6 canisters. Examining the results presented in Figure F-16, it is clear that 1.3 mol NaCl/ kg H₂O is sufficient to demonstrate subcriticality ($k_{eff} < 0.98$) for all Watts Bar canisters. In this context, it is also important to note that a saturated NaCl brine has a concentration of approximately 6 molal.

Figure G-33 shows the k_{eff} increase between the worst-misload scenario and the as-loaded configuration for the 6 analyzed Watts Bar canisters at the calendar year 22,000. The increase in k_{eff} varies between 1,578 and 2,459 pcm for Watts Bar canisters.

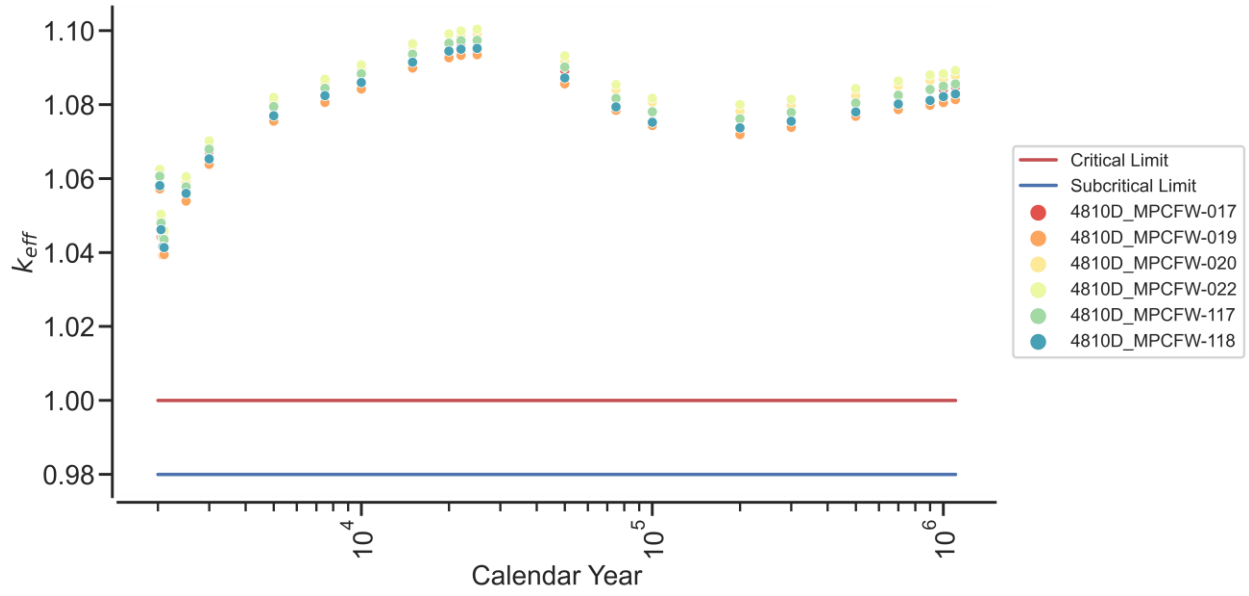


Figure G-31. k_{eff} vs. calendar year for the DB scenario based on actual loading and disposal isotopes for the SNF canisters at Watts Bar.

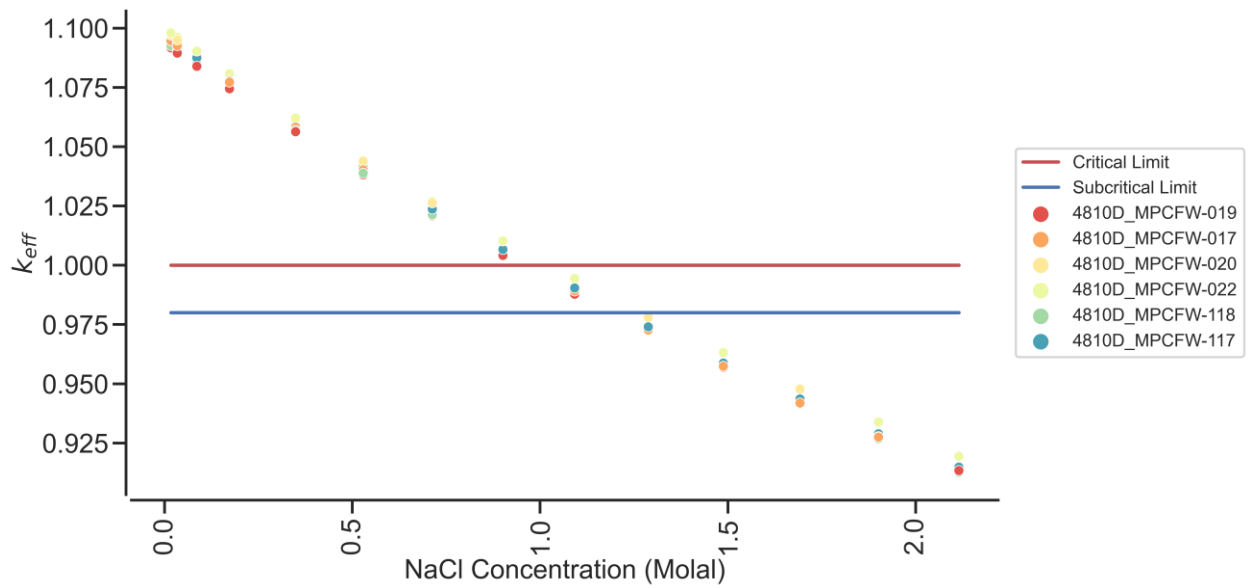


Figure G-32. k_{eff} vs. NaCl concentration for the DPCs with $k_{eff} > 0.98$ for the canisters analyzed at Watts Bar under the DB scenario (calendar year 22,000).

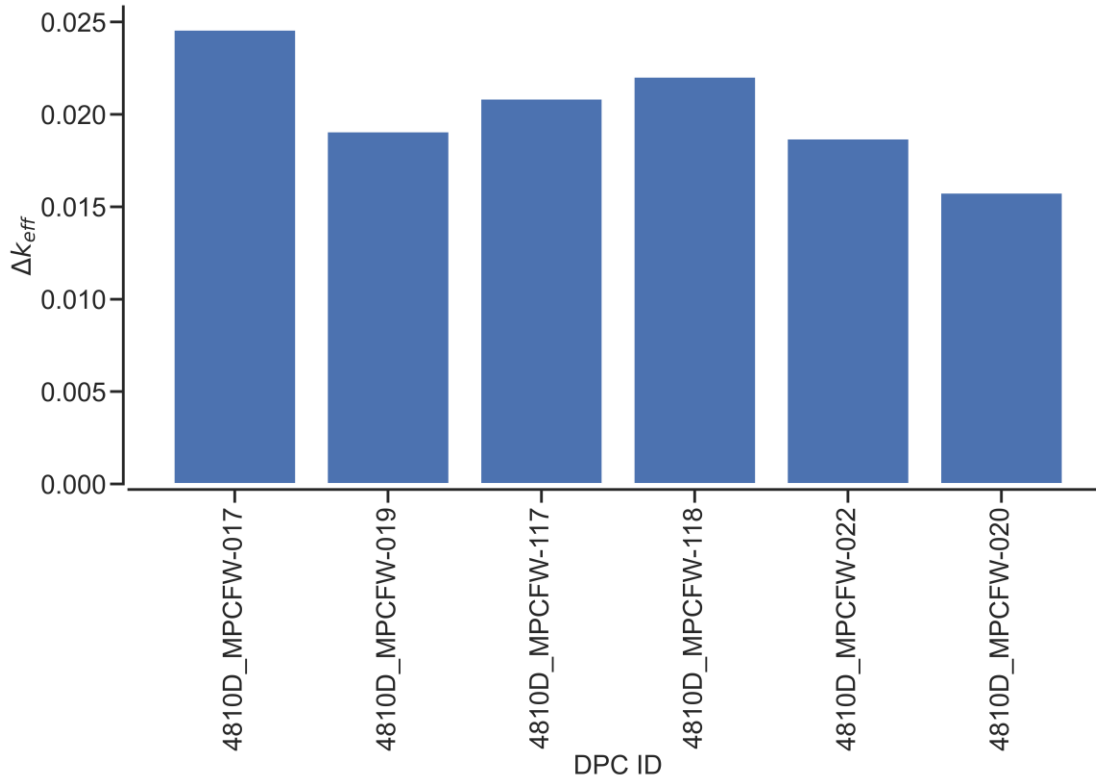


Figure G-33. k_{eff} increase between the worst-misload scenario and the as-loaded configuration for the MPC-37s at Watts Bar (calendar year 22,000).

G.12. BROWNS FERRY CRITICALITY CALCULATIONS

Post-closure disposal criticality calculations were performed as a function of decay time for the 27 SNF canisters at the Browns Ferry ISFSI. All 27 SNF canisters are MPC-89s. The MPC-89 basket is composed entirely of Metamic-HT, so for the MPC-89, the loss of neutron absorber is also the loss of the basket structure; therefore, only the DB condition is modeled. Figure G-34 shows results for the DB scenario for 23 decay times within the time interval between calendar years 2030 and 1,100,000. The results in Figure G-34 show k_{eff} variation as a function of calendar year. The one sigma statistical uncertainty for all k_{eff} values is 0.0003 or less for all cases.

The k_{eff} values are predicted to vary from 1.1342 to 1.1885 for the MPC-89s under the DB scenario. For canisters which had k_{eff} values greater than 0.98 under the degraded basket scenario, calculations were performed in which the pure water was replaced with groundwater compositions of various NaCl concentrations, and the models thus modified were used to determine k_{eff} as a function of NaCl concentration for the calendar year 22,000 (most reactive date). Figure G-35 presents k_{eff} variation as a function of NaCl concentration for those 27 canisters. Examining the results presented in Figure G-35, it is clear that 1.9 mol NaCl/ kg H₂O is sufficient to demonstrate subcriticality ($k_{eff} < 0.98$) for all Browns Ferry canisters. In this context, it is also important to note that a saturated NaCl brine has a concentration of approximately 6 molal.

Figure G-36 shows the k_{eff} increase between the worst-misload scenario and the as-loaded configuration for the 27 analyzed Browns Ferry canisters at the calendar year 22,000. The increase in k_{eff} varies between 454 and 2,958 pcm for Browns Ferry canisters.

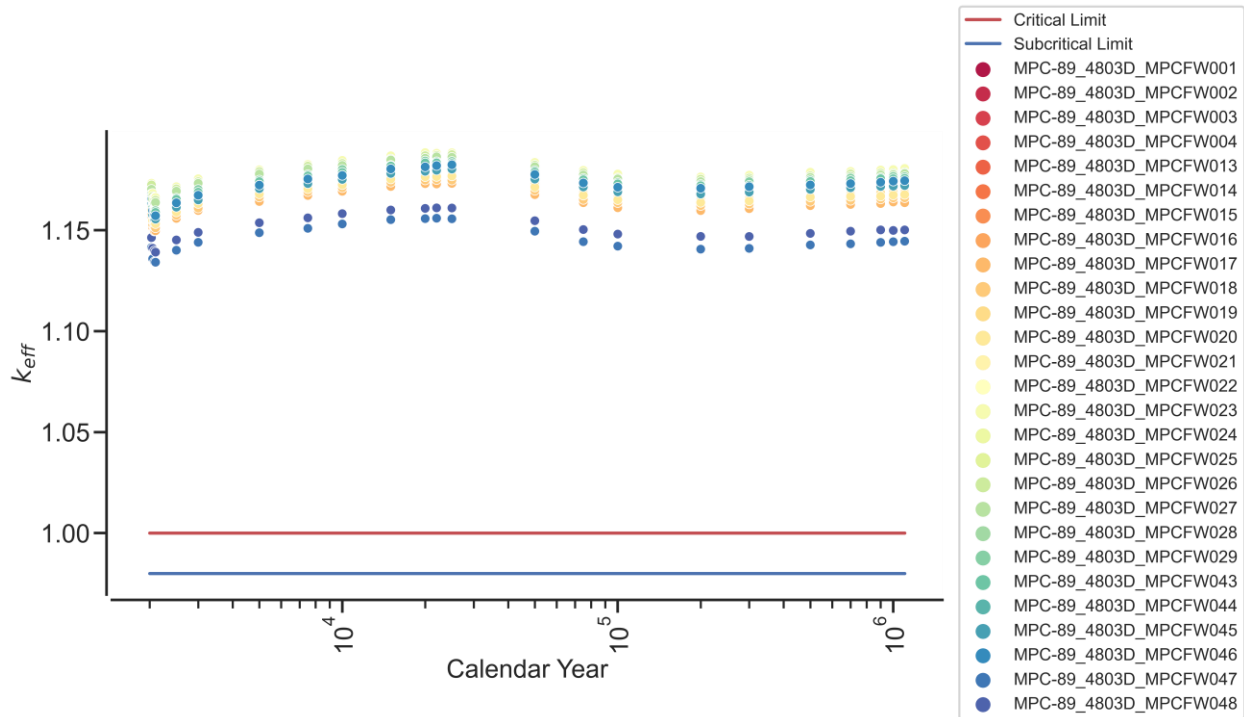


Figure G-34. k_{eff} vs. calendar year for the DB scenario based on actual loading and disposal isotopes for the SNF canisters at Browns Ferry.

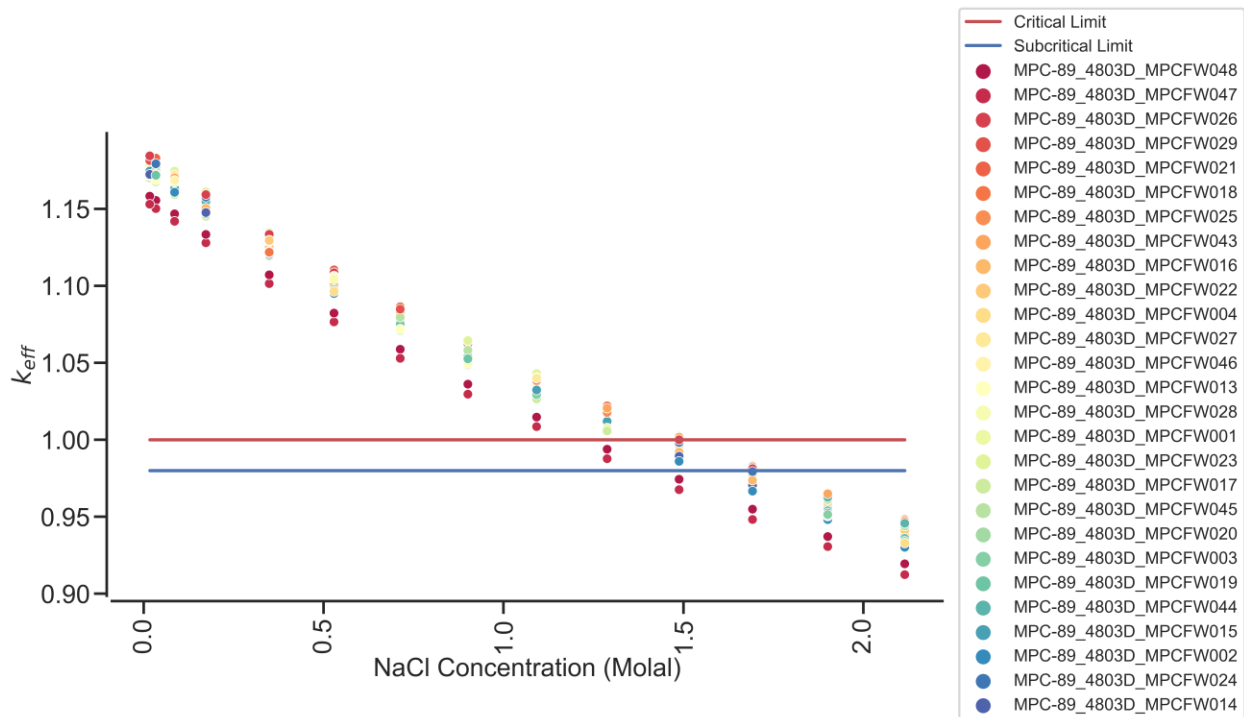


Figure G-35. k_{eff} vs. NaCl concentration for the DPCs with $k_{eff} > 0.98$ for the canisters analyzed at Browns Ferry under the DB scenario (calendar year 22,000).

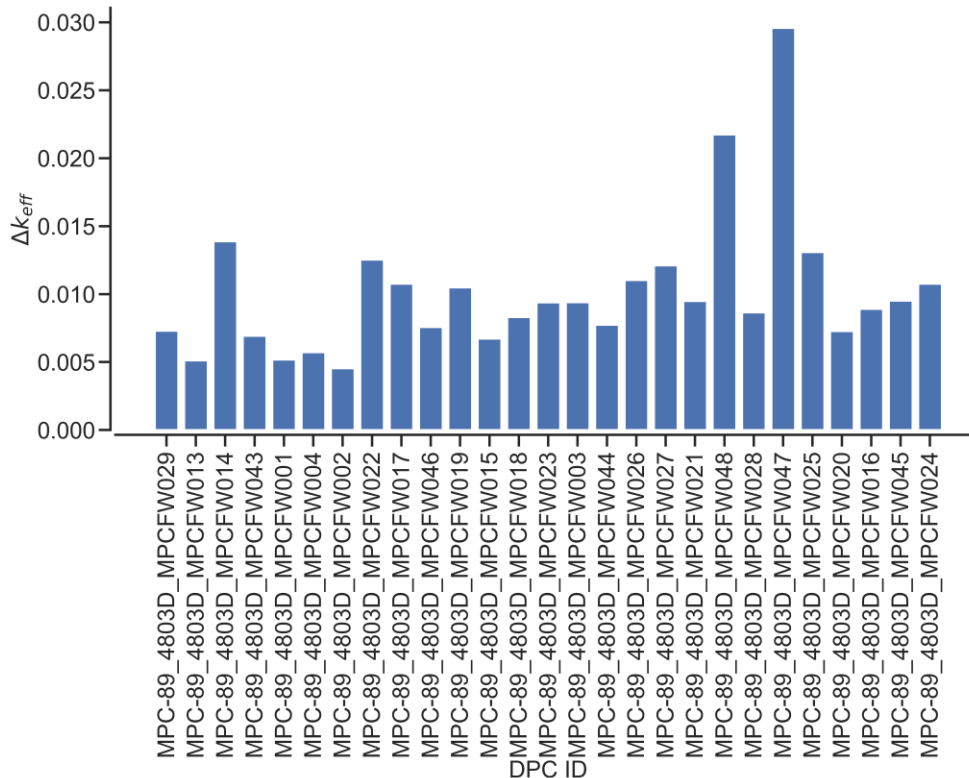


Figure G-36. k_{eff} increase between the worst-misload scenario and the as-loaded configuration for the MPC-89s at Browns Ferry (calendar year 22,000).

G.13. CONCLUSIONS

This appendix contains an update to the DPC reactivity assessment analysis carried out in previous years.

Previous FY21 post closure reactivity assessment activities include the analysis of fuel assembly/basket modification concepts and the initial investigation of DPC loading optimization while considering criticality as a criterion. The fuel assembly/basket modification work addressed guide tube based DCRA and ANA chevron inserts for PWR DPCs, as well as ANA fuel channel replacement absorbers for BWR DPCs. The DCRA showed good ability to demonstrate subcriticality for most highly reactive DPCs. Although the ANA chevron inserts did not perform as well, they showed the ability to demonstrate subcriticality for less reactive canisters. The ANA fuel channel replacements showed the ability to demonstrate subcriticality for the most reactive BWR DPCs. The fuel loading optimization work investigated the potential for reactivity reduction by reloading the fuel at Zion with the intention to reduce the reactivity of the set of DPCs. Whereas the Zion reloading work showed a dramatic decrease in DPC reactivity, it likely represents an idealized case which only addressed criticality. To incorporate post-closure criticality in a more holistic DPC loading algorithm, a neural network was trained and shown to be able to predict reactivity within an acceptable uncertainty.

Post-closure criticality analysis calculations for a total of 155 new as-loaded canisters from ten sites over the time interval between calendar years 2030 and 1,100,000 were performed using the burnup credit methodology described in this report. For the reactivity calculation, the NA configurations were modeled for DPCs with baskets composed of stainless steel, and the DB configurations were modeled for DPCs composed of other materials. A particular emphasis was placed on modeling DPCs with baskets composed of Metamic-HT (MPC-37, MPC-68M, MPC-89) because it performs both a neutron absorbing and structural function under normal storage and transportation conditions and may pose a concern for

post-closure criticality. Furthermore, four additional sites with MPC-32s, two sites with NUHOMS® 32PTH-DSCs, and one site with MPC-68s were analyzed. In all cases, the reactivity results were compared to a critical limit of 1.0 and a hypothetical limit of 0.98.

In addition to the as-loaded reactivity assessment calculations, canister misloading calculations and NaCl reactivity suppression calculations were performed. Canister misload criticality analyses were performed assuming a worst configuration in an as-loaded canister, which is based on the assumption that correct assemblies have been loaded into the canister, but they are loaded in the most reactive configuration. k_{eff} values for worst-misload configurations were determined assuming that all fuel assemblies in the canister have a decay time of 22,000 years and the neutron absorber is completely lost. The misload analysis was performed for all 155 new canisters containing intact fuel assemblies that were loaded to full capacity. All canisters that were shown to exceed the 0.98 subcritical limit were analyzed to determine the groundwater NaCl concentrations necessary to show subcriticality.

A summary of the DPC reactivity assessment results for 155 DPCs analyzed during FY21 are shown in Table G-2. For each site, Table G-2 contains the section of the report documenting the analysis, the type of DPC used at the site, the degradation scenario modeled, the minimum and maximum k_{eff} for the reactivity calculations, the minimum and maximum canister misload k_{eff} increases, and the maximum NaCl concentration needed to reduce the DPC k_{eff} values to 0.98. Based on the results in Table G-2, it is observed that all Metamic-HT baskets show very high reactivity as a result of the complete loss of neutron absorber and assembly spacing in the DB configuration. These DPCs are among the most reactive observed to date. It is also observed that, even with the elevated reactivity, a maximum of 1.9 m of NaCl would be required to suppress the reactivity of these canisters. The MPC-32, NUHOMS® 32PTH-DSC, and MPC-68 results were in alignment with previously calculated results for other canisters.

Table G-2. Summary of FY21 DPC reactivity assessment results.

Site	Section	DPC Type	Degradation scenario	Min k_{eff}	Max k_{eff}	Min misload Δk_{eff} (pcm)	Max misload Δk_{eff} (pcm)	Max required NaCl (molal)
Braidwood	G.3	MPC-32	NA	0.9218	1.0064	671	3,221	0.4
Diablo Canyon	G.4	MPC-32	NA	0.9327	1.0402	306	2,014	0.9
Byron	G.5	MPC-32	NA	0.9301	0.9967	219	2,183	0.4
La Salle	G.6	MPC-68	NA	0.9014	0.9371	550	1,887	N/A
La Salle	G.6	MPC-68M	DB	1.1335	1.1692	190	612	1.7
North Anna	G.7	32PTH-DSC	NA	0.9067	0.9718	325	2,456	N/A
Sequoyah	G.8	MPC-32	NA	0.9457	1.0056	455	1,438	0.6
Sequoyah	G.8	MPC-37	DB	1.0413	1.1097	936	1,833	1.5
Surry	G.9	32PTH-DSC	NA	0.8916	0.9548	288	1,856	N/A
Callaway	G.10	MPC-37	DB	1.0346	1.1009	2,746	4,510	1.3
Watts Bar	G.11	MPC-37	DB	1.0393	1.1004	1578	2,459	1.3
Browns Ferry	G.12	MPC-89	DB	1.1342	1.1885	454	2,958	1.9

A summary of the direct disposal criticality calculations is provided in Table G-3. For this project, 929 canisters have been analyzed through FY21. Of the canisters analyzed, it was shown that 68% would remain subcritical under the loss-of-neutron-absorber scenario. When considering complete degradation of the baskets of canisters with non-stainless-steel structural components, 60% of the canisters are shown to be subcritical. When further considering the potential for the worst-case arrangement of the most reactive fuel assemblies in each canister, it is shown that 58% of canisters would remain subcritical. The percentages of the canisters shown to be subcritical has dropped relative to the FY20 results. The drop is largely the result the inclusion of results for Metamic-HT basket DPCs, which show very high reactivity as a result of the complete loss of basket structure. Because these canisters are the latest generation of DPC and represent a large fraction of DPCs entering service, this trend is expected to continue as additional DPCs are loaded.

Table G-3. Summary of the number of canisters meeting the subcritical limit.

Description (analysis dates: 2030–1,100,000)	Value
Total DPCs analyzed	929
Total DPCs below subcritical limit with loss of neutron absorber (design-basis loading)	0 (0%)
Total DPCs below subcritical limit with loss of neutron absorber (as-loaded)	634 (~68%)
Total DPCs below subcritical limit with loss of neutron absorber and carbon steel structures (as-loaded)	557 (~60%)
Total DPCs below subcritical limit with loss of neutron absorber and carbon steel structures (as-loaded) considering misload	544 (~58%)

G.14. REFERENCE

- G-1. M. W. Swinney, J. B. Clarity, K. Banerjee, and L. P. Miller, *Criticality Process, Modeling and Status for UNF-ST&DARDS*, FCRD-NFST-2015-000440, Rev. 3, US Department of Energy, Integrated Waste Management, February 2021.
- G-2. J. B. Clarity, K. Banerjee, and L. P. Miller, *Basket Modification Concepts for Disposal Reactivity Control of Dual Purpose Canisters*, ORNL/SPR-2021/1780, Oak Ridge National Laboratory, January 2021.
- G-3. E. H. Hardin and K. P. Donovan, *Options for Future Fuel/Basket Modifications for DPC Disposition*, SAND2020-6236R, Sandia National Laboratories, Albuquerque, NM, June 2020.
- G-4. J. B. Clarity, L.P. Miller, and K. Banerjee, *Optimization of Canister Loading Patterns in Dual Purpose Canisters for Criticality Suppression*, ORNL/SPR-2021/2035, Oak Ridge National Laboratory, June 2021.

APPENDIX H. FY 2022 Criticality Study

H.1. INTRODUCTION

This appendix documents work performed supporting the US Department of Energy (DOE) Office of Nuclear Energy (NE) Spent Fuel and Waste Disposition (SFWD) under work breakdown structure element 1.08.01.03.05, “Direct Disposal of Dual Purpose Canisters.” In particular, this appendix fulfills the M3 milestone, M3SF-22OR0103050810, “Update of DPC Direct Disposal Criticality Analysis Report” within work package SF-22OR01030508, “DPC Reactivity and Criticality Modeling - ORNL.”

This appendix presents the dual-purpose canister (DPC) criticality evaluations performed in FY 2022 to support the feasibility determination of direct disposal of DPCs and extends the work reported in the main body and preceding appendices of this report. The main objective of the FY 2022 DPC disposal criticality study was as follows:

- Analyze an additional 225 as-loaded canisters from 14 sites for the time interval between calendar years 2030 and 1,100,000 using the burnup credit methodology described in the previous sections of this report. The analyzed canisters are organized by site in Table H-1.

Table H-1. Summary of Sites Analyzed in FY22.

Site	DPC Type	Canisters Analyzed	Section
Clinton	MPC-89	6	H.2
Fermi	MPC-68	12	H.3
Saint Lucie	NUHOMS® 32PTH	10	H.4
McGuire	TSC-37	16	H.5
Palo Verde	TSC-24	48	H.6
Summer	MPC-37	4	H.7
Susquehanna	NUHOMS® 61BT and 61BTH Type 1	30	H.8
Brown’s Ferry	MPC-68	5	H.9
Fitzpatrick	MPC-68M	5	H.10
Waterford	MPC-32	14	H.11
Perry	MPC-68	13	H.12
Farley	MPC-32	24	H.13
Indian Point	MPC-32	18	H.14
Comanche Peak	MPC-32	20	H.15

Criticality analysis models were developed for the intact canister configuration applicable to normal conditions of transport and storage, as described in the main report. The models were then modified for degraded material configurations applicable to the canister repository timeframe specified in this report. The degraded material configurations assume two scenarios: (1) complete loss of the fixed neutron absorber (i.e., ^{10}B) without fuel basket geometry changes and (2) complete degradation and loss of basket

materials, including neutron absorber plates and aluminum and carbon steel basket components (e.g., insert plates and basket support discs). As in FY21, the investigation was performed for baskets composed entirely of Metamic-HT poison material whose degradation—and thus neutron absorber loss—leads to a significant increase in k_{eff} . The degraded material configurations were analyzed for 23 analysis dates between 2030 and 1,100,000 years.

As mentioned in the main report, neutron moderation by water must occur for a waste package to achieve criticality. However, the groundwater (or pore water) that may flood a breached DPC will contain various dissolved aqueous species. Seventeen species were studied, as described in the main report, and it was determined that Cl, Li, and B provide the maximum reduction in canister reactivity because of their large neutron absorption cross sections. However, available groundwater data indicate that chlorine (as chloride) is the only naturally abundant neutron-absorbing element in groundwater that can provide a significant reduction in reactivity; chlorine is available in most of the repository concepts under consideration in varying quantities. Analyses were performed to determine the chlorine requirement to suppress the reactivity of canisters that could form a critical configuration in a repository timeframe. The impact of chlorine (in terms of NaCl) concentration in groundwater on the reactivity of as-loaded DPCs exceeding a k_{eff} value of 0.98 was evaluated for calendar year 22,000.

H.2. CLINTON CRITICALITY CALCULATIONS

Post-closure disposal criticality calculations were performed as a function of decay time for the six spent nuclear fuel (SNF) canisters at the Clinton ISFSI. All six SNF canisters are MPC-89s. The MPC-89 basket is composed entirely of Metamic-HT, so for the MPC-89, the loss of neutron absorber is also the loss of the basket structure; therefore, only the DB condition is modeled. Figure H-1 shows results for the degraded basket (DB) scenario for 23 decay times within the time interval between calendar years 2030 and 1,100,000. The results in Figure H-1 show k_{eff} variation as a function of calendar year. The one sigma statistical uncertainty for all k_{eff} values is 0.0003 or less for all cases.

The k_{eff} values are predicted to vary from 1.1414 to 1.1718 for the MPC-89s under the DB scenario. For canisters that had k_{eff} values greater than 0.98 under the degraded basket scenario, calculations were performed in which the pure water was replaced with groundwater compositions of various NaCl concentrations, and the models thus modified were used to determine k_{eff} as a function of NaCl concentration for the calendar year 22,000 (most reactive date). Figure H-2 presents k_{eff} variation as a function of NaCl concentration for those six canisters. Analysis of the results presented in Figure H-2 clearly shows that 1.7 mol NaCl/ kg H₂O is sufficient to demonstrate subcriticality ($k_{eff} < 0.98$) for all Clinton canisters. In this context, it is also important to note that a saturated NaCl brine has a concentration of approximately 6 molal.

Figure H-3 shows the k_{eff} increase between the worst-misload scenario and the as-loaded configuration for the six analyzed Clinton canisters at the calendar year 22,000. The increase in k_{eff} varies between 106 and 299 pcm for Clinton canisters.

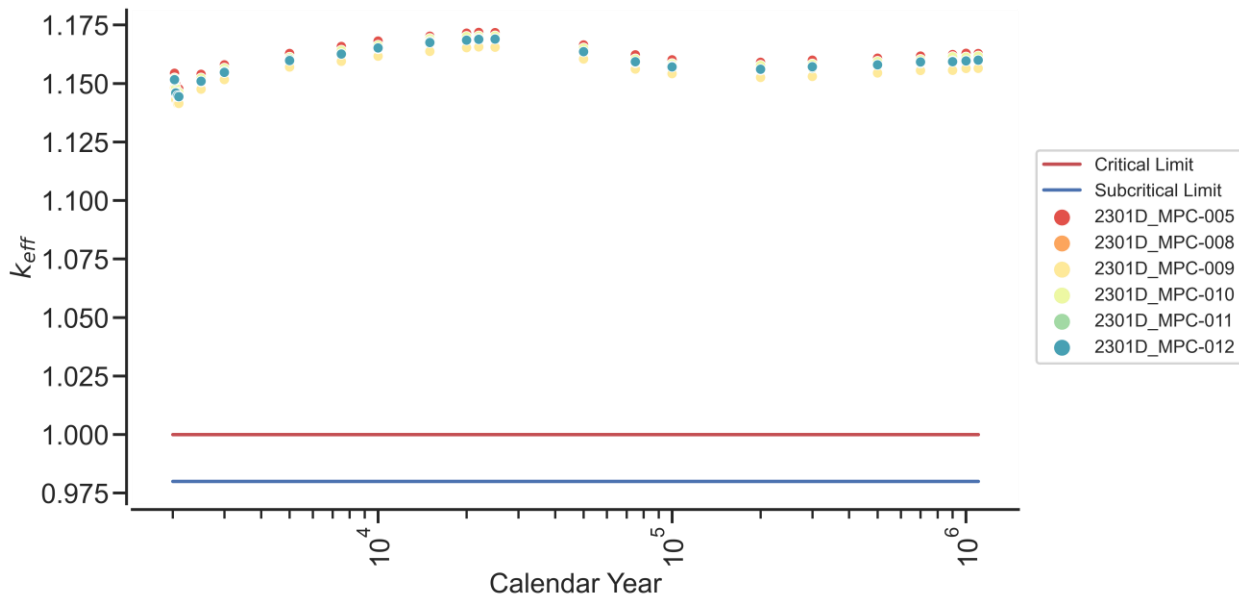


Figure H-1. k_{eff} vs. calendar year for the loss-of-neutron-absorber scenario based on actual loading and disposal isotopes for the SNF canisters at Clinton.

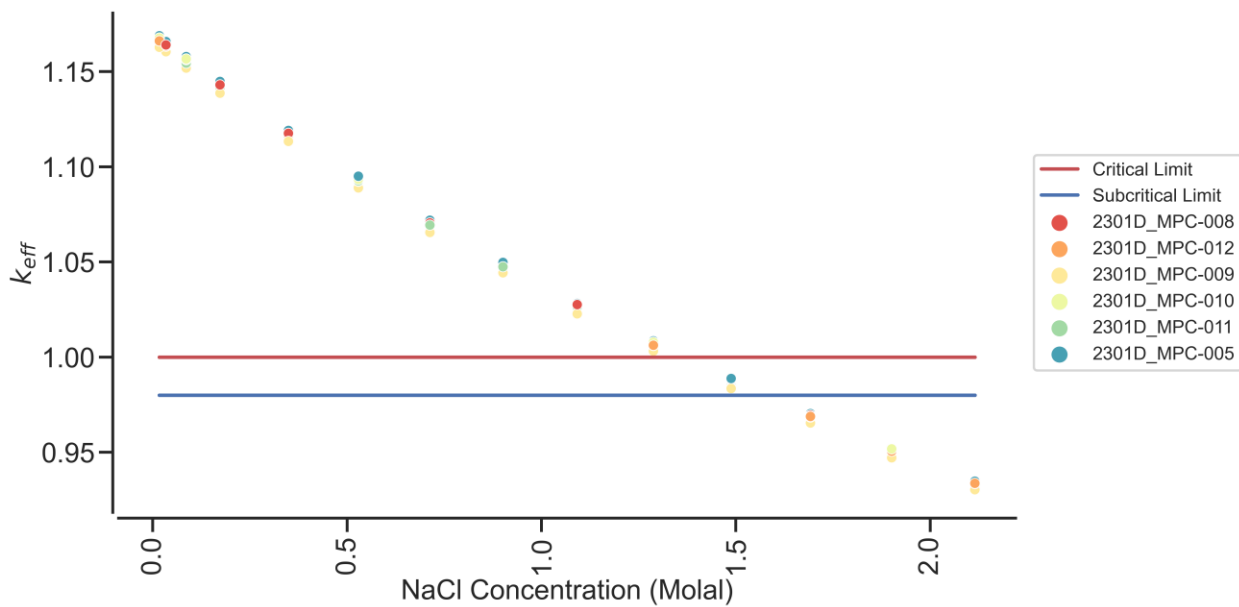


Figure H-2. k_{eff} vs. NaCl concentration for the DPCs with $k_{eff} > 0.98$ for the canisters at Clinton under the loss-of-neutron-absorber scenario (calendar year 22,000).

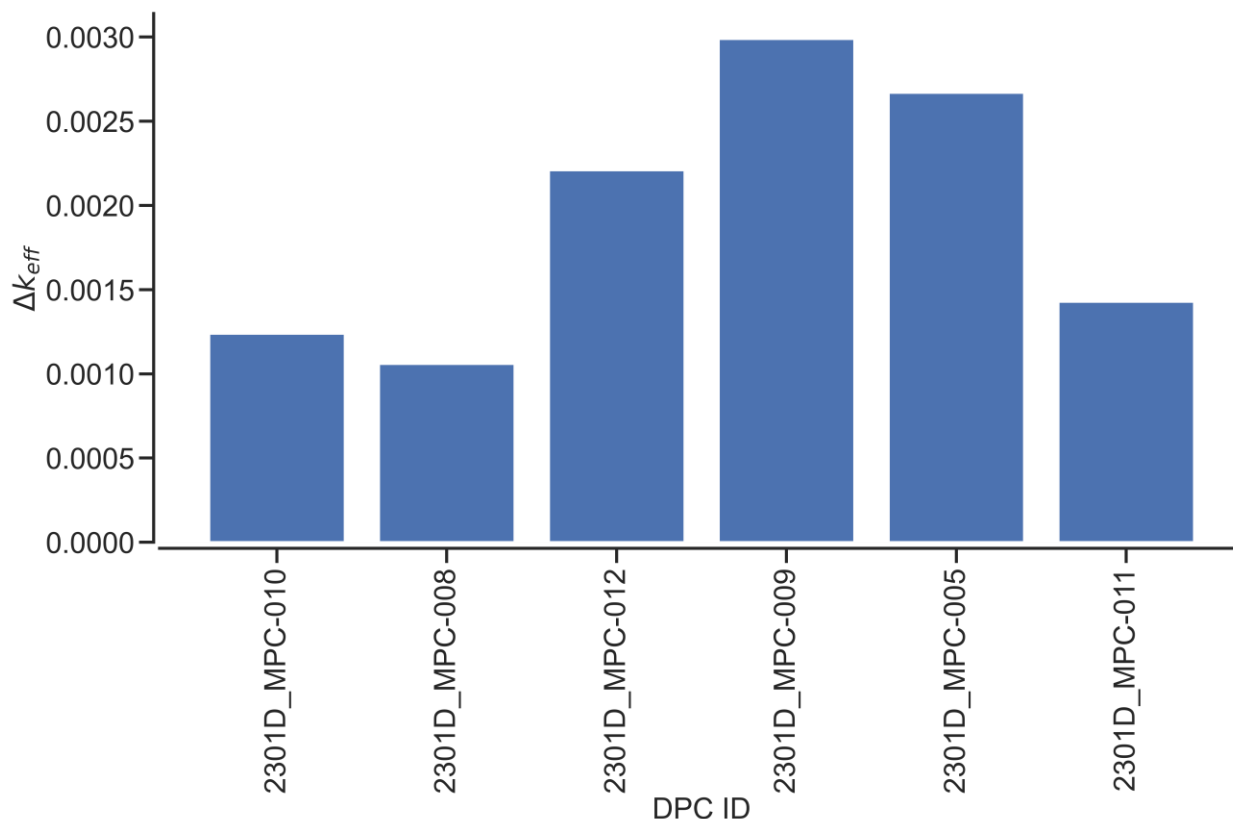


Figure H-3. k_{eff} increase between the worst-misload scenario and the as-loaded configuration for the MPC-89s at Clinton (calendar year 22,000).

H.3. FERMI CRITICALITY CALCULATIONS

Post-closure disposal criticality calculations were performed as a function of decay time for the 12 SNF canisters at the Fermi ISFSI. All 12 SNF canisters are MPC-68s. The MPC-68 contains no carbon steel structural components, so only the loss-of-neutron-absorber scenario is analyzed. Figure H-4 shows results for the loss-of-neutron-absorber scenario for 23 decay times within the time interval between calendar years 2030 and 1,100,000. The results in Figure H-4 show k_{eff} variation as a function of calendar year. The one sigma statistical uncertainty for all k_{eff} values is 0.0003 or less for all cases.

The k_{eff} values are predicted to vary from 0.9031 to 0.9337 for the MPC-68s under the loss-of-absorber scenario. No canisters had k_{eff} values greater than 0.98 under the loss-of-neutron-absorber scenario, and thus no calculations were performed in which the pure water was replaced with groundwater compositions of various NaCl concentrations.

Figure H-5 shows the k_{eff} increase between the worst-misload scenario and the as-loaded configuration for the 12 analyzed Fermi canisters at the calendar year 22,000. The increase in k_{eff} varies between 247 and 1,389 pcm for Fermi canisters.

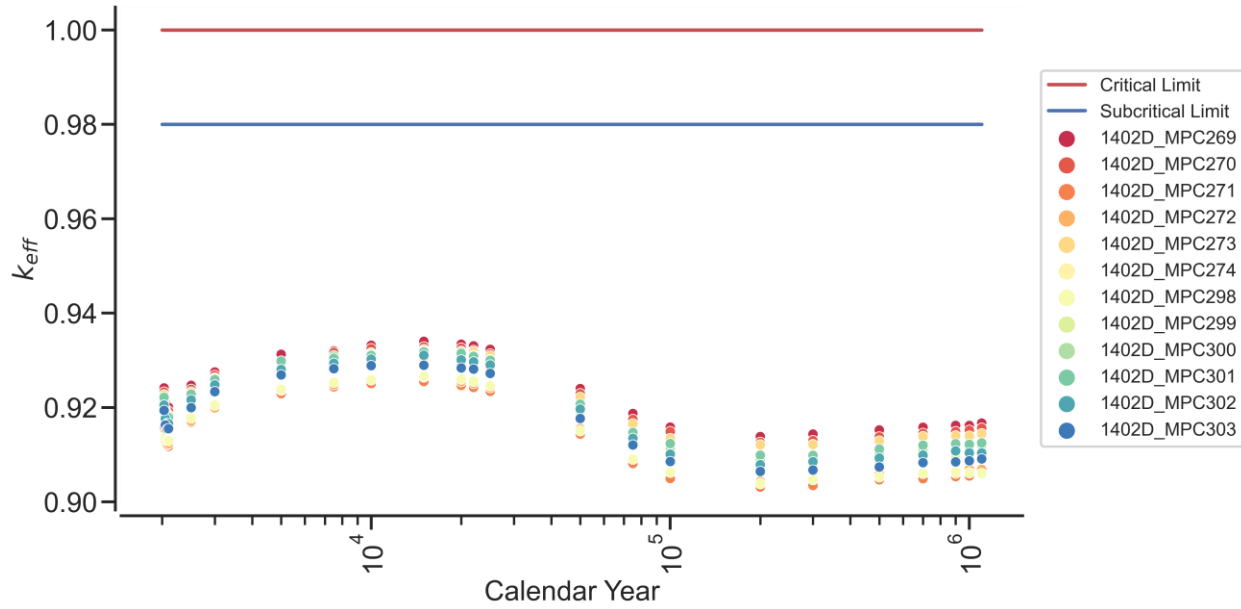


Figure H-4. k_{eff} vs. calendar year for the loss-of-neutron-absorber scenario based on actual loading and disposal isotopes for the SNF canisters at Fermi.

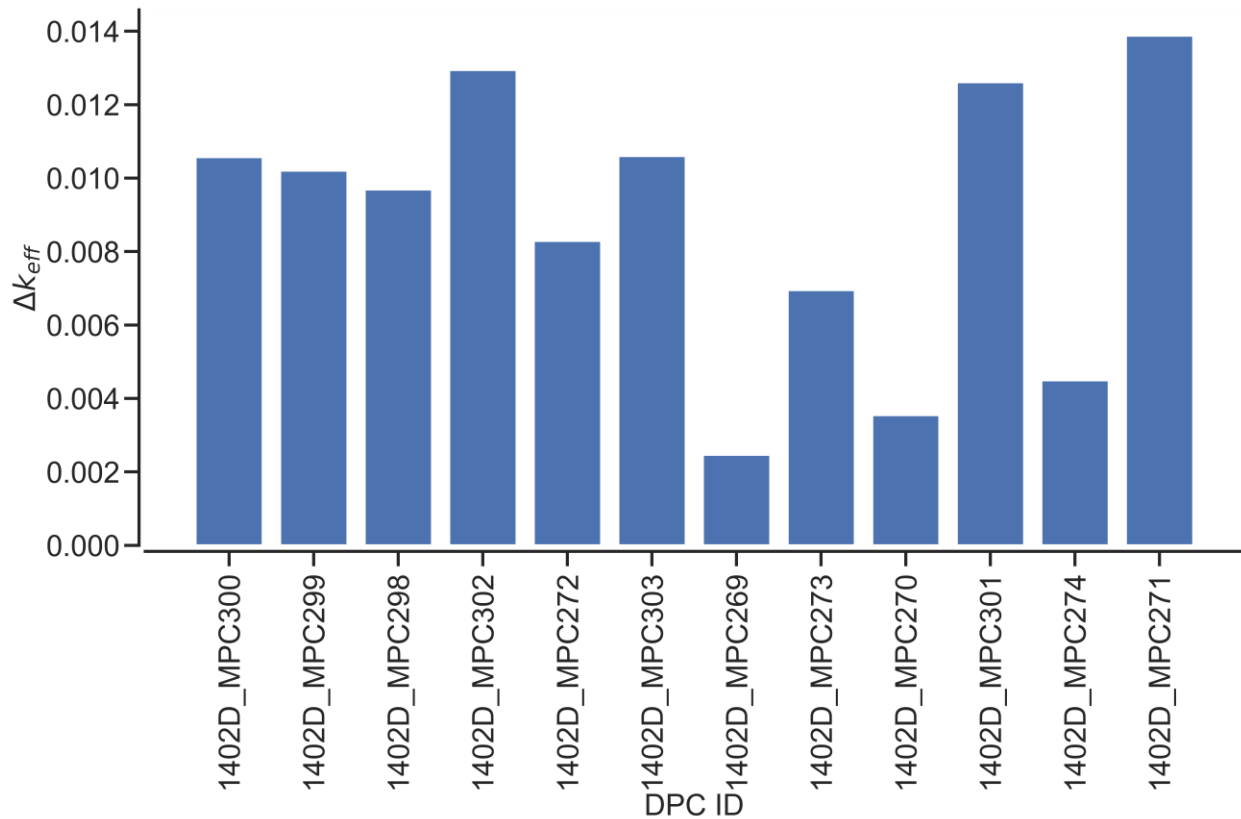


Figure H-5. k_{eff} increase between the worst-misload scenario and the as-loaded configuration for the MPC-68s at Fermi (calendar year 22,000).

H.4. SAINT LUCIE CRITICALITY CALCULATIONS

Post-closure disposal criticality calculations were performed as a function of decay time for the 10 SNF canisters at the Saint Lucie ISFSI. All 10 SNF canisters are NUHOMS® 32PTHs. The NUHOMS® 32PTH does not contain any carbon steel structural components, so only the loss-of-neutron-absorber scenario is analyzed. Figure H-6 shows results for the loss-of-neutron-absorber scenario for 23 decay times within the time interval between calendar years 2030 and 1,100,000. The results in Figure H-6 show k_{eff} variation as a function of calendar year. The one sigma statistical uncertainty for all k_{eff} values is 0.0003 or less for all cases.

The k_{eff} values are predicted to vary from 0.8232 to 0.9212 for the NUHOMS® 32PTHs under the loss-of-absorber scenario. No canisters had k_{eff} values greater than 0.98 under the loss-of-neutron-absorber scenario, and thus no calculations were performed in which the pure water was replaced with groundwater compositions of various NaCl concentrations.

Figure H-7 shows the k_{eff} increase between the worst-misload scenario and the as-loaded configuration for the 10 analyzed Saint Lucie canisters at the calendar year 22,000. The increase in k_{eff} varies between 178 and 2,371 pcm for Saint Lucie canisters.

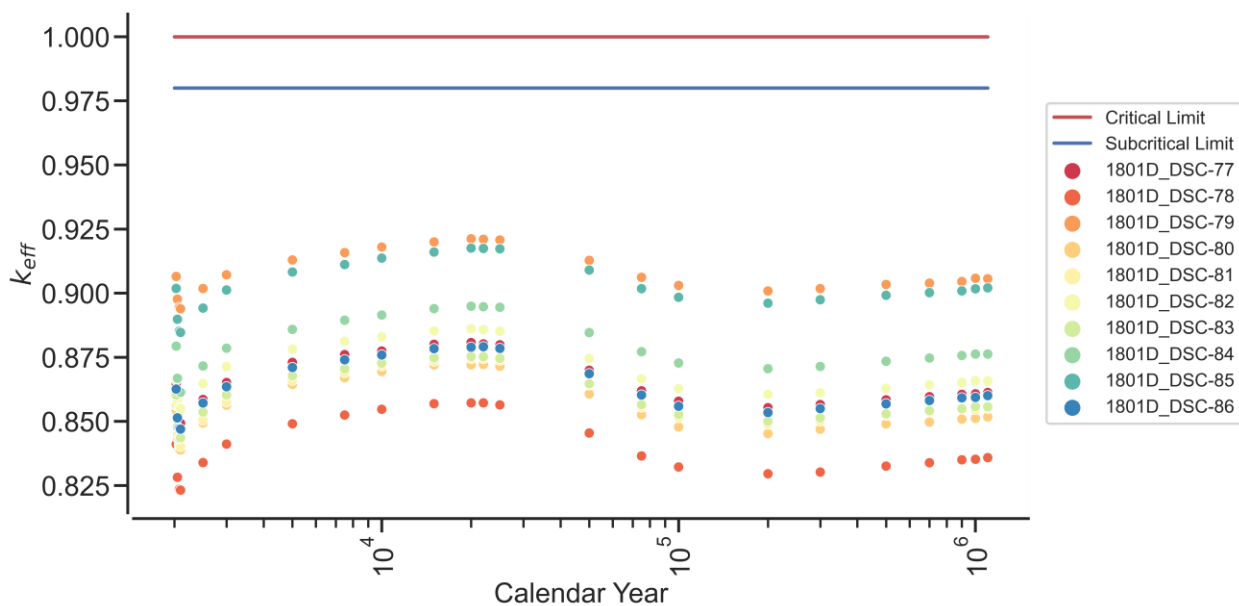


Figure H-6. k_{eff} vs. calendar year for the loss-of-neutron-absorber scenario based on actual loading and disposal isotopes for the SNF canisters at Saint Lucie.

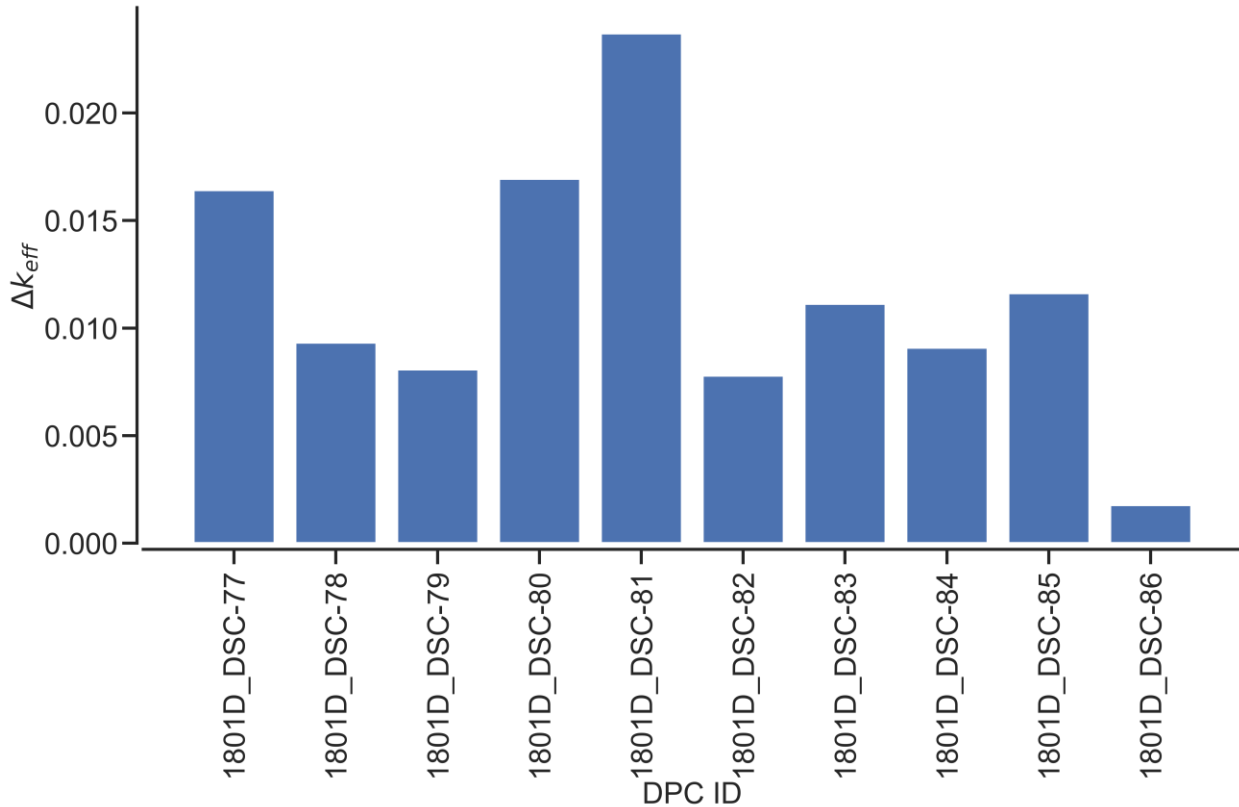


Figure H-7. k_{eff} increase between the worst-misload scenario and the as-loaded configuration for the NUHOMS® 32PTHs at Saint Lucie (calendar year 22,000).

H.5. MCGUIRE CRITICALITY CALCULATIONS

Post-closure disposal criticality calculations were performed as a function of decay time for the 16 SNF canisters at the McGuire independent spent fuel storage installation (ISFSI). All 16 SNF canisters are TSC-37s. The TSC-37 contains carbon steel or aluminum structural components, so the loss-of-neutron-absorber scenario is analyzed, and the DB condition is modeled. Figure H-8 shows results for the loss-of-neutron-absorber scenario for 23 decay times within the time interval between calendar years 2030 and 1,100,000. The results in Figure H-8 show k_{eff} variation as a function of calendar year. Figure H-9 shows results for the DB scenario for 23 decay times within the time interval between calendar years 2030 and 1,100,000. The results in Figure H-9 show k_{eff} variation as a function of calendar year. The one sigma statistical uncertainty for all k_{eff} values is 0.0003 or less for all cases.

The k_{eff} values are predicted to vary from 0.9386 to 1.0065 for the TSC-37s under the loss-of-absorber scenario, and they are predicted to vary from 1.0135 to 1.0871 under the DB scenario. All canisters had k_{eff} values greater than 0.98 under the loss-of-neutron-absorber scenario, and all 16 TSC-37 canisters under the DB scenario were above 0.98; thus, calculations were performed for TSC-37 canisters in which the pure water was replaced with groundwater compositions of various NaCl concentrations. Models thus modified were used to determine k_{eff} as a function of NaCl concentration for the calendar year 22,000 (most reactive DB date) and 22,000 (most reactive NA date). Figure H-10 and Figure H-11 present k_{eff} variation as a function of NaCl concentration for those 16 canisters. As the results presented in Figure H-10 and Figure H-11 show, 1.1 mol NaCl/ kg H₂O is sufficient to demonstrate subcriticality ($k_{eff} < 0.98$) for all McGuire canisters, with 0.4 mol NaCl/ kg H₂O sufficient for the NA condition. In this context, it is also important to note that a saturated NaCl brine has a concentration of approximately 6 molal.

Figure H-12 shows the k_{eff} increase between the worst-misload scenario and the as-loaded configuration for the 16 analyzed McGuire TSC-37 canisters for calendar year 22,000 (most reactive NA date). Figure H-13 shows the k_{eff} increase between the worst-misload scenario and the as-loaded configuration for the 16 analyzed McGuire TSC-37 canisters for calendar year 22,000 (most reactive DB date). The increase in k_{eff} varies between 657 and 1,874 pcm for McGuire TSC-37 canisters with the loss-of-neutron-absorber scenario, and it varies between 713 and 1,984 pcm for McGuire TSC-37 canisters with the DB scenario.

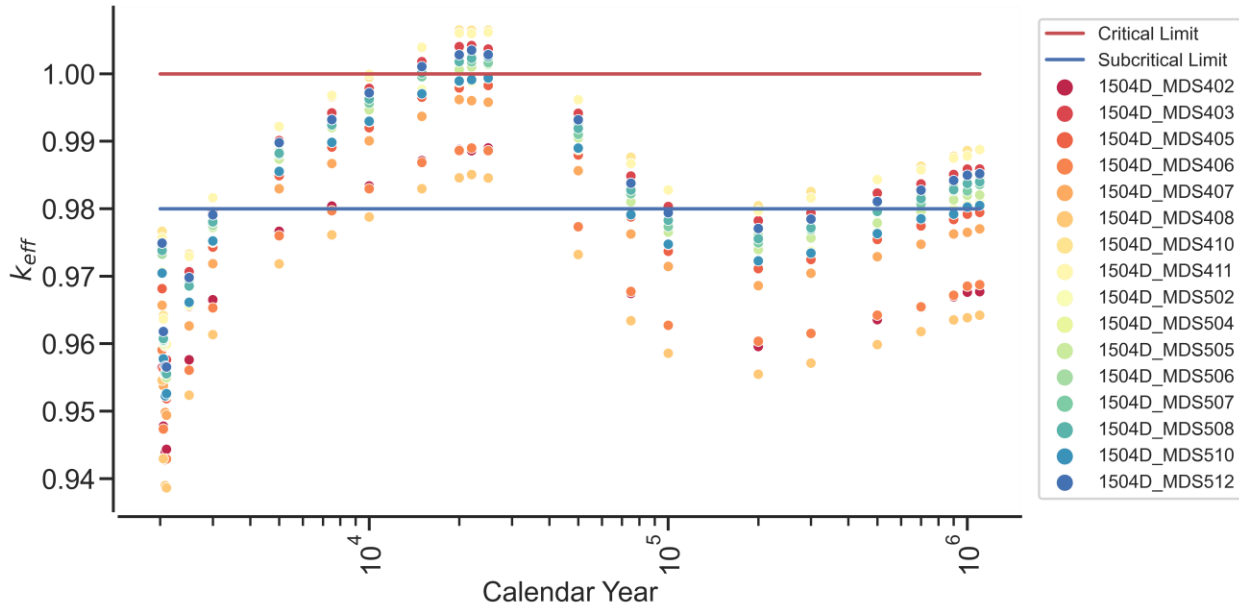


Figure H-8. k_{eff} vs. calendar year for the loss-of-neutron-absorber scenario based on actual loading and disposal isotopes for the TSC-37 SNF canisters at McGuire.

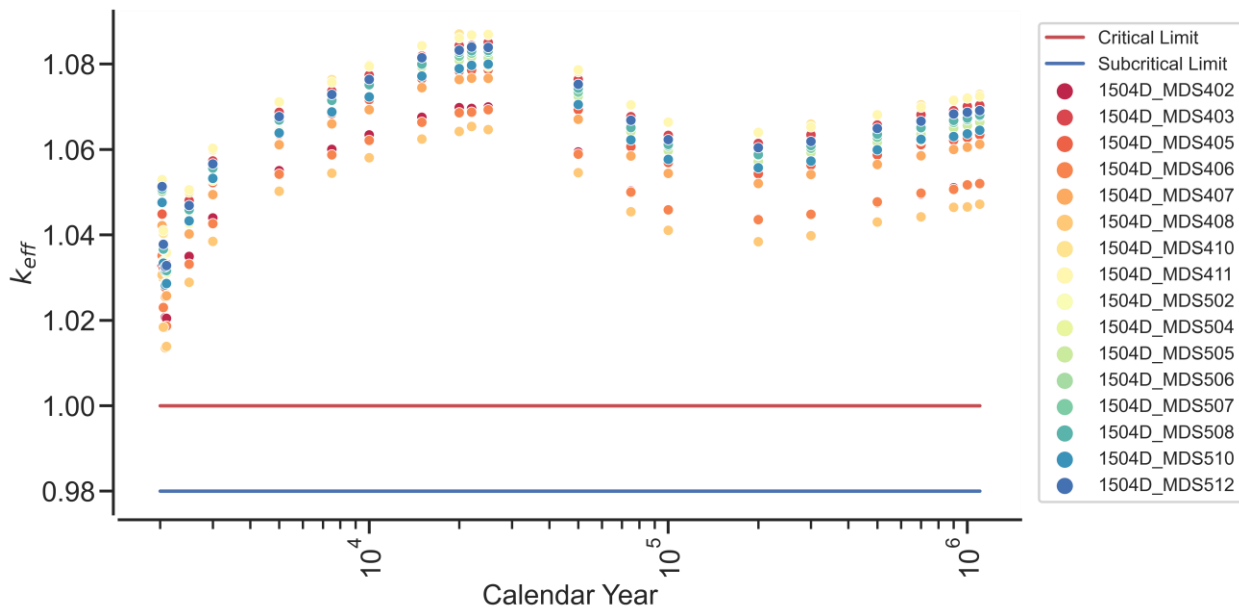


Figure H-9. k_{eff} vs. calendar year for the DB scenario based on actual loading and disposal isotopes for the TSC-37 SNF canisters at McGuire.

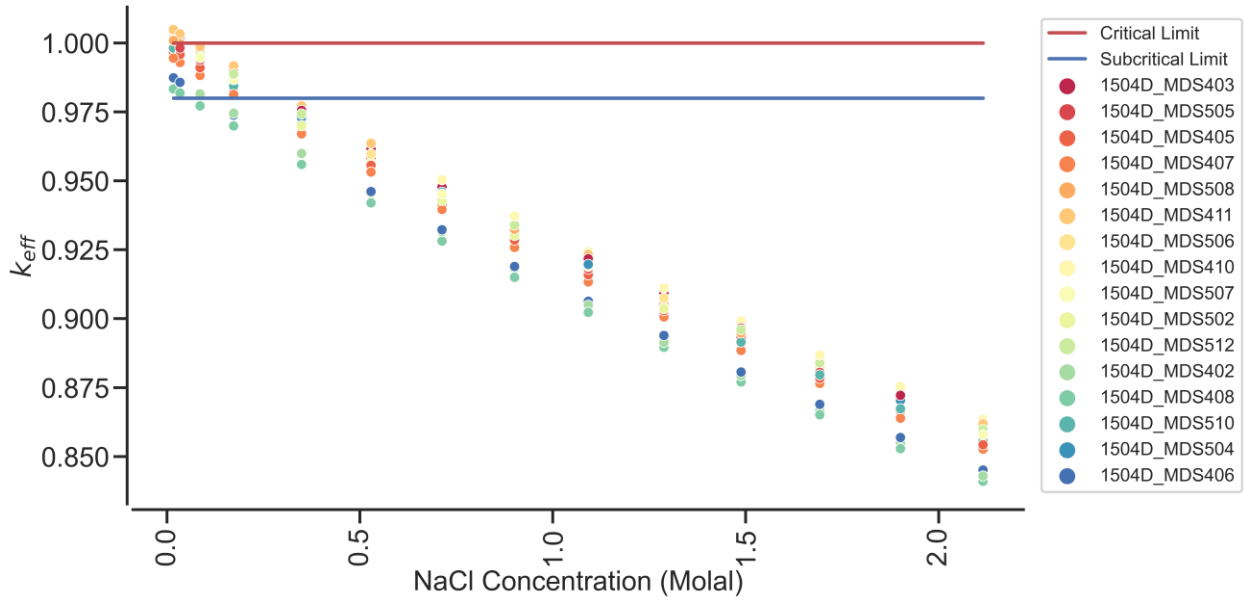


Figure H-10. k_{eff} vs. NaCl concentration for the DPCs with $k_{eff} > 0.98$ for the canisters analyzed in 2022 at McGuire under the NA scenario (calendar year 22,000).

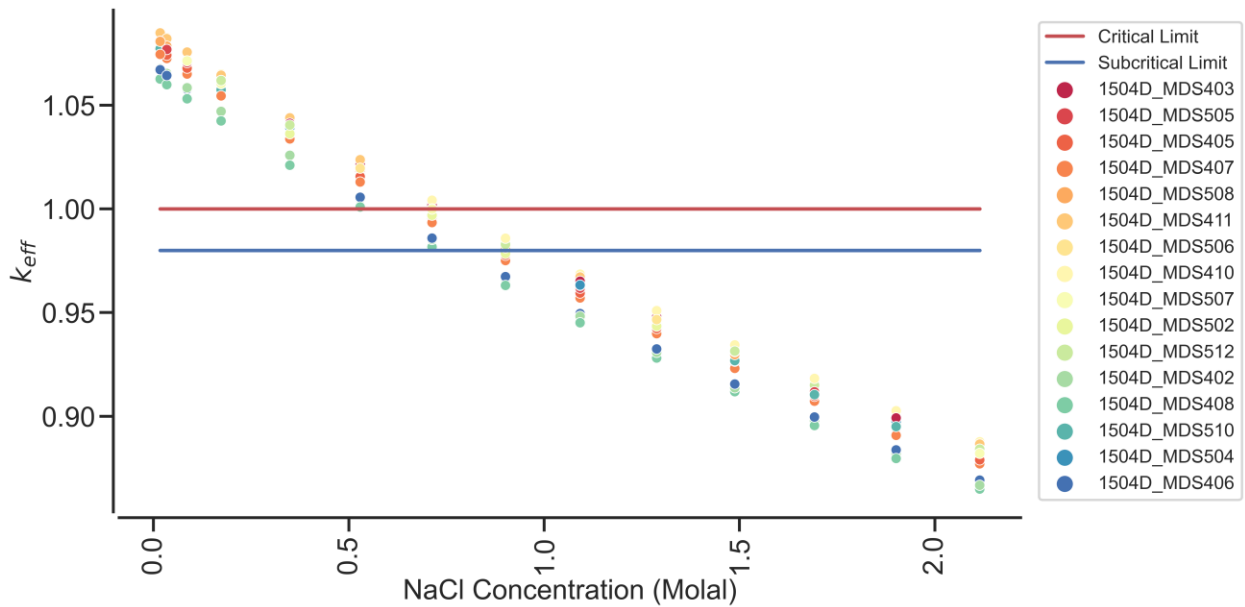


Figure H-11. k_{eff} vs. NaCl concentration for the DPCs with $k_{eff} > 0.98$ for the canisters analyzed in 2022 at McGuire under the DB scenario (calendar year 22,000).

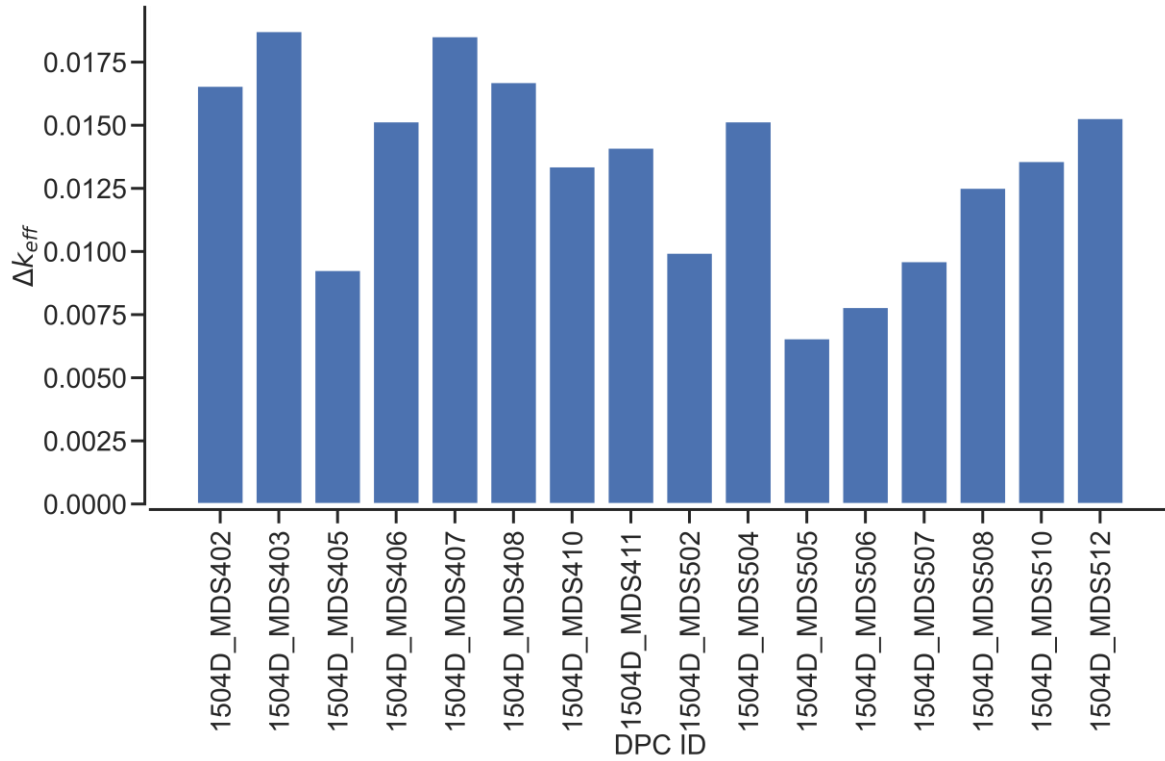


Figure H-12. k_{eff} increase between the NA worst-misload scenario and the as-loaded configuration for the TSC-37s at McGuire (calendar year 22,000).

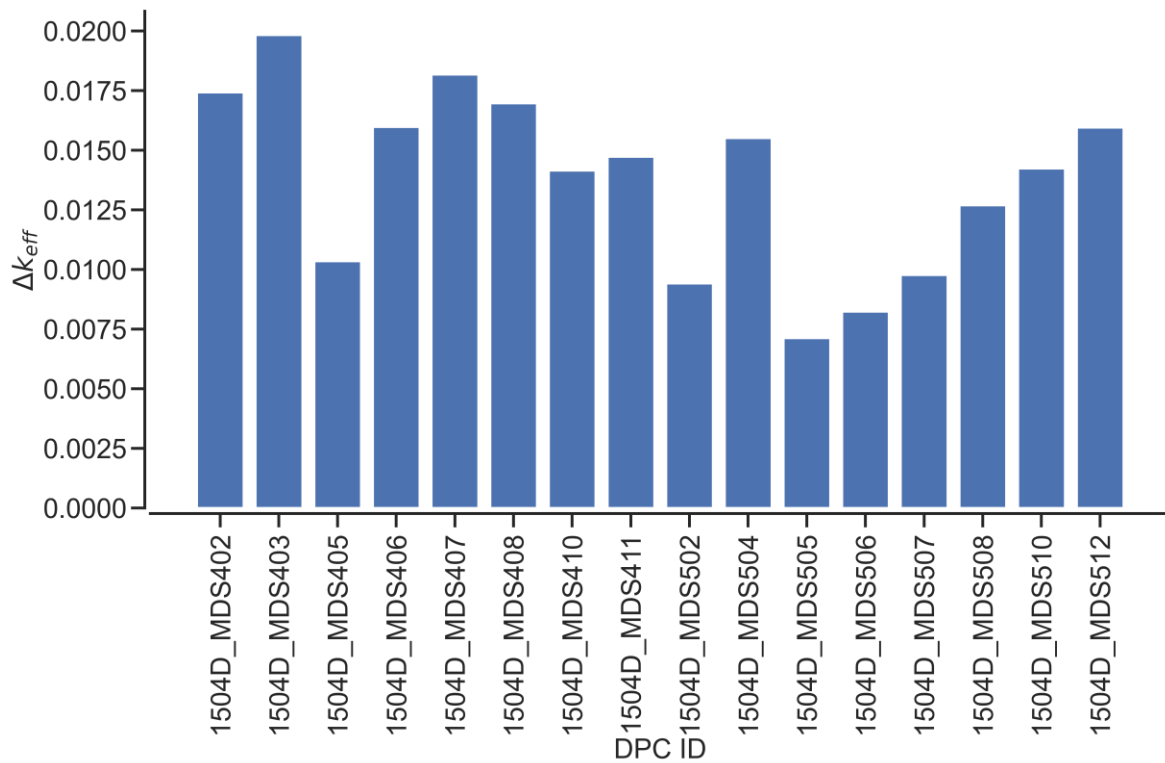


Figure H-13. k_{eff} increase between the DB worst-misload scenario and the as-loaded configuration for the TSC-37s at McGuire (calendar year 22,000).

H.6. PALO VERDE CRITICALITY CALCULATIONS

Post-closure disposal criticality calculations were performed as a function of decay time for the 48 SNF canisters at the Palo Verde ISFSI. All 48 canisters are TSC-24s. The TSC-24s contain no carbon steel structural components, so only the loss-of-neutron-absorber scenario was analyzed. Figure H-14 shows the results for the TSC-24 loss-of-neutron-absorber scenario for 23 decay times within the time interval between calendar years 2030 and 1,100,000. The results in Figure H-14 show k_{eff} variation as a function of calendar year. The one sigma statistical uncertainty for all k_{eff} values is 0.0003 or less for all cases.

The k_{eff} values are predicted to vary from 0.8072 to 0.8624 for the TSC-24s under the loss-of-absorber scenario. No canisters had k_{eff} values greater than 0.98 under the loss-of-neutron-absorber scenario, and thus no calculations were performed in which the pure water was replaced with groundwater compositions of various NaCl concentrations.

Figure H-15 shows the k_{eff} increase between the worst-misload scenario and the as-loaded configuration for the 48 analyzed Palo Verde TSC-24 canisters at the calendar year 22,000. The increase in k_{eff} varies between 442 and 3,835 pcm for TSC-24 Palo Verde canisters.

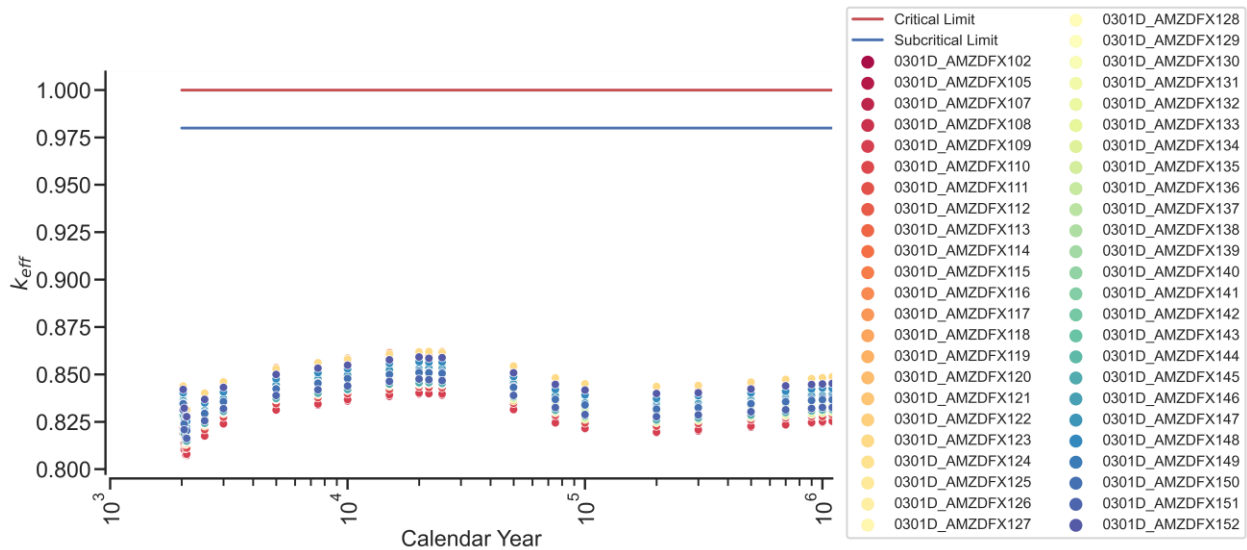


Figure H-14. k_{eff} vs. calendar year for the loss-of-neutron-absorber scenario based on actual loading and disposal isotopes for the TSC-24 SNF canisters at Palo Verde.

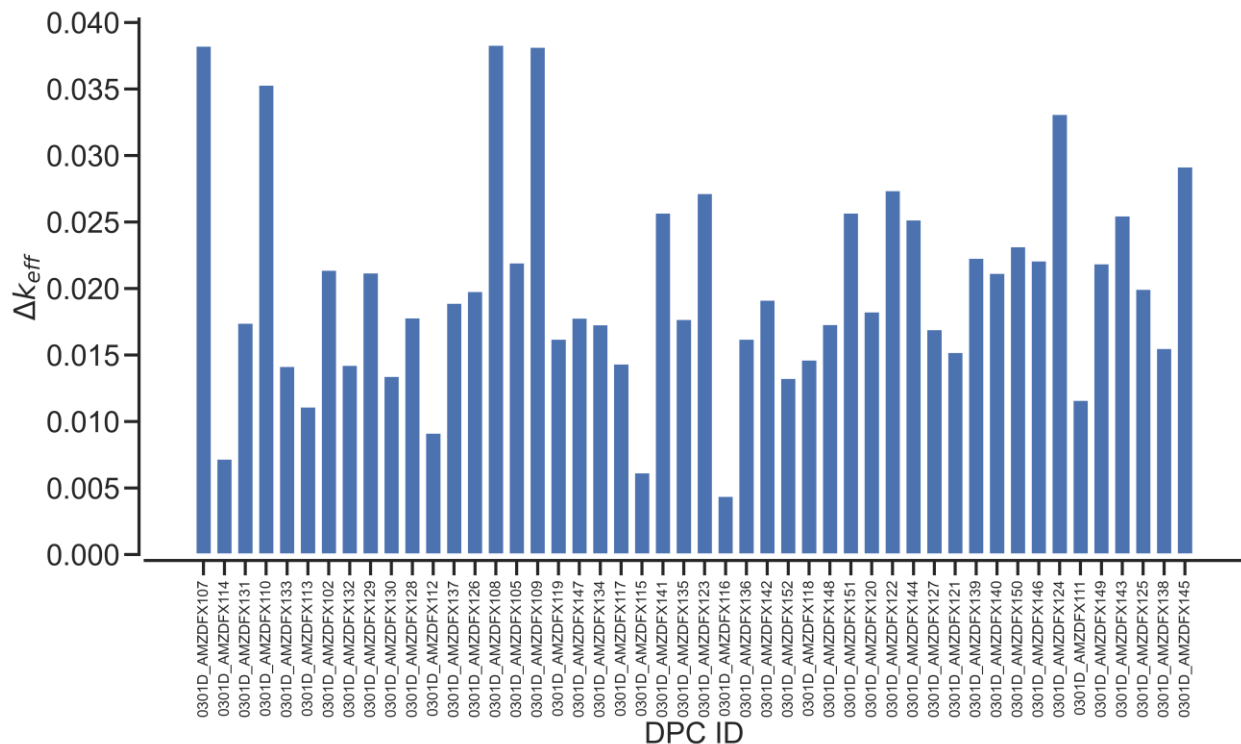


Figure H-15. k_{eff} increase between the worst-misload scenario and the as-loaded configuration for the TSC-24s at Palo Verde (calendar year 22,000).

H.7. SUMMER CRITICALITY CALCULATIONS

Post-closure disposal criticality calculations were performed as a function of decay time for the four SNF canisters at the Summer ISFSI. All four SNF canisters are MPC-37s. The MPC-37 basket is composed entirely of Metamic-HT, so for the MPC-37, the loss of neutron absorber is also the loss of the basket structure; therefore, only the DB condition is modeled. Figure H-16 shows the results for the DB scenario for 23 decay times within the time interval between calendar years 2030 and 1,100,000. The results in Figure H-16 show k_{eff} variation as a function of calendar year. The one sigma statistical uncertainty for all k_{eff} values is 0.0003 or less for all cases.

The k_{eff} values are predicted to vary from 1.0380 to 1.0935 for the MPC-37s under the DB scenario. For canisters that had k_{eff} values greater than 0.98 under the DB scenario, calculations were performed in which the pure water was replaced with groundwater compositions of various NaCl concentrations, and the models thus modified were used to determine k_{eff} as a function of NaCl concentration for the calendar year 22,000 (most reactive date). Figure H-17 presents k_{eff} variation as a function of NaCl concentration for those four canisters. As the results presented in Figure H-17 show, 1.1 mol NaCl/ kg H₂O is sufficient to demonstrate subcriticality ($k_{eff} < 0.98$) for all Summer canisters. In this context, it is also important to note that a saturated NaCl brine has a concentration of approximately 6 molal.

Figure H-18 shows the k_{eff} increase between the worst-misload scenario and the as-loaded configuration for the 4 analyzed Summer canisters at the calendar year 22,000. The increase in k_{eff} varies between 779 and 2,441 pcm for Summer canisters.

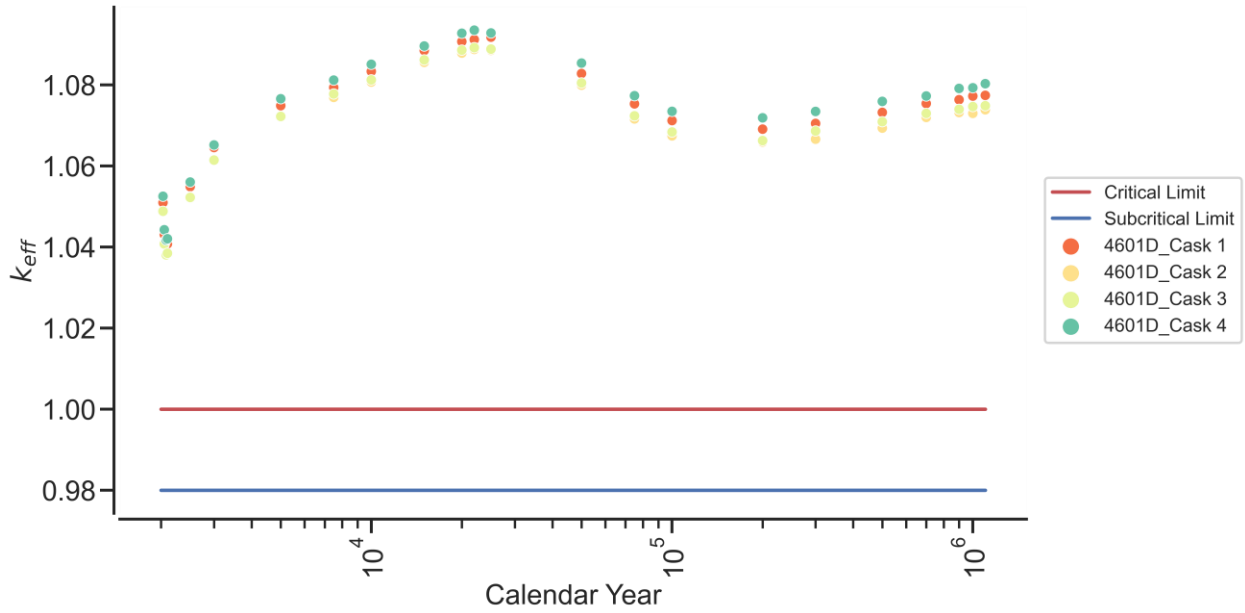


Figure H-16. k_{eff} vs. calendar year for the DB scenario based on actual loading and disposal isotopes for the SNF canisters at Summer.

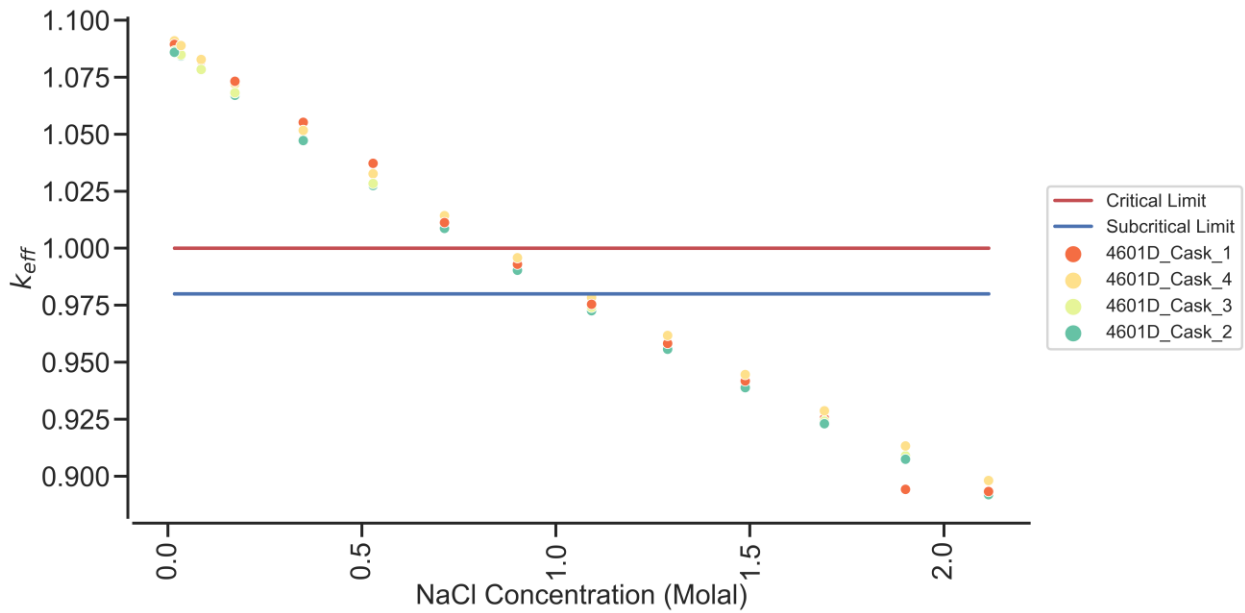


Figure H-17. k_{eff} vs. NaCl concentration for the DPCs with $k_{eff} > 0.98$ for the canisters analyzed at Summer under the DB scenario (calendar year 22,000).

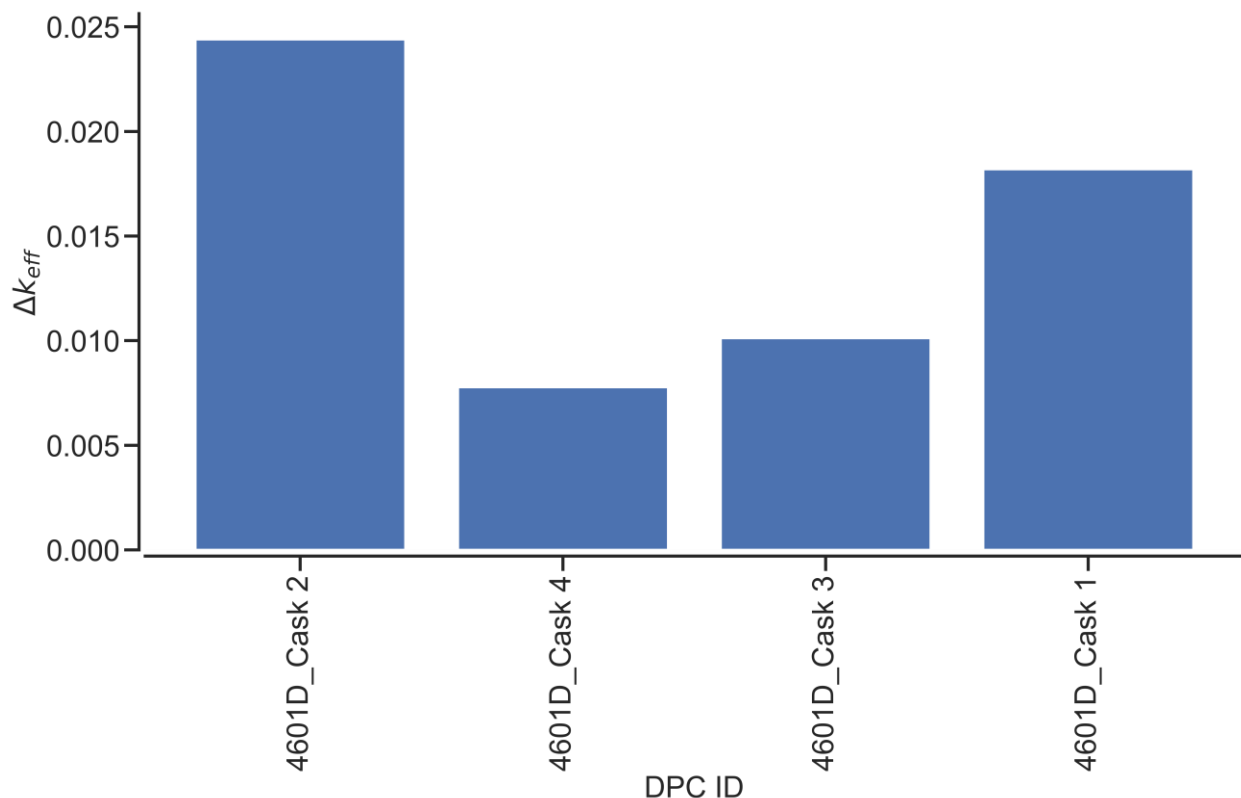


Figure H-18. k_{eff} increase between the worst-misload scenario and the as-loaded configuration for the MPC-37s at Summer (calendar year 22,000).

H.8. SUSQUEHANNA CRITICALITY CALCULATIONS

Post-closure disposal criticality calculations were performed as a function of decay time for the 30 SNF canisters at the Susquehanna ISFSI. Four of the 30 SNF canisters are NUHOMS[®] 61BT, whereas the remaining 26 are NUHOMS[®] 61BTH Type 1. Both the NUHOMS[®] 61BT and NUHOMS[®] 61BTH Type 1 contain no carbon steel structural components, so only the loss of neutron absorber is modeled. Figure H-19 shows results for the NA scenario for 23 decay times within the time interval between calendar years 2030 and 1,100,000. The results in Figure H-19 show k_{eff} variation as a function of calendar year for the NUHOMS[®] 61BT canisters and NUHOMS[®] 61BTH Type 1 canisters. The one sigma statistical uncertainty for all k_{eff} values is 0.0003 or less for all cases.

The k_{eff} values are predicted to vary from 0.8433 to 0.9541 for the NUHOMS[®] 61BTH Type 1s under the NA scenario, and from 0.9122 to 0.9387 for the NUHOMS[®] 61BTs. No canisters had k_{eff} values greater than 0.98 under the loss-of-neutron-absorber scenario, and thus no calculations were performed in which the pure water was replaced with groundwater compositions of various NaCl concentrations.

Figure H-20 shows the k_{eff} increase between the worst-misload scenario and the as-loaded configuration for the 30 analyzed Susquehanna canisters at the calendar year 22,000. The increase in k_{eff} varies between 126 and 2,684 pcm for NUHOMS[®] 61BTH Type 1 Susquehanna canisters and between 1,238 and 1,720 pcm for NUHOMS[®] 61BT canisters.

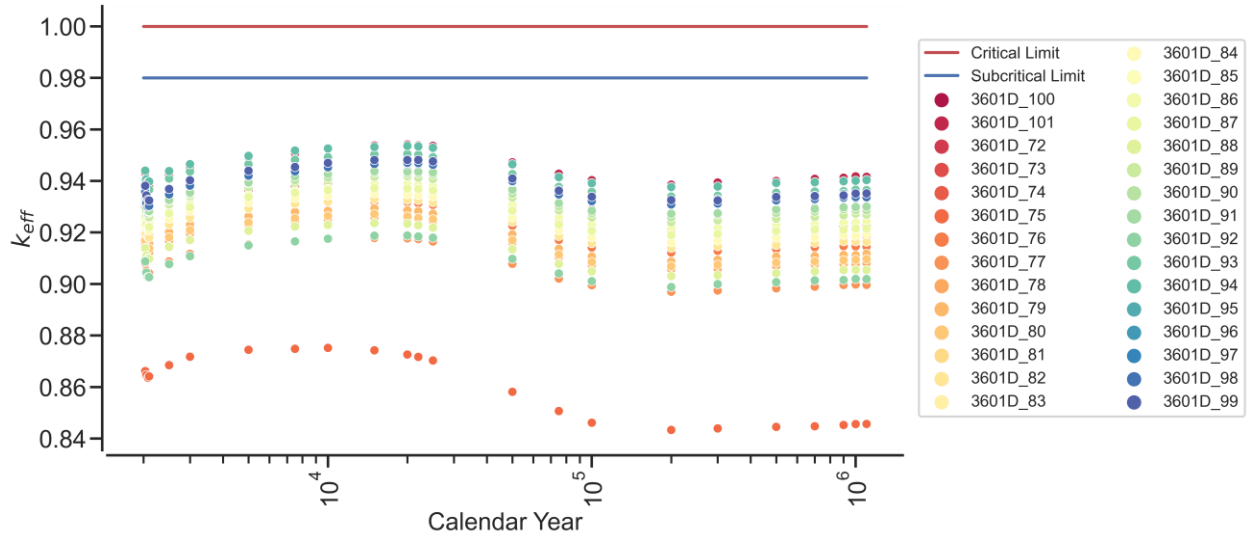


Figure H-19. k_{eff} vs. calendar year for the loss-of-neutron-absorber scenario based on actual loading and disposal isotopes for the NUHOMS[®] canisters at Susquehanna.

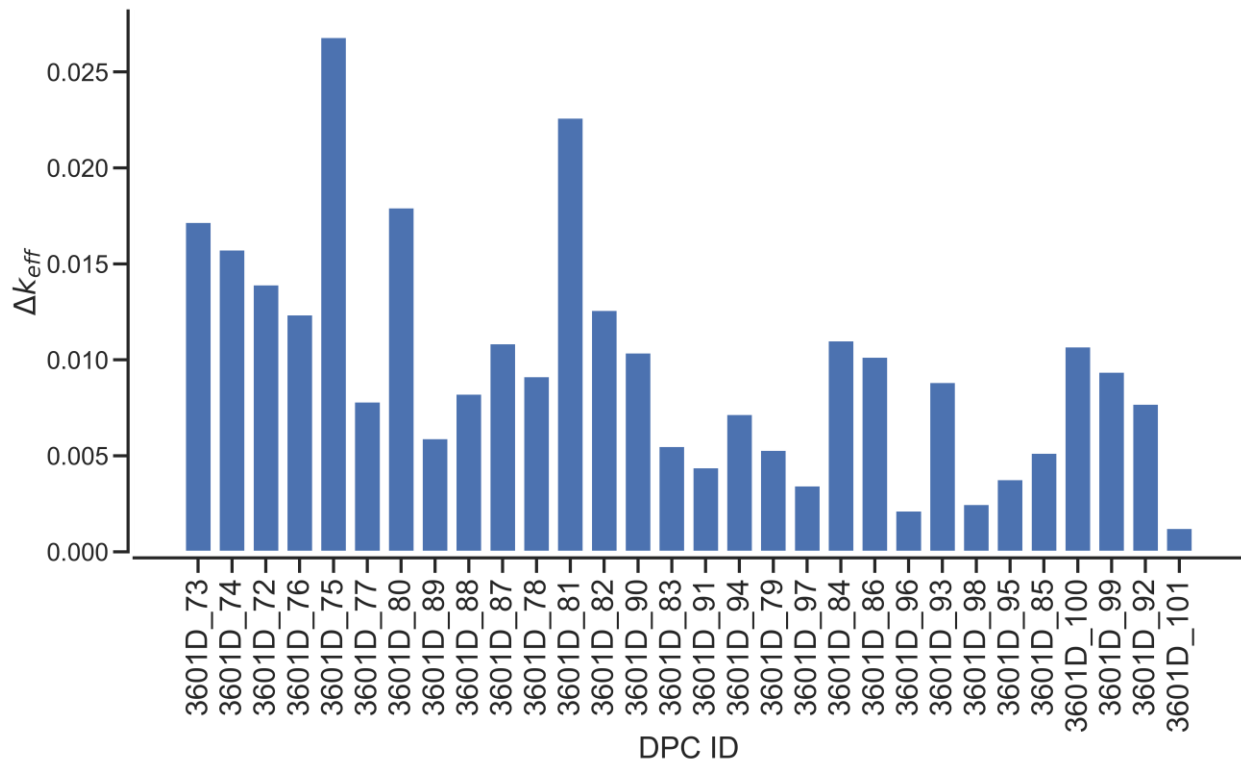


Figure H-20. k_{eff} increase between the worst-misload scenario and the as-loaded configuration for the NUHOMS[®] canisters at Susquehanna (calendar year 22,000).

H.9. BROWN’S FERRY CRITICALITY CALCULATIONS

Post-closure disposal criticality calculations were performed as a function of decay time for the five SNF canisters at the Brown’s Ferry ISFSI. All five SNF canisters are MPC-68s. The MPC-68 contains no carbon steel structural components, so only the loss-of-neutron-absorber scenario is analyzed. Figure H-21 shows results for the NA scenario for 23 decay times within the time interval between calendar years 2030 and 1,100,000. The results in Figure H-21 show k_{eff} variation as a function of calendar year. The one sigma statistical uncertainty for all k_{eff} values is 0.0003 or less for all cases.

The k_{eff} values are predicted to vary from 0.8929 to 0.9191 for the MPC-68s under the NA scenario. No canisters had k_{eff} values greater than 0.98 under the NA scenario, and thus no calculations were performed in which the pure water was replaced with groundwater compositions of various NaCl concentrations.

Figure H-22 shows the k_{eff} increase between the worst-misload scenario and the as-loaded configuration for the 5 analyzed Brown’s Ferry canisters at the calendar year 22,000. The increase in k_{eff} varies between 1,036 and 1,354 pcm for the Brown’s Ferry canisters.

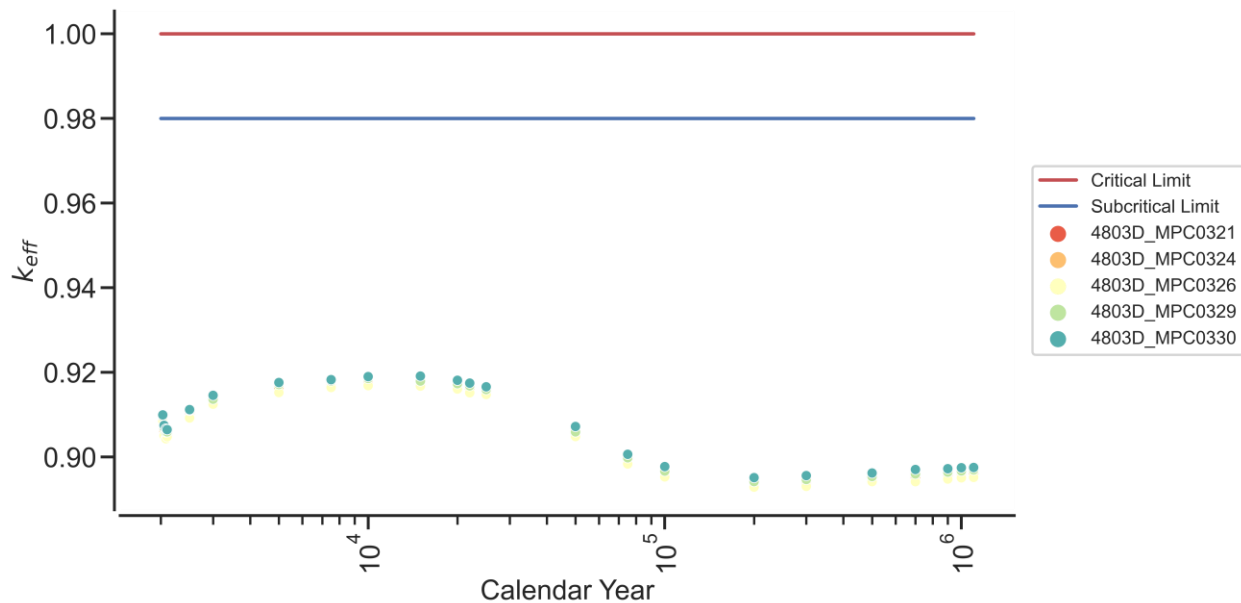


Figure H-21. k_{eff} vs. calendar year for the NA scenario based on actual loading and disposal isotopes for the SNF canisters at Brown’s Ferry.

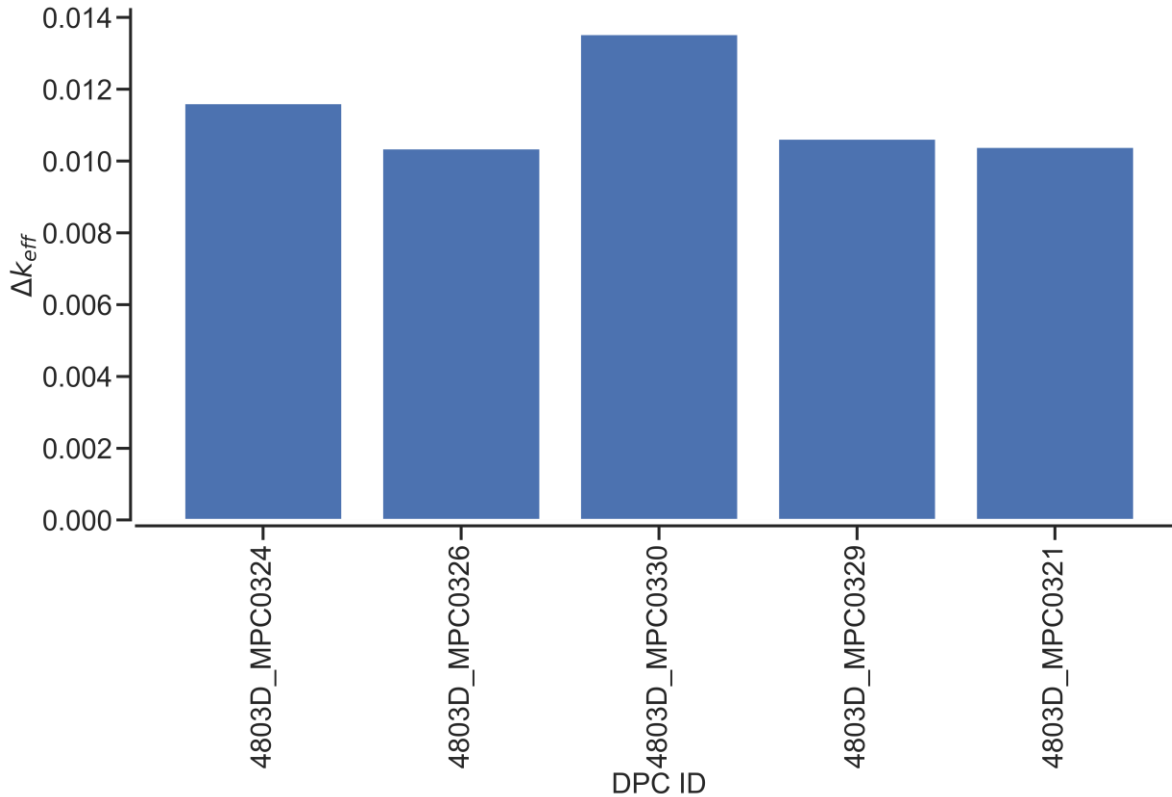


Figure H-22. k_{eff} increase between the worst-misload scenario and the as-loaded configuration for the MPC-68s at Browns Ferry (calendar year 22,000).

H.10. FITZPATRICK CRITICALITY CALCULATIONS

Post-closure disposal criticality calculations were performed as a function of decay time for the five SNF canisters at the Fitzpatrick ISFSI. All five SNF canisters are MPC-68Ms. The MPC-68M basket is composed entirely of Metamic-HT, so for the MPC-68M, the loss of neutron absorber is also the loss of the basket structure; therefore, only the DB condition is modeled. Figure H-23 shows results for the DB scenario for 23 decay times within the time interval between calendar years 2030 and 1,100,000. The results in Figure H-23 show k_{eff} variation as a function of calendar year. The one sigma statistical uncertainty for all k_{eff} values is 0.0003 or less for all cases.

The k_{eff} values are predicted to vary from 1.1433 to 1.1713 for the MPC-68Ms under the DB scenario. For canisters that had k_{eff} values greater than 0.98 under the DB scenario, calculations were performed in which the pure water was replaced with groundwater compositions of various NaCl concentrations, and the models thus modified were used to determine k_{eff} as a function of NaCl concentration for the calendar year 22,000 (most reactive date). Figure H-24 presents k_{eff} variation as a function of NaCl concentration for those 5 canisters. The results presented in Figure H-24 show that 1.7 mol NaCl/ kg H₂O is sufficient to demonstrate subcriticality ($k_{eff} < 0.98$) for all Fitzpatrick canisters. In this context, it is also important to note that a saturated NaCl brine has a concentration of approximately 6 molal.

Figure H-25 shows the k_{eff} increase between the worst-misload scenario and the as-loaded configuration for the 5 analyzed Fitzpatrick canisters for calendar year 22,000. The increase in k_{eff} varies between 445 and 1,038 pcm for Fitzpatrick canisters.

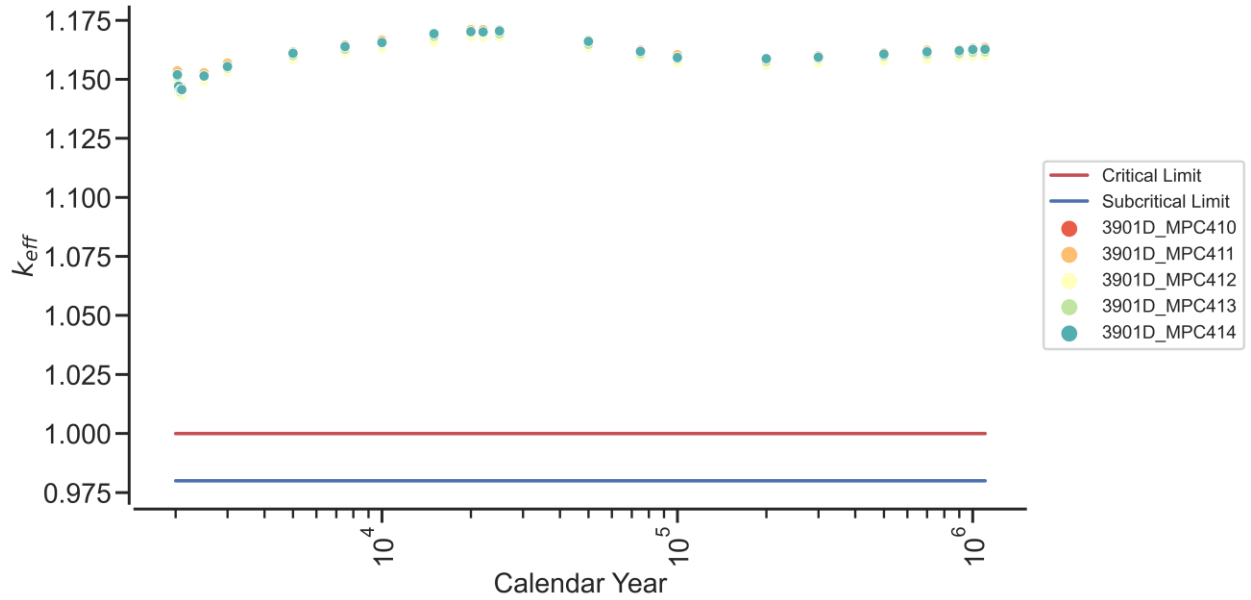


Figure H-23. k_{eff} vs. calendar year for the DB scenario based on actual loading and disposal isotopes for the SNF canisters at Fitzpatrick.

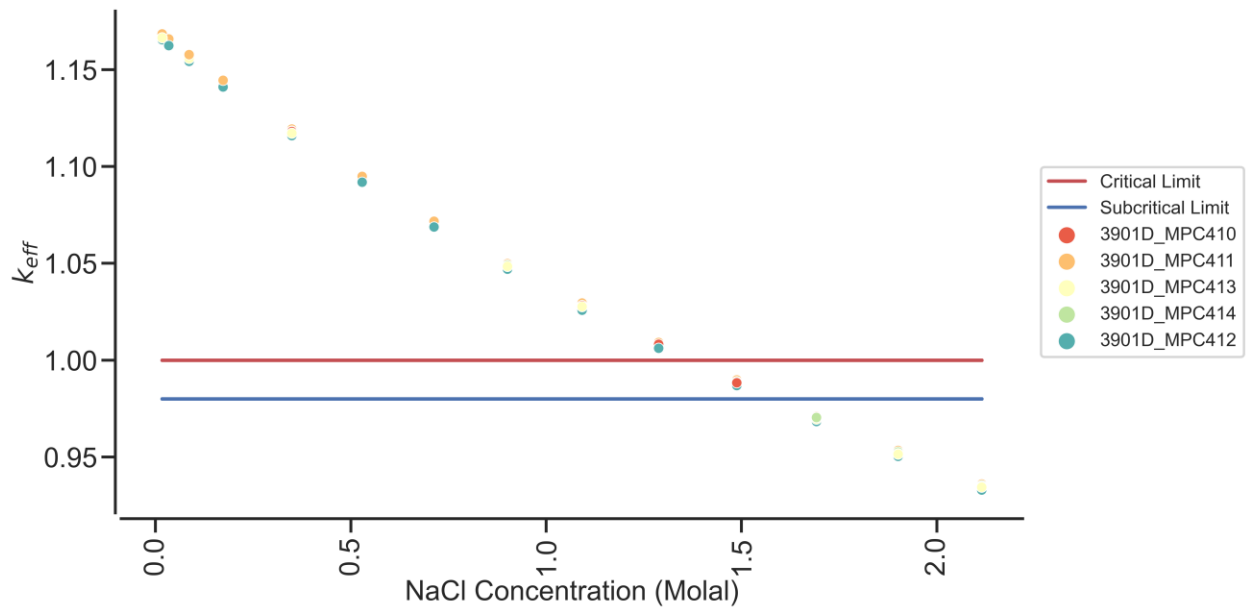


Figure H-24. k_{eff} vs. NaCl concentration for the DPCs with $k_{eff} > 0.98$ for the canisters analyzed at Fitzpatrick under the DB scenario (calendar year 22,000).

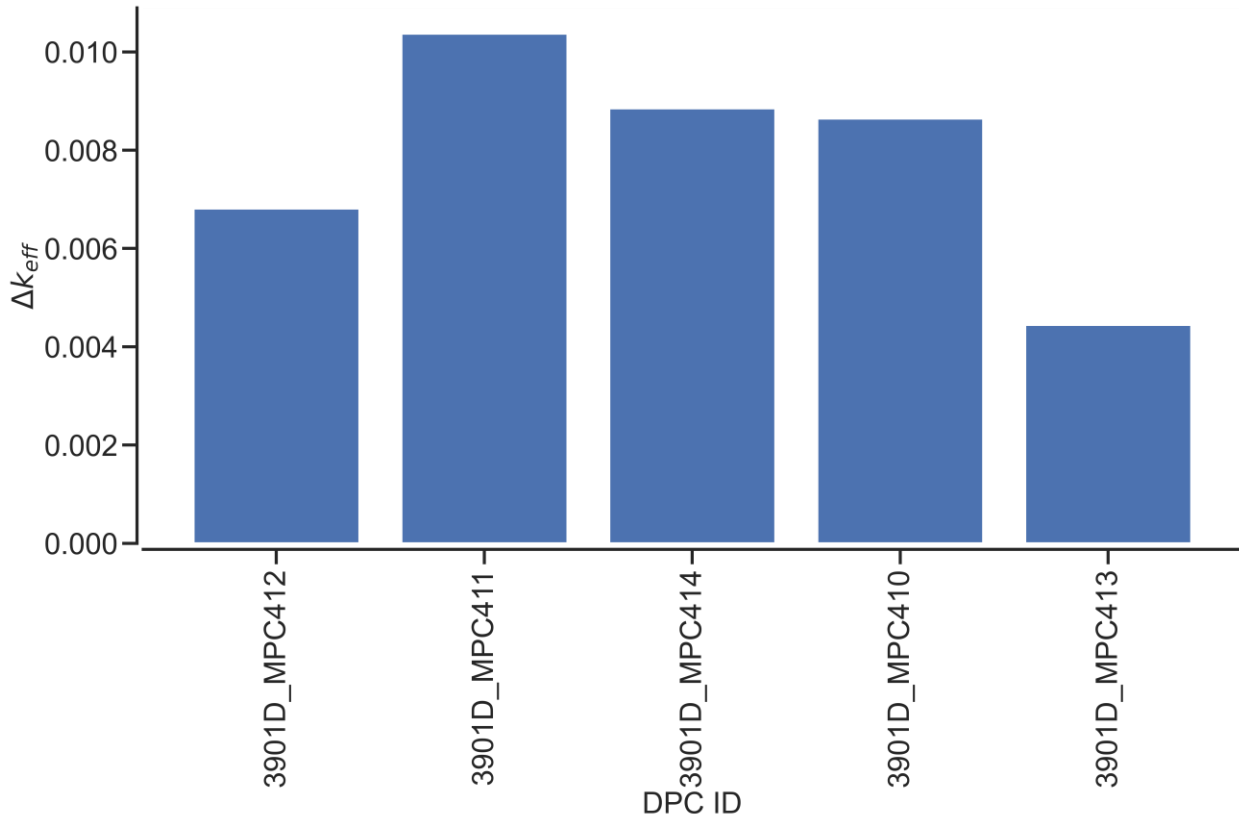


Figure H-25. k_{eff} increase between the worst-misload scenario and the as-loaded configuration for the MPC-68Ms at Fitzpatrick (calendar year 22,000).

H.11. WATERFORD CRITICALITY CALCULATIONS

Post-closure disposal criticality calculations were performed as a function of decay time for the 14 SNF canisters at the Waterford ISFSI. All 14 SNF canisters are MPC-32s. MPC-32s contain no carbon steel structural components, so only the loss-of-neutron-absorber scenario was analyzed. Figure H-26 shows results for the loss-of-neutron-absorber scenario for 23 decay times within the time interval between calendar years 2030 and 1,100,000. The results in Figure H-26 show k_{eff} variation as a function of calendar year. The one sigma statistical uncertainty for all k_{eff} values is 0.0003 or less for all cases.

The k_{eff} values are predicted to vary from 0.9060 to 0.9805 for the MPC-32s under the loss-of-neutron-absorber scenario. For the one canister that had k_{eff} values greater than 0.98 under the loss-of-neutron-absorber scenario, calculations were performed in which the pure water was replaced with groundwater compositions of various NaCl concentrations, and the models thus modified were used to determine k_{eff} as a function of NaCl concentration for the calendar year 22,000 (most reactive date). Figure H-27 presents k_{eff} variation as a function of NaCl concentration for the one canister. Examining the results presented in Figure H-27, it is clear that 0.1 mol NaCl/ kg H₂O is sufficient to demonstrate subcriticality ($k_{eff} < 0.98$) for all Waterford canisters. In this context, it is also important to note that a saturated NaCl brine has a concentration of approximately 6 molal.

Figure H-28 shows the k_{eff} increase between the worst-misload scenario and the as-loaded configuration for the 14 analyzed Waterford canisters for calendar year 22,000. The increase in k_{eff} varies between 890 and 2,369 pcm for Waterford canisters.

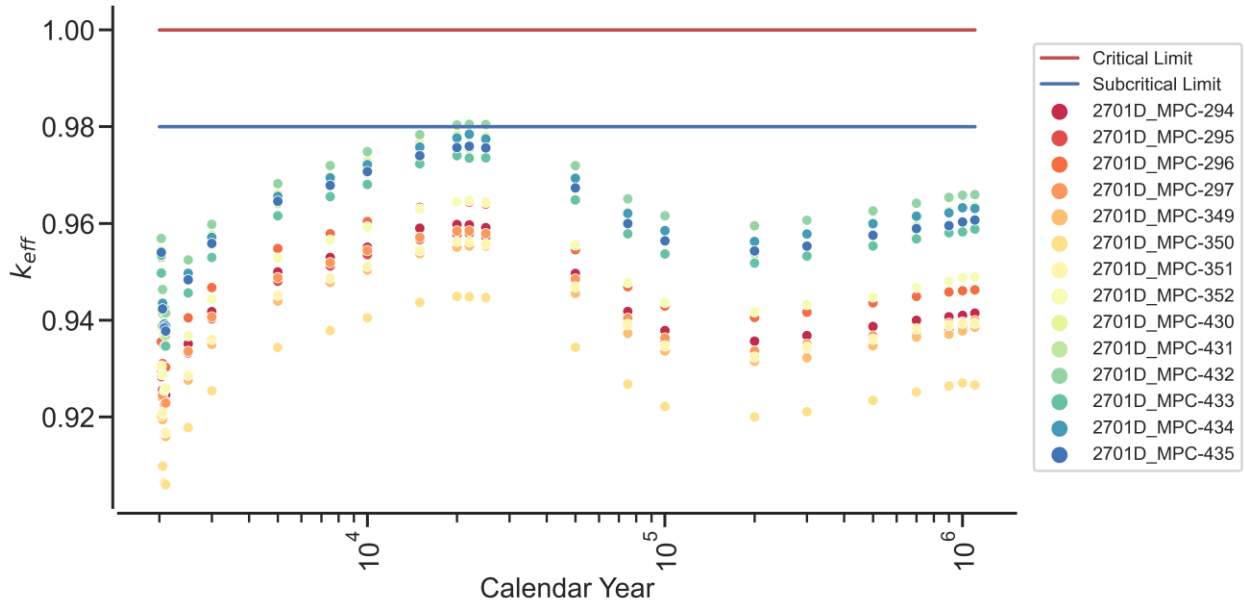


Figure H-26. k_{eff} vs. calendar year for the loss-of-neutron-absorber scenario based on actual loading and disposal isotopes for the SNF canisters at Waterford.

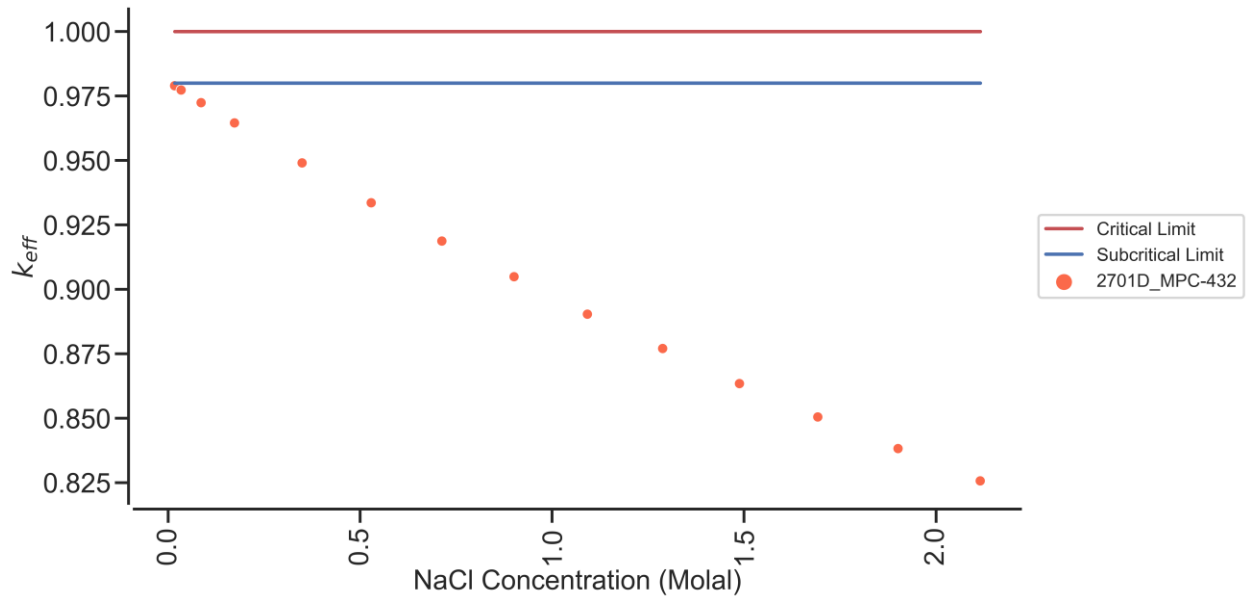


Figure H-27. k_{eff} vs. NaCl concentration for the DPCs with $k_{eff} > 0.98$ for the canisters analyzed at Waterford under the NA scenario (calendar year 22,000).

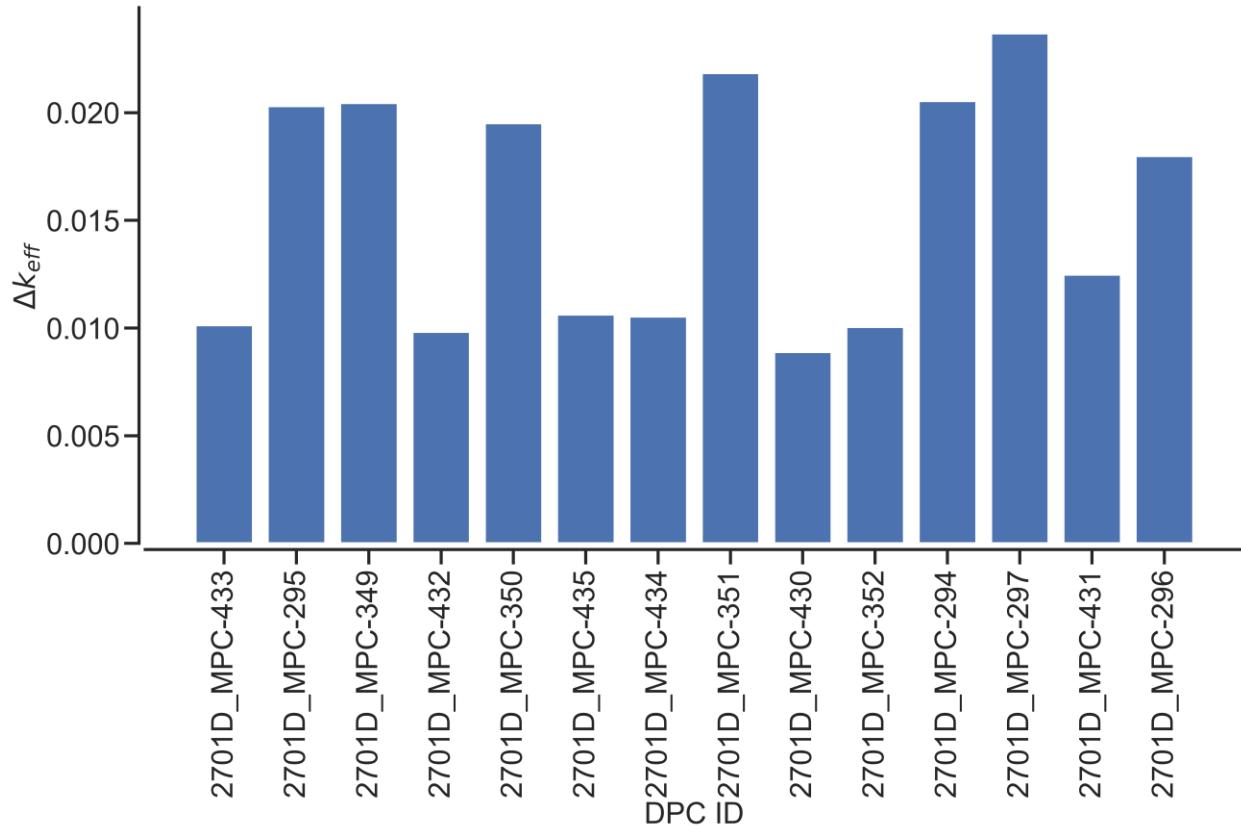


Figure H-28. k_{eff} increase between the worst-misload scenario and the as-loaded configuration for the MPC-32s at Waterford (calendar year 22,000).

H.12. PERRY CRITICALITY CALCULATIONS

Post-closure disposal criticality calculations were performed as a function of decay time for the 13 SNF canisters at the Perry ISFSI. All 13 SNF canisters are MPC-68s. The MPC-68 contains no carbon steel structural components, so only the loss-of-neutron-absorber scenario is analyzed. Figure H-29 shows results for the NA scenario for 23 decay times within the time interval between calendar years 2030 and 1,100,000. The results in Figure H-29 show k_{eff} variation as a function of calendar year. The one sigma statistical uncertainty for all k_{eff} values is 0.0003 or less for all cases.

The k_{eff} values are predicted to vary from 0.9212 to 0.9564 for the MPC-68s under the NA scenario. No canisters had k_{eff} values greater than 0.98 under the NA scenario, and thus no calculations were performed in which the pure water was replaced with groundwater compositions of various NaCl concentrations.

Figure H-30 shows the k_{eff} increase between the worst-misload scenario and the as-loaded configuration for the 13 analyzed Perry canisters at the calendar year 22,000. The increase in k_{eff} varies between 55 and 845 pcm for the Perry canisters.

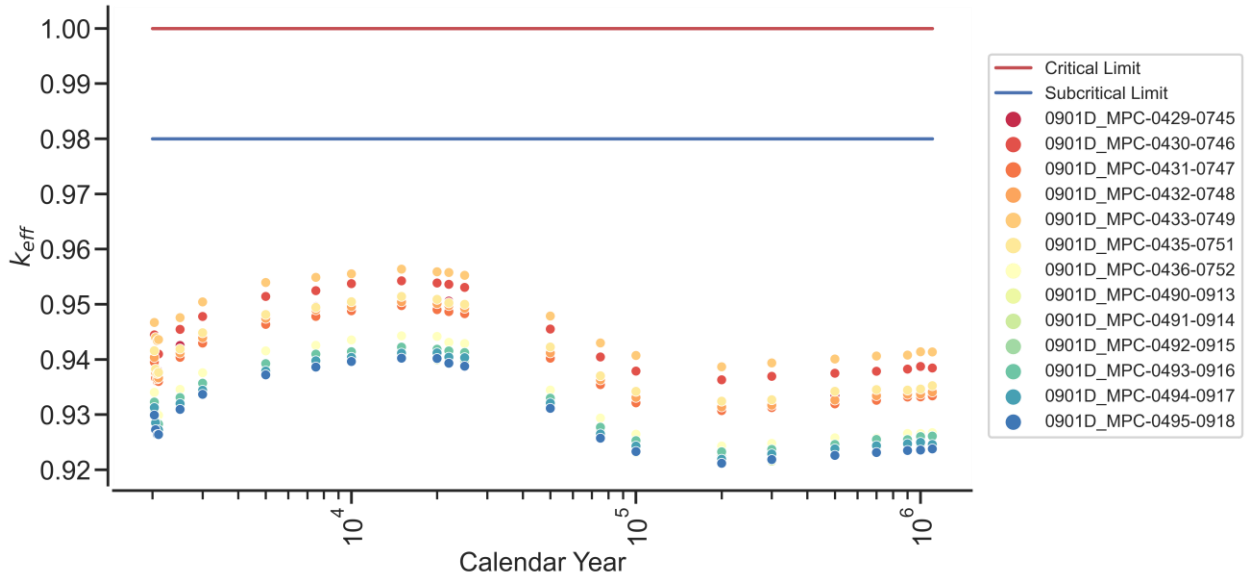


Figure H-29. k_{eff} vs. calendar year for the NA scenario based on actual loading and disposal isotopes for the SNF canisters at Perry.

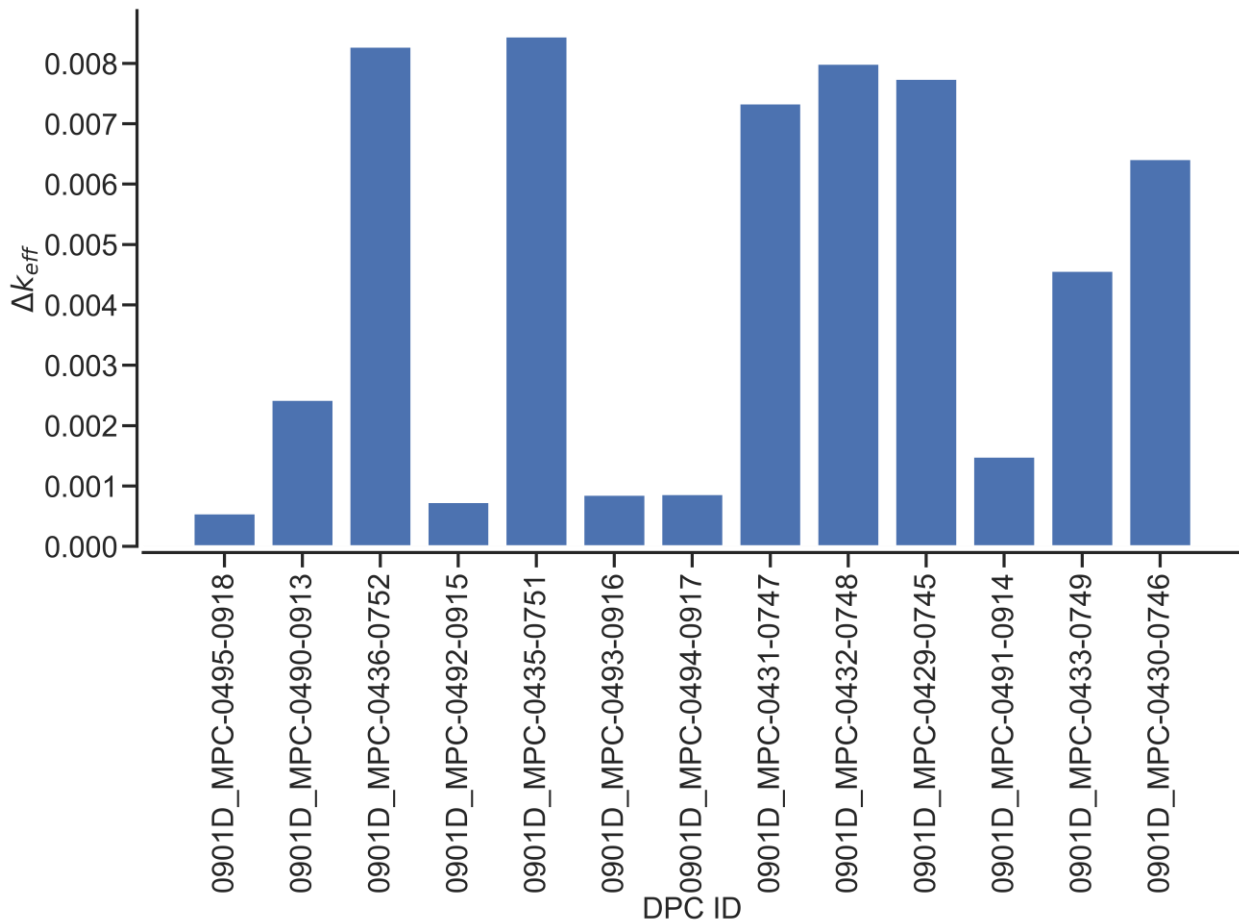


Figure H-30. k_{eff} increase between the worst-misload scenario and the as-loaded configuration for the MPC-68s at Perry (calendar year 22,000).

H.13. FARLEY CRITICALITY CALCULATIONS

Post-closure disposal criticality calculations were performed as a function of decay time for the 24 SNF canisters at the Farley ISFSI. All 24 SNF canisters are MPC-32s. MPC-32s contains no carbon steel structural components, so only the loss-of-neutron-absorber scenario was analyzed. Figure H-31 shows results for the loss-of-neutron-absorber scenario for 23 decay times within the time interval between calendar years 2030 and 1,100,000. The results in Figure H-31 show k_{eff} variation as a function of calendar year. The one sigma statistical uncertainty for all k_{eff} values is 0.0003 or less for all cases.

The k_{eff} values are predicted to vary from 0.9400 to 1.0176 for the MPC-32s under the loss-of-neutron-absorber scenario. Canisters that had k_{eff} values greater than 0.98 under the loss-of-neutron-absorber scenario, calculations were performed in which the pure water was replaced with groundwater compositions of various NaCl concentrations, and the models thus modified were used to determine k_{eff} as a function of NaCl concentration for the calendar year 22,000 (most reactive date). Figure H-32 presents k_{eff} variation as a function of NaCl concentration for all canisters. The results presented in Figure H-32 show that 0.5 mol NaCl/ kg H₂O is sufficient to demonstrate subcriticality ($k_{eff} < 0.98$) for all Farley canisters. In this context, it is also important to note that a saturated NaCl brine has a concentration of approximately 6 molal.

Figure H-33 shows the k_{eff} increase between the worst-misload scenario and the as-loaded configuration for the 24 analyzed Farley canisters at the calendar year 22,000. The increase in k_{eff} varies between 1,211 and 3,484 pcm for Farley canisters.

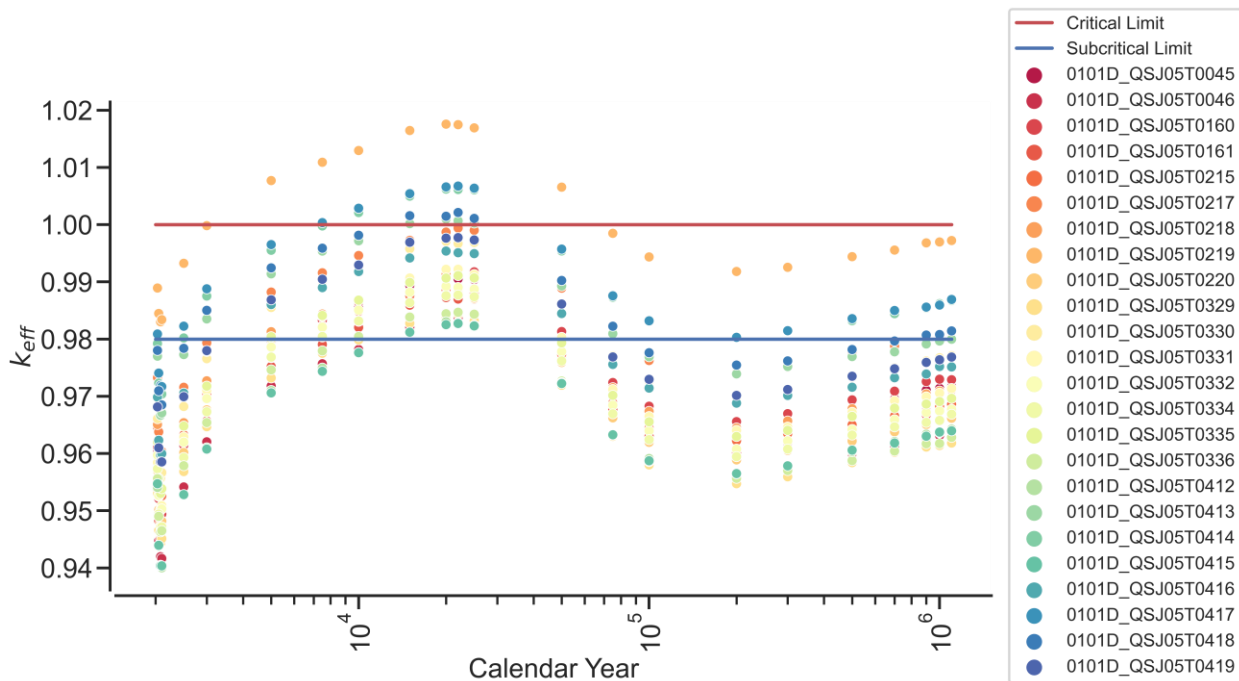


Figure H-31. k_{eff} vs. calendar year for the loss-of-neutron-absorber scenario based on actual loading and disposal isotopes for the SNF canisters at Farley.

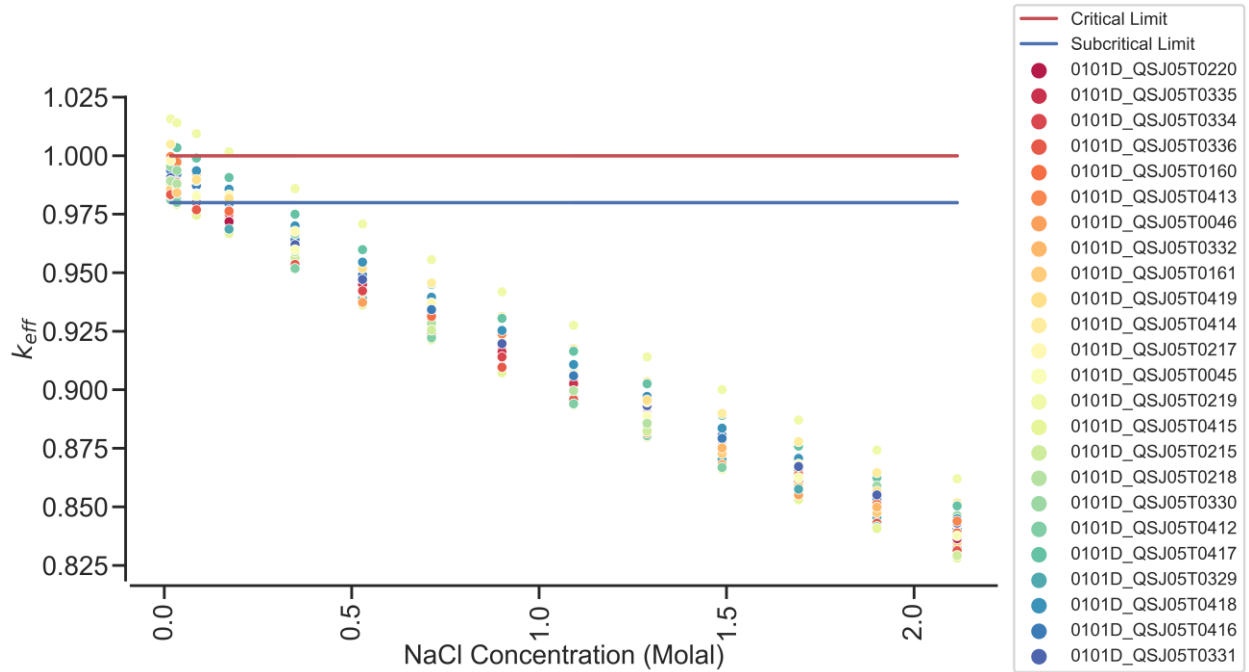


Figure H-32. k_{eff} vs. NaCl concentration for the DPCs with $k_{eff} > 0.98$ for the canisters analyzed at Farley under the NA scenario (calendar year 22,000).

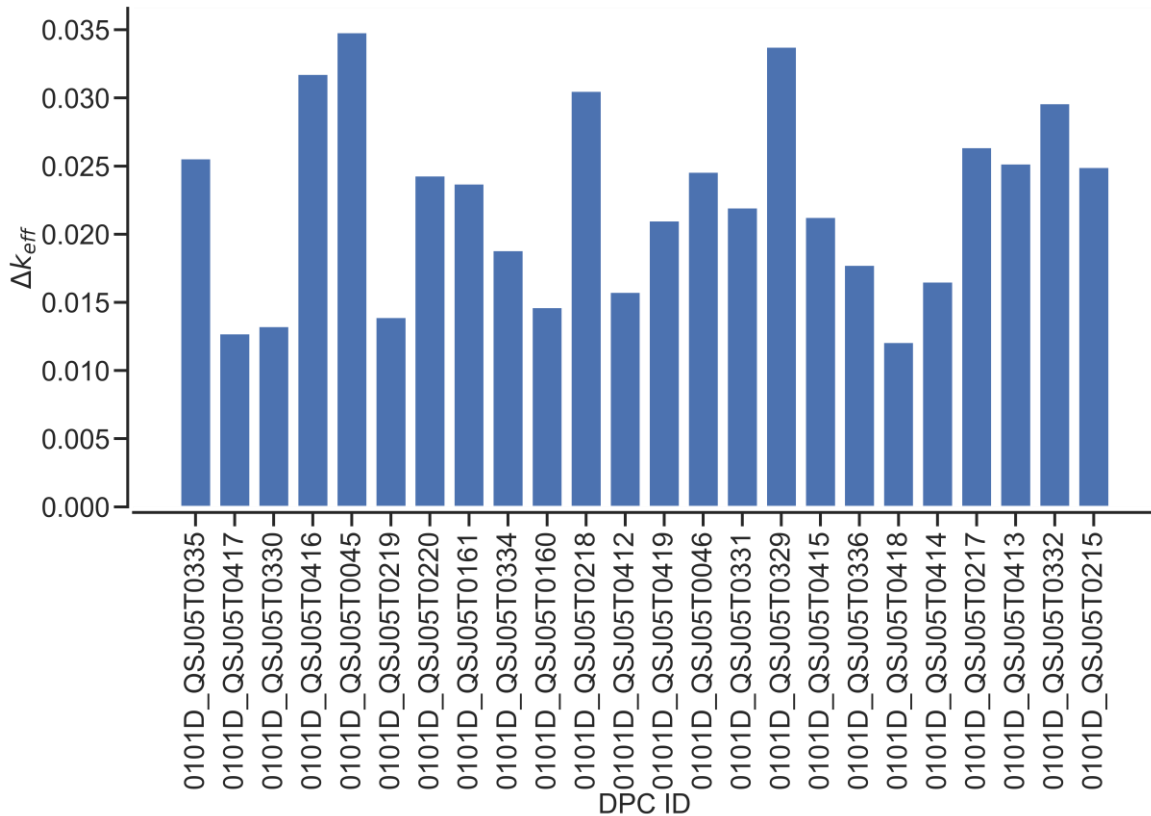


Figure H-33. k_{eff} increase between the worst-misload scenario and the as-loaded configuration for the MPC-32s at Farley (calendar year 22,000).

H.14. INDIAN POINT CRITICALITY CALCULATIONS

Post-closure disposal criticality calculations were performed as a function of decay time for the 18 SNF canisters at the Indian Point ISFSI. All 18 SNF canisters are MPC-32s. MPC-32s contain no carbon steel structural components, so only the loss-of-neutron-absorber scenario was analyzed. Figure H-34 shows results for the loss-of-neutron-absorber scenario for 23 decay times within the time interval between calendar years 2030 and 1,100,000. The results in Figure H-34 show k_{eff} variation as a function of calendar year. The one sigma statistical uncertainty for all k_{eff} values is 0.0003 or less for all cases.

The k_{eff} values are predicted to vary from 0.9093 to 1.0303 for the MPC-32s under the loss-of-neutron-absorber scenario. For canisters that had k_{eff} values greater than 0.98 under the loss-of-neutron-absorber scenario, calculations were performed in which the pure water was replaced with groundwater compositions of various NaCl concentrations, and the models thus modified were used to determine k_{eff} as a function of NaCl concentration for the calendar year 22,000 (most reactive date). Figure H-35 presents k_{eff} variation as a function of NaCl concentration for the one canister. The results presented in Figure H-35 show that 0.7 mol NaCl/ kg H₂O is sufficient to demonstrate subcriticality ($k_{eff} < 0.98$) for all Indian Point canisters. In this context, it is also important to note that a saturated NaCl brine has a concentration of approximately 6 molal.

Figure H-36 shows the k_{eff} increase between the worst-misload scenario and the as-loaded configuration for the 18 analyzed Indian Point canisters at the calendar year 22,000. The increase in k_{eff} varies between 1,171 and 4,091 pcm for Indian Point canisters.

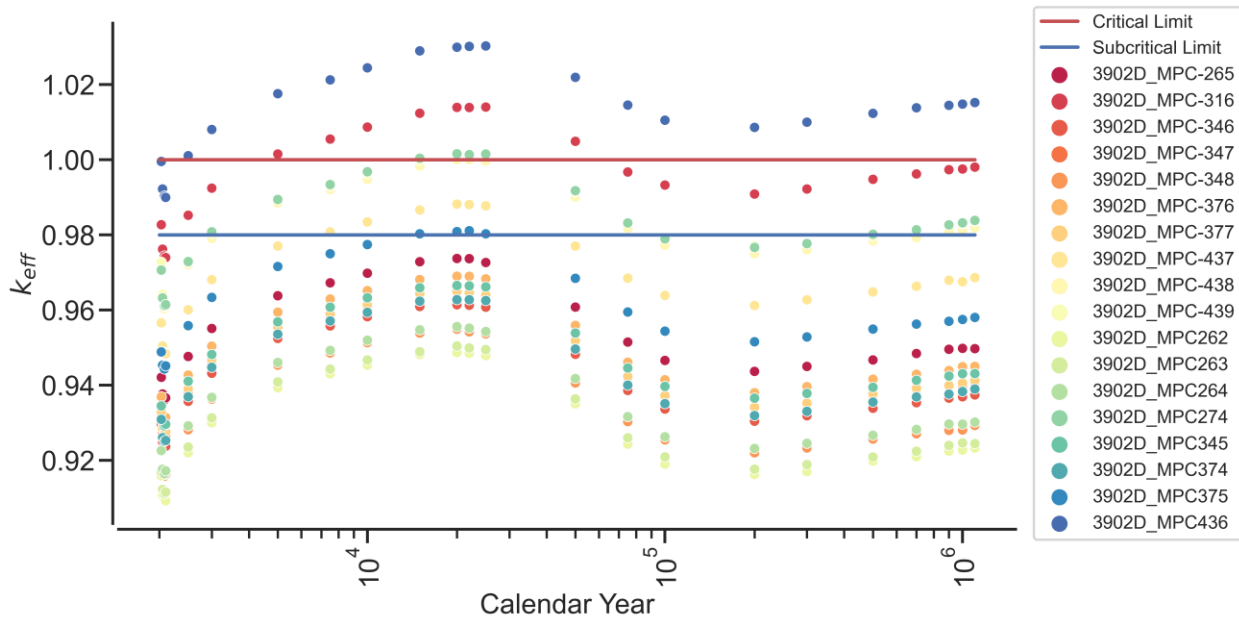


Figure H-34. k_{eff} vs. calendar year for the loss-of-neutron-absorber scenario based on actual loading and disposal isotopes for the SNF canisters at Indian Point.

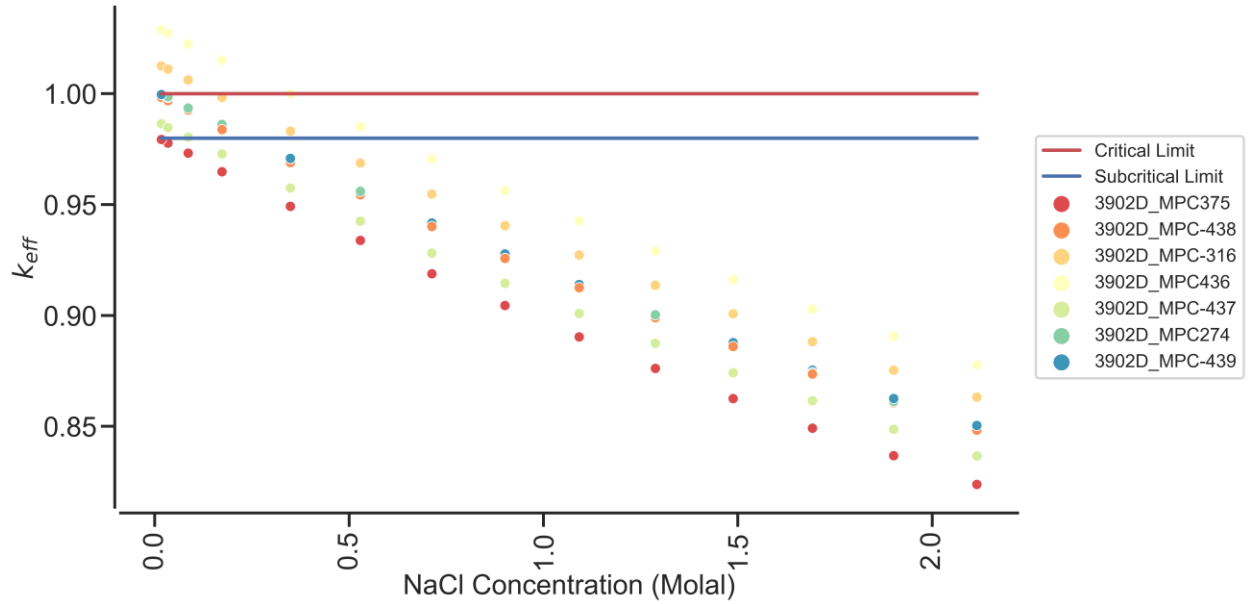


Figure H-35. k_{eff} vs. NaCl concentration for the DPCs with $k_{eff} > 0.98$ for the canisters analyzed at Indian Point under the NA scenario (calendar year 22,000).

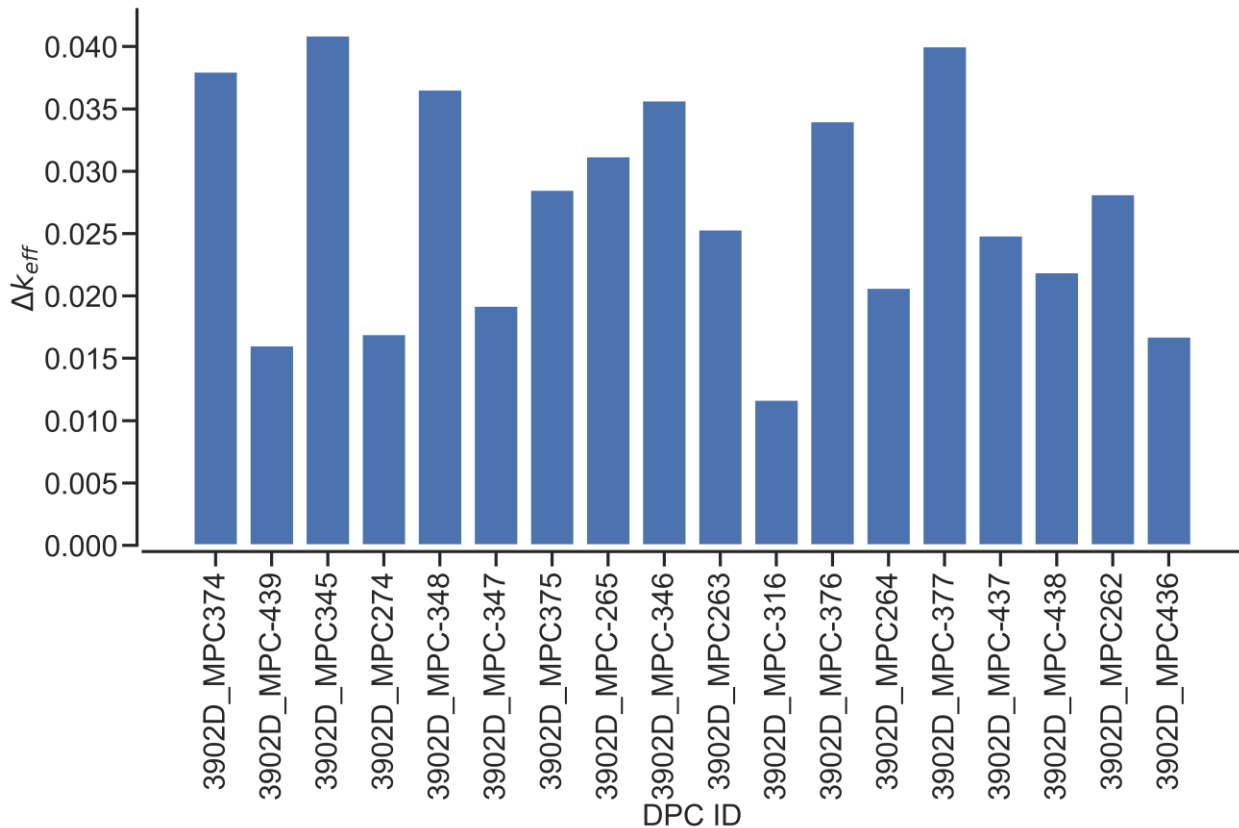


Figure H-36. k_{eff} increase between the worst-misload scenario and the as-loaded configuration for the MPC-32s at Indian Point (calendar year 22,000).

H.15. COMANCHE PEAK CRITICALITY CALCULATIONS

Post-closure disposal criticality calculations were performed as a function of decay time for the 20 SNF canisters at the Comanche Peak ISFSI. All 20 SNF canisters are MPC-32s. MPC-32s contain no carbon steel structural components, so only the loss-of-neutron-absorber scenario was analyzed. Figure H-37 shows results for the loss-of-neutron-absorber scenario for 23 decay times within the time interval between calendar years 2030 and 1,100,000. The results in Figure H-37 show k_{eff} variation as a function of calendar year. The one sigma statistical uncertainty for all k_{eff} values is 0.0003 or less for all cases.

The k_{eff} values are predicted to vary from 0.9546 to 1.0299 for the MPC-32s under the loss-of-neutron-absorber scenario. Canisters had k_{eff} values greater than 0.98 under the loss-of-neutron-absorber scenario, so calculations were performed in which the pure water was replaced with groundwater compositions of various NaCl concentrations, and the models thus modified were used to determine k_{eff} as a function of NaCl concentration for calendar year 22,000 (most reactive date). Figure H-38 presents k_{eff} variation as a function of NaCl concentration for the one canister. The results presented in Figure H-38 show that 0.7 mol NaCl/ kg H₂O is sufficient to demonstrate subcriticality ($k_{eff} < 0.98$) for all Comanche Peak canisters. In this context, it is also important to note that a saturated NaCl brine has a concentration of approximately 6 molal.

Figure H-39 shows the k_{eff} increase between the worst-misload scenario and the as-loaded configuration for the 20 analyzed Comanche Peak canisters at the calendar year 22,000. The increase in k_{eff} varies between 1,022 and 4,634 pcm for Comanche Peak canisters.

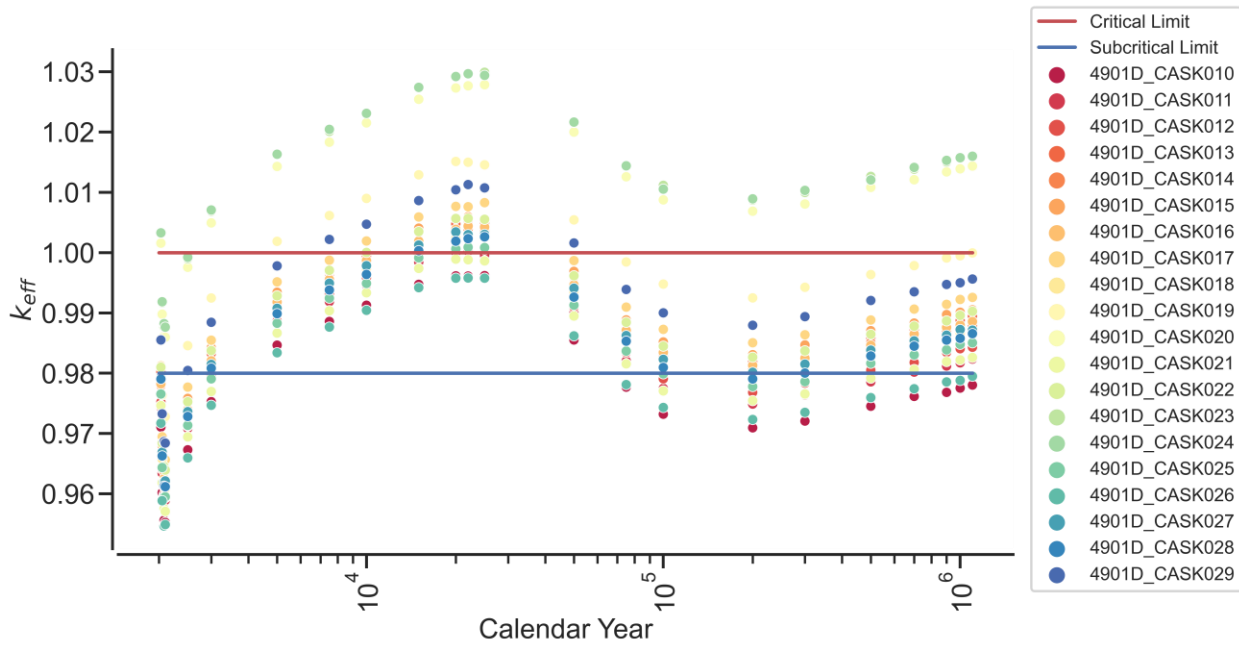


Figure H-37. k_{eff} vs. calendar year for the loss-of-neutron-absorber scenario based on actual loading and disposal isotopes for the SNF canisters at Comanche Peak.

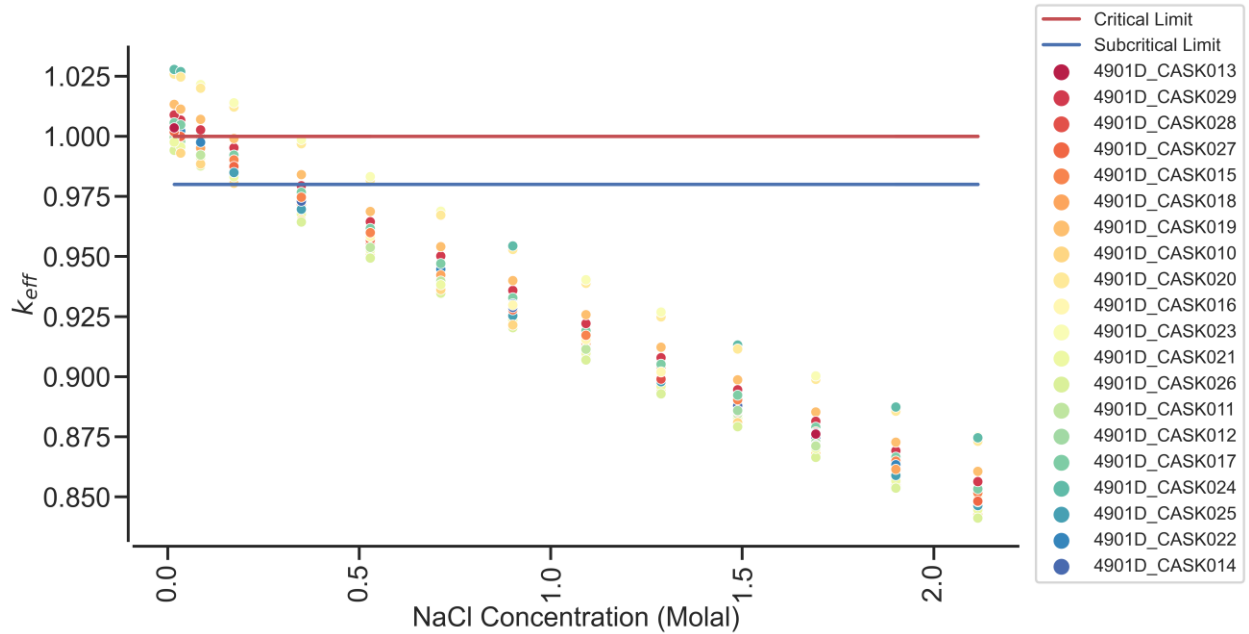


Figure H-38. k_{eff} vs. NaCl concentration for the DPCs with $k_{eff} > 0.98$ for the canisters analyzed at Comanche Peak under the NA scenario (calendar year 22,000).

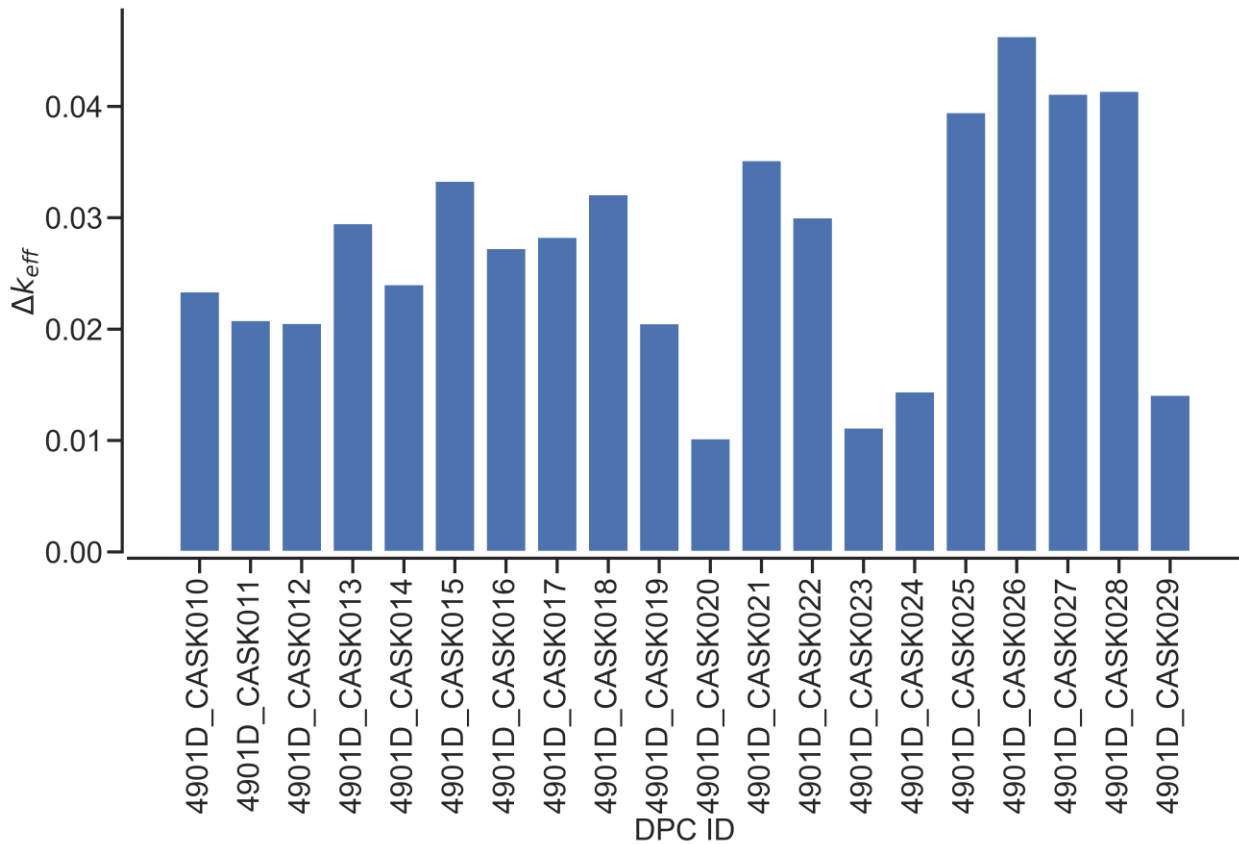


Figure H-39. k_{eff} increase between the worst-misload scenario and the as-loaded configuration for the MPC-32s at Comanche Peak (calendar year 22,000).

H.16. CONCLUSIONS

This appendix contains an update to the DPC reactivity assessment analysis carried out in previous years.

Post-closure criticality analysis calculations for a total of 225 new as-loaded canisters from 14 sites over the time interval between calendar years 2030 and 1,100,000 were performed using the burnup credit methodology described in this report. For the reactivity calculation, the NA configurations were modeled for DPCs with baskets composed of stainless steel, and the DB configurations were modeled for DPCs composed of other materials. A particular emphasis was again placed on modeling available DPCs with baskets composed of Metamic-HT (MPC-37, MPC-68M, MPC-89) when available because it performs both a neutron absorbing and structural function under normal storage and transportation conditions and may pose a concern for post-closure criticality. However, with a focus on these canisters last year, there are substantially fewer available to analyze. Three sites and 15 canisters utilized Metamic-HT, accounting for only 7% of the total canisters. Furthermore, four additional sites with MPC-32s, three sites with MPC-68s, one site with TSC-37s, one site with NUHOMS[®] 32PTH-DSCs, one site with TSC-24s, and one site with NUHOMS[®] 61BTs and NUHOMS[®] 61BTHs were analyzed. In all cases, the reactivity results were compared to a critical limit of 1.0 and a hypothetical limit of 0.98.

In addition to the as-loaded reactivity assessment calculations, canister misloading calculations and NaCl reactivity suppression calculations were performed. Canister misload criticality analyses were performed assuming a worst configuration in an as-loaded canister, which is based on the assumption that correct assemblies have been loaded into the canister, but they are loaded in the most reactive configuration. k_{eff} values for worst-misload configurations were determined assuming that all fuel assemblies in the canister have a decay time of 22,000 years and the neutron absorber is completely lost. The misload analysis was performed for all 225 new canisters containing intact fuel assemblies that were loaded to full capacity. All canisters that were shown to exceed the 0.98 subcritical limit were analyzed to determine the groundwater NaCl concentrations necessary to show subcriticality.

A summary of the DPC reactivity assessment results for 225 DPCs analyzed during FY22 is shown in Table H-2. For each site, Table H-2 refers to the section of the report documenting the analysis and includes the type of DPC used at the site, the degradation scenario modeled, the minimum and maximum k_{eff} for the reactivity calculations, the minimum and maximum canister misload k_{eff} increases, and the maximum NaCl concentration needed to reduce the DPC k_{eff} values to 0.98. Based on the results in Table H-2, it is observed that all Metamic-HT baskets show very high reactivity as a result of the complete loss of neutron absorber and assembly spacing in the DB configuration. This agrees with prior assessments involving Metamic-HT baskets, with these DPCs being among the most reactive observed to date. It is also observed that, even with the elevated reactivity, a maximum of 1.7m of NaCl would be required to suppress the reactivity of these canisters.

Table H-2. Summary of FY22 DPC reactivity assessment results.

Site	Section	DPC Type	Degradation scenario	Min k_{eff}	Max k_{eff}	Min misload Δk_{eff} (pcm)	Max misload Δk_{eff} (pcm)	Max required NaCl (molal)
Clinton	H.2	MPC-89	DB	1.1414	1.1718	106	299	1.7
Fermi	H.3	MPC-68	NA	0.9031	0.9337	247	1,389	N/A
Saint Lucie	H.4	NUHOMS® 32PTH	NA	0.8232	0.9212	178	2,371	N/A
McGuire	H.5	TSC-37	NA	0.9386	1.0065	657	1,874	0.4
McGuire	H.5	TSC-37	DB	1.0135	1.0871	713	1,984	1.1
Palo Verde	H.6	TSC-24	NA	0.8072	0.8624	442	3,835	N/A
Summer	H.7	MPC-37	DB	1.0380	1.0935	779	2,441	1.1
Susquehanna	H.8	NUHOMS® 61BT	NA	0.9122	0.9387	1,238	1,720	N/A
Susquehanna	H.8	NUHOMS® 61BTH Type 1	NA	0.8433	0.9541	126	2,684	N/A
Brown's Ferry	H.9	MPC-68	NA	0.8929	0.9191	1,036	1,354	N/A
Fitzpatrick	H.10	MPC-68M	DB	1.1433	1.1713	445	1,038	1.7
Waterford	H.11	MPC-32	NA	0.9060	0.9805	890	2,369	0.1
Perry	H.12	MPC-68	NA	0.9212	0.9564	55	845	N/A
Farley	H.13	MPC-32	NA	0.9400	1.0176	1,211	3,484	0.5
Indian Point	H.14	MPC-32	NA	0.9093	1.0303	1,171	4,091	0.7
Comanche Peak	H.15	MPC-32	NA	0.9546	1.0299	1,022	4,634	0.7

A summary of the direct disposal criticality calculations is provided in Table H-3. For this project, 1,154 canisters have been analyzed through FY22. Of the canisters analyzed, it was shown that 67% would remain subcritical under the loss-of-neutron-absorber scenario. When considering complete degradation of the baskets of canisters with non-stainless-steel structural components, 61% of the canisters are shown to be subcritical. When further considering the potential for the worst-case arrangement of the most reactive fuel assemblies in each canister, it is shown that 51% of canisters would remain subcritical. The percentages of the canisters shown to be subcritical have remained relatively stable relative to the FY21 results. There were notable drops observed for Metamic-HT basket DPCs, which show very high reactivity as a result of the complete loss of basket structure. However, as a fraction of examined canisters, Metamic-HT baskets were less available relative to FY21 reporting, and this along with non-Metamic-HT baskets resulted in largely consistent canister fractions. Although these canisters are the

latest generation of DPCs and represent a large fraction of DPCs entering service, this trend is expected to continue as additional DPCs are loaded but may exhibit a lagging effect in future reports as data are provided, input, and run with UNF-ST&DARDS.

Table H-3. Summary of the number of canisters meeting the subcritical limit.

Description (analysis dates: 2030–1,100,000)	Value
Total DPCs analyzed	1,154
Total DPCs below subcritical limit with loss of neutron absorber (design-basis loading)	0 (0%)
Total DPCs below subcritical limit with loss of neutron absorber (as-loaded)	776 (~67%)
Total DPCs below subcritical limit with loss of neutron absorber and carbon steel structures (as-loaded)	699 (~61%)
Total DPCs below subcritical limit with loss of neutron absorber and carbon steel structures (as-loaded) considering misload	583 (~51%)